Drought stress responses of the *Medicago truncatula* - *Ensifer meliloti* symbiosis on nodule senescence and nitrogen fixation

A thesis presented in fulfilment of the requirements for the degree of

Doctor of Philosophy

In

Plant Science

at Massey University, Palmerston North,

New Zealand.

Ramadoss Dhanushkodi

2018

Abstract

While the use of nitrogen (N) fertilizer has provided many benefits to agriculture, incessant use of it can reduce soil organic matter and fertility resulting in lower crop yields. Legume plants can fix its own N_2 through symbiotic nitrogen fixation (SNF) to promote plant growth by developing facultative root organs called nodules. Therefore, increasing the rate of SNF to reduce dependence on N fertilizer is a promising strategy for sustainable legume production. In legume cultivation this symbiotic process confronts two major challenges. First, SNF is suppressed by readily available N in the soil and second, the early senescence of N-fixing nodules can limit any further fixation to occur. Previous reports show that N fertilizer supresses SNF activity in many legumes and supports plant growth better than SNF. Moreover, suppression of SNF can also be induced by drought stress which causes early nodule senescence and subsequent reduced rates of plant growth. This thesis addresses the process of SNF suppression in two *Medicago truncatula* selected genotypes, Jemalong A17 and R108, in response to external N treatment and also delivers a molecular view on the regulation of drought-induced nodule senescence processes.

I first hypothesized that Jemalong A17 and R108 may respond differently to external N treatment and drought stress, which both lead to SNF suppression. To determine this, *M. truncatula* plants were grown with the N_2-fixing symbiont *Ensifer meliloti* and ^{15}N-labelled N fertilizer under well-watered and drought conditions. Plants were then harvested at different time points. N partitioned by SNF and N fertilizer were measured using isotope ratio mass spectroscopy. Results show that under well-watered conditions, N fertilized R108 plants used SNF for N uptake (upto 23% of total shoot N), when inoculated with *E. meliloti*, and reduced N fertilizer uptake to balance total N uptake. Under drought stress, both Jemalong A17 and R108 plants derived assimilated N from SNF (upto 45% of total shoot N) while they significantly reduced the N uptake from N fertilizer. Moreover I found that SNF in association with *E. meliloti* not only benefitted the host by increasing the N supply but also primed the host plant to better tolerate drought stress by controlling the expression of drought-associated genes.

In legumes, nodules are the first organs to be responsive to drought stress. Once drought conditions are perceived, the host plant induces early nodule senescence in order to reduce the carbon investment in the nodules. Therefore, nodule senescence can be part of a drought-survival strategy. However, as SNF becomes limited due to early nodule senescence, nutrient stress can develop in the legume in addition to the drought stress. Here, I then hypothesized that the intrinsically destructive senescence process must be tightly regulated to function as a part of drought-survival strategy. *M. truncatula* protease inhibitor and iron scavenging genes, possibly involved in controlling nodule senescence, were identified. RNAi lines were constructed in which expression of a *serpin* or *ferritins*

were knocked down. Both wild-type and RNAi lines were subjected to drought stress and the subsequent nodule activity and plant physiological responses were measured. Drought caused *M. truncatula* to initiate nodule senescence before plant growth was affected and before an increase in papain-like proteolytic activity and free iron levels were detected. Knock-down expression of *serpin6* and *ferritins* caused increased protease activity, free iron levels, early nodule senescence and reduced plant growth. These results suggest that *M. truncatula* expresses *serpin6* and *ferritins* in nodules to mediate ordered drought-induced senescence by regulating papain-like cysteine protease activity and free iron levels. This strategy may allow the drought-stressed plants to extract the maximum benefit from residual N fixation and nutrient recovery resulting from the breakdown of macromolecules.

Acknowledgement

Completion of my research work and doctoral study wouldn't have been possible without the support of following people. First and foremost, I would like to thank Associate Professor Paul Dijkwel, a mentor and an extradinaire dissertation supervisor for instilling in me the qualities of being a good plant scientist. His intellectual scientific advice, expertise and supervision during my doctoral study were greatly supportive to accomplish my targets. At this place, I would like to thank also Professor Emeritus Michael McManus, who has died in 2015 for his consent and offering me place to undertake my research. His support at the beginning of my course helped me to structure the thesis proposal and design preliminary experiments.

I would like to express my deep gratitude the to my co-supervisor Professor Cory Matthew for his scientific and moral support during the period. His advice, patience, immense scientific knowledge, expertise and feedback helped me a lot to improve my research and study. I would like to thank Associate professor Richard Macknight, University of Otago, New Zealand and Dr Peter Kalo for providing me *M. truncatula* seeds to undertake my research. I am greatly thankful to Dr Donald Hunter, Scientist, Plant and Food Research, Palmerston North for helping me in RNAi construction.

I also thank Dr Tina Sehrish a lab manager for her support in conducting various plant and lab experiments. I express my special thanks to my friends Dr Srishti Joshi, Nikolai Kondratev, Meriem, Elva, Xi Xu and colleagues of ScC5.19 lab for their friendly and moral support.

Coming last in order but nevertheless very important, my parents Dhanushkodi and Subbulakshmi for their wishes, support and encouragement to complete my PhD research. My sincere and heartful thanks to NZAid scholarship for financially supporting my living and education costs.

Table of Contents

Abstract ..... **II**

Acknowledgments ..... **IV**

Table of contents ..... **V**

List of figures ..... **XI**

List of tables ..... **XIV**

Abbreviations ..... **XV**

Chapter 1 ..... **1**

Introduction **1**

1.1 Plant immunity and rhizobial infection 2

1.2 Nitrogen fixation under N availability 3

1.3 Nitrogen fixation under drought 4

1.4 Effect of drought on symbiosis and the growth of SNF-dependent plants 6

1.5 Biological nitrogen fixation for plant growth 8

1.6 Rhizobia for stress amelioration 9

1.7 Nodule physiology of *M. truncatula* 9

1.8 Nodule senescence: stress-induced natural aging and the factors involved 11

1.9 Response and function of protease activity in various plant growth activities during natural and stress-induced nodule aging 12

1.10 Protease inhibitors as a proteolytic controlling mechanism in senescence 14

1.11 Attributes of plant serpins 15

1.12 Interaction of serpins with proteases and the involvement in programmed cell death and homeostasis 16

1.13 Expression and localization of serpins in plants 16

1.14 Role of lb in nodules and their stability during natural and stress-induced aging 17
1.15 Attributes of nodule iron and its toxicity 17
1.16 Reactive oxygen species (ROS) in natural aging and stress-induced senescence 18
1.17 Ferritins and their involvement in iron scavenging 20
1.18 Expression of serpin and ferritin in plants under drought 22
1.19 Medicago truncatula as a model plant for legume-rhizobium symbiosis 23
1.20 Concluding statement 24
1.21 Hypotheses 26
1.22 Research objectives 26

Chapter 2 28
Materials and methods 28
2.1 Plant growth and physiology protocols 28
2.1.1 Plant materials and growth 28
2.1.2 Measurement of growth kinetics of *E. meliloti* cells 28
2.1.3 *E. meliloti* inoculation for nodule formation 29
2.1.4 Measurement of field capacity (FC) 29
2.1.5 Water treatments 29
2.1.6 Physiological characterization 30
2.1.7 Chlorophyll estimation 31
2.1.8 Nitrogenase activity measurement by acetylene reductase assay (ARA) 32
2.1.9 Experimental set up for N fertilizer treatments in Chapter 4 32
2.1.10 Total N and ^{15}N measurement 33
2.2 Histology protocols 34
2.2.1 Histological analysis of nodule tissues 34
2.3 Molecular biology protocols 37
2.3.1 Sequence retrieval and primer design 37

2.3.2 RNA extraction 37
2.3.3 First strand cDNA synthesis 38
2.3.4 Quantitative Real-Time PCR 38
2.3.5 Ligation reaction 40
2.3.6 Competent cell preparation 40
2.3.7 Bacterial transformation 40
2.3.8 Colony PCR 41
2.3.9 Reverse transcriptase PCR 41
2.3.10 Agarose gel electrophoresis and gel elution 42
2.3.11 Restriction digestion reaction 42
2.3.12 Construction and transformation of RNAi knockdown *Ser6, Fer2* and *Fer3* constructs 43
2.3.13 Agrobacterium rhizogenes mediated root transformation 44
2.4 Biochemical assays protocols 45
2.4.1 Protein and protease activity measurement 45
2.4.2 Lb and iron content measurement 45
2.4.3 Protease inhibitory assay 46
2.5 Statistical analysis 47

Chapter 3 ..... **48**

A serpin and two ferritins are induced by drought in *M. truncatula* nodules **48**

3.1 Introduction **48**

3.2 Results **50**

3.2.1 Growth kinetics and optimum *E. meliloti* cell density 50
3.2.2 Nodulation and nitrogenase assay in *M. truncatula* 51
3.2.3 Effects of *E. meliloti* inoculation on *M. truncatula* plant growth 52
3.2.4 Identification of serpin and ferritin genes in *M. truncatula* 54
3.2.5 Multiple sequence alignment and primer design 55

3.2.6 Screening of serpin and ferritin genes in root, nodule and leaf tissues 57

3.2.6.1 cDNA amplification of serpin and ferritin groups 57

3.2.6.2 cDNA amplification of individual genes 58

3.2.7 Relative transcript abundance of serpin and ferritin genes in nodule under drought stress . 59

3.3 Discussion **65**

Chapter 4 ..... **67**

***M. truncatula* Jemalong A17 and R108 suppress SNF in different ways in response to N fertilizer and drought** **67**

4.1 Introduction **67**

4.2 Results **69**

4.2.1 Symbiosis phenotype varies between *M. truncatula* Jemalong A17 and R108 69

4.2.2 Symbiotic nitrogen fixation confers growth benefits to Jemalong A17 and R108 plants 69

4.2.3 Nitrogen fertilizer supresses the N uptake from SNF in Jemalong A17 but not R108 73

4.2.4 *E. meliloti* inoculation suppresses the N uptake from N fertilizer in R108 but not Jemalong A17 75

4.2.5 Jemalong A17 and R108 plants balance the N level by controlling N uptake 77

4.2.6 Jemalong A17 and R108 differ in nodule activity in response to external N fertilizer treatment 79

4.2.7 R108 alters the nodule plasticity in response to external N fertilizer treatment 79

4.2.8 N uptake from N fertilizer is suppressed in both Jemalong A17 and R108, when grown in water limiting conditions 82

4.2.9 Jemalong A17 and R108 acquired substantial N from SNF under drought stress 84

4.2.10 Jemalong A17 and R108 plants sustain nodule activity and active bacteroids under N fertilization and drought treatment 86

4.2.11 SNF sustains plant growth better than N fertilizer under drought stress 89

4.2.12 *E. meliloti*-inoculated plants induce expression of abscisic acid-related genes and reduce expression of stress-associated genes in *M. truncatula* leaves 91

4.3 Discussion **95**

4.4 Conclusion **99**

Chapter 5 ..... **100**

Drought-induced senescence of *Medicago truncatula* nodules involves serpin and ferritin to control proteolytic activity and iron levels **100**

5.1 Introduction **100**

5.2 Results **102**

5.2.1 Prolonged drought stress affects the growth of *M. truncatula* 102

5.2.2 Prolonged drought stress disrupts the nodule activity of *M. truncatula* 106

5.2.3 Drought induced nodule senescence involves the elevation of proteolytic activity and iron content 107

5.2.4 Nodule expresses *MtSer6*, *MtFer2* and *MtFer3* genes during early drought stress 110

5.2.5 Down-regulated expression of *MtSer6*, *MtFer2* and *MtFer3* in RNAi knockdown lines 113

5.2.6 Knockdown of *MtSer6* in *RNAiMtSer6* nodules results in increased papain-like cysteine protease activity, iron levels and *MtFer3* expression 116

5.2.7 Knockdown of *ferritins* result in excess iron increase and nodule protein and lb degradation 116

5.2.8 Reduced expression of *MtSer6*, *MtFer2* and *MtFer3* in triple RNAi nodules exhibits further nodule protein and lb degradation 117

5.2.9 Knockdown of *Mtser6* and *ferritins* causes early nodule senescence and reduced plant growth 119

5.3 Discussion **124**

5.4 Conclusion **126**

Chapter 6 Summary and conclusion **127**

Bibliography **131**

Appendices **159**

Appendix 1. Growth media and nutrients used in this study 159

Appendix 2. Primers used in this study 162

Appendix 3. Nucleotide sequence of the genes used for qRT-PCR 165

Appendix 4. RNAi sense strand with introduced restriction sites for generating *MtSer6*, *MtFer2* and *MtFer3* RNAi lines 170

Appendix 5. Multiple alignment of members of serpin and ferritin family 171

Appendix 6. Supplementary figures for chapter4 178

Appendix 7. Statement of contribution to doctoral thesis containing publications 194

List of Figures

Chapter 1

Fig. I. Schematic pathway of energy carbon source and bacteroid respiration in nodule under drought stress 5

Fig. II. Structural physiology of determinant and indeterminant nodules 11

Fig. III. Network of protein transformations under stress 14

Fig. IV. Generation of reactive hydroxyl radicals through the Fenton reaction 18

Fig. V. Possible role of senescence-induced regulation of iron homeostasis and protease - mediated programmed cell death (PCD) 19

Fig. VI. Schematic regulation of ferritin in *Arabidopsis* depending on iron availability 21

Chapter 2

Fig. 1. Growth kinetics of *E. meliloti* in YEM medium 50

Fig. 2. Growth and symbiotic attributes of *M. truncatula* 52

Fig. 3. Impact of SNF on plant growth 53

Fig. 4. Molecular phylogenetic analysis of the serpin and ferritin families 56

Fig. 5. Reverse transcriptase PCR of 7 serpin groups (S1-S7) and the ferritin group (F1) 57

Fig. 6. Reverse transcriptase PCR of 9 serpin genes and 3 ferritin genes 58

Fig. 7. Expression of serpin and ferritin genes in response to drought**.** 62

Fig. 8. Comparison of relative expression of serpin (a) and ferritin (b) genes in response to drought in the nodule 63

Fig. 9. Transcriptional changes of 5 serpin and 3 ferritin genes in nodule of *M. truncatula* under well-watered and drought conditions. 64

Chapter 4

Fig. 1. Symbiotic attributes of WT *M. truncatula* plants and non-N fixing mutants 71

Fig. 2. Impact of SNF on plant growth**.** 72

Fig. 3. Effect of external N fertilizer treatment on N uptake from SNF 74

Fig. 4. Effect of *E. meliloti* inoculation on ^{15}N uptake in shoots of external N fertilizer treated *M. truncatula.*..... 76

Fig. 5. Effect of external N fertilizer treatment and *E. meliloti* inoculation on total N level 78

Fig. 6. Effect of external N fertilizer treatment on nodule localization in roots of *M. truncatula* R108 81

Fig. 7. Effect of drought stress on uptake of ^{15}N in shoots of external N fertilizer treated *M. truncatula.*..... 83

Fig. 8. Effect of drought stress and external N fertilizer treatment on N uptake from SNF and total shoot N level 85

Fig. 9. Effect of drought stress on nodule morphology 87

Fig. 10. Effect of *E. meliloti* inoculation and N fertilization on plant growth under drought stress..... 90

Fig. 11. Transcriptional changes of genes involved in ROS and ethylene synthesis under drought stress. 93

Fig. 12. Transcriptional changes of genes involved in ABA biosynthesis and the post-ABA regulating pathway under drought stress 94

Chapter 5

Fig. 1. Drought-induced changes of leaf-water content in *M. truncatula*……..103

Fig. 2. Effect of drought on *M. truncatula* leaves……104

Fig. 3. Effect of drought stress on *M. truncatula* growth and nodule nitrogenase activity……106

Fig. 4. Change of *M. truncatula* nodule colour under drought stress……107

Fig. 5. Drought-induced changes in *M. truncatula* nodules……109

Fig. 6. Expression of 9 *serpin* and 3 *ferritin* genes in *M. truncatula* nodules……112

Fig. 7. Response of to drought stress of *serpin* and *ferritin* genes in the nodule of *M. truncatula*…..112

Fig. 8. Effect of RNAi KD on expression of targeted genes in *M. truncatula* nodules grown under drought stress……..114

Fig. 9. Effect of RNAi knockdown of *MtSer6, MtFer2* and *MtFer3* expression in *M. truncatula* nodules under drought……..115

Fig. 10. Effect of reduced *MtSer6, MtFer2* and *MtFer3* expression on nodules……118

Fig. 11. Ectopic effects of RNAi KD on *Mtser6*, *MtFer2* and *MtFer3* expression……120

Fig. 12. Impact of reduced *MtSer6, MtFer2* and *MtFer3* expression on nodule senescence of drought-stressed *M. truncatula*……121

Fig. 13. Effect of reduced *MtSer6, MtFer2* and *MtFer3* expression on *M. truncatula* nodule bacteroids at the senescence zone……122

Fig. 14. Effect of reduced *MtSer6*, *MtFer2* and *MtFer3* expression on *M. truncatula* nodule nitrogenase activity and plant growth 123

List of Tables

Chapter 2

Table 1. List of experiments with duration and sampling time points 30

Table 2. Experimental setup for N fertilizer treatments in chapter 4 32

Chapter 3

Table 1. Chromosome locus tags and NCBI accession numbers of 28 serpin genes from *M. truncatula* 54

Table 2. Chromosome locus tag and NCBI accession number of 3 ferritin genes from *M. truncatula* 55

Chapter 4

Table. 1. Effect of external N fertilizer treatment in nodule activity 80

Table 2. Effect of drought stress and N fertilization on nodule nitrogenase activity 88

Chapter 5

Table 1. Chromosome locus tag and accession number of 28 *serpin* and 3 *ferritin* genes retrieved from *Medicago* genome database (MGDB) 111

List of abbreviations

AA	Amino acid
ABA	Abscisic acid
Acds	1-amino cyclopropane carboxylate deaminase
ACO	1-Aminocyclopropane-1-Carboxylic Acid oxidase
ACS	1-Aminocyclopropane-1-Carboxylic Acid synthase
BNF	Biological nitrogen fixation
CFU	Colony forming unit
CP	Cysteine protease
DAD	Days after drought
DAT	Days after treatment
DPI	Days post inoculation
FC	Field capacity
GA	Gibberrilic acid
H_2O_2	Hydrogen peroxide
ICS	Iso citrate synthase
IDRS	Iron dependent regulatory sequences
KD	Knock down
LB	leghaemoglobin
mRNA	Messenger RNA
NCED	9- cis-epoxycarotenoid dioxygenase

NCR’s	Nodule cysteine rich peptides
NIF	Nitrogen fixation
OD	Optical density
P5CS3	Delta-1-pyrroline-5-carboxylate synthase
PAL	Phenylalanine ammonia lyase
PBS	Peribacteroid membrane
PCD	Programmed cell death
PCR	Polymerase chain reaction
PGPR	Plant growth promoting rhizobacteria
PI	Protease inhibitor
qRT-PCR	Quantitative realtime-PCR
RCL	Reactive centre loop
RD1	Responsive to dessication1
ROS	Reactive oxygen species
RT-PCR	Reverse transcriptase PCR
SA	Salicylic acid
SNF	Symbiotic nitrogen fixation
ZEP	Zeathanxin epoxidase
ZIP	Leucine zipper transcription factor

Chapter 1

Introduction

Currently, there are two important tasks that must be addressed in the field of agriculture. First, the risks that climate change imposes on plants must be reduced. Second, food security must be ensured. Crop and forage legumes in agriculture are two important food sources for highly nutritious food for both humans and livestock feed. In addition to these fundamental benefits, the majority of legumes are grown for sustainable agricultural production as it improves the soil fertility. In agriculture, legumes are also often used for crop rotation as this can also benefit non-legumes by increasing soil N fertility. However, in an intensive agriculture system synthetic N fertilizers are being widely used as the host plant ca uptake N at low carbon cost (Crews & Peoples, 2004; Fischer *et al*., 2010). Excessive use of these chemical fertilizers for crop yield causes extensive fertilizer runoff into waterways and causes adverse effects on the environment (Udvardi *et al*., 2015). Therefore, legume-based cropping systems are an example of a natural resource management practice which can reduce the use of synthetic fertilizers (Pislariu, 2012). These plants maintain soil nitrogen (N) fertility through symbiotic association with N_2-fixing soil bacteria called rhizobia (Pierre *et al*., 2014). This symbiotic interaction between rhizobia and legumes leads to the formation of facultative root organs called nodules where atmospheric N_2 is fixed and exported to other parts of the plant as a usable form (ammonia) (Gourion *et al*., 2015). In return, rhizobia are provided with energy carbon by the host plant for various cellular activities. The whole process of nitrogen fixation requires eight electrons and at least sixteen ATP molecules to fix one molecule of N_2 gas.

$$N_2+8H^++8e^- \longrightarrow 2NH_3+ H_2$$

The efficiency of this symbiosis may depend on rhizobial invasion into root cortices and their ability to colonize. Initially, a rhizobium enters the root cortex through a signal exchange which involves the interaction of rhizobial lipochitin oligosaccharide molecules called Nod factors and root flavonoids. This signal interaction leads to the formation of nodule primordia (Quintana *et al*., 2013; Maunoury *et al*., 2010). After invasion into infection threads, rhizobia undergo cellular differentiation, become surrounded by a plant membrane and form organelle-like symbiosomes. At this stage, rhizobia are known as bacteroids as they can start fixing N_2 (symbiotic nitrogen fixation). The symbiosome membrane encloses the bacteria into individual cortical cells and the bacteroids are surrounded by plant plasma membrane called periplasmic membrane (Lodwig *et al*., 2003).

1.1 Plant Immunity and rhizobial infection

In general, a plant defence response is elicited upon the initial stages of rhizobial infection and then will be suppressed at later stages. The plant immune response towards the rhizobial infection is well described for several legumes like *Glycine max* (L) Merr*, Medicago* and *Phaseolus* (Gourion *et al*., 2015). A transcriptomic study in soybean demonstrated that plant defence-related genes are induced strongly in roots after 12 hours of *Bradyrhizobium japonicum* infection, and the same genes are then suppressed after24 hours of infection (Libault *et al*., 2010). Similar results were found in *M. truncatula* where defence-related genes in roots were expressed 1 hour after inoculation with *S. meliloti* but then suppressed as early as 6 hours after inoculation (Lohar *et al*., 2006). This might be due to inactive bacterial MAMPs (microbe-associated molecular patterns) where plant immune responses rely on to recognize rhizobial infection (Gourion *et al*., 2015). It has been demonstrated that exopolysaccharides like the succinoglycan found in various rhizobia suppresses MTI (MAMP triggered immunity) by chelating the cellular signalling molecule calcium (Jones *et al*., 2008; Aslam *et al*., 2008). In addition, the bacterial type III or type IV secretion systems (T3SS/T4SS) found in many pathogenic bacteria, including the rhizobia, can also help to suppress MTI through releasing nodulation outer proteins (NOPs) (Deakin *et al*., 2009). Once this defence mechanism is established in roots upon the initial infection of rhizobia, plants use reactive oxygen species (ROS) through H_2O_2 production to subsequently recruit more rhizobia. Jamet et el. (2007) described a mutant strain of *Sinorhizobium meliloti* that is deficient in H_2O_2 production which caused inefficient infection and reduced nodule numbers in *M. truncatula* due to limited ROS production. This indicates that H_2O_2 and ROS production upon rhizobial infection is essential for optimal rhizobial invasions in roots.

There are two important hormones that have been identified in nodules that reduce rhizobial infection and nodule numbers. The plant defence hormone salicylic acid (SA) was shown to affect rhizobial infection and nodule numbers in both indeterminate nodule-forming *M. truncatula* and determinate nodule-forming *Lotus japonicus* (Stacey *et al*. 2006). For controlling SA levels in nodules, Nod factors (NFs) were identified as a key controlling factor. Martínez-Abarca *et al*. (1998) and Blilou *et al*. (1999) demonstrated that *Medicago sativa* and pea plants inoculated with incompatible (Nod genes absent) or Nod factor-deficient mutant strains of rhizobia resulted in an increased accumulation of SA in the roots. In the meantime, non-nodulating pea mutant *Pssym30* (defective in nod factor induction), inoculated with a compatible rhizobia strain increased the root SA content. This indicates that control of SA in the nodules is also dependent on the compatibility of the rhizobia which express NF's. NF's are produced by the bacteria to initiate nodulation and promote development. This has been shown by previous studies that NFs are not only expresses in the root cortex upon rhizobial infection, but the

genes also actively transcribe when the rhizobia enter the nitrogen fixation zone in order to maintain the nodule organogenesis (Sugawara *et al*., 2014; Liang *et al*., 2013; Roux *et al*., 2014).

Ethylene is another defence-related hormone produced in plants during natural aging and stress-induced early bacteroid senescence. However, an *acdS* gene (1-amino cyclopropane carboxylate deaminase) which catalyses the degradation of ACC (an ethylene precursor) into ammonium and α-ketobutyrate has been found in many rhizobia (Blaha *et al*., 2006). Through the activity of this enzyme, ACC deaminase-containing bacteria can reduce ethylene biosynthesis in plants and increase nodulation (Ma *et al.,* 2003). Nascimento *et al*. (2012) described that rhizobial strains expressing the ACC deaminase enzyme displayed an optimal symbiotic performance. This optimal performance is a consequence of lowering the ethylene levels that typically inhibit the nodulation process.

1.2 Nitrogen fixation under N availability

For optimisation of N uptake and assimilation, plants use complex molecular networks such as signalling molecules, transporters and sensors. Based on the availability of N in the soil rhizosphere, this network can be fine-tuned according to the plant's N demand. Plants have so-called PII signal transduction proteins that are involved in controlling N assimilation under low and high N availability. Under low N conditions, the intracellular concentration of glutamine, which is known as a key signal for nitrogen status, is reduced. Therefore, the uridylyl transferase or uridylyl-removing enzyme modifies the trimeric protein of PII and inhibits its interaction with target genes. As a result, phosphorylation is activated and the expression of nitrate transporter genes is induced. Under sufficient or high a nitrogen status, intracellular glutamine molecules cause de-uridylylation of the PII proteins thereby changing the PII receptor interaction (D'Apuzzo *et al*., 2015; Dixon & Kahn, 2004). N transporters (NRT's) are the major molecules involved in N sensing and acquisition (Xuan *et al*., 2017). Plants have at least 4 major NRT families with distinct functions. In rice, a high affinity transporter of nitrate, *OsNRT2*, is highly expressed in most types of root cells but it is weakly expressed in shoots. This transporter is induced by nitrate but repressed by ammonium (Feng *et al*., 2011). Members of the nitrate/peptide transporter family (NPF/NRT1) are low affinity transporters that are unresponsive to N supply but are highly expressed in root, shoot, leaf blade and sheath. In legumes, once the rhizobia are established in the nitrogen fixation zone after differentiation into nitrogen fixing bacteroids, nitrogenase activity starts to convert the atmospheric nitrogen to ammonia. This ammonia will later be converted into amino acids and loaded into the xylem. This symbiotic nitrogen fixation process is regulated systemically depending on a plant's N demand (Marino *et al*., 2007). Response of the nitrate transporters in nodulating legumes was studied recently and it was shown that primary

transporter genes are expressed in nodules when N is supplied (Straub *et al*., 2014). The increased expression of these transporter genes altered nodule activity by downregulating the 9 leghaemoglobin (lb) genes which are essential for buffering the concentration of oxygen in nodules to assist with rhizobial respiration. On the other hand, nitrogen-fixing bacterium are also known to be involved in controlling nitrogen fixation through NIF (nitrogen fixing genes) gene regulation. In many bacteria including rhizobium, *nifA* is involved as a positive regulator of N fixation and uptake. However, under high N status, a bacteroid encounters an increase in intracellular glutamine concentration and thus activates the *nifL* gene (a negative fixation regulatory gene). It has been shown in soybean by several studies that high N availability can reduce nitrogenase activity, nodule numbers, nodule density and biomass as a result of the action of the rhizobial *nifL* gene (Harper & Gibson 1984; Streeter, 1985; Streeter, 1988; Walch-Liu *et al*., 2006). Goh *et al*. (2016) suggested that rhizobia can induce root architectural changes to control the N uptake from soil and internal N levels.

1.3 Nitrogen fixation under drought

Among the various categories of environmental stresses, drought is a major abiotic stress which affects symbiotic nitrogen fixation (SNF) by inhibiting the nitrogenase complex. Drought stress induces structural changes to the oxygen diffusion barrier, which lowers the symbiosome O_2 concentration and consequently bacteroid respiration. In most legumes, Ureides are the exported N compounds and drought-induced reduction of ureides catabolic compounds such as allantoate, allantoin results in accumulation of ureids in the nodule (King & Purcell, 2005). It has been demonstrated that reduction of nitrogenase activity is a result of the accumulation of ureides which decrease nodule permeability to oxygen (pO_2) (Serraj *et al*., 1999). The sensitivity of N_2 fixation to drought among legume species results in the export of ureides from the nodule. Nodules in species like soybean and cowpea have the highest levels of ureide export under drought. This indicates that increased accumulation of ureides in plant xylem sap would enhance sensitivity to drought. Such accumulation can affect nitrogenase activity through N feedback regulation. By contrast, it has also been shown that legumes with low accumulation of ureides were discovered to be relatively drought tolerant (Serraj, 2003). For bacteroid respiration and activity, considerable nodule carbon influx is required and the plant provides carbon in the form of photosynthates. Sucrose is the major carbon source that bacteroids require to fuel the fixation of N (Fig. I). Once sucrose is transported into the nodule cortex, it is being cleaved to fructose and UDP-glucose by the enzyme sucrose synthase to feed bacteroids with carbohydrates (Gordon *et al*., 1997). It has been shown in many legume nodule function studies that drought stress may cause a reduction in sucrose synthase activity, which results in a reduction of carbohydrate availability and

subsequent inhibition of nitrogenase activity (Gonzalez *et al*., 1995; Gordon *et al*., 1997; Galvez *et al*., 2005; Arrese-Igor *et al*., 1999).

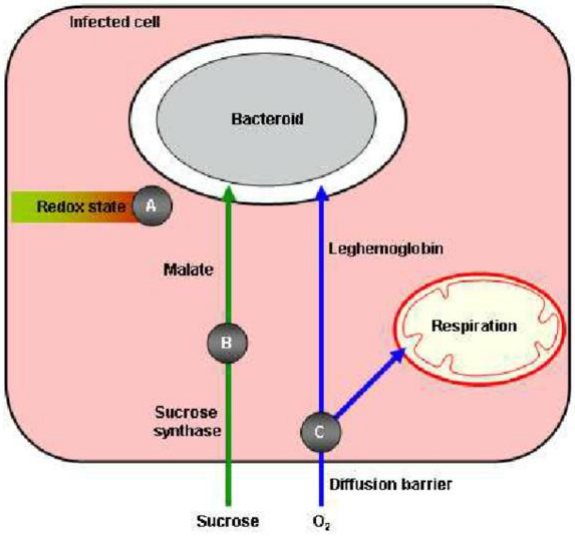

Fig. I. Schematic pathway of energy carbon source and bacteroid respiration in nodule under drought stress. A, modification of the redox balance; B, alteration of the bacteroid nutrition; C, alteration of O_2 homeostasis (Figure copied from Dupont *et al.,* 2012).

However, different observations were noted in chickpea by Esfahani *et al*. (2014). The rapid decrease of nitrogenase activity immediately after water withholding affected neither sucrose synthase, a synthesiser of sucrose to provide carbon, nor malate dehydrogenase, a provider of malate for bacteriods. This suggests that nitrogenase activity does not correlate with sucrose content, sucrose synthase or malate dehydrogenase levels but instead bacteroid respiration. This result in chickpea was found to be similar in *M. truncatula* and *M. sativa* but not in *Phaseolus vulagaris, Pisum sativum* or *G. max.* Drought stress can also affect bacteroid protein levels and the bacteroid metabolism that attributes the symbiotic nitrogen fixation in *M. truncatula* though oxidative damage as described by Larrainzar *et al*. (2009). Reduction of CO_2 metabolism, and malate and succinate upon early drought stress would also cause a decline in respiratory capacity of bacteroids (Talbi *et al*., 2012). Effect of this early drought was also resulted in the increased accumulation of amino acids and organic acids in chickpea. There are two reasons behind this increase in accumulation. First, the accumulation of amino acids through a nitrogen feedback mechanism increases the transport of amino acids from phloem to nodules (Esfahani *et al*., 2014). Second, organic acids, such as malate and succinate, shutdown malate and succinate dehydrogenase activities. This N feedback mechanism is most common in the legumes through which nitrogen fixation is affected under drought stress. By contrast, Gil-Quintana *et al*. (2013) recently reported that local amino acid accumulation may occur prior to any

measurable decline in nitrogen fixation rates, thus the role of N feedback mechanisms are downplayed.

1.4 Effect of drought on symbiosis and the growth of SNF-dependent plants

Under drought stress, plants perform various functions primarily to keep hydration levels under control and maximize their survival. A plant's dependence on water is an important factor in maintaining plant growth, metabolic activities and photosynthesis. This includes leaf water potential, transpiration and stomatal conductance (Mansfield & Davies, 1981; Brodribb & Holbrook, 2003; Lawlor & Tezara, 2009). This scenario is common for most plants. Stomatal conductance, which controls the photosynthesis and transpiration of plants, is a major factor affecting plant adaptation to drought. Regulation of stomatal opening and the restriction of leaf expansion and growth of young leaves are among key plant strategies for improved drought adaptation (Lawlor & Cornic, 2002). The secondary responses of a plant to drought stress are the metabolic changes and reprogramming of the expression of various genes (Ozturk *et al*., 2002; Zhu, 2002; Oono *et al*., 2003; Benjamin & Nielsen 2006). Drought causes the decline in CO_2 assimilation, affects photochemical and biochemical reactions and decreases plant biomass and seed yield (Chaves *et al*., 2002). Ramos *et al*. (1999) reported that drought can decrease nitrogen fixation up to 70-80% and plant biomass up to 35-45%. N is an essential component of proteins, including the enzyme ribulose-bisphosphate-carboxylase-oxygenase (RuBisCo), an enzyme which catalyzes the incorporation of CO_2 into an organic molecule. Drought stress would cause the reduction of photosynthesis by various factors like chlorophyll degradation, the decline of RuBisco activity and protein degradation. These outcomes would suggest that the reduction of nitrogen fixation in SNF-dependent legumes would negatively affect chlorophyll content and RuBisco activity by limiting the N supply. This hypothesis has been proved in *M. truncatula* when a reduction of nitrogenase activity resulted in a reduced photosynthesis rate and plant growth after 6 days of water withholding (Baena-Gonzalez *et al*., 2007).

Drought is a major limiting stress factor for legume growth and yield and it has become the most important threat to soybean (Daryanto *et al*., 2015; Kunert *et al*., 2016), chickpea (Yadav *et al*. 2006; Toker *et al*. 2006), bean plant (Barrios *et al*.,2005) and lentil (Alami-Milani *et al*.,2013) cultivation and yields worldwide. Hence, it is important to select and breed drought tolerant cultivars to minimize future impacts of drought. It has been shown that drought affects the yield of major legume crops such as chickpea (Ha *et al*., 2014), soybean (Quintana *et al*., 2013) and mungbean (Ranawake *et al*., 2011), and also causes biomass reduction in forage legumes such as white clover (Luscher *et al*., 2014) and alfalfa (Moghaddam *et al*., 2015) due to decline of N_2 fixation. Researchers have made an effort to develop suitable cultivars for increasing the growth and yield of major food legumes such as

soybean (Ku *et al*., 2013), chickpea (Talebi *et al*., 2013), peas and beans (Grzesiak *et al*., 1997). As drought stress severely affects the N fixation process by degrading bacteroid proteins and minimizing nitrogenase activity, it is important for SNF-dependent plants to regulate the N fixation and nodule senescence processes. Moghaddam *et al*. (2015) reported that stabilized biological N fixation under drought increased the total biomass and shoot dry matter in *M. sativa.* This finding was further confirmed by Sulieman *et al*. (2015) who reported that a drought tolerant cultivar, DT2008, which could produce higher nodule numbers, showed a 67% increase in shoot dry weight and a 42% increase of root dry weight as compared to another drought tolerant cultivar, W82, which had lower nodule numbers. This evidence clearly suggests that the biological significance of SNF on plant growth in a water-scarce environment can be achieved by developing suitable rhizobium-legume partners. However, there is still a lack of clarity about the correlation between SNF and plant growth adaptation to drought stress.

A recent study has shown that although drought affects plant growth, a plant may still use complex molecular networks to overcome the drought stress and damage. Such complex molecular networks, including ABA, ethylene and metabolic regulatory networks, are primary tools that plants activates upon drought conditions (Luo *et al*., 2016). A transcriptomic study by Van de Velde (2006) suggested that nodules express some stress related genes, such as APETALA/ETHYLENE RESPONSE FACTOR (*AP2*/*ERF*), the DEAD-box RNA helicase gene and other key genes, for jasmonic acid production (JA) during the initiation of different developmental stages of nodules. However, there is no clear evidence about role or involvement of SNF in plant drought tolerance. Thus, understanding the role and involvement of SNF in legume crop productivity in water-scarce environments would enable breeders to develop more drought tolerant cultivars.

In addition to the effect of drought on plant growth and survival, drought stress also affects the population of rhizobia in soil under water deficit condition (Barthelemy-Delaux *et al*., 2014). Low soil-moisture conditions affect rhizobial movement towards plant root hairs (Yanni *et al.,* 2016). It has been shown by some studies that the drought effect on rhizobia depends on the bacteria's ability to tolerate drought. Multiple attempts have been made to isolate drought-tolerant rhizobia to minimize the negative effects of drought on the symbiosis (Mohammad *et al.,* 1991; Rehman & Nautiyal, 2002; Naveed *et al.,* 2017). While a suitable rhizosphere environment is essential for a successful legume-*Rhizobium* interaction, the rate of symbiosis inhibition may depend on the severity of the stress and the plant growth and developmental phase. For example, it was shown in soybean that mild drought stress reduced only the number of root nodules, while moderate and severe stress reduced both the number and size of the nodules (Zahran, 1999).

1.5 Biological nitrogen fixation for plant growth

SNF is a plant-associated nitrogen fixation process, which is being carried out in legumes by rhizobium. In addition, free-living bacteria can also fix N by living in the plant root rhizosphere region. Examples of such bacteria are *Azospirillum, Azotobacter* and *Bacillus* (Steenhoudt & Vanderleyden, 2000; Kizilkaya, 2009). These two processes together are called biological N_2 fixation (BNF). Some field experiments proved that BNF can provide 50-70 Tg of N annually in agriculture systems (Herridge *et al*. 2008). Through BNF, some grass species were reported to achieve sufficient N for maintaining plant growth (Boddey & Victoria. 1986; Morais *et al*., 2012). Recently Pankievicz *et al*. (2015) showed that N acquisition of plants via BNF can support more robust plant growth than control plants that were inoculated with a non-nitrogen fixing bacteria Their study was focused on the contribution of BNF to the growth promotion of *Setaria viridis*, a model C4 grass which forms an associative interaction with N-fixing *Azospirillum brasilense*. Plants inoculated with N-fixing *A. brasilense* under N-limited conditions showed a 24% shoot dry weight, a 28% root length and a 38% lateral root number increase higher than the control plant inoculated with a non-N fixing bacteria Moreover, inoculated plants produced a higher seed yield. Fixed N was found to be used by plants for RuBisco synthesis and photosynthesis. It was also shown that an increase in CO_2 fixation correlates with increased BNF in inoculated plants. This study strongly emphasized that under an N-limited soil environment, efficient BNF would certainly enhance N assimilation and support plant growth through CO_2 fixation, sugar accumulation and photosynthesis. N is essential for RuBisco, chlorophyll and nucleic acid synthesis (Karim *et al*., 2016). Hence, crop management which can enhance SNF is proposed as a natural resource management practice which can avoid the need of N fertilizer. Esfahani *et al*. (2014) reported that *Mesorhizobium cicer*-inoculated chickpea, which had higher nodule numbers and nitrogen fixation rates, also showed a significant increase of shoot and root dry weight, N fixing gene expression (*nifH*, *nifD* and *nifK*), malate content and soluble proteins as compared to less nodulated plants. Moreover, the selection of suitable nodulating rhizobia as well as the development of a microbial consortium for the host plant which would involve co-inoculating plants with plant growth rhizobacteria (PGPR) such as *Bacillus subtilis, Paenibacillus polymyxa, Azospirillum brasilense* and *Azotobacter vinelandii*, would provide the plant with multiple mechanisms to support plant growth. The availability of metabolites for plant growth and development would also be achieved with this two-pronged strategy (Larrainzar *et al*., 2009; Annapurna *et al., 2013*). These studies suggest that enhancing the nodulation and N fixation efficiency in legumes may help for sustainable plant growth production under changing climatic conditions.

1.6 Rhizobia for stress amelioration

Rhizobia that protect a host plant from environmental stresses are called PGPR. Rhizobia can produce antioxidants, osmolytes, and stress proteins for plant growth promotion. It has been reported that some rhizobia can survive under drought stress up to −1.5 and −3.5 MPa soil water potential (Elboutahiri *et al*. 2010; Abolhasani *et al*., 2010). Many studies reports that rhizobia can protect legume and non-legume plants and promote their growth under environmental stresses by producing compounds such as, sugars, the stress enzyme ACC deaminase, exopolysaccharides (EPS), low molecular weight organic compounds (trehalose), phosphate solubilisation, siderophores and phytohormones. *Ensifer meliloti* was found to induce metabolic activities such as proline synthesis for stress adaptation in *Cicer arietinum* and *M. sativa* (Mhadhbi *et al*. 2011; López-Gómez *et al*., 2014). Using a microbial ecological perspectives, selection and inoculation of potential PGPR's for stress amelioration has become a strategic approach in sustainable agricultural production (Tilak, 2005; Souza *et al.,* 2015).

1.7 Nodule physiology of *M. truncatula*

Based on the mode of growth and development, nodules are classified as indeterminate or determinate (Fig. II). Determinate nodules are spherical in shape and are initiated from the meristematic cells in the outer root cortex. Cell division is not sustained after 10-12 days after the rhizobial infection. There is a radial gradient of development (development zone) where senescence begins and develops towards the infection zone. Examples of legume genera with this type of nodule development are *Glycine* (soybean), *Phaseolus* (common bean), and *Vigna* (mung bean). Indeterminate nodules have an active apical meristem that produces new cells for growth over the life of the nodule. They are elongated due to the addition of new cells at the end of the nodule and distal from the meristem. Hence, these nodules have a cylindrical shape with five distinct zones (Fig. II). Zone I, made up of meristematic cells where no microsymbionts persist; zone II, known as the infection zone, where rhizobial infection occurs; zone III, a nitrogen fixation zone where bacteria are housed in the symbiosome and actively fix atmospheric N; zone IV, a senescence zone which appears only after the nodule starts developing and can be seen clearly as the plant ages; and finally zone V which is very close to the root and contains free-living bacteria and do not show any structural features of the symbiosome. Examples of genera with indeterminate nodules are *Pisum* (pea), *Medicago sativa* (alfalfa), *M. truncatula* (barrel medic), *Trifolium* (clover), and *Vicia* (vetch). In indeterminate nodules, senescence-associated signals are transferred from the root and endodermis and senescence begins from zone IV (Muller *et al*., 2001; Timmers *et al*., 2000; Mao *et al*., 2013).

Rhizobia in the root cortex can adapt to the endosymbiotic life cycle of plant cells and start gaining usable N from the environment. In certain legume-rhizobial symbioses, bacteroids become non-cultivable polyploids and undergo cellular differentiation rather than multiplication (Kondorosi *et al*., 2013; Mergaert *et al*., 2006). Similar results were reported in the symbiosis between the legume *M. truncatula* and the bacterium *S. meliloti* where bacteroid differentiation was provoked by nodule cysteine rich peptides (NCR) which are specifically expressed in rhizobium-infected symbiotic cells (Farkas *et al*., 2014; Van de Velde *et al*., 2010). In *M. truncatula*, more than 500 nodule-specific cysteine rich coding peptides have been identified as participating in the symbiotic interaction (Durgo *et al.,* 2015). Among them, NCR247 is known to arrest bacterial cell division and promote cell elongation. Farkas *et al*. (2014) noted that *S. meliloti*-inoculated *M. truncatula*, which has a functional NCR247, produced elongated pink N-fixing nodules like wild-type strains. Rhizobia usually multiply in the non-dividing youngest cells below the meristem (non-N_2 fixing rhizobial cells) and only differentiate in the nitrogen fixation zone to become N_2 fixing bacteroids. Therefore, this suggests that bacteroid differentiation could help to increase N-fixing activity rather than only multiplication. However, drought stress may induce a wide range of protease activities which cause the degradation of functional bacteroid proteins and a consequent reduction nitrogenase activity (Pierre *et al*., 2014; Pladys & Vance, 1993). Moreover, drought stress may also induce ROS levels which in turn affect the N fixation by causing oxidative damage to bacteroids (Clement *et al*., 2008). A visual diagnosis of senescence can be made by observing nodule colour changes (pink to green or brown), which indicates the degradation of haemoglobins (Roponen, 1970), and when the senescence is more advanced, symbiosome membrane disintegration (Timmers *et al*., 2000). Benefits of N fixation during pod filling has been shown in many legumes to help improve seed protein levels and is suggested by several researchers that extending the nodule activity and delaying the senescence could play an essential role in increasing the crop productivity and yield (Merbach & Schilling, 1980; Bethlenfalvay & Phillips, 1977; Van de Velde *et al*., 2006).

Fig. II. Structural physiology of determinant (a) and indeterminant nodules (b) (Figure copied from Puppo *et al*., 2005)

1.8 Nodule senescence: stress-induced natural aging and the factors involved

Decline of lb content and the subsequent reduction of nitrogenase activity in the nodule is called nodule senescence (Pfeiffer *et al*., 1983). Nodule senescence includes symptoms such as loss of turgidity and colour changes in the fixation zone from pink to brown. *M. truncatula* is a model legume plant for nodule-rhizobium symbiosis studies. The plant can efficiently interact with *E. meliloti* and fix nitrogen from the atmosphere in quantities that have economic significance in the cultivation of forage or pasture legumes as well as environmental value in non-managed ecosystems (Gubry-Rangin *et al*., 2013). It has been shown that *M. truncatula* nodule senescence starts between approximately 65 to 85 days after sowing (Mhadhbi *et al.,* 2011). For many leguminous crops, nodule senescence coincides with pod filling (Lawn & Brun, 1974; Bethlenfalvay & Phillips, 1977). However, age-related molecular changes might occur before the visible nodule senescence is observed. These changes include the induction of proteolytic activity and degradation of nodule proteins (Guerra *et al*., 2010).

As discussed above, N fixation can only be efficient under low N availability in the soil. If the plants are supplied with nitrite or ammonium fertilizers, they don't undergo rapid and efficient nodulation. Hence the soil should have a low N status before inoculating crops with rhizobia. Under low N availability, signals for nodule initiation are induced upon rhizobial inoculation. It has been shown that if plants are supplied (especially at pod filling) with adequate amounts of N through SNF, additional

nodule initiation does not occur while active nodules cease N fixation and begin to senesce (Puppo *et al*., 2005). However, it has also been reported that nodules may still fix N_2 to a limited extent during seed maturation which results in an increase in seed protein content (Merbach & Schilling. 1980). The major consequence of nodule senescence is a wide range of uncontrolled proteolytically-mediated degradation reactions affecting larger-sized proteins such as N fixation proteins (*nif*) and symbiosome membrane proteins (Pladys & Vance. 1993; Berrabah *et al*., 2014). Besides lb degradation, N_2 feedback regulation and the liberation of free iron (Fe^{2+}) would also cause rapid senescence and programmed cell death (PCD) in bacteroids by increasing ROS levels (Lampl *et al*., 2013).

1.9 Response and function of protease activity in various plant growth activities during natural and stress-induced nodule aging

During the natural nodule aging process, large scale protein remobilization occurs through aproteolytic process. Among other proteases, cysteine, serine and aspartic proteases are involved predominantly in the removal of misfolded or degraded proteins in the nodule and remobilization of nutrients (Malik *et al*., 1981; Drake *et al*., 1996; Cercos *et al*., 1999; Puppo *et al*., 2005). After protein degradation, the released amino acids can be used for *de novo* protein synthesis (Fig. III). It has been previously reported (Groten *et al.,* 2006) that there are two major proteases involved in nodule senescence: i) cysteine proteases and ii) serine proteases (Trypsin-like/Subtilisin-like). Wyk *et al*. (2014) reported that 14 weeks after the rhizobial inoculation of soybean, almost 80% of the cysteine protease gene family exhibited greatly enhanced expression compared to the expression levels in the early stages of nodule development. A possible consequence of proteolysis associated with nodule senescence is enhanced plant survival through nutrient remobilization. However, uncontrolled proteolytic activity is deleterious for nodules and plants as it may prematurely affect the N fixation and nodulation process by degrading key N fixing enzymes and co-factors. This scenario of early nodule senescence in *M. truncatula* being linked to overexpression of papain and legumain-like proteases was demonstrated by Pierre *et al.*, (2014). The identified genes which code papain and legumain proteases are *MtCP6* (cysteine protease) and *MtVPE* (vacuolar processing enzyme) respectively (Pierre *et al.,* 2014). Through transcript profiling analysis in *M. truncatula,* these two genes were also found to be rapidly induced at the onset of developmental nodule senescence. *MtVPE* was shown to be also induced during the early stages of nodule development. Toluidine blue stained *M. truncatula* nodules where cysteine protease and papain protease genes were knocked down exhibited a small senescence zone and elongated nitrogen fixation zone. Similar results were observed in the transcriptomic analysis of soybean nodule developmental stages where the *MtVPE* genes (of

which there are 6) were found to be highly expressed in 14-week-old senescing nodules but were not expressed in the early stages of senescence (Wyk *et al*., 2014). In an experiment with *M. truncatula* papain and legumain protease knock-out lines, only small senescence zones and elongated nitrogen fixation zones were observed. As a result, longer nodule lengths and a higher nitrogenase activity were observed in *M. truncatula* (Pierre *et al.,* 2014). This study indicates that these proteases are involved in controlling nodule senescence. The involvement of these two proteases in inducing nodule senescence was further demonstrated in *M. truncatula* where overexpression of *MtVPE* and *MtCP6* genes in zone III (Mergaert *et al*., 2003) resulted in an elongated senescence zone and caused early nodule senescence. As a result, the cumulative N fixation was reduced and nodule lengths were shortener in the overexpression lines (Fricker & Meyer, 2001; Li *et al*., 2008). The symbiosome is known as a form of a lytic compartment because of the presence of nuclease, vacuole phosphatase and protease activities in the peribacteroid membrane (PBS). Pierre *et al*. (2013) reported that PBS is acidic at the interface of the N_2-fixing and senescence zones where the optimum environment is provided for papain and legumain protease activity. Because of the direct delivery of proteases into the PBS, symbiosome degradation begins immediately and leads to the disruption of the symbiotic interaction between *M. truncatula* and *S. meliloti*.

The negative effects of uncontrolled proteolytic activity were also previously reported in *Astragalus sinicus* where a nodule-specific cysteine protease, *AsNOD 32,* was silenced in an *RNAi* background. As a result, a shortened senescence zone was observed in nodules 45 and 60 days post inoculation. The *RNAi AsNOD 32* plants showed a visible phenotypic difference including greener, healthier leaves than control plants. Interestingly, *in situ* microscopic analysis proved that greater bacteroid nucleoid fragmentation was detected in the symbiosome of wild type (WT) plant nodules as compared to the *RNAi* plants. This is due to the cysteine protease activity (Li *et al*., 2008). In addition to cysteine proteases, serine proteases (SP) are also one of the largest groups of proteolytic enzymes which possesses a serine residue at their active site. It has been reported that trypsin and subtilisin-like serine proteases are strongly expressed during the early stages of nodule development in *Lotus japonicus* (Takeda *et al*., 2012; Kusumawati *et al*., 2013).

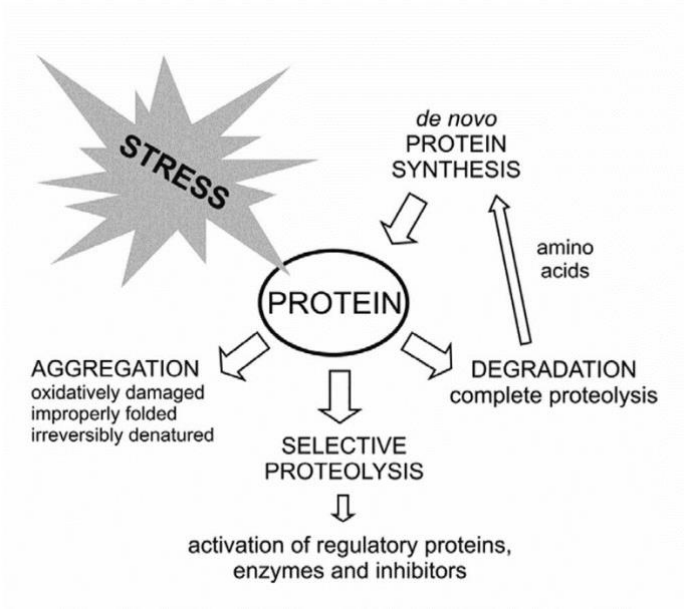

Fig. III. **Network of protein transformations under stress.** Stress causes proteolytic degradation which leads to greater amino acid release which is followed by *de novo* protein synthesis. Proteins can also be aggregated either by misfolding or denaturation under stress conditions (Copied from Kidric *et al*., 2014).

Djordjevic *et al*., (2011) reported that CLE (CLAVATA3/ESR-related) peptides are specifically cleaved by serine proteases and an active form of CLE peptide is liberated in the nodules of most legume species. In soybean, overexpression of CLV3/ESR-related (CLE) pre-propeptide encoding genes, *GmNIC1* (nitrate-induced and acting locally) and *GmRIC1* (*Bradyrhizobium*-induced and acting systemically), suppresses soybean nodulation (Reid *et al*., 2013). *M. truncatula* knock-down lines of CLE genes also were found to result in an increase in nodule numbers as compared to the control plants (Mortier *et al*., 2012).

1.10 Protease inhibitors as a proteolytic controlling mechanism in senescence

Protease inhibitors are small proteins which prevents protease activity by binding with the active site of a protease. There are two types of inhibition by which protease inhibitors inhibit enzyme activities: i) competitive inhibition where an inhibitor binds to the active site and prevents the enzyme-substrate interaction ii) non-competitive inhibition where the inhibitor binds to an allosteric site altering the active site making it inaccessible to the substrate. Protease inhibitors (PI's) undergo complex interactions with proteases thereby inhibiting the proteolytic activity. PIs also serve as storage proteins in plant storage organs. These PIs are divided into 4 major classes: cysteine (cystatins), serine (serpins and trypsin), and aspartic and metalloprotease inhibitors. Of these, the most abundant are

serine and cysteine inhibitors in the leaves, roots and nodules of most plants. As discussed above, uncontrolled proteolysis occurs as the plants age or are subjected to stress. Concurrently to proteolytic activity, protease inhibitors were also found to be expressed in most plant organs and play an endogenous response to environmental stresses and pathogenic attack (Huang *et al*., 2001). Sharma *et al*. (2015) demonstrated the differential expression of protease inhibitors in 5 different plant tissues of *C. arietinum*. This study reported that among all protease inhibitors, those predominantly expressed in most of the vegetative organs and aerial parts of the plant were the serine (Kunitz PIs and serpins) and cysteine PIs.

It has been reported that Kunitz PIs are expressed to protect plants from oxidative damage under salinity, alkalinity, heat and drought stresses (Gosti *et al*., 1995; Kang *et al*., 2002). Another serine PI, trypsin PI, was suggested to be a factor in multiple stress tolerances in tobacco. Srinivasan *et al*. (2009) reported that transgenic tobacco carrying an *NtPI* (trypsin PI) gene conferred tolerance to NaCl, alkalinity, drought and insect pest stresses by controlling the elevation of proteolytic activity in leaves. These transgenic plants showed enhanced seed germination, chlorophyll content, root-shoot ratio and root length when compared to the control plants. This indicates that protease inhibitors are essential players in controlling proteolytic mediated cell death and senescence.

1.11 Attributes of plant serpins

Serine protease inhibitors are ubiquitous in plants and have a rigid bait loop that can form covalent and irreversible complexes with proteases. The mode of action of serpins is the inactivation of endoproteases whose mechanism depends on the formation of acyl enzyme intermediates such as cysteine and serine proteases. The mechanism by which serpins inactivate the target proteases is comprised of 3 steps: i) the protease recognizes the reactive centre loop (RCL) at the serpin and forms an irreversible Michalis complex;, ii) the protease cleaves in the reactive centre at the peptide bond of P1 and P1' residues forming an acyl intermediate between the active site Ser/Cys of the protease and the carbonyl carbon of P1; and iii) the RCL inserts a new antiparallel stand into β sheet A, rotating the protease ~70 A^{o} to the bottom of the serpin. These three steps cause a deformity in the active site of the protease, thus resulting in a decrease in the rate of the hydrolysis of the acyl-enzyme intermediate (Huntington *et al*., 2000; Fluhr *et al*., 2012).

1.12 Interaction of serpins with proteases and the involvement in programmed cell death and homeostasis

Atserpin1 was shown to interact with and inactivate the papain-like proteases responsive to desiccation (*RD1*) and Atmetacaspases (*AtMC9*). Vercammen *et al*. (2006) reported that a suicide inhibitor of *AtMC9,* which regulates the programmed cell death (PCD), might have been controlled by the interaction of *Atserpin1*. Another important interaction of *Atserpin1* with the papain-like protease RD1 was shown to control PCD in *Arabidopsis* leaves. Plant vacuoles are at the centre of the PCD process and where *RD1* localization was identified in *Arabidopsis*. Detached leaves from a line of wild type *Arabidopsis* containing overexpressed *Atserpin1HA* (hemagglutinin epitope-tagged) and leaves from mutant lines were inoculated individually with *Sclerotinia sclerotiorum* (a plant pathogen) and *Botrytis cinerea* (a common necrotroph). The decay spot diameter and ROS levels of all leaves was observed. Interestingly, the overexpressed *Atserpin1* and mutant *RD1* lines showed much smaller decay diameters than the wild type and *atserpin1* (lack in *serpin1* expression) mutant lines. Similarly, the rapid decline of ROS levels was noted in lines with overexpressed *Atserpin1* and mutant *RD1* genes than the wild type and *Atserpin1* mutant lines. This study confirms that inhibition of papain-like *RD1* proteases controls PCD through interaction with *AtSerpin1* (Vercammen *et al*., 2006).

1.13 Expression and localization of serpins in plants

Initial studies of serpins and their expression were carried out in vegetative and grain tissues of barley by Roberts *et al*. (2003). They observed the expression of the Serpins BSZx, BSZ4 and BSZ7 in the meristems and vascular tissues of roots and embryonic leaves *Arabidopsis thaliana Atserpin1* was extensively studied for its expression and localization in the endoplasmic reticulum (ER), cytoplasm and vacuoles. These results were further corroborated by subcellular fractionation which showed an increased endogenous serpin content in the cytoplasm of overexpressed *Atserpin1* cells as compared to the wild type. Serpin expression was found in all organs, particularly in the lateral root, root elongation zone and root hair zone except in the pollen. Some *Arabidopsis* serpins, such as *At2g26390* and *At1g47710*, were found to be significantly upregulated under salt and cold stress (Zimmerman *et al*., 2004; Lampl *et al*., 2010). In *M. truncatula*, 28 serpin genes were identified through whole genome sequencing. Based on the number of hits and expression index of recent microarray data (the *M. truncatula* gene expression atlas) produced by the Nobel foundation (http://mtgea.noble.org/v3/search_result.php?s=201501), 8 out of 28 genes in the nodules and 24 out of 28 genes in the roots of *M. truncatula* are identified as highly expressed at 28 dpi (Unpublished

data). However, expression of serpins in the nodules of legumes at later growth stages and under drought stress are not well-studied.

1.14 Role of lb in nodules and their stability during natural and stress-induced aging

Lb are N and oxygen carriers and are exclusively expressed in symbiotic legume root nodules. Lb are considered to be an essential component in symbiotic nodules for buffering the free oxygen flux during nitrogen fixation. Symbiotic Lb can scavenge O_2 and facilitate its diffusion to the N_2-fixing microbial symbionts in nodules. Specifically, Lb are synthesized at a 2–3 mM concentration and function to maintain an O_2 free environment (20–40 nM concentration) in the cytosol of nodule cells (Appleby *et al*., 1980; Becana & Klucas, 1992). Ott *et al*. (2005) reported that Lb are only essential for nitrogen fixation and not for plant growth and development. The researchers developed Lb*RNAi* lines of *Lotus japonicus* and studied the phenotypic changes and nitrogen fixing activity. The Lb*RNAi* lines have white coloured non-nitrogen-fixing nodules and exhibit highly reduced growth compared with control plants. Predictably, all the lines grown with N fertilizer were unaffected and showed similar growth and development to that observed in the controls. It was also shown that Lb are crucial for ATP/ADP production in the form of bacteroid nitrogenase and that they enhance the energy metabolism of nodules by increasing the amount of oxygen for respiration (Ott *et al*., 2005). The degradation of Lbs which occurs during nodule aging or drought-induced early aging would negatively affect the nodule function by increasing ROS accumulation through the Fenton reaction. Degradation of Lbs could potentially liberate large amounts of free iron which could then react with H_2O_2 and increase ROS levels in the cytosol (Becana *et al*., 1998). Under this scenario, the positive role of Lb in nitrogen fixation during healthy nodule development may reverse to a negative impact due to the Lb action of increasing ROS accumulation and oxidative damage under drought stress.

1.15 Attributes of nodule iron and its toxicity

Iron plays a significant role in SNF by acting as a co-factor of the nitrogenase enzyme (Brear *et al*., 2013). This is one of the catalytic molecules of iron-sulfur clusters and heme- containing proteins. Plants generally obtain Fe from the rhizosphere and reduce Fe^{3+} to Fe^{2+} through Fe(III) chelate reductase. The intracellular iron concentration should be maintained at levels adequate for cellular metabolism, photosynthesis, respiration and nucleic acid synthesis. An excess of free iron is potentially detrimental to cells because of its tendency to react with oxygen to produce harmful free hydroxyl radicals through the Fenton reaction (Fig. IV). Under drought stress, more free Fe ions are liberated in

the nodule from heme- containing proteins like Lbs. As discussed above, this Fe ions can react with H_2O_2 and increase the ROS accumulation and subsequent nodule senescence (Briat & Lobreaux. 1997; Ravet *et al*., 2009). On the other hand, iron homeostasis in plants is achieved by the actions of transport and storage mechanisms. The transport of iron is mediated by iron transporters in the nodule. Rodriguez-Haas *et al*. (2013) reported that transported iron was released into the apoplast of the infection zone (Fig. II) from the vasculature. The final delivery of this iron into the symbiosome is carried out by infected cells in order to synthesize ferroproteins. Plants can recover some of this iron during the senescence stage for flowering and seed maturation.

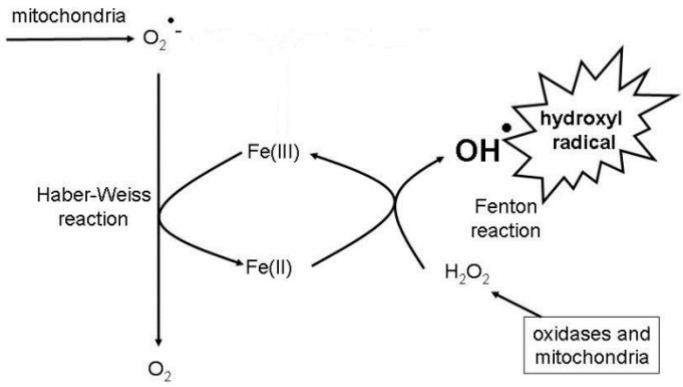

Fig. IV. Generation of reactive hydroxyl radicals through the Fenton reaction. Liberated free iron reacts with H_2O_2 and produces highly reactive hydroxyl radicals (Figure copied from Prousek, 2007).

1.16 Reactive oxygen species (ROS) in natural aging and stress-induced senescence

ROS is a by-product from the metabolism of oxygen-peroxidases which are involved in cell signalling and the oxidative process. Superoxide anions and H_2O_2 are generated through photosynthesis and respiration in plants. Drought stress can cause enormously elevated levels of these superoxide anions and H_2O_2, and thereby cause oxidative damage in the plant organs. ROS in plants also play a positive role by acting as secondary messengers for the synthesis of plant hormones such as auxin, abscisic acid (ABA) and ethylene (Noctor *et al*., 2002; Pei *et al*., 2000; Moeder *et al*., 2002). A certain amount of ROS accumulation helps powerful cell signalling cascades underpinning the development of embryonic axes, lateral root formation, leaf expansion and coleoptile growth (Joo *et al*., 2001; Foreman *et al*., 2003). Foreman *et al*. (2003) proposed that root hairs are the first site for rhizobial infection and ROS regulate root hair growth through the activation of calcium channels. Abscisic acid (ABA) is synthesized more in root and leaf tissues when nodulating plants are under stress. In a reduced water potential state, ABA is translocated to the leaves where it rapidly alters stomatal guard

cells causing them to shrink. As the stomata close, transpiration is reduced and further water loss from the leaves is prevented (Steuer *et al*., 1988). During natural nodule aging the synthesis of ROS through the Fenton reaction may act as a signalling mechanism to regulate hormones involved in flowering and seed development. However, under stress conditions early degradation of Lb would liberate excess free iron that could potentially react with hydroxyl radicals and cause excessive ROS accumulation in the symbiosome membrane and the bacteroids (Tang *et al*., 2017). Under such conditions, nodules and associated bacteroids may be subjected to severe oxidative damage leading to early senescence (Delaat *et al*., 2014). Puppo *et al*. (2005) proposed a model of regulation of senescence-inducing signals involved in ROS accumulation and proteolytic mediated PCD. Free iron accumulation and uncontrolled proteolytic activity are the two major negative factors that cause oxidative damage to bacteroids in response to drought stress (Fig. V).

Fig. V. Possible role of senescence-induced regulation of iron homeostasis and protease - mediated programmed cell death (PCD). Signals induced by plant-derived senescence affect N_2 fixation by disturbing the symbiosome membrane. Under stress, senescence associated signals induce proteolytic activity and cause catalytic iron release. This iron will further react with hydroxyl radicals and disrupt the symbiosome membrane. The increased levels of ROS would also cause DNA fragmentation, which culminates in PCD (Figure copied from Puppo *et al*., 2005).

1.17 Ferritins and their involvement in iron scavenging

Ferritins are 24-mer iron scavenging proteins which can accommodate ~4000 iron atoms. Plant ferritins are significantly regulated by excess iron. As discussed above, environmental stresses like drought, salinity, and high temperatures can cause the liberation of free iron radicals (Fe^{2+}) which cause oxidative damage to bacteroids and trigger early nodule senescence. Therefore, ferritin is a potential damage-limiting factor expressed by plants to scavenge the excess of free iron molecules. Several transcriptomic studies of gene expression in the leaves of *Arabidopsis* have identified ferritin encoding genes which are associated with senescence (Gaymard *et al*., 1996; Bhalerao *et al*., 2003; Wollaston *et al*., 2003). Petit *et al*. (2001) reported that there are 4 different ferritin proteins expressed in *Arabidopsis,* and their expression is stimulated by different factors. *Atfer1, Atfer3* and *Atfer4* are induced by an excess of iron and *Atfer2* is regulated by abscisic acid (ABA). In addition, *Atfer1* is also induced by H_2O_2 in *Arabidopsis*. In legume nodules ferritins are reported to be localized in the amyloplasts and plastids (Lucas *et al*., 1993).

Control of ferritin expression depends on iron concentrations in the cytosol. Under low iron availability, repressors inhibit the transcription factors which are bound with iron-dependent regulatory sequences (IDRS). This binding leads to the inhibition of the positive regulation of ferritin transcription. Under high iron availability, ubiquitination and proteasome-dependent degradation of the repressors occurs after a nitrous oxide (NO) burst originates in the plastids. Concurrently, PP_2A phosphatase activity causes the de-phosphorylation of repressors and consequently the de-repression of ferritin gene expression. After transcripts are produced, ferritin precursor polypeptides are synthesized through translation and transported to plastids where they undergo assembly to the 24-mer ferritin protein (Fig. VI) (Briat *et al*., 2010).

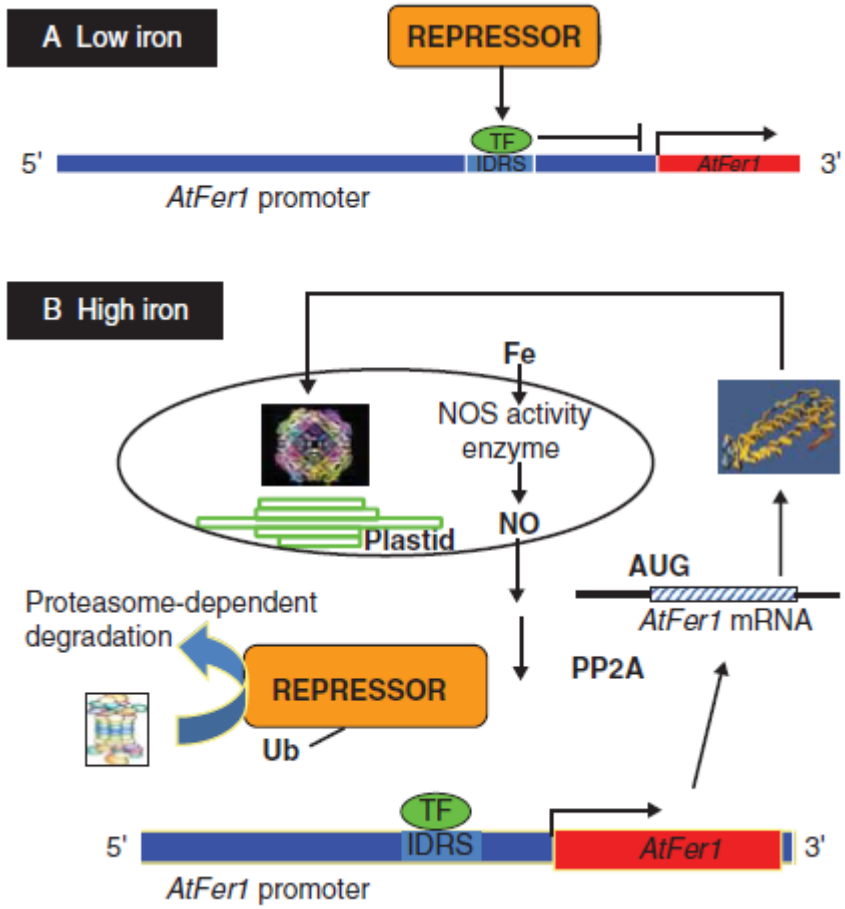

Fig. VI. Schematic regulation of ferritin in *Arabidopsis* depending on iron availability. Under low Fe availability, repressors bind with iron dependent regulatory sequences (IDRS) and prevent transcription. At high iron concentrations, nitrous oxide mediated cell bursts occur in the plastids and subsequently the derepression of ferritin expression is affected by protein phosphatase (PP_2A). (Figure copied from Briat *et al*., 2010)

The interaction between iron homeostasis and oxidative stress was well described by Ravet *et al*. (2009). The authors knocked out 3 ferritin genes expressed in the vegetative organs and reproductive tissues of *Arabidopsis* and then characterized the mutant plants. An *Atfer2* knock-down mutant was also developed. As *Atfer2* is known to be expressed only during seed germination, research with this mutant demonstrated that ferritin2 protects the seed from free iron-mediated oxidative damage but does not store the iron for plant development. Triple knock-down mutant (*Atfer1, Atfer3* and *Atfer4*), 35S::*Atfer1* (overexpressing line with 35S promoter background) and wild type lines were grown for 50 days under normal water irrigation and 2mM FeEDDHA. In this experiment, the dry matter, photosynthesis rate and quantum yield of photosystem II were measured. None of the lines showed any difference in dry matter until the 30 days after sowing, but the triple mutant exhibited a drastic

reduction in biomass at later growth stages and, under iron irrigation as compared to the wild type control. At 50 days after planting and before bolting, the mutant line showed a 65% reduction in dry matter compared to the wild type. Interestingly, the leaf size was also significantly decreased in the triple mutant line as compared to the wild type, but no changes in leaf numbers were observed in any of the lines. These results indicate that in the absence of ferritin excess iron reduces the rosette growth. This study also confirms that the absence of ferritin affects CO_2 fixation for photosynthesis but doesn't affect the photosynthetic electron transfer. Likewise, the absence of ferritin in the floral stalk affected the flower phenotype by altering the iron transport. This resulted in a 70% decrease in seed yield in the triple mutant line under iron irrigation.

In addition, several enzymes known to be involved in ROS regulation, including superoxide dismutase (SOD), catalase (CAT), ascorbate peroxidase (APX) and glutathione reductase were measured in the triple mutant under water and iron irrigation. All levels of all four enzymes were found to be significantly increased in the ferritin-lacking triple mutants as compared to wild type plants. These results indicate that in the absence of ferritin, an excess of free iron can increase the ROS accumulation. In *M. truncatula* three ferritins (*Fer1, Fer2* and *Fer3*) have been identified and shown to be expressed until plants are 28 days of age in *S. meliloti*inoculated *M. truncatula* nodules according to microarray data released by the Nobel Foundation (http://mtgea.noble.org/v3/). However, involvement of ferritins in nodule activity and senescence under different environmental stresses has not yet been studied.

1.18 Expression of serpin and ferritin in plants under drought

Serpin-Z2B is a drought-responsive protein reported in wheat by Jiang *et al*. (2012). Their studies into serpin Z2B indicated that the accumulation of serpin in seeds is likely to be involved in the regulation of defence activation and programmed cell death under drought. Experimental evidence suggests that protease activity is relatively higher in stress sensitive plants than stress tolerant plants (Simova-Stoilova *et al*., 2006). In order to prove the hypothesis that certain protease inhibitors are expressed under drought in tolerant plants, Vaseva *et al*. (2014) studied protein expression analysis of serpins and cystatins (cysteine protease inhibitors) in drought tolerant and susceptible verities of wheat. They found that two serpins (*Ser1* and *Ser2*) and two cystatins were expressed under drought stress in the tolerant variety. This study suggests that drought stress may result in the upregulation of protease inhibitors in drought tolerant plants in order to control proteolysis-mediated cell death. However, further study is needed to investigate the potential role of serpins in controlling the proteolysis which causes symbiosome damage in nodules and proteolytic mediated PCD.

In the case of ferritins, Kang & Udvardi, (2012) reported that drought stress induces the expression of ferritin more rapidly in alfalfa nodules. Moreover, ferritin mRNAs were found to be expressed at a 2-fold higher level than other gene families in soybean nodules under drought stress (Yamaguchi *et al*., 2010; Clement. 2008). A recent study by DeLaat *et al*. (2014) examined levels of ferritin transcripts in the leaf tissue of three common bean cultivars. The study found that three ferritin proteins (*Pvfer1, Pvfer2* and *Pvfer3*) were actively transcribed in an intracellular environment of iron excess caused by drought stress. However, temporal expression and involvement of ferritins in reducing iron toxicity in nodules is yet to be demonstrated.

1.19 *Medicago truncatula* as a model plant for legume-rhizobium symbiosis

M. truncatula is used as a model plant for studying legume-rhizobial symbiosis, functional genomics, proteomic studies and functional physiology because of its fast tissue regeneration capacity, ease of transformation, reproductive self-compatibility and small diploid genome. Among many genotypes of *M. truncatula*, Jemelong A17 is widely used for functional physiological studies while R108 is used for transformations because of its fast tissue regeneration capacity. These two genotypes, however, differ in their response to various environmental stresses (Wang *et al*., 2014; Branca *et al*., 2011; Ellwood *et al*., 2006; Rodriguez-Celma *et al*., 2013).

1.20 Concluding statement

Legumes are grown agriculturally both for human and stock feed and to aid sustainability in crop rotations through their N-fixing ability. Legumes are classified into two broad types: i) grain legumes for human and animal consumption, and for the production of oils for industrial use, e.g. beans, lentils, lupins, peas, and peanuts; ii) forage legumes for livestock feed such as alfalfa and clover.

Legume plants are a well-known source of nitrogen supply to the symbiotic host through the action of SNF. During the senescence of host tissues, the N from SNF may be transferred to soil and other crops. Enhancement of the symbiotic potential in legumes is an essential strategy for sustainable agricultural production. Moreover, the importance of nitrogen fixation in global environmental conditions has been considered. Studies on improving the symbiotic performance of legumes are being focussed currently by several researchers to improve the productivity of economically valuable crops such as legumes and eliminate the use of synthetic nitrate fertilizers. It has been identified in agriculture systems that legume-rhizobial symbiosis confronts two major issues: SNF suppression by leached N in felid soil and drought stress, and drought-induced early nodule senescence. The addition of nitrate fertilizer or an available leached field N can reduce the SNF process by affecting the resistance of O_2 diffusion in nodules. In addition, drought stress, which is a major constraint for legume-rhizobial symbiosis, can affect the SNF by increasing the amino acid and ureides loading in nodules. However, this effect may vary from plant to plant depending upon the symbiotic response to external N and drought stress. Recent studies reported that *M. truncatula* genetic backgrounds, Jemalong A17 and R108, show differential variations to aluminum toxicity, salt stress, iron deficiency and drought stress (Wang *et al*., 2014; Luo *et al*., 2016). Hence, it is speculated in this study that these genetic backgrounds may also differentially respond to external N treatment on SNF suppression.

A reduction of SNF can also take place if a plant nodule precedes to senesce where nitrogen-fixing bacteroids die. In legumes, nodule senescence is a developmental process which is programmed to remobilize nutrients when a plant ages (Puppo *et al*., 2005). At this stage, nitrogen fixation may be reduced but it will not completely cease until seed packaging begins as seed proteins require N. This natural senescence process begins by the induction of senescence-related signals through signal transduction. Under drought, symbiotic interaction between the legume host and the rhizobial symbiont is constrained due to the early initiation of the breakdown of nodule proteins, degradation of bacteroids and the consequent senescence process. In *M. truncatula* nodules, drought causes early nodule senescence through the enhancement of uncontrolled proteolytic activity and iron-mediated ROS accumulation (Delaat *et al*., 2014; Pierre *et al*., 2014). However, plant nodules were identified to involve protease inhibitors like serpin and cystatins as a controlling factor to limit protease-mediated cell death. Among the protease inhibitors, serpins are known to interact with papain and legumain

proteases and would therefore be considered as an important factor in the control of protease-mediated cellular damage. Lampl *et al*. (2013) reported that *AtSerpin1* is involved in controlling the proteolytic (papain RD1 protease and legumain like caspase1) mediated PCD and necrotrophic mediated PCD induced by fungal pathogens. A transcriptomic study in wheat (Vensel *et al.,* 2005) revealed that serpins are induced at higher levels under drought as a defensive shield to protect storage proteins from digestion. Localization of serpin was previously observed in the ER, protoplast and cytoplasm (section 1.13). However, the expression of serpins in nodules and their involvement in the nodule senescence process are not known. Iron mediated ROS damage in nodules could be the result of Lb degradation under drought stress. As discussed above (Section 1.15), an excess of free iron is always harmful for cellular activity since it produces deleterious ROS through the Fenton reaction (Fig. IV) (Kang & Udvardi 2012). Iron scavenging by ferritin would only be an effective controlling factor for excess iron-mediated ROS increase since plants do not have another alternative source for capturing the free Fe ions liberated during drought stress. Ferritin is a protein which can accommodate ~4000 iron atoms in its central cavity. Previous localization studies in *Arabidopsis* reported that ferritin localizes to plastids and amyloplasts (Ravet *et al*., 2009) and captures free Fe ions released in cells.

Considering the importance of SNF in legumes, improved knowledge of the physiological factors that affect and determine the performance of the symbiosis would be extremely useful. This study begins this investigation by elucidating the physiological and molecular responses of the *M. truncatula- E. meliloti* symbiosis to external N fertilizer treatment and drought stress. Having known the functional attributes of serpin and ferritins, this study also gives insight into investigating the mechanisms involved in the drought-induced nodule senescence process.

1.21 Hypotheses

Considering the context of this research, the two following hypothesises were formulated:

1. The *M. truncatula* genetic backgrounds, Jemelong A17 and R108, may differentially suppress SNF in response to external N fertilizer treatment under well-watered and drought conditions. Difference discovered between those two genotypes may reveal how SNF suppression is regulated and the benefit of SNF.
2. *M. truncatula* may initiate nodule senescence in the early stages of growth limitation in adverse conditions such as drought stress but regulate the process of senescence by involving serpin and ferritin to maintain residual SNF for longer than in an uncontrolled senescence process and increase the ecological fitness of the plant.

1.22 Research objectives

To test the first hypothesis, the following three objectives were developed:

1. Investigate the symbiotic characteristics of *M. truncatula* Jemelong A17 and R108 and the impact of SNF on plant growth by comparing non-N fixing mutants under N limitated conditions.
2. Determine the suppression of SNF by external N treatment in two different genotypes, Jemelong A17 and R108, under well-watered and drought conditions.
3. Investigate and decipher the impact of SNF/N fertilizer on plant growth under drought stress by evaluating drought tolerant genes.

To test the second hypothesis, the following 4 objectives were formulated:

1. Determine the changes in the physiological and nodule activities of SNF-dependent *M. truncatula* in response to drought stress and the biological relevance of SNF on plant growth.
2. Investigate the key features of drought-induced nodule senescence such as proteolytic activity and excess iron levels.
3. Identify the expression of key serpin and ferritin genes in nodules in response to drought stress and generate *RNAi* knock down lines to investigate the effects of the loss of function.

4. Knock down serpin and ferritin genes in nodule and investigate the effects on proteolytic activities and changes in iron levels in order to make inferences about the regulation of the nodule senescence process under drought.

Chapter 2

Materials and methods

2.1 Plant growth and physiology protocols

2.1.1 Plant materials and growth

The seeds of *M. truncatula* wild type genotypes, Jemalong A17 and R108, used in this study were kindly provided by Associate Professor Richard Macknight, School of Biomedical Sciences, University of Otago. The mutant seeds used from Jemalong A17 *dnf5-2* (*defective in nitrogen fixation2,* defective in nodule organogenesis) and Jemalong A17 *dmi1-3* (*does not make infection1,* fails in bacteroid invasion) were kindly provided by Dr Peter Kalo, Agricultural Biotechnology Centre, Hungary. For germination, seeds were scarified by gently rubbing them between two pieces of sand paper (fine quality) until small signs of abrasion appeared. Scarified seeds were incubated in the dark at 4^{o}C on 0.8% soft agar for 3 days to overcome embryonic dormancy. The seeds were then left at 22^{o}C in the dark for another 24 hours until radicle development occurred. Germinated seedlings were sown in a soil mix consisting of 50% vermiculite, 30% perlite and 20% sand. Plants were grown under 16 h light (200 µM photons/m^2/s^1)/ 8 h dark at 22^{o}C and watered every other day with 1X nitrogen-free Jenson's seedling media (Jones *et al*., 2008; Appendix 1).

2.1.2 Measurement of growth kinetics of *E. meliloti* cells

A single colony of *Ensifer meliloti* (ICMP 19861- [Dangeard 1926] Young 2003) was inoculated in 100 ml Rhizobium-specific liquid medium yeast extract mannitol broth (YEMB) (Sigma Aldrich, Germany; Appendix1) and grown at 25^{o}C for 60 hours. One ml of culture was sampled every 10 hours, and the optical cell density was measured spectrophotometrically at 565 nm. Serial dilutions using 1 ml of culture was also performed as described by Sieuwerts *et al*. (2008). One ml of serially diluted samples were spread on YEM agar plates and the number of colonies was counted after 16 hours of incubation at 22^{O}C. The number of colony forming units (CFU) were calculated per ml of bacterial samples based on dilution factors as described by Sieuwerts *et al*. (2008).

2.1.3 *E. meliloti* inoculation for nodule formation

E. meliloti cells were cultured for 16 h and showed an optical density of 0.5 at 565 nm without dilution. The cells were harvested by centrifugation and resuspended in sterile water. Two days after *M. truncatula* seedlings had been sown into pots, 1 ml of the harvested *E. meliloti* culture was injected in the soil near the rhizospheric region of each plant using a sterile micropipette. For uninoculated control, Jemalong A17 genotype was used for all the experiments. Uninoculated treatment pots were instead inoculated with sterile distilled water.

2.1.4 Measurement of field capacity (FC)

Potting mix comprised of 50% vermiculite, 30% perlite and 20% sand was packed into pots constructed from plastic piping (50 cm L x 13 cm W), fitted with a tubular plastic film liner and well saturated with distilled water. After complete saturation the pots were kept overnight to drain excess water from the potting mix. The next day, the potting mix from all the pots was emptied into trays which were placed in a hot air draft herbage drying oven at $105^{O}C$ for 2-3 days to dry completely. The mass of solids before and after drying was measured to calculate the water holding capacity after saturation and drainage overnight (FC) using the following formula as described by Samarah (2005):

$$\text{Field capacity} = \frac{\text{Mass of solids at field capacity - Mass of oven dried solids}}{\text{Mass of oven dried solids}} \text{ X } 100$$

2.1.5 Water treatments

This thesis has experiments that were conducted over two different time periods. The first group of experiments were conducted for a duration of 32 days, and the second group had durations of 72 days. For the experiments that had a 72-day duration, two different soil moisture contents 95%, a well-watered condition and 70%, a moderate drought stress (Yousfi *et al.,* 2016) were maintained beginning from 30 days post inoculation (dpi) with *E. meliloti*. For the well-watered treatments, pots were watered every other day to bring the soil moisture content to 95% FC. For the drought treatments, pots were left unwatered from 30 dpi until the soil moisture fell to 70% FC. Thereafter, pots were weighed daily. Water was added to replace evapotranspiration and bring each pot back to the desired % of FC. Both water regimes were maintained for another 42 days. Plants were uprooted at different time points, washed with sterile distilled water and then used for further analysis. For the

experiments that had a 32days duration, water was withheld completely at 20 dpi for 12 days to impose the drought treatment. For the well-watered control treatment, plants at 20 dpi were well-watered for the same 12 day period. A list of experiments used in this study are as follows:

Table 1. List of experiments with duration and sampling time points.

Experiments	**Duration**	**Sampling time point for various measurements**
1	72 days	10, 15, 20, 25, 30, 35, 60 and dpi.
2	72 days	14, 25 and 42 days after well-watered (DAT+W) and drought stressed treatments (DAT-W) from at 30 dpi.
3	32 days	20, 26 and 32 dpi well-watered and drought stressed plants
4	32 days	20, 26 and 32 dpi well-watered and drought stressed plants
5	32 days	20, 26 and 32 dpi well-watered and drought stressed plants
6	72 days	0, 7, 14, 25, 37, and 42 days after drought stressed (DAD) and control plants (well-watered) from at 30 dpi
7	32 days	0, 6 and 12 days after drought stressed (DAD) and control plants (well-watered) from at 20 dpi

2.1.6 Physiological characterization

Leaf water potential was measured at each harvesting time point using a Wescor HR 33T Dew-point microvolt meter (Wescor Inc, USA). During the dark period, 6 mm diameter leaf discs from fully expanded leaves were cut from 4 plants of each treatment and kept in psychrometer chambers for

60-90 min. Then πv values (cooling coefficient) were measured in Dew-point mode as described in the instrument instruction manual. The πv values of the leaf discs were converted to MPa by comparison with calibration curves obtained using different filter paper discs soaked in NaCl solutions of known concentrations. Using a CIRAS-2 photosynthesis system (PP systems, USA), CO_2 concentration, transpiration rate, vapour pressure deficit, stomatal conductance and net photosynthesis rate were measured for fully expanded leaves inserted into the measurement chamber of the instrument. Conditions inside the chamber were set to 80% relative humidity, 1400 µmol m^{-2} s^{-1} photosynthetically active radiation (PAR), and 400 ppm CO_2 (Zegada-Lizarazu & Monti, 2012). The relative water content of leaves was measured by first imbibing fully expanded trifoliate leaves from each treatment by overnight (saturation) in water and then drying them at 65^{O}C for 2 days. The weight of the leaves was measured before and after saturation and again after drying. RWC of leaves was calculated by the following formula:

$$RWC = \frac{\text{Fresh weight - dry weight}}{\text{Saturated weight - dry weight}} \text{ X } 100$$

After plant harvesting, nodule numbers were counted and shoot biomass was measured. For acetylene reductase assay, 100 mg of fresh nodules were kept separately and the rest of the nodules, root and leaf tissues were stored at –80^{O}C.

2.1.7 Chlorophyll estimation

Ten mg of frozen leaf tissue were homogenized in 1.7 ml Eppendorf tubes with a pestle using liquid nitrogen. To the powder 100 µl of 95% ethanol was added and the samples were stored in the dark overnight at 4^{O}C. Samples were subsequently centrifuged at 10,000 g for 10 min. Supernatant was collected and optical density was measured at two different wavelengths, 665 and 649nm. From the absorbance value, the amount of chlorophyll content in µg/mg of FW was calculated by using the following formula as described by Ritchie (2006),

Chlorophyll a = 13.70xAbs665-5.76xAbs649

Chlorophyll b = 25.80xAbs649-7.60xAbs665

Total Chlorophyll = 6.1xAbs665+20.04xAbs649

2.1.8 Nitrogenase activity measurement by acetylene reductase assay (ARA)

At each time point, the ARA method was followed to determine nitrogenase activity in nodules as described by David *et al.* (1980). For each sample, 100 mg of nodules were detached from the roots and placed in a 6 ml tube. The tube was closed with an air tight rubber stopper. Acetylene (0.6 ml, 98% pure) was injected into Gas chromatography using a sterile syringe to reach a 10% final concentration and the samples were incubated for 1 hour at 22^{O}C. After incubation, 1 ml was injected into a GS-8A Gas chromatograph (Shimadzu, Japan). All samples were run at attenuation 16 and the total area of the ethylene peak (40 sec. retention time) was calculated. For the ethylene standards, samples of 0.0038, 0.338, 3.386, 33.868, 338.68 and 3386.8 nM of ethylene gas were prepared in sterile air-tight tubes of 6 ml volume. A 1 ml sample from each standard was injected into the gas chromatograph, and the total ethylene peak area was measured. The peak area of ethylene from each sample was converted to nM/µM of C_2H_4 produced/hr/g FW.

2.1.9 Experimental set up for N fertilizer treatments in Chapter 4

Seeds were germinated as described above and sown in prepared potting mix (2.1.1). Plants were treated with unlabelled or ^{15}N labelled N fertilizer and inoculated with or without *E. meliloti* as mentioned in the following table:

Table 2. Experimental setup for N fertilizer treatments in chapter 4.

Experiments	Treatments	Rhizobium (*E.meliloti*) inoculation	Watering	N fertilization (Potassium nitrate)
Experiment 3	1	+	+	-
	2	-	+	-
Experiment 4	1	+	+	+ (^{15}N isotope labelled)
	2	+	-	+ (^{15}N isotope labelled)
	3	-	+	+ (^{15}N isotope labelled)

	4	-	-	+ (^{15} isotope N labelled)
Experiment 5	1	-	-	+
	2	+	-	-

Rhizobia culture was inoculated as mentioned above and nitrogen fertilizer was supplied in the form of either 10 mM unlabelled potassium nitrate or ^{15}N labelled potassium nitrate (10 atom % ^{15}N; Sigma Aldrich, Germany) based on the above treatments. For the N fertilizer treatment, labelled fertilizer (as a component in Janson's solution) was prepared and supplied to plants from 3 days after sowing as described by Hellmann *et al*. (2015). For each treatment, a minimum of 3 plants were kept in all experiments to allow for biological replications. Nodules and plants were then harvested from all treatments at 20, 26 and 32 dpi. As mentioned above, nitrogenase activity and physiological measurements were carried out for each plant at all harvesting time points. In addition, the location of nodules (distance from the root-shoot junction) and nodule dry mass were measured.

2.1.10 Total N and ^{15}N measurement

Plant shoot samples were dried at 40 to 60^{O}C, ground to a <200 um particle size using a ball mill, and N content was measured using a Dumas elemental analyser (Europa Scientific ANCA-SL, UK) interfaced to an isotope ratio mass spectrometer (Europa Scientific 20-20 Stable Isotope Analyser, UK). This measurement was performed at Waikato stable isotope unit, University of Waikato, New Zealand. Atom percentage, delta ^{15}N and total N content of shoot were measured as described by Unkovich *et al*. (2008). The relative contribution of N from nitrogen fixation was also calculated from the percentage and amount of total N in shoots as described by Goh *et al*. (2016). The formulae used for ^{15}N and total N content measurement were as follows:

$$\text{At\%}^{15}\text{N} = \left(\frac{^{15}\text{N}}{^{14}\text{N} + ^{15}\text{N}} \right) (100\ \text{At\%})$$

where

$$\delta^{15}\text{N‰ vs. [std]} = \left(\frac{\text{R}_{\text{sample}} - \text{R}_{\text{std}}}{\text{R}_{\text{std}}} \right) (1000\ \delta\text{‰})$$

$$R = \left(\frac{At\%^{15}N}{At\%^{14}N} \right)$$

%Ndfix (nitrogen derived from fixation)

= $\delta^{15}N$ of reference plant- $\delta^{15}N$ of N fixing plant x 100/ $\delta^{15}N$ of reference plant- $\delta^{15}N$ of N_2 in air.

2.2 Histology protocols

2.2.1 Histological analysis of nodule tissues

For light microscopy, nodules were fixed in a solution containing 50% ethanol, 5% acetic acid and 10% formalin. The samples were kept in a vacuum to allow the fixative solution to penetrate the tissue by removing the air bubbles. The following washing steps were then performed prior to embedding.

Steps	Solution	Time	temperature
1	50% isopropanol	1 hour	RT
2	70% isopropanol	1 hour	RT
3	85% isopropanol	1 hour	RT
4	95% isopropanol	1 hour	RT
5	100% isopropanol	1 hour	RT
6	100% isopropanol	1 hour	RT
7	5:1 isopropanol: mineral oil	1 hour	50^0C
8	2:1 isopropanol: mineral oil	1 hour	50^0C
9	100%mineral oil	1 hour	50^0C
10	50% mineral oil + 50% paraplast	1 hour	60^0C
11	100% paraplast extra	Overnight	60^0C
12	100% paraplast extra	3 hours	60^0C
13	100% paraplast extra	3 hours	60^0C
14	100% paraplast extra	3 hours	60^0C
15	100% paraplast extra	3 hours	60^0C
16	100% paraplast extra	3 hours	60^0C

The prepared nodule tissues were embedded using Leica EG1150 tissue embedder according to the manufacturer's instructions and as described by Cam *et al*. (2012).

- The nodule(s) from each plant were placed into a metal mould preheated to 60^OC, and the mould was filled with paraplast wax.
- A labelled plastic cassette was then placed on top of the mould to be a part of the wax cast. After pouring each mould, the samples were placed on a cooling surface (-4^OC) to let the wax solidify quickly.

- Each nodule was sectioned on a Leica RM2235 microtome (Leica Microsystems, Germany) to yield 5 µm slices. For each tissue, 5 strip slices were taken to ensure that a full longitudinal section was obtained.
- Each strip was then gently placed on the surface of a 42^{O}C deionised water bath and mounted onto a labelled frosted glass microscope slide by raising the slide out of the water underneath the strip of sections.
- Slides were left on a 42^{O}C warming tray until dry, at which point they were stored in microscope slide boxes.
- The slides were then washed in xylene to remove the wax, leaving the root nodule tissue in place.
- Slides were first submerged in a tub of "histoclear II" (xylene + terpenes) for 10 min.
- After 10 min, the slides were then submerged in a separate tub of the same solution for 2 min, and finally a third tub of the same solution for a further 2 min.
- The washed slides were placed again on a 42^{O}C warming tray to dry off excess solvent. Then the slides were stained with toluidine blue as described by van de Velde *et al*. (2006) and imaged using a Leica DM3 XL (Leica Microsystems, Germany) light microscopic system and mounted with DPX (Merck, Germany).
- Once all slides had cover slips mounted, and the DPX had dried, images of the tissue on each slide were taken at Manawatu microscopic and imaging centre (MMIC) using Leica DFC320 microscope either at 4x Zeiss objective lens or 20x Zeiss objective lens, based on the size of the tissue being observed.

2.3 Molecular biology protocols

2.3.1 Sequence retrieval and primer design

Using the *M. truncatula* genome database (*Mt*GDB) (http://www.plantgdb.org/MtGDB/), *MtCat, MtRboh, MtAco, MtAcs, MtZep, MtNced, MtZip, MtPal, MtIcs* and *MtP5cs3* genes were identified and the full coding sequence was retrieved (Appendix 3). Primers were designed for each gene using IDT (Integrated DNA Technologies) oligo designing tool (https://sg.idtdna.com/calc/analyzer) and according to the requirements for Quantitative Real Time PCR like amplicon length of 80-200bp, minimum secondary structure, and reduced ability to form self-dimer and $60^{O}C\pm1$ melting temperature. The primer efficiency for each set was determined by using the LinReg PCR software (Appendix 2; Ruijter *et al*., 2009).

2.3.2 RNA extraction

100 mg of frozen tissue from nodules, leaves and roots from the two different harvesting time points were ground in a mortar using liquid nitrogen. The powder was then used for RNA extraction using Quick-RNA™ MiniPrep-Zymoresearch kit (Zymo Research, USA). Manufacturer instructions were used and are as follows:

- The tissue was ground in liquid nitrogen using a mortar and pestle.
- 800 µl of RNA lysis buffer was added to the tube and vortexed vigorously for 15 sec.
- Samples were centrifuged at 13,000 x g for 1 min at room temperature.
- The supernatant was collected and transferred to Spin-Away™ Filter in a collection tube and centrifuged again at 10,000 x g for 1 min to remove genomic DNA.
- The sample was collected in the collection tube after centrifugation and was thoroughly mixed with 1 volume of 100% ethanol by pipetting the solution up and down.
- This mixture was transferred to a Zymo-Spin™ IIICG column in a collection tube and centrifuged at 10,000 x g for 1 min. This step was repeated until all of the mixture was filtered.
- 400 µL of RNA prep buffer was added to the column and centrifuged for 1 min at 10,000 x g.
- Then, 700 µL of RNA wash buffer was added to the column and centrifuged at 10,000 x g for 1 minute.

- The column was placed in a DNAse and RNAse free 1.7 ml Eppendorf® tube and 50 µL of DNAse/RNAse free water was adde.
- The column was centrifuged at 13,300 x g for 1 minute and RNA was eluted into the collection tube.

The purity and quantity of RNA was measured spectrophotometrically at 206/280 nm using Nanodrop (Thermo scientific, USA) according to the manufacturer's instructions.

2.3.3 First strand cDNA synthesis

The protocol used for first strand cDNA using Transcriptor First Strand cDNA Synthesis Kit (Roche Life Science, Germany) was as follows:

- After RNA extraction 2.5 µg of each RNA sample and 1 µl of DnaseI (1U) (Roche Life Science, Germany) were combined and made into a 24.3 ul reaction volume and the tubes were incubated for 30 min at 37^{O}C.
- At the end of the incubation period, 1.6 µl of 125 mM EDTA was added to stop the reaction. The samples were incubated again at 75°C for 10 min to inactivate the DnaseI.
- For first strand cDNA synthesis (Transcriptor First Strand cDNA Synthesis Kit - Roche Life science, Germany), 1 µg of DnaseI treated RNA (10 µl) and 1 µl of oligod(T) were combined and the total volume adjusted to 13 µl with sterile distilled water.
- Tubes were incubated at 65°C for 10 min in a thermal block cycler and the following components were added immediately at the end of incubation: 4 µl of Reverse transcriptase buffer, 0.5 µl of protector Rnase inhibitor, 2 µl of dNTP mix and 0.5 µl of Reverse transcriptase.
- Tubes were incubated at 55°C for 30 min in a thermal block cycler.

2.3.4 Quantitative Real-Time PCR

To make cDNA dilutions, nodule cDNA's were diluted 20-fold using Rnase/Dnase free water. Three biological replicates for each gene and 3 technical replicates for each sample were kept for qPCR reactions. *Mt β Tubulin* and *MtPDF* 2 housekeeping gene primers were used (Kakar *et al*., 2008) and were found to remain stably expressed throughout the different experimental treatments and timepoints. Primers for the genes used in this study are listed in Appendix 2. The qPCR reaction was performed in a LightCycler 480 Real-Time PCR system (Roche Life Science, Germany). The reaction components and conditions were followed as per the manufacturers' instructions.

In an opaque 96-well plate the following components were added to each cell:

2 X LightCycler 480 SYBR Green I Master Mix	5 µl
Forward primer (10 µM)	0.5 µl
Reverse primer (10 µM)	0.5 µl
cDNA	2.5 µl
Rnase/Dnase free water	1.5 µl
Total volume	10 µl

Reaction conditions in the light cycler was as follows:

Steps	Temperature	time	cycle
Initial denaturation	95°C	5 min	1
Amplification: Denaturation	95°C	10 sec	35
Annealing	60°C	10 sec	
Extension	72°C	10 sec	
Melting curve	95°C	5 Sec	1
	65°C	1 min	
	97°C	4 min	
Cooling	40°C	30 sec	1

After each run, data was exported as a ".txt" file and converted to MS Excel format using 'Conversion-LightCycler 480 to LinReg PCR' software. The raw data from the excel sheet was further analysed to get Cq values (quantitation cycle) and primer efficiency using LinReg PCR (version 2015.0). For all samples, the geometric mean of 3 technical replicates was calculated. Relative expression of each gene in response to drought and age was calculated using the following formula.:

$$R = (E_{Target})^{\Delta Cq\ Target\ (Control-sample)} / E_{Reference}^{\Delta Cq\ Reference(Control-sample)}$$

Where,

E = Primer efficiency

R = Relative expression

Reference = Geometric mean of housekeeping gene

Target = Geometric mean of target gene

2.3.5 Ligation reaction

In a sterile Eppendorf® tube the following reaction was prepared using NEB T4 DNA ligase reaction (NEB, UK) according to manufacturer's instruction and incubated at 16°C for 1 hour:

Template DNA	~150 ng
Vector	50 ng
T4 DNA ligase	1 µl
T4 DNA Ligase Buffer (10X)	2 µl
Water	To 20 µl

2.3.6 Competent cell preparation

Competent cells for *E. coli* DH5α and *A. rhizogenes* were prepared using the protocol of Sambrook & Joseph, (2001):

- Freshly grown bacterial cells were inoculated in LB broth (Appendix 1) and grown overnight at 37°C with shaking (180 rpm).
- After cultured as above, bacterial cells were centrifuged at 3000 x g for 5 min at 4°C and the pellet was re-suspended in 10 ml of ice-cold 60 mM $CaCl_2$.
- The cells were left on ice for 1 hour and washed twice with 60 mM CaCl2 as above.
- The cells were pelleted again at 3000 x g and re-suspended in 4 ml of 60 mM $CaCl_2$ along with 15% (v/v) glycerol. Aliquots of 100 µl of the solution containing suspended cells were used for transformation.

2.3.7 Bacterial transformation

The prepared competent cells were then transformed using the protocol of Sambrook & Joseph, (2001):

- ~50 ng of the ligated vector was mixed gently with 100 µl of competent cells and incubated on ice for 1 hour.
- After 1 hour, tubes were heat-shocked at 42°C for 1.5 min and then immediately placed on ice.

- From each tube, 25 µl of cells were spread on LB solid media (see appendix) and cultured overnight at 37°C.
- Single colonies were selected and colony PCR or plasmid extraction was conducted to verify presence of the insert.

2.3.8 Colony PCR

A freshly developed single colony from the transformation plate was used to perform colony PCR as follows (Sambrook & Joseph. 2001):

- The selected single colony was touched with a sterile toothpick and mixed in an Eppendorf tube containing 10 µl of sterile MilliQ water.
- Tubes were incubated at 95°C for 5 min and the PCR reaction was initiated.

2.3.9 Reverse transcriptase PCR

In a sterile 0.2 ml Eppendorf tube, the following reaction mix was prepared and run in a thermal cycler for template amplification:

Forward Primer (10 µM)	0.5 µL
Reverse Primer (10 µM)	0.5 µL
2 x PCR Master Mix (Promega)	10 µL
cDNA	1 µL
PCR grade water	8 µL
Total Volume	20 µL

The reaction conditions in the thermal cycler were as follows,

Steps	Temperature	Time	Cycle
Predenaturation	95°C	10 min	
Denaturation	95°C	30 sec	1
Annealing	4°C less than the melting temperature of primers	30 sec	30
Extension	72°C	Time is given as per the amplicon length (1 min/per kb)	
Final Extension	72°C	10 min	

2.3.10 Agarose gel electrophoresis and gel elution

- In 100 ml of 1X TAE buffer, 1% of UltraPURETM agarose (Life Technologies, USA) was added and melted in a microwave oven until the solution was transparent. For smaller fragments (<200bp), a 2% (w/v) TBE (See appendix) gel was used to measure the optimal resolution.
- Melted agarose gel was poured into the gel tray along with a comb and allowed to solidify for 30 min.
- 2 µl of the PCR product was then mixed with 1X loading dye [10 X SUDS (0.1 M EDTA, pH 8.0, 50% (v/v) Glycerol, 1% (w/v) SDS, 0.025% (w/v) bromophenol blue)] and loaded into wells along with a 1 kb/100 bp DNA ladder (NEB, USA).
- The gel was run for 1 hour at 100 V for 45 min. The gel was then stained with 0.1 ug ml^{-1} ethidium bromide for 10 min. The fragments were visualised using a Gel Doc 2000 Gel Documentation System from Bio-rad Laboratories, CA, USA.

For gel extraction, Zymoclean™ Gel DNA Recovery Kit (Zymo Research, USA) was used, and the fragments were purified as follows:

- The gel portions containing the fragments were sliced from the gel using a sterile blade and 3 volumes of ADB buffer was added.
- Tubes were kept at 50°C for 10 min with continuous inverted mixing.
- After the gel slices had dissolved completely in the buffer, the solution was transferred into a Zymo-Spin™ Column in a collection tube.
- Tubes were centrifuged at 10,000 rpm for 30 sec and the flow through was discarded.
- To the column, 200 µl of DNA wash buffer was added and centrifuged again for 30 sec.
- After decanting the flow through, 20-30 µl of sterile MilliQ water or elution buffer was added and centrifuged for 30 sec to collect the purified DNA.

2.3.11 Restriction digestion reaction

For the digestion of DNA fragments used in the preparation of the template for ligation and transformation, the following protocol was used according to NEB (UK) manufacturer's instructions:

Restriction Enzyme 1	1 µl (10U)
Restriction Enzyme 2 (only for double digestion)	1 µl (10U)
DNA	1 µg
10X NEBuffer (NEB, UK)	5 µl (1X)
Total Reaction Volume	50 µl
Incubation Time	1 hour
Incubation Temperature	37°C

2.3.12 Construction and transformation of RNAi knockdown *Ser6*, *Fer2* and *Fer3* constructs

The complete coding regions of the *Ser6, Fer2 and Fer3* genes were used and customized to the target region of 150–250 bp using IDT Custom Dicer-Substrate siRNA (DsiRNA) tool. Fragments from these 3 genes were synthesised from Genscript, USA by introducing restriction sites and then cloned in a pUC19 vector as mentioned in Appendix 4. Single RNAi constructs for *Ser6, Fer2* and *Fer3,* a double RNAi construct for *Fer2* and *Fer3*, and a triple construct for *Ser6Fer2Fer3* were construed as described below.

Triple gene knockdown construct

The insert was digested out with *SpeI* and *BglII* and the gel insert (A) was purified. This insert was cloned into the *SpeI/BglII* site of pDAH2 to make Plasmid B. Plasmid B was then digested with *BamHI/NheI* and insert A was cloned to get Plasmid C, which is an inverted repeat of the three sequences.

Double gene knockdown construct (*MtFer2* and *MtFer3*)

An inverted repeat of *MtFer2* and *MtFer3* was made by digesting pUC19 with *AvrII* and *BglII*, purifying insert G and cloning into *SpeI/BglII* site of pDAH2. This plasmid was considered as plasmid H digested with *BamHI* and *NheI* to get insert G. Insert G was then cloned to get Plasmid I.

Single knock down

The *MtSer6, MtFer2* and *MtFer3* genes were amplified from nodule cDNA (*XbaI* at 5' and *BamHI* at 3' end). Each gene was digested individually with *XbaI* and *BamHI*. The inserts were then cloned into the *SpeI/BglII* site of pDAH2 to get Plasmid S. Plasmid S was digested and the insert was cloned into *BamHI/NheI* site to get Plasmid T.

All constructs were then cloned in an *RNAi* vector carrying a 35S promoter, *pDAH2* (Davies *et al*., 2012). *pDAH2* plasmids carrying the RNAi constructs were cut with *NotI* (NEB, UK) restriction enzyme and fragments containing the RNAi modules were cloned into *pGreen 0229* (Hellens *et al*., 2000). For the control construct, an empty *pDAH2* vector carrying only the 35S promoter (no insert) was cut with *NotI* and the cassette was cloned in *pGreen 0229*. This vector was transformed into *A. rhizogenes* along with the helper plasmid, *pSoup* (Tahir *et al*., 2012).

2.3.13 *Agrobacterium rhizogenes* mediated root transformation

Vectors were transformed into *M. truncatula* R108 using *Agrobacterium rhizogenes* mediated root transformation as described by Chabaud *et al*. (2006):

- An *A. rhizogenes* culture was grown over night and prepared in a TY/calcium medium (Appendix 1). The culture was then spread on a TY/calcium agar plate with antibiotics and grown for another 24 hours.
- After 30 hours of seed germination on 0.8% soft agar, root tips (3 mm) were excised from the 1 cm long seedlings using a sterile scalpel.
- After the formation of a bacterial layer on the agar plate, the seedlings were gently rubbed on the bacterial layer and placed on a petri dish (approx. 4-6 cm from the top) containing agar with modified Fahraeus medium (Appendix 1) with Kanamycin at 25 mg/l.
- Several incisions with a scalpel were made along the upper edge of the petri dish were made to allow for adequate gas exchange and then the plates were sealed with parafilm.
- Petri dishes were kept at an angle of approximately 45°C for 2–3 days (to reduce the risk of the seedlings falling) and then were vertically positioned for another 4–5 days in a 20°C growth chamber (16/8 L/D period).

Three weeks after *A. rhizogenes* inoculation when the transgenic roots were sufficiently developed, plants were transferred into pots containing the vermiculite, perlite and sand potting mix described above, and grown with *E. meliloti* inoculation. DNA was isolated from 20-d-old transformed roots using the CTAB method (Latif & Osman, 2017) and PCR was performed using NAN forward and NOS reverse primers (Appendix 7.2) to confirm successful transformation events. All plants with roots that tested positive were considered transformants and were transferred to a vermiculte/perlite/sand mixture and were inoculated with *E. meliloti* as described in 2.1.3.

2.4 Biochemical assays protocols

2.4.1 Protein and protease activity measurement

- Nodules (50 mg) were homogenized with 300 µl of extraction buffer (50 mM MOPS, 20 mM KCL, 1 mM Na_2EDTA ,5 mM $MgCl_2$, 1.5 mg/ml DTT and 0.7 µl/ml β mercaptoethenol) using a mortar and pestle.
- Homogenates were centrifuged at 15,000 x g for 15 min at 4ºC. The supernatant from the samples was collected and used for protein quantification and protease activity.
- In 100 µl of protein sample, 1 ml of 1x Bradford reagent (Bio-Rad) was added and incubated at room temperature for 5 min.
- The optical density of each sample was then measured spectrophotometrically at 595 nm and the concentration of protein (mg/g fresh weight) was calculated using bovine Serum albumin as standard (Sigma Aldrich, Germany).
- To measure protease activity in 100 µl of the protein sample, 100 µl of FTC-Casein working solution (1 µg) (Fluorescent protease assay kit, Thermo Fisher Scientific, USA) was added and incubated at room temperature for 30 min (96 well black plate).
- Samples were then measured fluorimetrically at excitation and emission wavelengths of 485 and 538 nm, respectively.
- Protease activity was assessed was assessed using trypsin as a standard to measure fluorescence of protease per min.
- Protease activity was determined by measuring the fluorescence emitted by the digestion of fluorescent isothio-cyanate labelled casein substrate by protease enzymes present in the sample.

2.4.2 Lb and iron content measurement

Fluorometric analysis of Lb content was performed as described by Larue and Child (1979).

- 100 mg of frozen nodule tissue was homogenised in 400 µl of extraction buffer containing 0.02% potassium ferricyanide and 0.1% sodium bicarbonate.
- Homogenates were centrifuged at 10,000 x g for 10 min and the supernatant (a red coloured supernatant appears in nodule samples) was mixed with 2ml of saturated oxalic acid.
- Tubes were then heated for 30min at 120^{o}C and measured fluorometrically at excitation wavelength of 405nm and emission wavelength of 650nm.

- Concentrations of Lb (µM/mg of nodule fresh weight) were calculated using bovine serum albumin as a standard.
- Iron content of the nodule tissues was quantified as described by Ravet *et al*. (2009).
- 100 mg of nodule tissues were dried completely overnight at 80^{O} C and homogenized with a mortar and pestle in 200 µl of 0.1 M phosphate buffer.
- From the homogenates 100 µl samples were taken in sterile tubes and 0.1 ml 98% H_2SO_4 and 70% HNO_3 were added.
- Samples were completely digested by heating at 100°C for 3 hours, and then 50 µl of 60% perchloric acid was added and dried completely at 100°C.
- The following were added to the sample ash: 0.5ml sterile water, 0.25 ml 1% thioglycolic acid, 1.5 ml saturated sodium acetate and 1.0 ml bathophenanthroline solution (200mg/250ml isoamyl alcohol) and mixed well.
- Samples were centrifuged at 12,000 x g for 10 min. The red aqueous layer (~1.0 ml) was collected and read spectrophotometrically at 535 nm.
- The quantity of iron in µg/g DW of nodule tissues was calculated using standard iron solution (Sigma Aldirch, Germany).

2.4.3 Protease inhibitory assay

Protein samples were prepared as described above and used for measuring papain-like cysteine legumain protease activity. Protease specific substrates, benzyloxycarbonyl-Arg-7-Amino-4-Methylcoumarin (ZR-AMC) for papain-like cysteine activity, and AC-YVAD-PNA for legumain like caspase activity, were used in this assay (Pereira & Song.,2008) (Sigma Aldrich, germany). A reaction mix was prepared by mixing 100 mM sodium acetate buffer (pH 5.5), 1 mM EDTA, 1 mM dithiothreitol, 10 µg/ml of total protein and 50 µM of substrate. The reaction was incubated at 28°C for 20 min. Samples were then measured fluorimentrically at 485nm excitation/538nm emission. Fluorescence absorbance was measured by cleavage of substrate over 1min and values are expressed as Δ (fluorescence) min^{-1} (Pierre *et al*., 2013).

2.5 Statistical analysis

The statistical analysis for plant physiological and qRT-PCR data were performed in Microsoft Office Excel 2010, MiniTab® 16 statistical package and Sigmaplot version 14. Standard errors of means (SEM) were calculated from a minimum of 3 independent biological replicates. Mean separations were evaluated by the Student's *t*-test, performed in Microsoft Excel using the standard formula and significance levels of 5% ($p < 0.05$) and 0.1% ($p<0.001$). Experiments with multiple treatments were statistically analysed by Two-way ANOVA with Post Hoc Tukey's test using MiniTab® 16 statistical package.

Chapter 3

A serpin and two ferritins are induced by drought in *M. truncatula* nodules

3.1 Introduction

The efficacy of SNF varies depending upon the host, host-rhizobial specificity and the symbiotic interaction. Each legume has its own specific rhizobial partner for symbiotic processes (Westhoek *et al*., 2017). Therefore, identifying suitable host-rhizobial partners and determining the symbiotic characteristics are important aspects in legume-rhizobial symbiosis and molecular studies. Nitrogen fixing nodules undergo various developmental stages such as the initial rhizobial infection into the root cortex, rhizobia multiplication and bacteroid differentiation, nodule development, nitrogen fixation and senescence. Nodule senescence is either part of the natural ageing process of a plant or it can be an induced process in a plant in response to biotic or abiotic stresses (Van de Velde *et al*., 2006). Natural nodule senescence coincides with a wide range of proteolytic activities which are essential to remove damaged or unfolded bacteroid and nodule proteins. However, this proteolytic activity might be induced at high intensity by the plant in response to drought stress and as a result, nodule senescence might be induced rapidly because of the degradation of functional nodule proteins. This senescence process could therefore, lead to bacteroid degradation and nitrogenase activity reduction (Pladys & Vance, 1993; Wyk *et al*., 2014). Pierre *et al*. (2014) described that increases of papain and legumain protease activity causes early nodule senescence in *M. truncatula.* Furthermore, uncontrolled proteolytic activity would also degrade leghaemoglobins and release toxic iron which in turn causes oxidative damage to bacteroids through deleterious ROS production (Delaat *et al*., 2014). However, plants have their own mechanisms to control proteolytic activity and excess iron- based ROS toxicity such as protease inhibitors and iron scavengers. Serpins are highly abundant protease inhibitors which are known to inhibit endoproteases such as cysteine and serine proteases (Fluhr *et al.,* 2012; Alvarez-Alfageme *et al.,* 2011). It has been shown in *Arabidopsis thaliana* that a serpin, *Atserpin1,* inhibits the activity of cysteine proteases and rescues the leaves from programmed cell death. To control iron toxicity, ferritin has been proposed as a key controlling factor by several studies (Gaymard *et al*., 1996; Bhalerao *et al*., 2003; Wollaston *et al*., 2003). Ravet *et al*. (2009) reported that ferritin can accommodate approximately 4000 iron atoms in its central cavity to reduce toxic damage in *A. thaliana* leaves.

This study investigates the characteristics of *M. truncatula* symbiotic interactions with *E. meliloti* and hypothesizes that serpins and ferritins may be expressed in *M. truncatula* nodules during nodule

senescence in response to stress conditions such as drought. I used herein the *M. truncatula*-specific rhizobium *E. meliloti* and studied symbiotic performance and gene expression in *M. truncatula* Jemalong A17 genotype.

3.2 Results

3.2.1 Growth kinetics and optimum *E. meliloti* cell density

For optimal nodulation efficiency, 10^8 cells ml^{-1} of *Rhizobium* must be supplemented in the rhizosphere region of legumes (Terpolilli *et al*., 2008; Simsek *et al*., 2007). This study hypothesizes that *E. meliloti* will develop the optimum cell density during a particular growth period prior to its use as an inoculum. To investigate this, a freshly prepared colony on YEMA medium (Appendix 1) was inoculated in YEM broth and grown for 60 hours. One millilitre of broth culture was sampled every 10 hours and the density of active cells was measured by counting colony forming units (CFU) as described in Chapter 2. Results showed that after 30 hours of incubation and at 0.5 optical density (OD), CFU reached approximately 10^8 cells/ml. While a prolonged incubation time increased the optical density, CFU counts decreased (Fig. 1b). This study showed the optimum density of *E. meliloti* cells, approximately 10^8 cells/ml, was reached after 30 hours of incubation and at 0.5 OD.

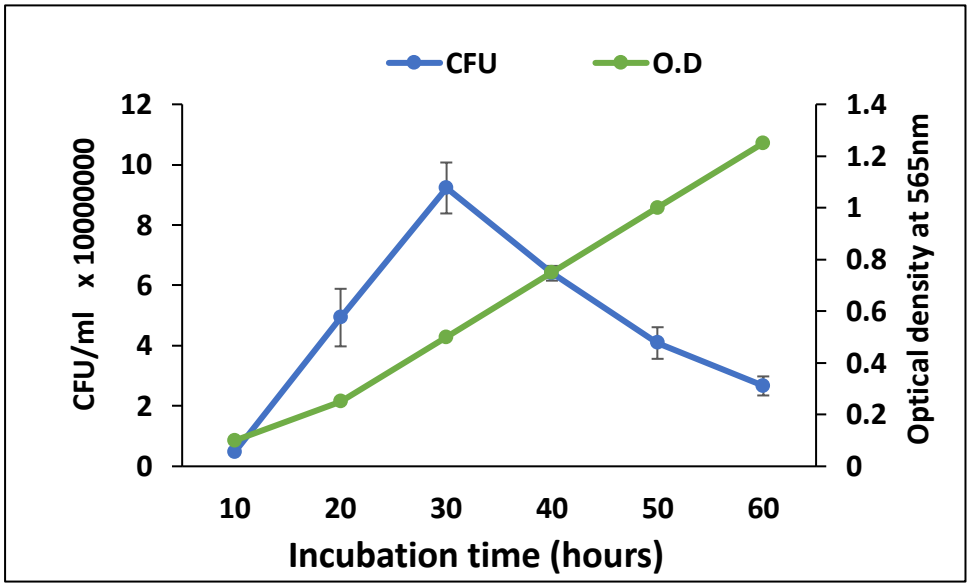

Fig. 1. **Growth kinetics of *E. meliloti* in YEM medium.** Cells were grown for 60 hours (green line) and optical density was spectrometrically measured at 600 nm. CFU's (blue line) were counted at each indicated time point after serial dilution. Values are the means of three biological replicates and error bars represent the standard errors of the means.

3.2.2 Nodulation and nitrogenase assay in *M. truncatula*

Each legume species has a different nodulation pattern and nitrogenase activity based on its interaction and compatibility with rhizobia. Post inoculation, nodule initiation has been observed to starts at 3 days, developing nodules are seen between 10-18 days, and nitrogenase activity begins at 20 days (Heynes *et al*., 2004; Suzaki *et al*., 2015). This study hypothesizes that similar time-frames are needed to establish a nitrogen-fixating symbiosis between *M. truncatula* Jemalong A17 and *E. meliloti*. To examine the nodulation properties of *M. truncatula*, the rhizosphere of *M. truncatula* was inoculated with *E. meliloti* cells under nitrogen free conditions (Experiment 1, Chapter 2). Nodules were then counted throughout the period of plant growth. Visible nodules were seen at 15 dpi and their numbers increased gradually to reach approximately 35 nodules/plant at 72 dpi. To determine the nitrogenase activity in *M. truncatula,* the ARA method (Chapter 2) was performed during the plants' growth period. The result of the assay showed that increased nitrogenase activity coincided with a higher number of nodules. Nitrogenase activity began at 20 dpi and increased until 60 dpi. At later plant growth stages (e.g. 72 dpi) nitrogenase activity dropped rapidly (Fig. 2b). This study showed that *M. truncatula* in association with *E. meliloti* performs efficient nitrogenase activity from 30 dpi to 60 dpi.

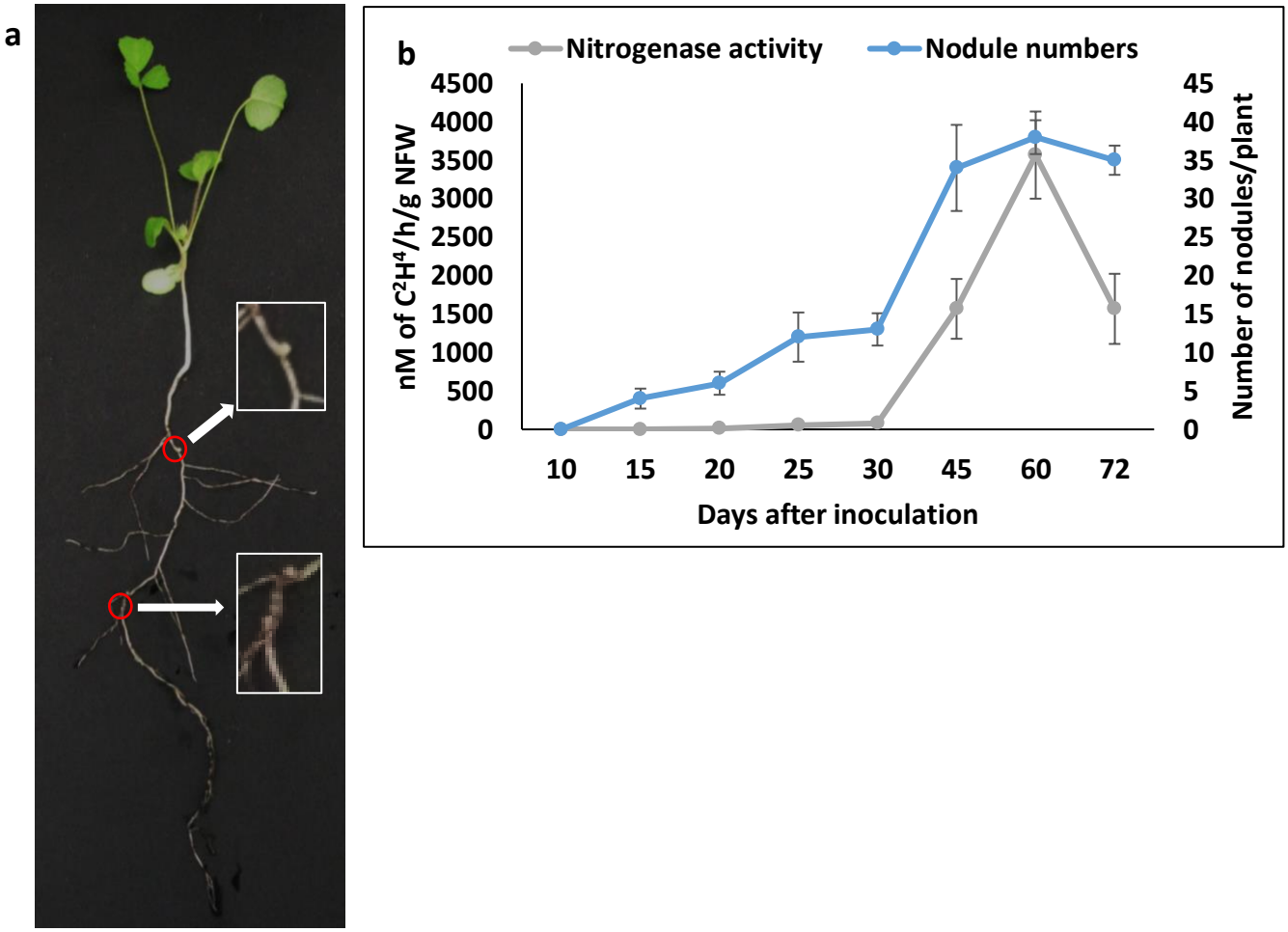

Fig. 2. Growth and symbiotic attributes of *M. truncatula* (a) 20 days old *E. meliloti* inoculated *M. truncatula* plants grown under N limited conditions and (b) nodule nitrogenase activity and nodule count. Red circles indicate the nodules. NFW denotes nodule fresh weight. Values are the means of three biological replicates and error bars represent the standard error of the means.

3.2.3 Effects of *E. meliloti* inoculation on *M. truncatula* plant growth

SNF fixation is a requirement of SNF-dependent legume growth (Remans *et al.,* 2008; Mus *et al*., 2016). This study hypothesizes that nitrogen fixation in the *M. truncatula* - *E. meliloti* symbiosis affects plant growth when grown in an N-free growth condition. To determine the effect of nitrogen fixation on *M. truncatula* growth, plants were grown in N-free conditions for 72 days with and without *E. meliloti* inoculation (Experiment 1, Chapter2). The photosynthetic rate, chlorophyll content and shoot biomass were measured. Results showed that N-fixing *M. truncatula* exhibited a significantly higher photosynthetic rate (3 fold) as compared to the uninoculated control. In the case of chlorophyll content, the results showed a 2 fold higher content than that of the uninoculated control. Moreover, we observed that these changes were found to be correlated with shoot biomass. As compared to the uninoculated control, the inoculated N- fixing plants showed a 5 fold higher

shoot biomass (Fig. 3a). As a result of the reduction of SNF, the shoot biomass of uninoculated *M. truncatula* was significantly reduced as compared to *E. meliloti* inoculated plants (Fig. 3b). Thus, SNF is required for optimal growth of the SNF-dependent *M. truncatula* Jemalong A17 inoculated with *E. meliloti.*

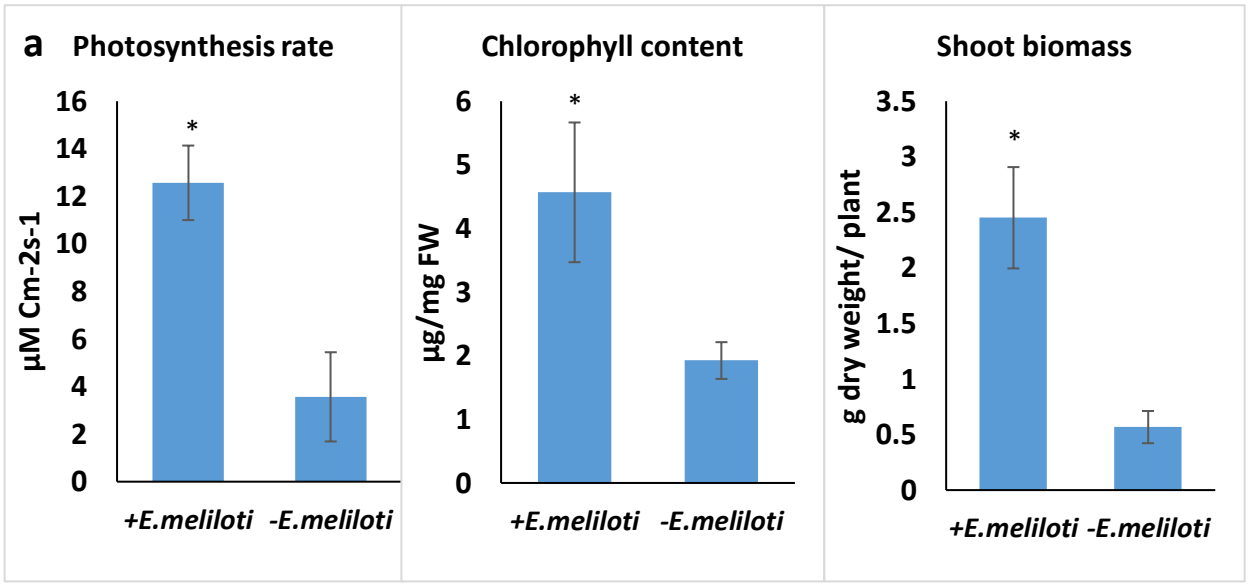

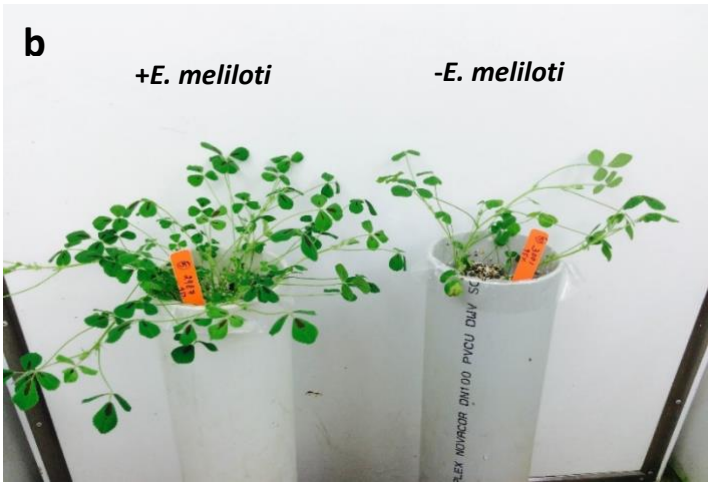

Fig. 3. Impact of SNF on plant growth. (a) Photosynthetic rate, chlorophyll content and shoot biomass of 72-day-old *E. meliloti* inoculated and uninoculated *M. truncatula* and (b) visible plant growth. Values are the means of three biological replicates and error bars represent the standard error of the means. Asterisks indicate the significant difference between uninoculated and *E. meliloti* inoculated plants at $p<0.05$ according to student's *t*-test.

3.2.4 Identification of serpin and ferritin genes in *M. truncatula*

To study the expression of serpin and ferritin genes in the nodules of *M. truncatula,* serpin and ferritin gene sequences were first retrieved from the *Medicago* genome database (MGDB) (Chapter 2) based on the number of matching sequences found on different chromosome loci. There were 28 serpin and 3 ferritin gene sequences identified from the database. Using the locus tag provided for individual genes, sequences were retrieved using the NCBI BLAST tool. The BLAST result of all these genes showed that 24 serpin and 3 ferritin *M. truncatula* genes were found to have 100% similarity with the respective *Medicago* serpins and ferritins from the database (with individual NCBI accession numbers), (Table 1, 2) whereas the remaining 4 serpin genes, *MtSer2, MtSer3, MtSer4* and *MtSer7* (from different chromosome loci), showed no specific accession numbers in NCBI database and 100% match with *M. truncatula* serpins. However, *MtSer2, MtSer3,* and *MtSer4* showed partial similarity (79%, 82%, and 79% respectively) with *MtSer1,* a gene with 100% similarity to the database/ annotated genes. Likewise, *MtSer7* showed 81% similarity with *MtSer6,* another gene with 100% similarity to the database. This indicates that these genes were not annotated in the database as serpins but still partially matched other annotated serpins (Table 1).

Table 1. **Chromosome locus tags and NCBI accession numbers of 28 serpin genes from *M. truncatula.*** All the serpins retrieved from the MGD database showed 100% similarity with their respective genes except *MtSer2* (79% similarity with *MtSer1)*, *MtSer3* (82% similarity with *MtSer1), MtSer4* (79% similarity with *MtSer1)* and *MtSer7* (81% similarity with *MtSer6)*. Asterisks (*) indicate the genes which don't have NCBI accession numbers but partially match other serpin genes as indicated.

Gene ID	Locus tag	Accession number	Organism	Similarity
MtSer1	MTR_3g018740	XM_003598595	*Medicago truncatula*	100%
**MtSer2*	MTR_2g045980	XM_003598595	*Medicago truncatula*	79%
**MtSer3*	MTR_8g027420	XM_003598595	*Medicago truncatula*	82%
**MtSer4*	MTR_2g046030	XM_003598595	*Medicago truncatula*	79%
MtSer5	MTR_3g101030	XM_003602927	*Medicago truncatula*	100%
MtSer6	MTR_3g101010	XM_003602925	*Medicago truncatula*	100%
**MtSer7*	MTR_4g045707	XM_003602925	*Medicago truncatula*	81%
MtSer8	MTR_7g050810	XM_003622635	*Medicago truncatula*	100%
MtSer9	MTR_3g10120	XM_003602943	*Medicago truncatula*	100%
MtSer10	MTR_3g101180	XM_003602941	*Medicago truncatula*	100%
MtSer11	MTR_3g015760	XM_003598529	*Medicago truncatula*	100%
MtSer12	MTR_3g101190	XM_003602942	*Medicago truncatula*	100%
MtSer13	MTR_7g050830	XM_003622637	*Medicago truncatula*	100%
MtSer14	MTR_3g099970	XM_003602833	*Medicago truncatula*	100%
MtSer15	MTR_3g100990	XM_003602923	*Medicago truncatula*	100%
MtSer16	MTR_3g101110	XM_003602934	*Medicago truncatula*	100%
MtSer17	MTR_3g101050	XM_003602929	*Medicago truncatula*	100%
MtSer18	MTR_3g111160	XM_003603640	*Medicago truncatula*	100%
MtSer19	MTR_3g100520	XM_003602885	*Medicago truncatula*	100%
MtSer20	MTR_3g101130	XM_003602936	*Medicago truncatula*	100%

MtSer21	MTR_7g050750	XM_003622631	*Medicago truncatula*	100%
MtSer22	MTR_3g111150	XM_003603639	*Medicago truncatula*	100%
MtSer23	MTR_3g048000	XM_003599803	*Medicago truncatula*	100%
MtSer24	MTR_3g015620	XM_003598519	*Medicago truncatula*	100%
MtSer25	MTR_3g101020	XM_003602926	*Medicago truncatula*	100%
MtSer26	MTR_4g093550	XM_003608337	*Medicago truncatula*	100%
MtSer27	MTR_3g101120	XM_003602935	*Medicago truncatula*	100%
MtSer28	MTR_6g046890	XM_003619290	*Medicago truncatula*	100%

Table 2. Chromosome locus tag and NCBI accession number of 3 ferritin genes from *M. truncatula.* All the gene's sequences were matched 100% similarity with *M. truncatula* ferritin genes with individual accession number.

Gene ID	Locus tag	Accession number	Organism	Similarity
MtFer1	MTR_7g069980	XM_003623311	*Medicago truncatula*	100%
MtFer2	MTR_5g083170	XM_003616637	*Medicago truncatula*	100%
MtFer3	MTR_4g014540	XM_003604515	*Medicago truncatula*	100%

3.2.5 Multiple sequence alignment and primer design

To determine the sequence-based diversity among the members of serpin and ferritin gene families in *M. truncatula*, complete coding regions of all the genes were aligned using MEGA7 (Molecular Evolutionary Genetics Analysis) and phylogenetic analysis was also performed. A phylogenetic tree showed that members of the serpin such as *MtSer5, MtSer2, MtSer11, MtSer8* and *MtSer16* are closely related (>90% similarity) with *MtSer17, MtSer4, MtSer24, MtSer13* and *MtSer27* respectively and other members of serpin and ferritin are not similar to each other or closely related (Fig. 4). Furthermore, no specific groups could be delineated among these gene families. To find any conserved regions among the serpin and ferritin families, all genes were grouped using the MUSCLE (Multiple Sequence Comparison by Log- Expectation) tool. Based on this process, 28 serpin genes were separated into serpin group 1 -serpin group 7 (SG1-SG7) and 3 ferritin genes into ferritin group 1 (FG1). This particular alignment and grouping of gene family members (based on conserved regions) was completely different from the genetic diversity the of gene members (tree build based on complete coding sequence) shown in the phylogenetic tree (Appendix 5, Fig. 4). In groups where two conserved regions were identified (Appendix 5), forward and reverse primers were designed (Chapter 2). In groups where only one conserved region was detected (Appendix 4 c, d, e, f and g) anchored oligo(dT) primers were used as a reverse primer (Appendices 2 and 5).

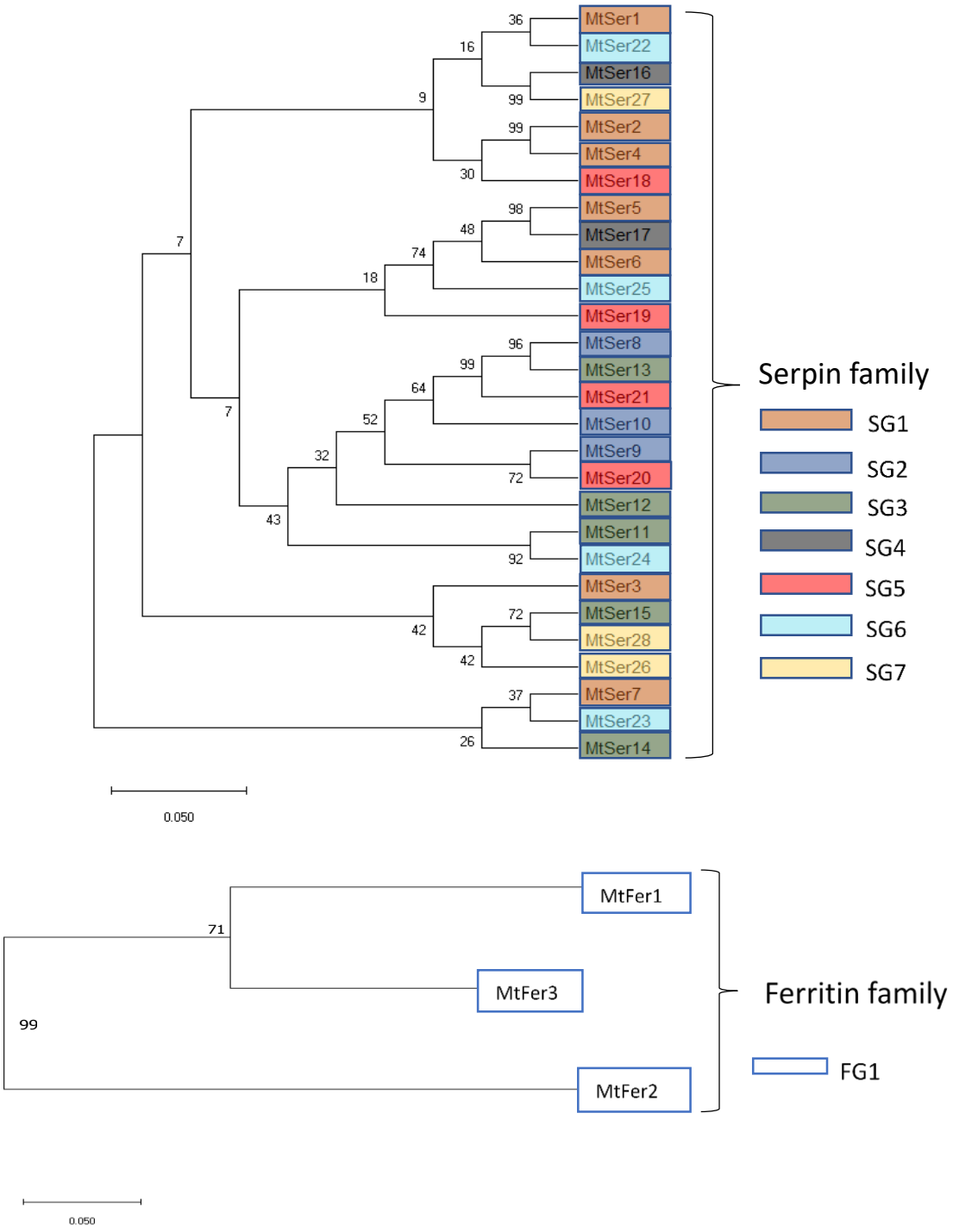

Fig. 4. Molecular phylogenetic analysis of the serpin and ferritin families. Evolutionary history of the families was inferred by using the Maximum Likelihood method based on the Tamura-Nei model. Evolutionary analyses were conducted in MEGA7 using the complete coding sequence of respective genes. Numbers indicate bootstrap values. Colours indicate the groups that were created using the MUSCLE alignment tool based on conserved regions found in coding sequences.

3.2.6 Screening of serpin and ferritin genes in root, nodule and leaf tissues

As seen above, it was determined that *M. truncatula* has 28 serpins and 3 ferritins genes. Therefore, this study hypothesized that certain serpin and ferritin genes are expressed in *M. truncatula* nodules. To identify the serpin and ferritin genes which are expressed in the nodules, a reverse transcriptase PCR approach was used to amplify the cDNA of the genes.

3.2.6.1 cDNA amplification of serpin and ferritin groups

M. truncatula plants were grown for 30 days with *E. meliloti* and treatment of 95% field capacity (FC) of soil moisture content was maintained for another 42 days (days after treatment) (Experiment 2, Chapter 2). To identify the expression of serpin and ferritin gene groups in the nodule, root and leaf tissues of *M. truncatula*, reverse transcriptase PCR was used to amplify the groups (Fig. 4). At 14 and 25 days after treatment (DAT), plant nodules were harvested and reverse transcriptase PCR was performed using the primers (Appendix 2). After 2 rounds of PCR amplification (60 cycles), S1, S2 and ferritin groups gave positive amplification in the nodule, root and leaf tissues, whereas other serpin groups did not show expression in any selected tissues except for the root tissue in serpin group 3 (S3) (Fig. 5).

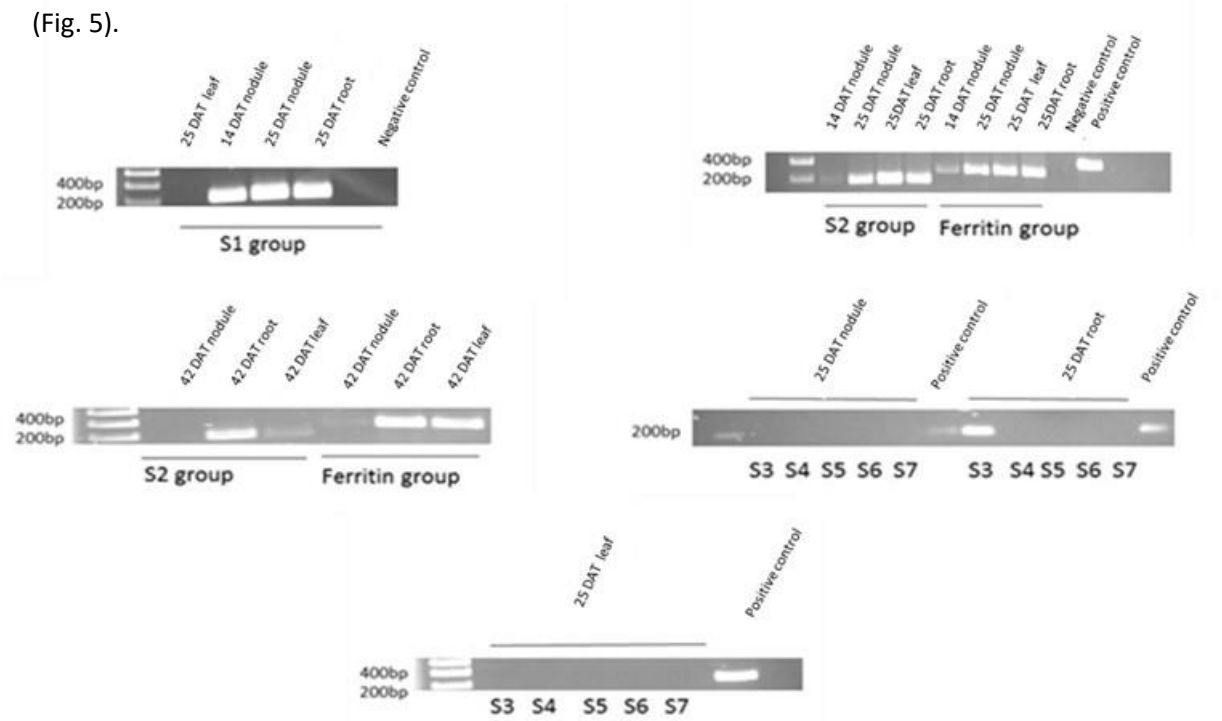

Fig. 5. Reverse transcriptase PCR of 7 serpin groups (S1-S7) and the ferritin group (F1) in well-watered nodules, roots and leaves of *M. truncatula* at different days after treatment (DAT). Water treatment (Day 0) started at 30 dpi to keep the field capacity of soil at 95%. *MtELF1* was used as a positive control.

3.2.6.2 cDNA amplification of individual genes

We observed that the SG1 and SG2 serpin groups and the FG1 ferritin group from the 14 and 25 DAT nodules showed positive amplification. Therefore, to screen the individual genes in the nodules of the SG1, SG2 and FG1 groups, specific primers were designed for all the genes (Appendix 2). As mentioned above, 2 rounds of PCR were carried out for all genes in the plant nodules at 14 and 25 DAT. The PCR products of all positively amplified genes were confirmed by sequencing followed by a BLAST (Basic local alignment search tool) analysis. After the second PCR round (~after 60 cycles), among *MtSer1*, *MtSer5*, *MtSer2*, *MtSer3*, *MtSer6* and *MtSer7* from the S1 group, *MtSer6* was found to be expressed at 14 and 25 DAT nodules while *MtSer5* was expressed only at 14 DAT. From the S2 group, *MtSer8*, *MtSer9* and *MtSer10* were found to be expressed only at 14 DAT. Among 3 ferritins (*MtFer1*, *MtFer2* and *MtFer3*) *MtFer2* and *MtFer3* were found to be expressed at 14 and 25 DAT nodules while *MtFer1* was expressed only at 14 DAT (Fig. 6). Taken together, these results showed that *MtFer1*, *MtSer2*, *MtSer5*, *MtSer6* and *MtSer10* were expressed only at 14 DAT and *MtSer6*, *MtFer2* and *MtFer3* were expressed at 25 DAT in the nodules.

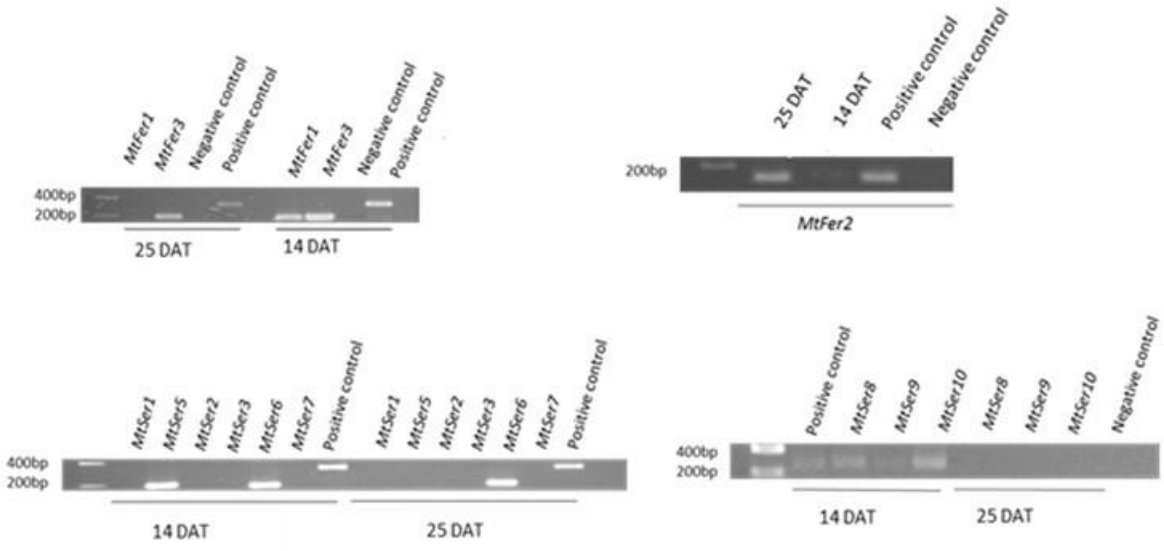

Fig. 6. Reverse transcriptase PCR of 9 serpin genes (*MtSer1*, *MtSer5*, *MtSer2*, *MtSer3*, *MtSer6*, *MtSer7*, *MtSer8*, *MtSer9* and *MtSer10*) and 3 ferritin genes (*MtFer1*, *MtFer2* and *MtFer3*) in well-watered nodules at 14 and 25 days after treatment (DAT). Water treatment (Day 0) was started at 30 dpi to keep the field capacity of soil at 95%. *MtELF1* was used here as a positive control.

3.2.7 Relative transcript abundance of serpin and ferritin genes in nodule under drought stress

As 5 serpins (*MtSer5*, *MtSer6*, *MtSer8*, *MtSer9* and *MtSer10*) and 3 ferritins (*MtFer1*, *MtFer2* and *MtFer3*) were confirmed as positively expressed genes in the nodules of *M. truncatula* through PCR cDNA amplification (Fig. 3), the following study hypothesized that nodules might express serpin and/or ferritin genes in response to drought stress. The serpin and ferritin genes identified above were then selected to further investigate relative transcript abundance in nodules in response to drought stress (70% FC) at 25 and 42 DAT. *M. truncatula* plants were grown for 30 days with *E. meliloti* and two different soil moisture contents were maintained for another 42 days (Experiment 2, Chapter 2). Soil moisture contents were maintained at 75% FC (DAT-W) for drought treatment and at 95% FC (DAT+W) for well-watered control treatment (Chapter 2). Nodules from well-watered plants (95% FC) harvested at 25 and 42 DAT+W were used as a control. To determine the transcript abundance changes of the genes, the relative transcript abundance of each gene was studied using quantitative real time PCR as mentioned in Chapter 2. We observed that *MtSer5* expression was unchanged in the 25 and 42 DAT-W nodules as compared to control nodules (Fig. 7a). Interestingly, *MtSer6* was found to be expressed 18- and 25-fold higher at 25 and 42 DAT-W respectively as compared to the 25 DAT+W control nodules (Fig. 7b). Other serpin genes such as *MtSer8*, *MtSer9* and *MtSer10* were expressed only in control plant nodules but not in drought-stressed nodules (Fig. 7c,d,e). In the case of ferritins, a significant difference of *MtFer1* expression was not seen in drought stressed nodules as compared to control nodules (Fig. 7f). However, *MtFer2* expression was found to be 2.5- and 3.5-fold higher in the nodules at 25 and 42 DAT-W respectively as compared to the nodules in the control plants at 25 DAT+W (Fig. 7g). Interestingly, *MtFer3* expression was seen to be 3.5- and 8-fold higher in the 25 and 42 DAT-W nodules respectively as compared to control nodule at the same timepoints. It may be noted that expression of *MtFer3* in the control nodules was 2.5-fold significantly higher at 42 DAT+W than 25 DAT+W. Similarly, in drought stressed nodules, expression of *MtFer3* was seen to increase to 7-fold higher at 42 DAT-W as compared to 25 DAT-W (Fig. 7h). To further confirm the genes which are expressed predominantly in nodules in response to drought, we performed a comparative expression analysis based on relative expression. Results showed that among 5 serpin genes and 2 ferritin genes chosen for analysis, only *MtSer6* and *MtFer3* showed a significant increase in expression in response to drought stress (Fig. 8a,b). It may also be noted that expression of these genes in nodule increases by days of plant growth. A heat map figure (Fig. 9) also confirms that among 28 serpin and 3 ferritin genes present in *M. truncatula*, only *MtSer6, MtFer2* and *MtFer3* genes are being expressed in nodules in response to drought stress.

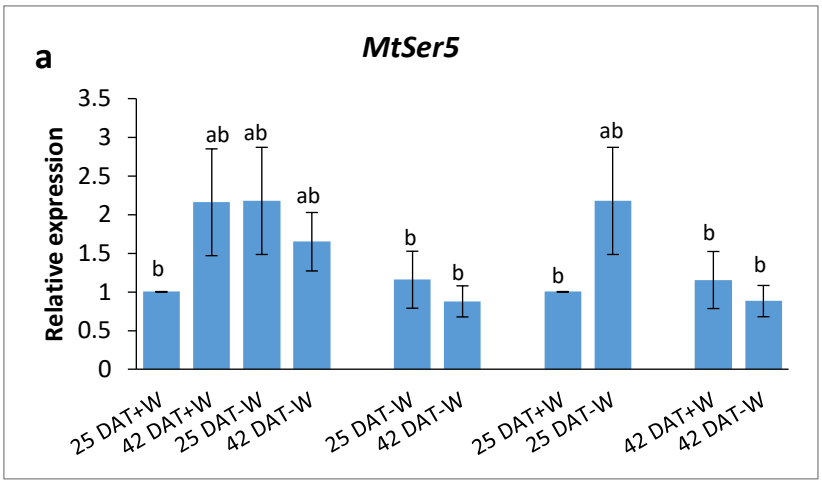
a
MtSer5
Relative expression
3.5
3
2.5
2
1.5
1
0.5
0
b
ab
ab
ab
b
b
b
ab
b
b
25 DAT+W
42 DAT+W
25 DAT-W
42 DAT-W
25 DAT-W
42 DAT-W
25 DAT+W
25 DAT-W
42 DAT+W
42 DAT-W

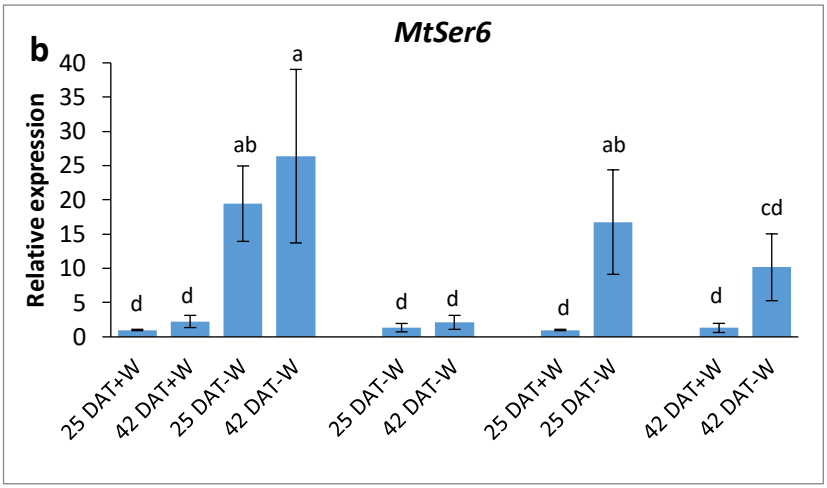
b
MtSer6
Relative expression
40
35
30
25
20
15
10
5
0
d
d
ab
a
d
d
d
ab
d
cd
25 DAT+W
42 DAT+W
25 DAT-W
42 DAT-W
25 DAT-W
42 DAT-W
25 DAT+W
25 DAT-W
42 DAT+W
42 DAT-W

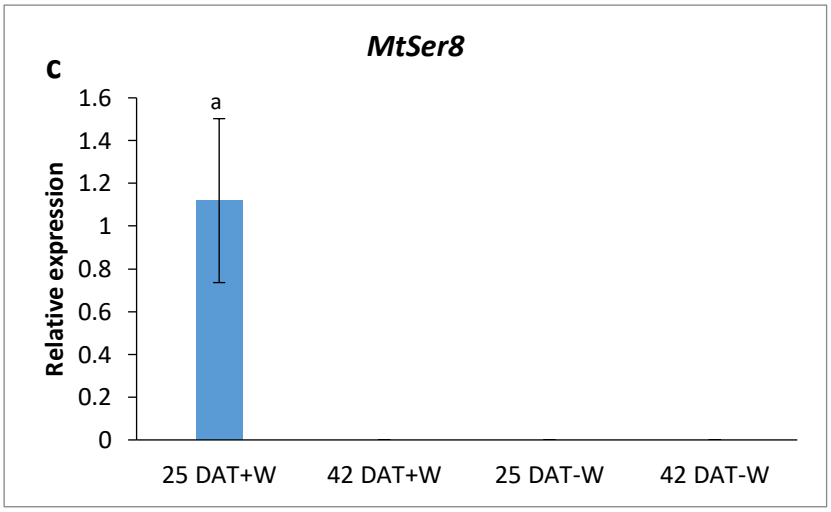
c
MtSer8
Relative expression
1.6
1.4
1.2
1
0.8
0.6
0.4
0.2
0
a
25 DAT+W
42 DAT+W
25 DAT-W
42 DAT-W

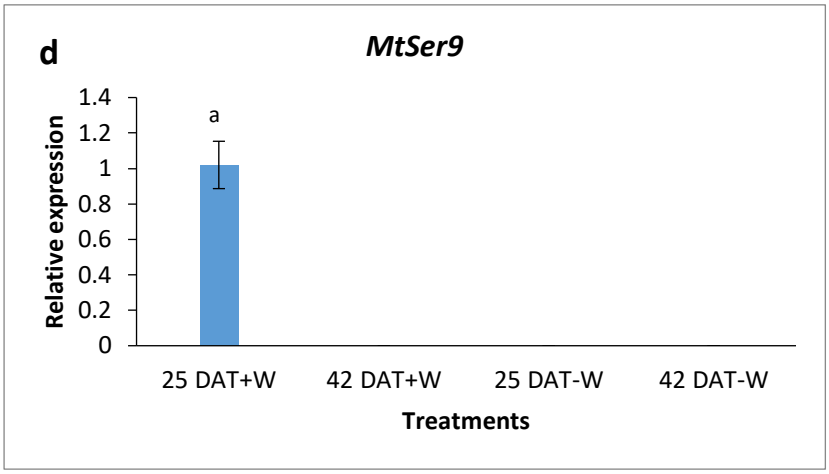
d
MtSer9
Relative expression
1.4
1.2
1
0.8
0.6
0.4
0.2
0
a
25 DAT+W
42 DAT+W
25 DAT-W
42 DAT-W
Treatments

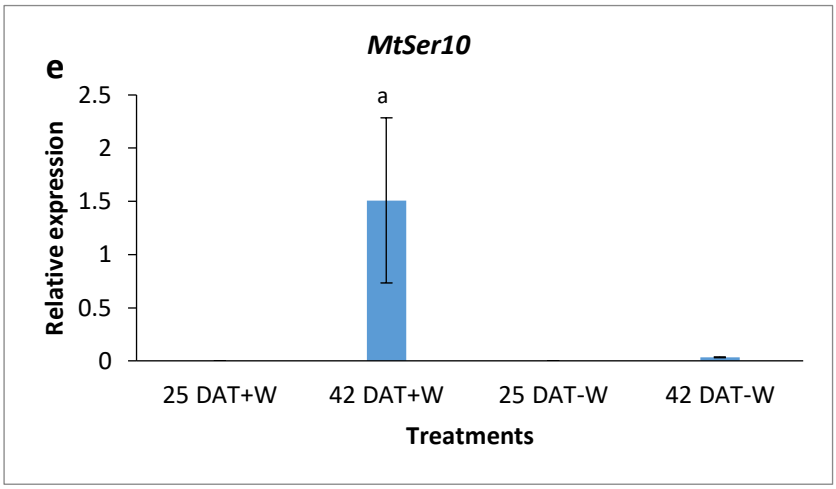
e
MtSer10
Relative expression
2.5
2
1.5
1
0.5
0
a
25 DAT+W
42 DAT+W
25 DAT-W
42 DAT-W
Treatments

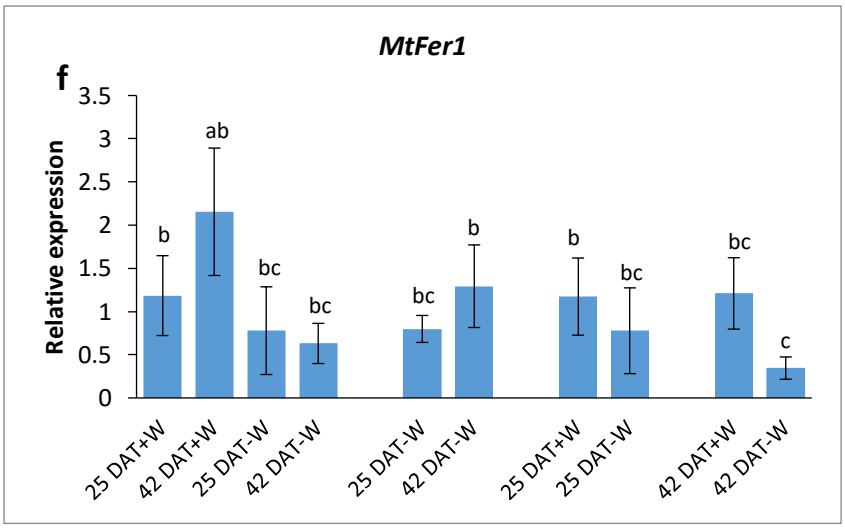
f
MtFer1
Relative expression
3.5
3
2.5
2
1.5
1
0.5
0
b
ab
bc
bc
bc
b
b
bc
bc
bc
c
25 DAT+W
42 DAT+W
25 DAT-W
42 DAT-W
25 DAT-W
42 DAT-W
25 DAT+W
25 DAT-W
42 DAT+W
42 DAT-W

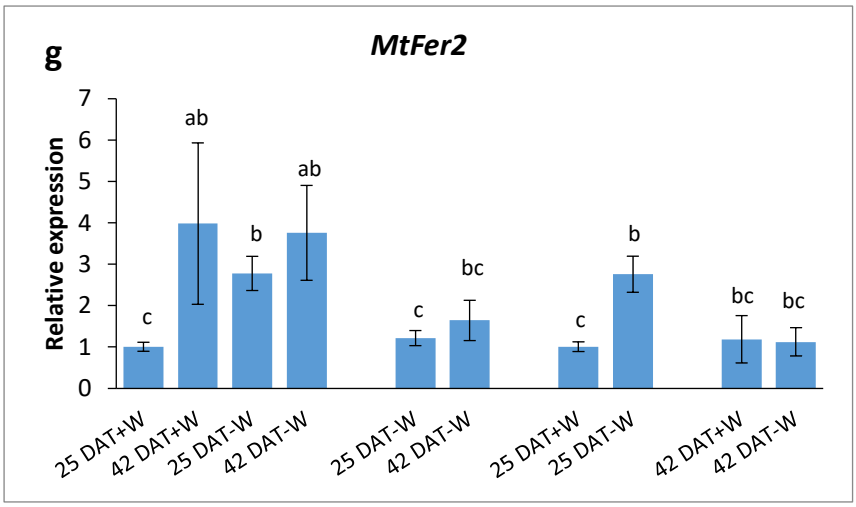

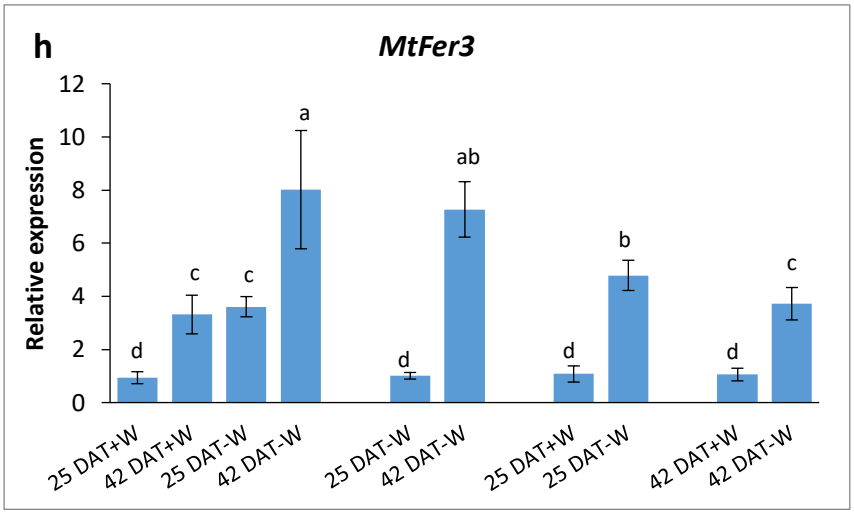

Fig. 7. Expression of serpin and ferritin genes in response to drought. Relative expression of *MtSer5* (a), *MtSer6* (b), *MtSer8* (c), *MtSer9* (d), *MtSer10* (e), *MtFer1* (f), *MtFer2* (g) and *MtFer3* (h) in in nodules in response to drought. Relative transcript abundance (fold change) was determined by qRT-PCR and was normalized to the control treatment using two internal reference control genes (*βTubulin* and *MtPDF2*). Same treatments were used multiple times for relative comparison with other treatments, where necessary. Bars represent the standard errors of means different letters on each bar represents the significant differences at $p<0.05$ according to ANOVA-Post Hoc Tukey's test. Water levels in the plant soil mixture was maintained at 95% (+W) for the control treatment and 70% (-W) for the drought treatment. DAT is days after treatment.

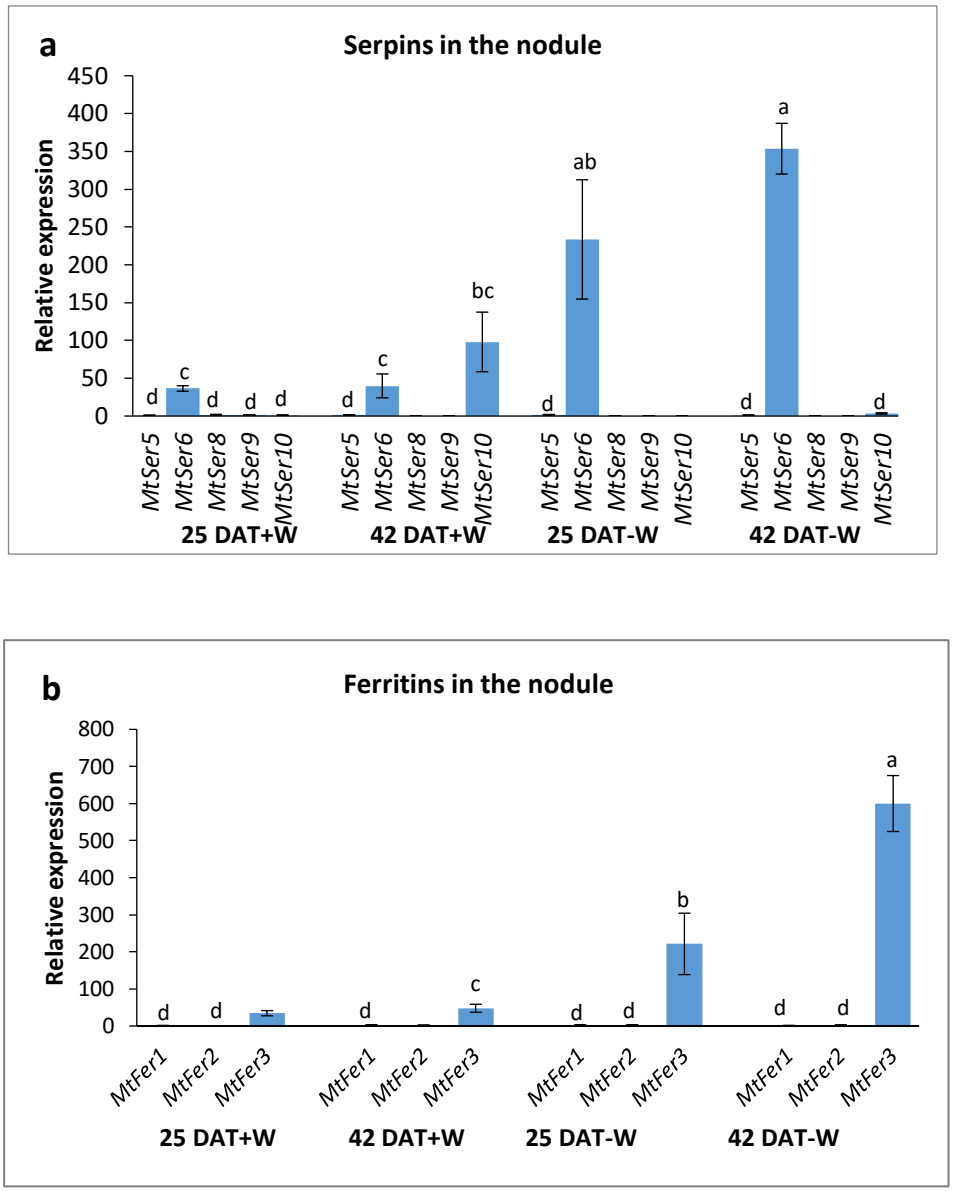

Fig. 8. **Comparison of relative expression of serpin (a) and ferritin (b) genes in response to drought in the nodule.** Water level in plant soil mixture was maintained at 95% (+W) for control treatment and 70% (-W) for drought treatment. DAT is days after treatment. Relative transcript abundance (fold change) was determined by qRT-PCR and was normalized to control treatment using two internal reference control genes (*βTubulin* and *MtPDF2*). Bars represent the ± standard errors of mean and different letters on each bar represents the significant differences at $p<0.05$ according to ANOVA-Post Hoc Tukey's test.

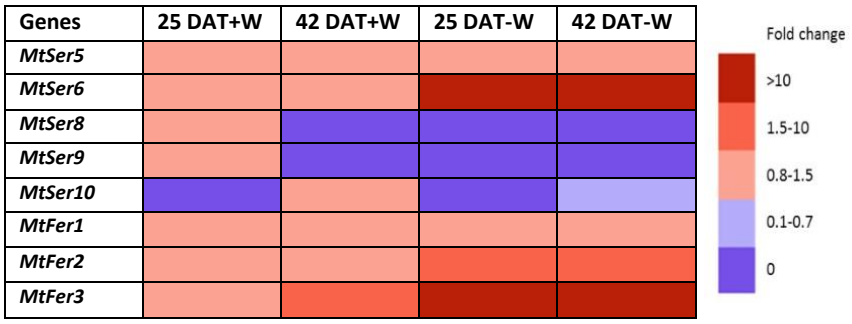

Fig. 9. Transcriptional changes of 5 serpin and 3 ferritin genes in nodule of *M. truncatula* under well-watered and drought conditions. Water levels in the plant soil mixture was maintained at 95% (+W) for control treatment and 70% (-W) for drought treatment. DAT is days after treatment. The scale at the right denotes transcript abundance (fold change). The relative expression of all genes was determined using qRT-PCR and data were normalized using two internal reference controls (β*Tubulin* and *MtPDF2*).

3.3 Discussion

The nitrogen fixation capability of legume nodules is sensitive to drought stress as the nodules were reported to be the first organ affected by drought (Marquez-Garcia *et al.,* 2015). Under such a stress condition, nodules may undergo early senescence to avoid a plant investing more carbon or to remobilize protein rich nodule nutrients for plant growth recovery (Fenta *et al*., 2014; Guerra *et al*., 2010). Major causes of early nodule senescence are both a wide range of proteolytic activity and excess iron toxicity according to previous studies (Pierre *et al*., 2014; Delaat *et al*., 2014; Ravet *et al*., 2014). However, it has been shown in *Arabidopsis thaliana* that serpin can inactivate the cysteine proteases which cause cell damage, and ferritins can scavenge toxic irons which cause cellular homeostasis and PCD in plants. Therefore, I speculated that *M. truncatula* nodule may involve serpin and ferritin to control the proteolytic activity and excess iron release which causes early nodule senescence. To begin answering this question, I aimed to identify the key serpin and ferritin genes in the *M. truncatula* nodule expressed under drought stress.

This chapter began with characterizing the symbiosis of *M. truncatula- E. meliloti* under N free condition. A study of symbiotic characteristics in the *M. truncatula-E. meliloti* association showed that at 14 dpi the first root nodules become visible and the number of nodules increased to reach ~35 per plant by 72 dpi. However, nitrogenase activity started at only 20 dpi and increased until 60 dpi. At the late plant growth stage (72 dpi), a sudden drop of nitrogenase activity was seen but there was no drop in nodule numbers (Fig. 2b). These results may be explained by the observation that that when a plant ages it may reduce nitrogenase activity due to N redundancy (plant senses sufficient N) as described by Soper *et al*. (2014). Nodules at this late stage may undergo senescence but not a complete shutdown of nitrogenase activity as flowering and seed development still requires N (Van de Velde *et al*., 2006). Nitrogen fixation in SNF-dependent plants is a major component for photosynthesis and plant growth as the fixation provides aminoacids required for RuBisCO synthesis (Kirizii *et al*., 2007). Results from this study also confirm that the SNF-dependent *M. truncatula* sustains its growth and photosynthetic rate in part by active N fixation (Fig. 3a, b). Environmental stress is an important limiting factor for nodule-rhizobia symbiosis in legumes which affects the nitrogen fixation by increasing ureides accumulation in nodule and nodule aging by increasing the proteolytic activity and iron toxicity (Marquez-Garcia *et al.,* 2015; Van de Velde *et al*., 2006; Guerra *et al*., 2010). Under such stress, senescence associated genes (SAGs), such as protein kinases and cysteine proteases, were shown to be involved in stress-induced nodule senescence of *M. truncatula* (Guerra *et al*., 2010). In addition, plants may also have many defence and environmental stress-responsive regulatory genes in every organ, including nodules. Serpins and ferritins are gene families reported to be present in different organs of *A. thaliana*, *M. truncatula*, and *Zea mays* such as leaf, root, seeds etc. (Rustgi *et al*.,

2017; Vercammen *et al*., 2006; Bournier *et al*., 2013; El-Yahyaoui *et al*., 2004; Thoiron *et al*., 1997). The present study showed that *M. truncatula* possess, 28 serpin genes and 3 ferritin genes and expresses 5 serpins (*MtSer5*, *MtSer6*, *MtSer8*, *MtSer9* and *MtSer10*) and 2 ferritins (*MtFer2* and *MtFer3*) genes in the nodule. As discussed above, induction of proteolytic activity and excess iron release in nodule by a plant in response to drought stress are deleterious to nodule senescence. Plant may however control these deleterious factors by regulating serpin and ferritin in order to reduce the risk of early nodule senescence and consequent plant growth reduction. I identified that serpin *MtSer6* and ferritins *MtFer2* and *MtFer3* are expressed in nodule in response to drought stress (Fig. 7b,g,h). In particular, the expression of *MtFer3* increased with age under drought stress (Fig. 8b). This data suggests that the identified serpin *MtSer6* and ferritins *MtFer2* and *MtFer3* might be involved in the drought-induced nodule senescence process of *M. truncatula.*

Chapter 4

M. truncatula Jemalong A17 and R108 suppress SNF in different ways in response to N fertilizer and drought

4.1 Introduction

In intensive agricultural systems, N fertilizers are still used in legume cultivation because plants can uptake N directly from the soil at a lower carbon cost than fixing N through forming symbiotic relationships. However, it is concerning that the use of N fertilizer creates serious negative consequences such as decline of soil organic matter, fertility, eutrophication and global warming (Minchin & Witty, 1997; Crews & Peoples, 2003).

Previous studies have shown that SNF in legumes is suppressed under N availability in the soil or during drought stress (Goh *et al*., 2016; Pierre *et al*., 2014; Pladys & Vance, 1993). Nitrate supplements may decrease the nodulation efficiency by reducing the root flavonoid synthesis, which acts as a primary signalling molecule to induce nodulin genes for rhizobial infection (Waterer & Vessey, 1993; Bollman & Vessey, 2006; Xia *et al.,* 2017). To maintain a balanced energy carbon investment in order to avoid excessive nodule formation and reduce the carbon investment in the presence of nitrate in soil, plants control the symbiosis through autoregulation of nodulation (AON). In the presence of nitrate in the soil, plant-induced CLAVATA-like root signal peptides activate a shoot acting leucine rich receptor-like kinase which inhibits the nodulation (Okamoto *et al.,* 2009). However, growth of nodules already differentiated could not be prevented by AON (Saito *et al.,* 2014). Legume plants under excess N availability may then inhibit nitrogenase activity through N feedback regulation. N compounds such as glutamine and asparagine are being loaded in the phloem sap, which then exports to roots and nodules. Accumulation of these amino acids in nodules negatively affected nitrogenase activity, present in nodules, by reducing nodule permeability to O_2 (Neo & Layzell, 1997; Bacanambo & Harper, 1997).

Water limiting growth conditions affect carbon fixation, which in turn can affect bacteroid respiration and root nitrogenase activity because of carbon shortage and oxygen limitation (Serraj *et al*., 1999). It has been shown that drought stress affects the activity of sucrose synthase, which is essential for supplying a major carbon source, sucrose to bacteroids (Arrese-Igor *et al*., 1999). Moreover, drought stress may reduce the nitrogenase activity by inducing early nodule senescence (Schiltz *et al*., 2004; Distelfeld *et al*., 2014). Considering the importance of SNF in sustainable agriculture system, it is necessary to determine how SNF is affected by external N availability and drought to improve crop productivity, particularly in dry environments.

To investigate the response of symbiosis to N fertilizer treatment, two *M. truncatula* wild type genetic backgrounds, Jemalong A17 and R108 were used in this study. Wang *et al*. (2014) demonstrated that *M. truncatula* genotypes, Jemalong A17 and R108, differ in response to aluminium toxicity, salt stress and iron deficiency and show genomic variations. A recent study by Luo *et al*. (2016) described that the two *M. truncatula* genotypes, Jemalong A17 and R108, differentially responded to drought stress and N fertilizer treatments when not inoculated with rhizobia and therefore unable to perform SNF; in particular, Jemalong A17 was seen to be more drought tolerant than R108.

In this chapter, I therefore hypothesized that symbiotic N-fixing *M. truncatula* Jemalong A17 and R108 may differentially suppress SNF in response to external N fertilizer treatment under well-watered and water limiting growth conditions.

4.2 Results

4.2.1 Symbiosis phenotype varies between *M. truncatula* Jemalong A17 and R108

SNF characteristics vary from plant to plant and I first evaluated the phenotype of symbiosis on selected WT genotypes, Jemalong A17 and R108, and mutants Jemalong A17 *dnf5-2* and Jemalong A17 *dmi1-3* in a 32-days experiment. Plants were grown with and without (control) *E. meliloti* for 32 days and nodule phenotypes such as nodule biomass and nodule morphology were observed at 20, 26 and 32 days post inoculation (dpi). Nodule dry weight was seen significantly higher in the Jemalong A17 and R108 plants as compared to the mutants (Fig. 1a). To examine the size and physiology of nodules in mutants and WT genotypes, nodules were sectioned, stained with toluidine blue and observed under the microscope. Microscopic images showed an absence of meristem development in the *dmi1-3* mutant, minor bacteroid differentiation or division in the *dnf5-2* mutant. In contrast, well-differentiated bacteroids were found in Jemalong A17 and R108 plants (Fig. 1b). Interestingly, when the symbiotic phenotype differences between Jemalong A17 and R108 were observed, R108 nodules were visibly seen longer with a higher nodule biomass and contained more bacteriods than Jemalong A17 nodules (Fig. 1a, b, Appendix 6.1). In particular, R108 showed a 30-40% higher nodule biomass than Jemalong A17 (Fig. 1b). Thus, symbiotic phenotypes exist between the Jemalong A17 and R108 WT genotypes.

4.2.2 Symbiotic nitrogen fixation confers growth benefits to Jemalong A17 and R108 plants

As the symbiotic phenotypes were different between the genotypes Jemalong A17 and R108, I hypothesized that SNF and the effect on plant growth would also vary in both genotypes. WT plants, Jemalong A17 and R108, and mutant plants, Jemalong A17 *dnf5-2* and Jemalong A17 *dmi1-3,* were grown with and without (control) *E. meliloti* for 32 days and physiological and growth measurements were performed at 20, 26 and 32 days post inoculation (dpi). I first tested the nodule nitrogenase activity and found that there was zero activity in uninoculated plants, very low activity in mutants and high activity in the WT plants. Specifically, the *dmi1-3*, *dnf5-2*, Jemalong A17 and R108 plants produced 0, 200, 2900 and 3500 nM of ethylene/hour/g of nodule fresh weight respectively at 32 dpi (Fig. 1c.). I then investigated the chlorophyll content and photosynthetic rate in all plants. Results showed that chlorophyll content and photosynthetic rates were significantly lower in the leaves of uninoculated wild types and the two mutants as compared to *E. meliloti*-inoculated WT Jemalong A17 and R108 plants (Appendix 6.2a,b). Furthermore this was found coincided with significantly higher shoot biomass and plant growth in *E. meliloti* -inoculated WT plants than that of mutants (Fig. 2a,b). It was

also found that R108 root nodules contained significantly higher nitrogenase activity as compared to Jemalong A17 nodules (Fig. 1c, 2a,b). In addition, R108 shoots showed a nearly 50% higher shoot biomass than Jemalong A17 at 32 dpi (Fig. 2a). This study showed that the effect of symbiosis on plant growth was well pronounced in WT plants and, R108 exhibited a better growth than Jemalong A17.

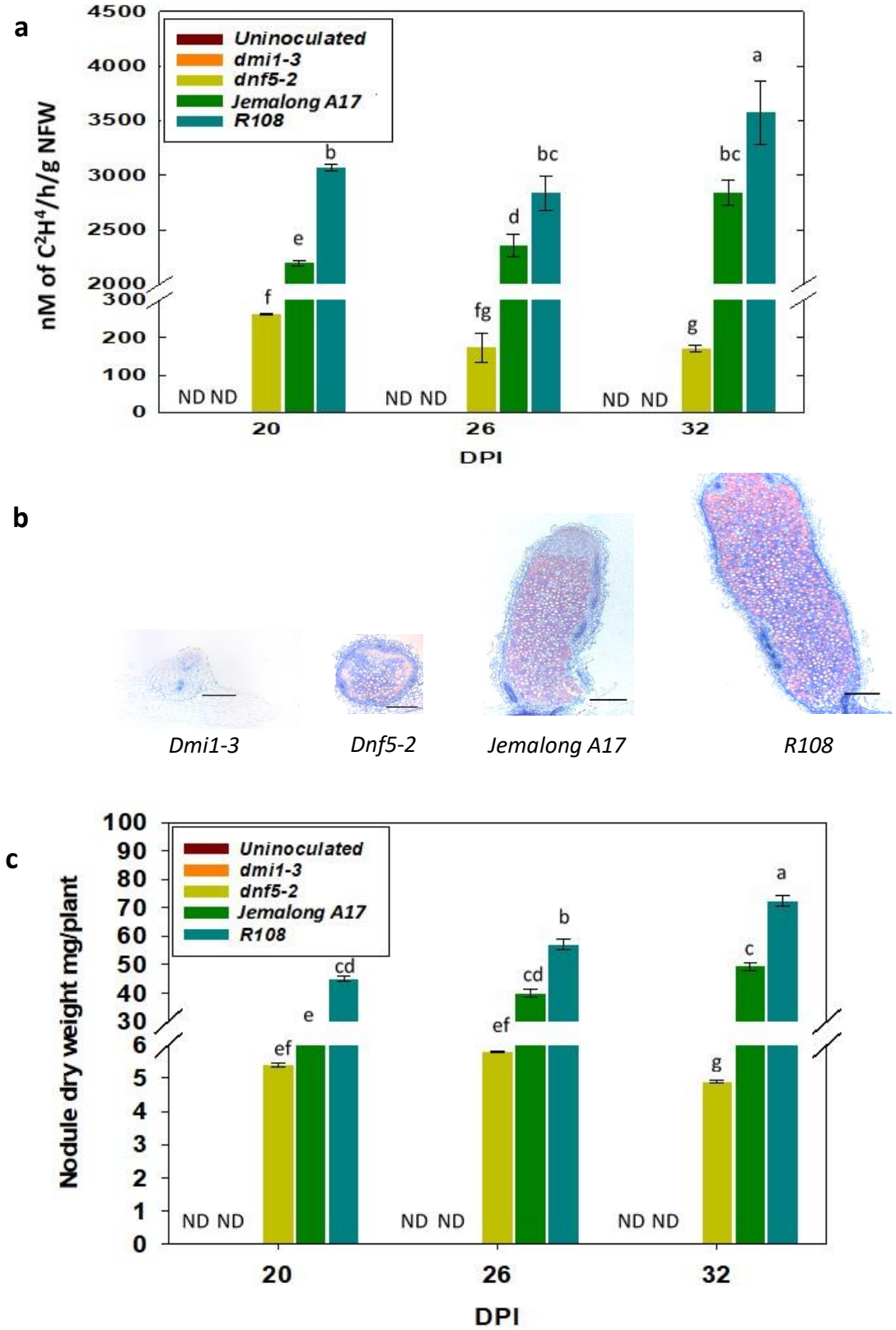

Fig. 1. Symbiotic attributes of WT *M. truncatula* plants and non-N fixing mutants. Nitrogenase activity (a), nodule morphology (b) and nodule dry weight (c) of plants grown under N-free medium for 32 days. Values are the mean of three biological replicates. Error bars represent the standard errors of mean and different letters on each bar represents the significant differences at $p<0.05$ according to ANOVA-Post Hoc Tukey's test. ND is not detectable and the scale bar in the nodule images indicates 200µm length. Uninoculated control is a WT Jemalong A17.

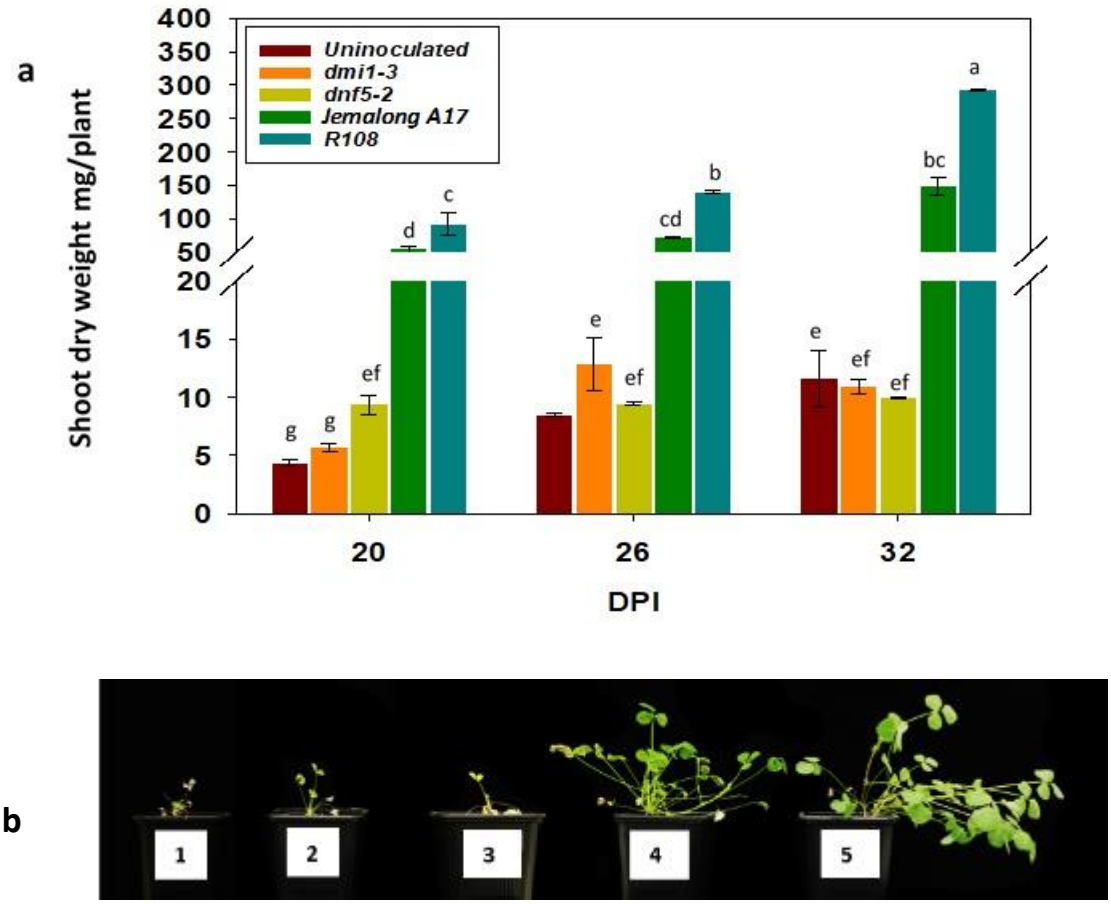

Fig. 2. Impact of SNF on plant growth. Shoot dry weight (a) and 32-day old *M. truncatula* WT genotypes (Jemalong A17 and R108) and non-N fixing mutants (*dnf5-2* and *dmi1*-3) grown under N-deficient medium (b) (Pot 1, uninoculated; pot 2, *dnf5-2*; pot 3, *dmi1-3*; pot 4, Jemalong A17; pot 5, R108). Values are the mean of three biological replicates. Error bars represent the standard errors of mean and different letters on each bar represents the significant differences at $p<0.05$ according to ANOVA-Post Hoc Tukey's test. Uninoculated control is WT Jemalong A17.

4.2.3 Nitrogen fertilizer supresses the N uptake from SNF in Jemalong A17 but not R108

As seen above, SNF is important for plant growth of Jemalong A17 and R108 genotypes as it is a primary source of N under N limited conditions. According to the previous reports, addition of high nitrate (10mM) during legume growth reduces SNF completely (Liu *et al*., 2006; Goh *et al*., 2016). This study therefore hypothesizes that N fertilizer treatment would result in reduction of N uptake from SNF in Jemalong A17 and R108 plants under well-watered conditions. To determine the amount of N partitioned in the shoot from N fertilizer and nodules, plants were treated with heavy isotope labelled ^{15}N fertilizer at 10mM concentration. In biological materials, ^{14}N is most abundant and ^{15}N is rare (99.6337% and 0.3663% of atmospheric N, respectively). By measuring the ratio of ^{14}N (derived from SNF) over ^{15}N (derived from N fertilizer), the relative contribution of SNF in plants can be calculated (He *et al.,* 2009; Chapter 2). From the data of this study we found that, N derivation from N_2 fixation process was completely suppressed at all tested time points in *E. meliloti*-inoculated Jemalong A17 plant as compared to untreated *E. meliloti*-inoculated plants (Fig. 3a, Appendix 6.3a). In contrast, the percentage of N derived from N_2 fixation process in the ^{15}N treated *E. meliloti* R108 plants was seen to increase to 10.23% and 23.18% at 26dpi and 32dpi respectively as compared at 20 dpi (0%) while untreated *E. meliloti* R108 showed complete N derivation from SNF (Fig. 3b, Appendix 6.3b). The data showed that under well-watered conditions, N derivation from N_2 fixation process was completely suppressed in Jemalong A17 by external N fertilizer treatment but not in R108.

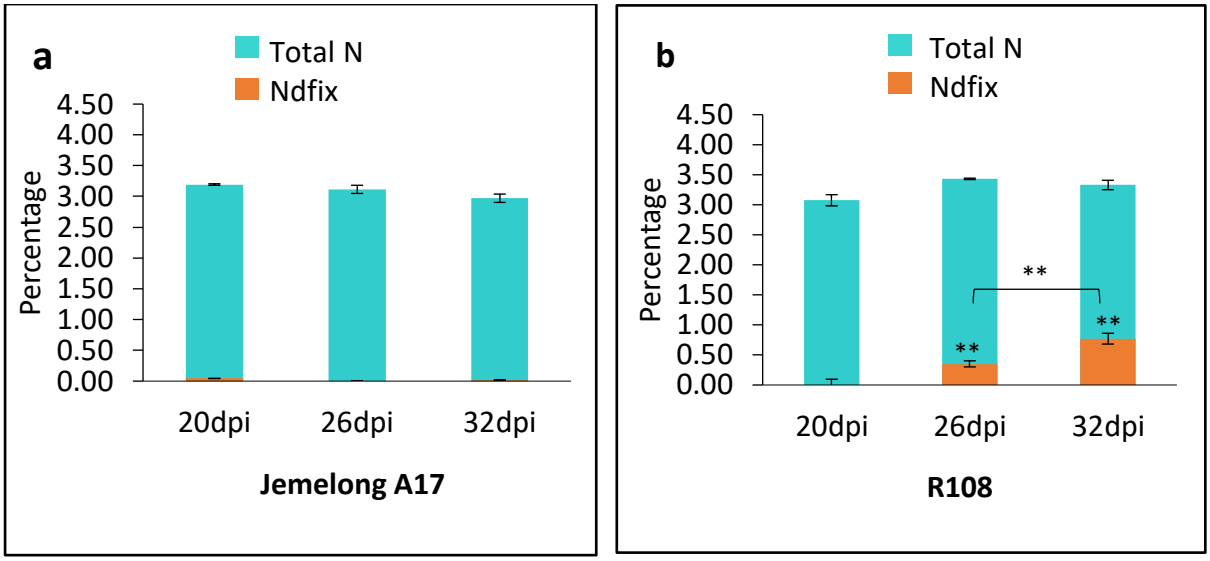

Fig. 3. Effect of external N fertilizer treatment on N uptake from SNF. Percentage of total N and Ndfix (N derived from fixation) per shoot biomass of ^{15}N treated and *E. meliloti* inoculated Jemalong A17 (a) and R108 plants (b). Plants were inoculated at 0 days post-inoculation (dpi) and measurements were taken at 20, 26 and 32 dpi. Values are the mean of three biological replicates. Error bars represent the standard errors of mean and asterisks indicate the significant differences from 20dpi at $p<0.01$ according to student's *t*- test.

4.2.4 *E. meliloti* inoculation suppresses the N uptake from N fertilizer in R108 but not Jemalong A17

N uptake from SNF was seen suppressed in Jemalong A17 and not in R108 upon N fertilizer treatment. I therefore hypothesized that ^{15}N fertilized Jemalong A17 plant may not supress the N uptake from N fertilizer to balance the N level in shoot as it completely inhibits the N uptake from SNF. In contrast, since genotype R108 did not fully suppress SNF, it is expected that N uptake from fertilizer is suppressed in the presence of the two N sources. N uptake from N fertilizer was determined by measuring the ^{15}N percentage in shoot of ^{15}N treated and *E. meliloti* inoculated or uninoculated Jemalong A17 and R108 plants (Fig. 4). This data showed that the ^{15}N percentage in *E. meliloti*-inoculated and uninoculated Jemalong A17 plants, grown under well-watered conditions, did not drop at any point during the time-course (Fig.4a). While uninoculated R108 plants did not show a reduction of ^{15}N uptake, *E. meliloti*-inoculated R108 plants showed significant reduction of ^{15}N levels by 13% and 25% at 26 dpi and 32 dpi treatments, respectively as compared to levels at 20 dpi (Fig. 4b). Taken together, this study showed that in Jemalong A17 N uptake from N fertilizer was not suppressed, while in *E. meliloti*-inoculated R108 plants, the uptake of fertilizer was suppressed.

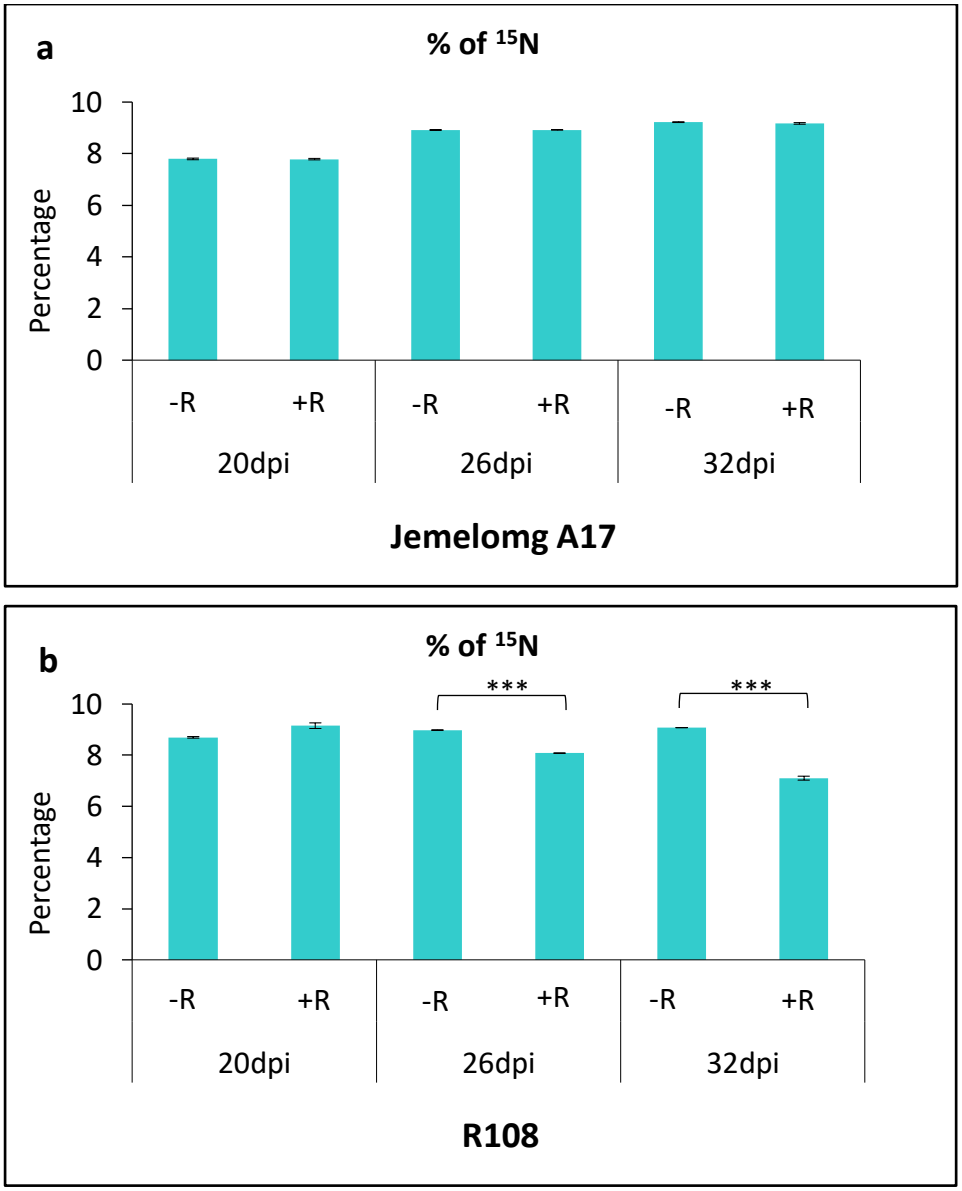

Fig. 4. Effect of *E. meliloti* inoculation on ^{15}N uptake in shoots of external N fertilizer treated *M. truncatula*. Percentage of ^{15}N from well-watered *E. meliloti* inoculated (+R) at 0 dpi and uninoculated (-R) *M. truncatula* genotypes Jemalong A17 (a) and R108 (b) grown with ^{15}N labelled N fertilizer. Percentage ^{15}N was measured 20, 26 and 32 dpi. Values are the mean of three biological replicates. Error bars represent the standard errors of mean and asterisks indicate the significant differences at $p<0.001$ according to students *t*-test. dpi, days post-inoculation.

4.2.5 Jemalong A17 and R108 plants balance the N level by controlling N uptake

The *M. truncatula* Jemalong A17 and R108 genotypes suppressed the N uptake from N fertilizer and SNF in different ways. This study hypothesizes that both the Jemalong A17 and R108 genotypes, however can balance the N uptake, such that the total N uptake is not affected by the availability of two N sources. To determine the level of total N in both plants, the N percentage as a fraction of dry weight was measured in Jemalong A17 and R108 plants inoculated with *E. meliloti* and treated with ^{15}N fertilizer. Result for Jemalong A17 plants showed that the total N percentage in the *E. meliloti* inoculated and N fertilizer treated plants was maintained at levels similar to that of the uninoculated and ^{15}N fertilizer treated plants (Fig. 5a). In regards of R108 plants, significantly higher N percentage was found at 26dpi in *E. meliloti*-inoculated and ^{15}N fertilized plant as compared to uninoculated and ^{15}N fertilizer treated plants, but a similar N level was seen at 32dpi as that of uninoculated and ^{15}N fertilizer treated plants (Fig. 5b). The results specify that both Jemalong A17 and R108 can balance the N level despite of two different N sources.

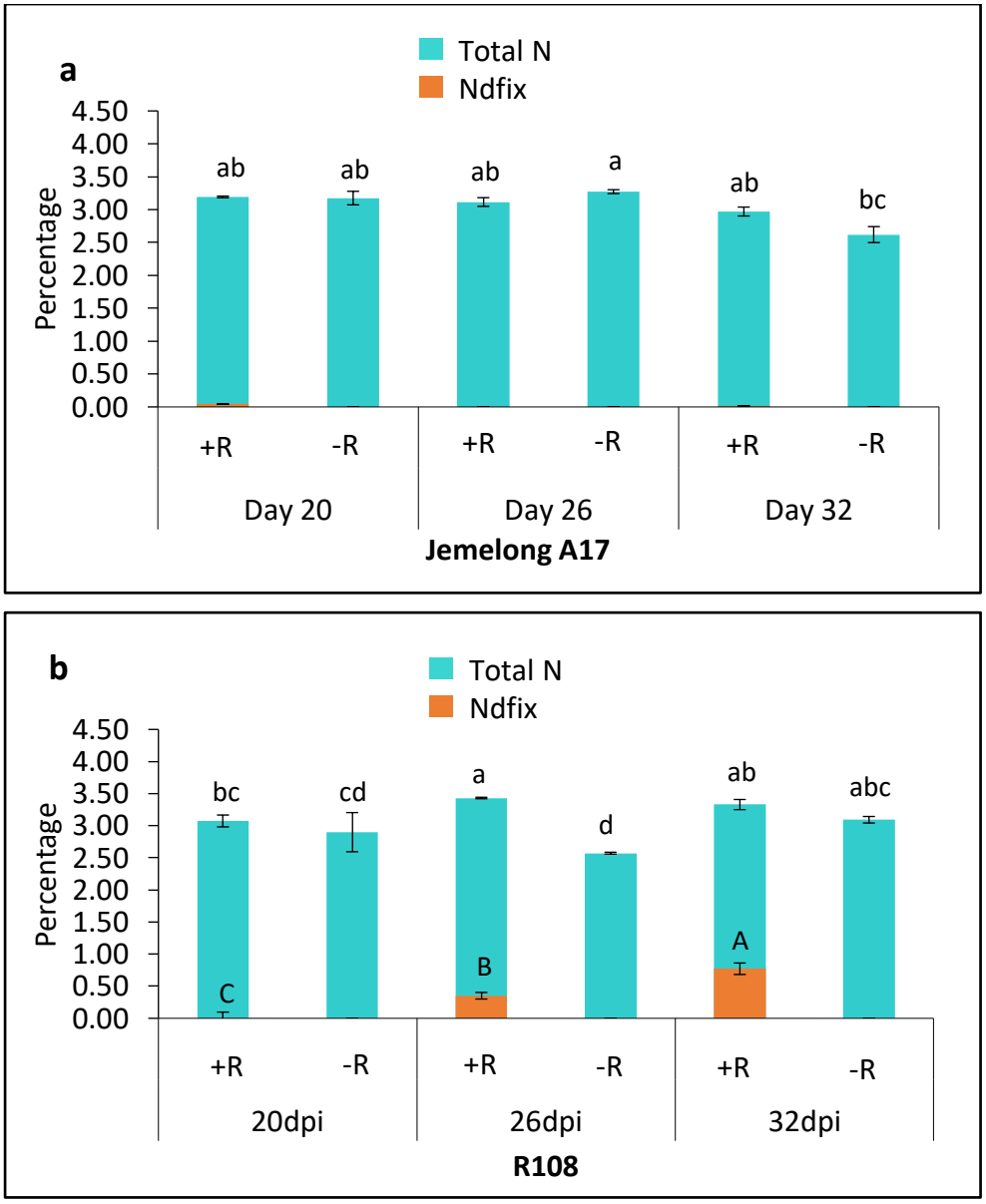

Fig. 5. Effect of external N fertilizer treatment and *E. meliloti* inoculation on total N level. Percentage of total N and Ndfix in shoots of ^{15}N treated and *E. meliloti* inoculated (+R) and uninoculated (-R) Jemalong A17 (a) and R108 plants (b). Inoculation took place at 0 days post-inoculation (dpi) and measurements were taken at 20, 26 and 32 dpi. Values are the mean of three biological replicates. Error bars represent the standard errors of mean and different letters (upper cases indicate between Ndfix values; lower cases between total N values) on each bar represents the significant differences at $p<0.05$ according to ANOVA-Post Hoc Tukey's test.

4.2.6 Jemalong A17 and R108 differ in nodule activity in response to external N fertilizer treatment

N fertilizer can suppress SNF by reducing nodule numbers and nitrogenase activity (Ohyama *et al*., 2011). Data from this study shows that N contribution from SNF in R108 was not completely suppressed in response to external N fertilizer treatment under well-watered conditions. Therefore, I hypothesized that nitrogenase activity, nodule and bacteroid numbers are less suppressed in R108 than Jemalong A17 under external N fertilizer treatment. Jemalong A17 and R108 plants were grown under well-watered conditions for 32 days with *E. meliloti* and with or without an external N fertilizer. Nodule numbers were first counted in both the plants to investigate the effects of N fertilization on nodulation. Results showed that nodule numbers in R108 plants treated with external N was not significantly different from non-treated R108 plants, while Jemalong A17 plants treated with external N fertilizer showed significantly less nodules at 26 and 32 dpi as compared to non-treated plants (Table 1a). Similarly, nitrogenase activity was not affected by external N fertilizer treatments in R108, while the Jemalong A17 plants showed significantly less nitrogenase activity upon N fertilizer treatment as compared to non-treated plants (Table 1b). As bacteroid numbers in nodules also influence nitrogenase activity as described by Barraza *et al*. (2012), I measured the number of mature bacteroids microscopically from similar sized nodules of N fertilizer treated and untreated Jemalong A17 and R108 plants. The data showed that in response to N fertilizer treatment, Jemalong A17 nodules contained significantly lower bacteroid numbers at 32 dpi as compared to nodules of untreated plants. In contrast, bacteroid numbers R108 nodules did not depend on the presence of N fertilizer (Appendix 6.4). The overall data herein specifies that nodule numbers, nitrogenase activity and bacteroid numbers in response to N fertilizer treatment were not suppressed in R108 while these characteristics were suppressed in Jemalong A17.

4.2.7 R108 alters the nodule plasticity in response to external N fertilizer treatment

During the course of the experiments, it was noted that nodule positioning differed between Jemalong A17 and R108 treated with N fertilizer. Therefore, I hypothesized that nodule spacing may correlate with SNF suppression. To investigate the position of nodules in the root systems, external N fertilizer treated and untreated *E. meliloti*-inoculated plants were uprooted and the distance of the nodules from root collar was measured at 32 dpi. Results showed that in the absence of external N in untreated *E. meliloti* inoculated Jemalong A17 and R108 plants, the distance and position of the nodules from root collar were similar in both genotypes. Interestingly, in response to N fertilizer treatments, the location of R108 nodules were altered as compared to N fertilizer treated Jemalong A17 and non-

treated R108 plants. Points of nodulation in N fertilizer-treated R108 plants were observed close to root collars, and the nodules were clustered (Fig. 6a,b). In the case of Jemalong A17 plants, there was no change in nodule localization in the external N fertilizer treated plants as compared to untreated plants (Fig. 6b, Appendix 6.5). This study highlights that nodule clustering correlates with a reduced suppression of SNF.

Table. 1. Effect of external N fertilizer treatment in nodule activity. Nodule numbers (a), nitrogenase activity (b) and of Jemalong A17 and R108 plants measured at 20, 26 and 32 dpi grown with or without N fertilizer. Treatments are watered (+W) and N fertilizer treated (+/-N). Values are the mean of three biological replicates. Means followed by the same letter were not significantly different at p≤0.05 according to ANOVA-Post Hoc Tukey's test. ± represent the standard error of mean.

a	Jemalong A17		R108	
Dpi	+W+N	+W-N	+W+N	+W-N
20	18.0±1.73^{d}	21.3±1.45^{cd}	14.0±1.15^{e}	17.6±1.45^{d}
26	18.6±1.20^{d}	24.0±1.70^{bc}	22.3±1.20^{c}	18.3±0.88^{d}
32	22.6±1.05^{c}	26.0±0.57^{a}	25.6±0.88^{a}	24.0±1.73^{ab}

b	Jemalong A17		R108	
Dpi	+W+N	+W-N	+W+N	+W-N
20	1620±12.1^{e}	2194±26.6^{cd}	3131±23.1^{de}	3069±27.6^{def}
26	1986±24^{d}	2353±203^{b}	3338±200^{cd}	2835±260^{ef}
32	2206±34.7^{bc}	2835±114^{a}	3370±70.0^{bc}	3572±295^{ab}

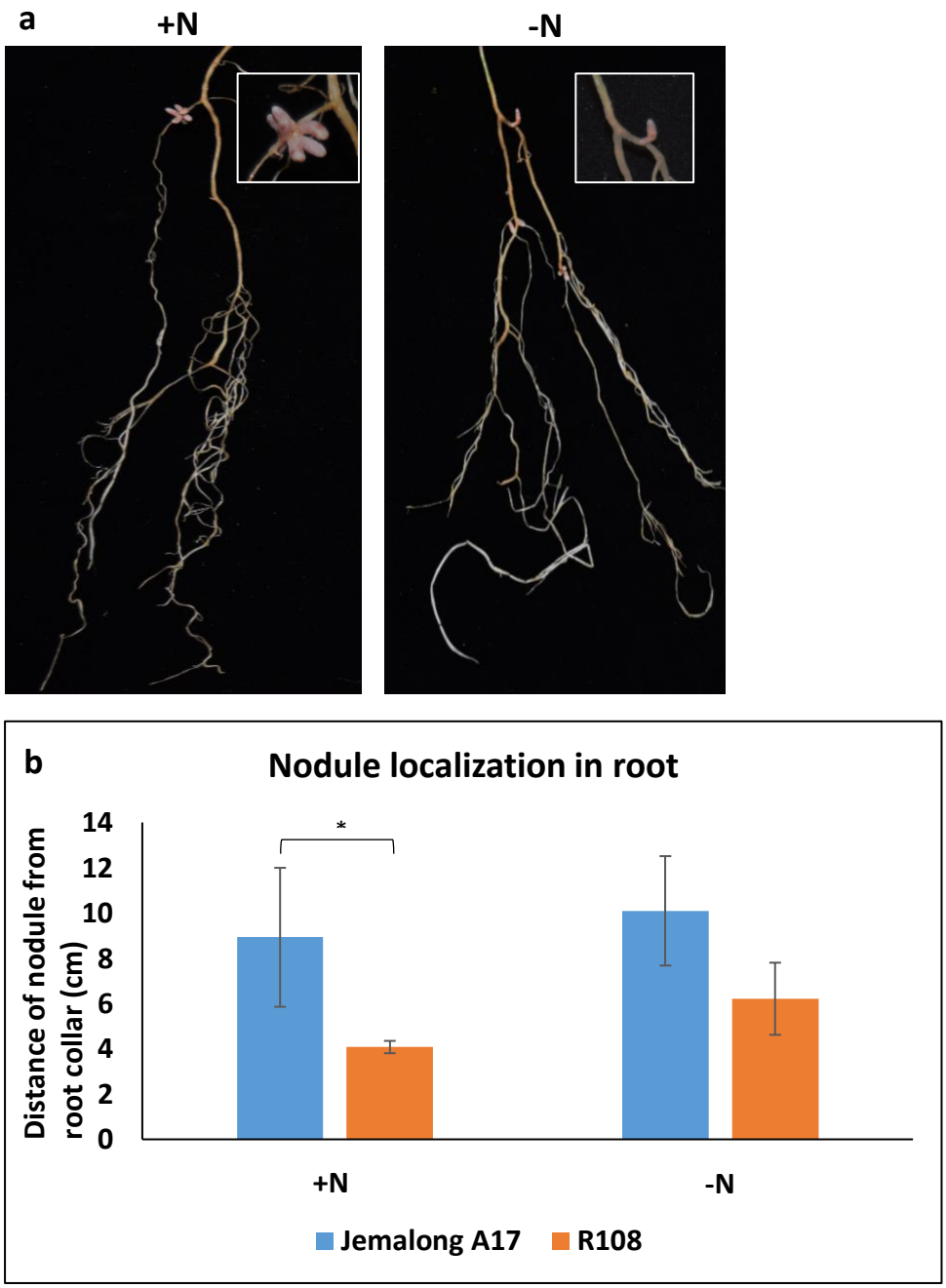

Fig. 6. Effect of external N fertilizer treatment on nodule localization in roots of *M. truncatula* R108. Root image containing nodules (a) and distance of nodules from root collar (b) at 32 dpi. Distance of 20 nodules from the root collars of three plants were measured. Plants were grown with (+N) or without (-N) N fertilizer. Error bars represent the standard errors of mean and asterisk indicates the significant differences at $p<0.05$ according to students *t*-test.

4.2.8 N uptake from N fertilizer is suppressed in both Jemalong A17 and R108, when grown in water limiting conditions

N uptake from N fertilizer was seen suppressed only in R108 and not in Jemalong A17 when grown under well-watered condition. Under water limiting conditions, reduced soil moisture may have significant impact on N uptake from N fertilizer as water is essential for nutrient movement in soil (He and Dijkstra, 2014). I hypothesized that N uptake from N fertilizer may become limited in both Jemalong A17 and R108. To determine the level of N uptake from N fertilizer, ^{15}N percentage was measured in shoots of *E. meliloti*-inoculated plants grown under drought stress. The result showed that under drought stress, the N uptake from N fertilizer was reduced by 26% and 35% at 26 and 32 dpi, respectively in Jemalong A17 as compared to 20 dpi (Fig. 7a). R108 plants showed further reduction (37% at 26 dpi and 45% at 32 dpi) as compared to 20 dpi (Fig. 7b). The data highlight that both genetic backgrounds reduce the N uptake from fertilizer when grown under water limiting conditions.

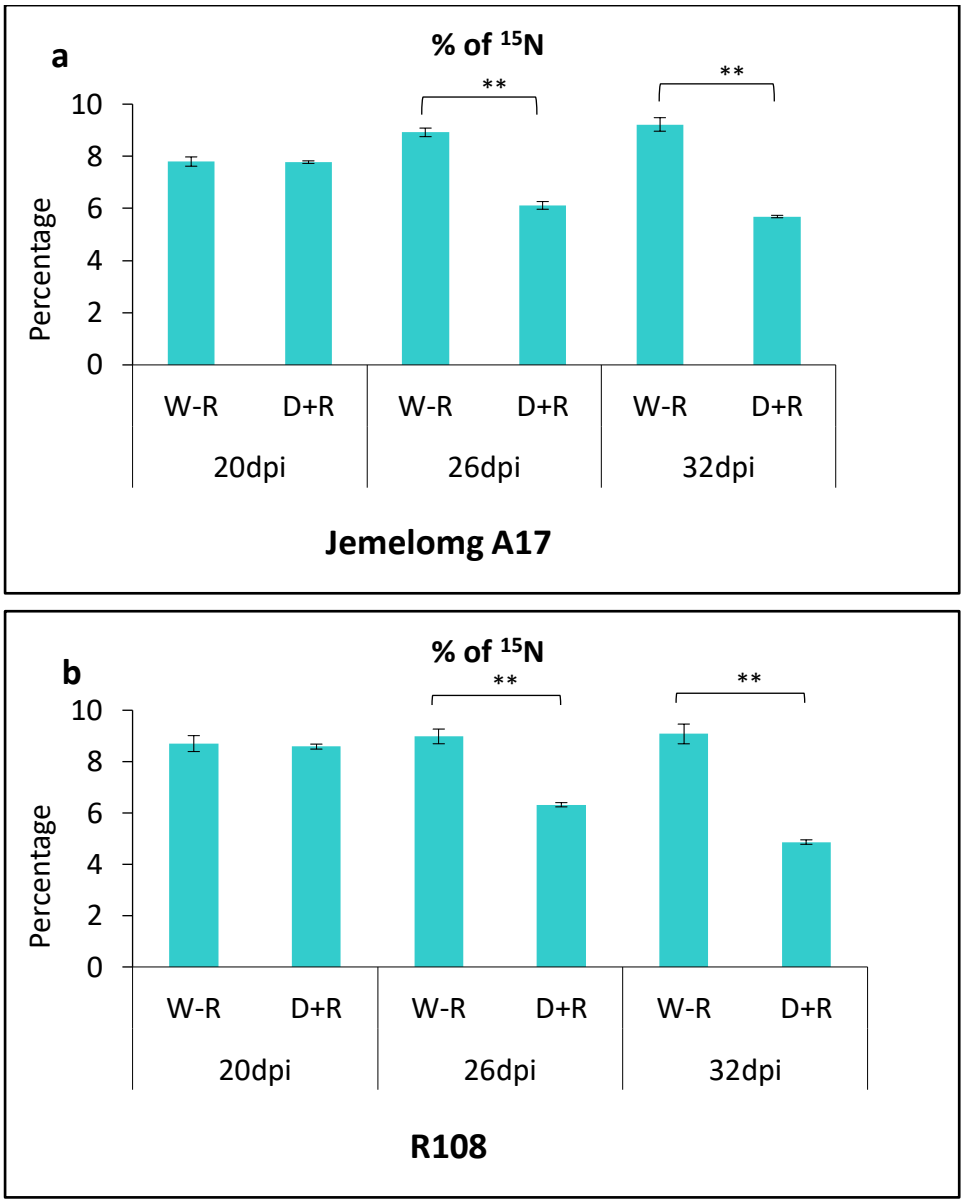

Fig. 7. Effect of drought stress on uptake of ^{15}N in shoots of external N fertilizer treated *M. truncatula*. Percentage of ^{15}N out of total N from drought stressed *E. meliloti* inoculated (+R) at 0 dpi and uninoculated (-R) *M. truncatula* genotypes Jemalong A17 (a) and R108 (b) grown under ^{15}N labelled N fertilization. Plant were well-watered until 20 dpi and were subsequently watered normally (W) or water was with-holded (D). Values are the mean of three biological replicates. Error bars represent the standard errors of mean and asterisks indicate the significant differences between two treatments at $p<0.01$ according to student's *t*-test.

4.2.9 Jemalong A17 and R108 acquired substantial N from SNF under drought stress

M. truncatula Jemalong A17 and R108 plants show differential drought response (Luo *et al*., 2016). According to previous reports, drought stress and the addition of N during legume growth reduces the process of SNF and limits the N export from nodules (Liu *et al*., 2006; Goh *et al*., 2016; Kunert *et al*., 2016). Data from above study showed that N uptake from N fertilizer is limited in both the genetic backgrounds under drought stress. I hypothesized that to maintain a sufficient N level for plant growth, Jemalong A17 and R108 plants may not have suppressed the N uptake from SNF in response to drought stress and N fertilization. To detect the amount of N partitioned in shoots from N fertilizer and/or nodules, the relative ^{14}N and ^{15}N contribution in total shoot N was determined from *E. meliloti*-inoculated Jemalong A17 and R108 plants treated with ^{15}N labelled N fertilizer. As a control, well-watered, uninoculated plants were treated with N fertilizer. Interestingly, in both Jemalong A17 and R108, the percentage of relative N derived from SNF increased over time to 40 and 48% in the case of Jemalong A17 and R108, respectively (Fig. 8a,b, Appendix 6.3a,b). As a result of continued N uptake from SNF, level of shoot N in Jemalong A17 and R108 plants under drought stress was maintained to the same level as well-watered plants (Fig. 8a,b). This data shows that suppression of N uptake from SNF by N fertilizer is reduced in both Jemalong A17 and R108 that are grown under water limiting conditions, likely to maintain shoot N levels.

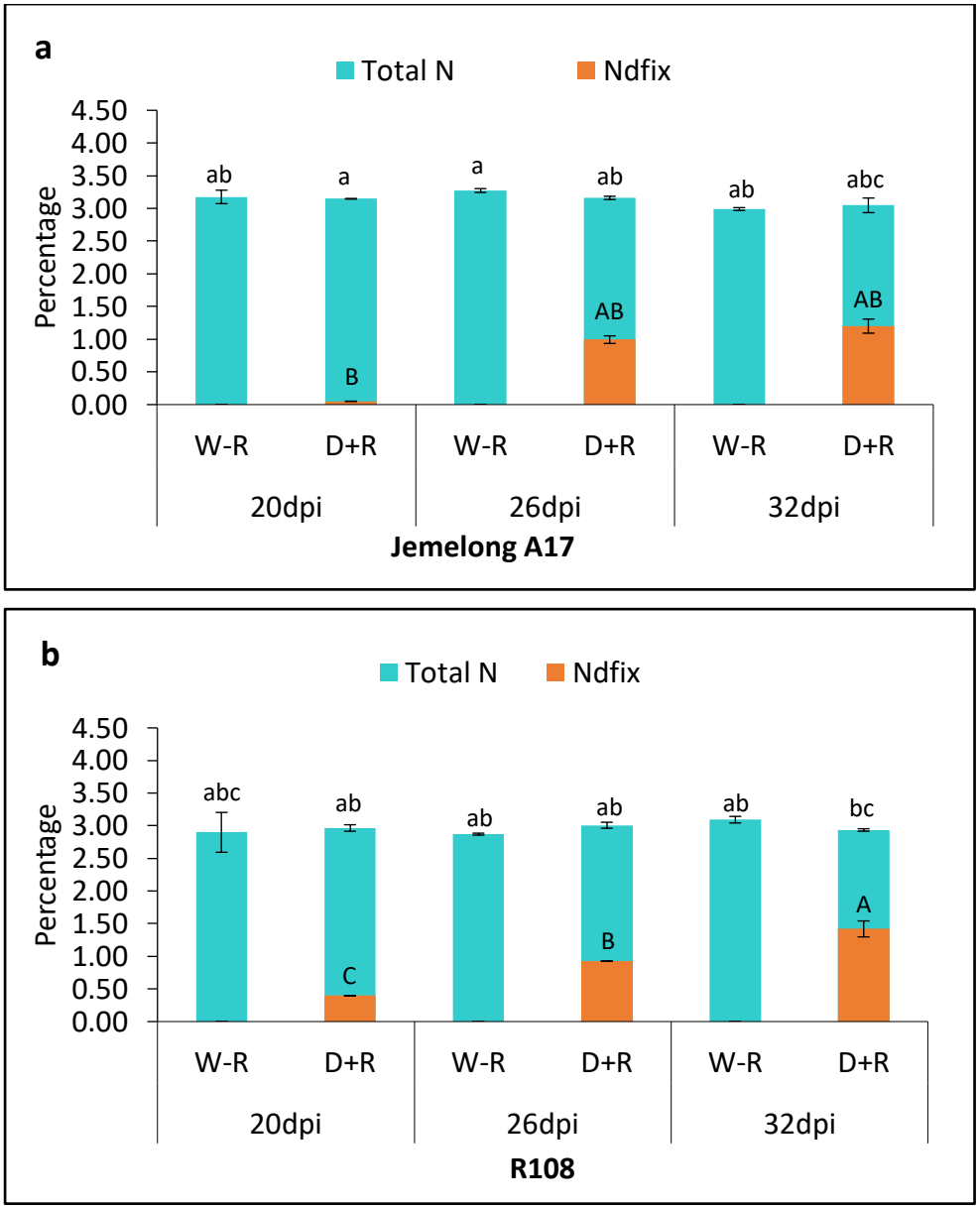

Fig. 8. Effect of drought stress and external N fertilizer treatment on N uptake from SNF and total shoot N level. Percentage of total N and Ndfix in shoots of ^{15}N treated and *E. meliloti* inoculated Jemalong A17 (a) and R108 plants (b). D, droughted; W, watered; +R, + *E. meliloti* inoculation; -R, -*E. meliloti* inoculation. Values are the mean of three biological replicates. Error bars represent the standard errors of mean and different letters (upper cases indicate between Ndfix of samples; lower cases indicate between total N of samples) on each bar represents the significant differences at $p<0.05$ according to ANOVA-Post Hoc Tukey's test.

4.2.10 Jemalong A17 and R108 plants sustain nodule activity and active bacteroids under N fertilization and drought treatment

As the N input from SNF in both Jemalong A17 and R108 was not suppressed under drought stress, I hypothesize herein that these plants might have sustained the nodule activity under drought stress. Therefore, I measured several parameters of nodule activity such as, nodule senescence, nodule numbers, bacteroid numbers and nitrogenase activity. External N fertilizer-treated and *E. meliloti*-inoculated plants were grown until 20 dpi, after which water was withheld for a subset of plants to induce drought stress, while control plants continued to receive water. Nodules harvested at 32 dpi were first observed under the microscope after sectioning and staining with toluidine blue to determine the extent of nodule senescence. Microscopic results show that some nodule senescence was induced in drought-treated WT Jemalong A17 and R108 plants, as compared to well-watered plants. Both Jemalong A17 and R108 plants showed highly packed matured bacteroids in 70-80% of nodule tissue area (Fig. 9a). I then measured the effect of drought on nodulation and bacteroids, by counting the nodule and healthy bacteroids numbers (counted microscopically from similar sized nodules) at 20, 26 and 32 dpi in plants. Results showed that the number of nodules was maintained consistently without a significant increase or decrease (Appendix 6.6). Concomitantly, the number of bacteroids per nodule were significantly increased at 26 and 32 dpi in both Jemalong A17 and R108 plants as compared to nodules sampled at 20 dpi (Appendix 6.7). Then to investigate the effects of drought stress on nodule nitrogenase activity, ARA analysis was performed in roots of Jemalong A17 and R108 plants. The result showed that the activity was maintained at a constant level without significant decrease over the measurement period (Table 2), as compared to that of well-watered plants. This study specifies that both Jemalong A17 and R108 plants maintain active bacteroids and N_2 fixation and that nodule senescence is limited to a small area under drought stress, despite of external N fertilizer treatment.

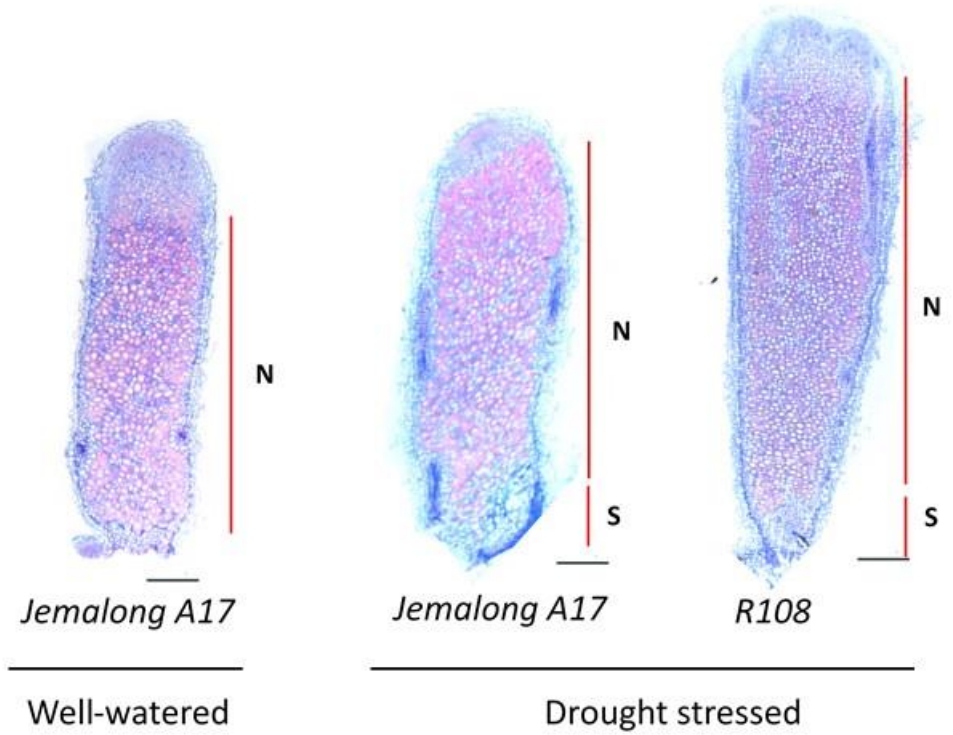

Fig. 9. Effect of drought stress on nodule morphology. Nodule physiology of 32 days-old post *E. meliloti*-inoculated plants grown under drought stress. Drought treatment in N fertilizer treated plants began at 20 dpi and plants were grown for another 12 days. Scale bar indicates 200µM. Senescence (S) and active N_2 fixation (N) zones are indicated in the image (red).

Table 2. Effect of drought stress and N fertilization on nodule nitrogenase activity. At 20 dpi, plants continued to receive water (W) or water was withheld (D) for the following 12 days and an ARA analysis was performed at 20, 26 and 32 dpi. Values are the mean of three biological replicates and ± represent the standard errors of mean. Mean values followed by the same letter belong to the same group and are not significantly different to each other according to ANOVA-Post Hoc Tukey's test.

Dpi	Jemalong W+N	Jemalong A17 D+N	R108 W+N	R108 D+N
20	1620±12^{e}	2200±50.8^{d}	3131±23^{bc}	3050±12.4^{b}
26	2586±254^{d}	2210±71.3^{d}	3338±200^{ab}	3250±51.9^{b}
32	2206±34^{d}	2175±42.1^{d}	3370±70^{ab}	3200±120.3^{b}

4.2.11 SNF sustains plant growth better than N fertilizer under drought stress

Previous studies show that drought stress negatively affects the symbiotic process and nitrogenase enzyme activity in legumes (Marino *et al*., 2007). In contrast, I observed that both of the *M. truncatula* genotypes, Jemalong A17 and R108, sustained SNF but decreased the N uptake from fertilizer. I therefore hypothesize herein that SNF can maintain plant growth better than N fertilizer under drought. To determine the difference between the effect of *E. meliloti* inoculation (0mM KNO_3) and external 10mM KNO_3 N fertilizer treatment (Uninoculated) on plant growth under drought stress, the Jemalong A17 and R108 plants were first grown for 20 days under well-watered conditions. Water was then withheld in group of pots at 20 dpi for 12 days to impose drought stress and continued watering in group of pots for well-watered control treatment. The observed field capacity of soil mixture used here was 95%, 74% and 51% at 20, 26 and 32 dpi respectively (Appendix 6.8). To determine the effect of drought on the plant water relations, stomatal conductance and the transpiration rate were measured in both drought stressed and well-watered *E. meliloti*-inoculated plants. The results showed that the transpiration rate and stomatal conductance were reduced significantly in the drought stressed plants at 26 and 32 dpi as compared to the well-watered plant (Appendix 6.9, 6.10). Subsequently, the effects of SNF and N fertilization on leaf photosynthetic rates was measured in plants grown under water limiting conditions. Results showed that as compared to N fertilizer-treated plants, both *E. meliloti*-inoculated Jemalong A17 and R108 plants had significantly higher photosynthetic rates (Appendix 6.11): N fertilizer-treated Jemalong A17 plants showed a 47% and 50% reduction in photosynthesis rates as compared to *E. meliloti*-inoculated plants at 26 and 32 dpi respectively, while N fertilizer treated R108 plant showed 23% and 42% reduction in photosynthesis rates as compared to *E. meliloti*-inoculated plants at 26 and 32 dpi respectively. Furthermore, to investigate and compare between the effect of *E. meliloti* inoculation and N fertilization on plant growth under drought stress, shoot dry weight was measured. Results showed that as compared to N fertilization, *E. meliloti* inoculation (SNF) significantly increased plant shoot biomass. N fertilizer-treated Jemalong A17 plants showed a 32% and 34% growth reduction as compared to *E. meliloti*-inoculated plants at 26 and 32 dpi, respectively. Similarly, N fertilizer treated R108 plants showed a 33% and 57% growth reduction as compared to *E. meliloti*-inoculated plants at 26 and 32dpi, respectively (Fig. 10a,b, Appendix 6.12, 6.13, 6.14). In addition, comparative data of nodule biomass and shoot biomass exhibited that nodule biomass increase coincided with a shoot biomass increase in Jemalong A17 and R108 during the 12-day drought period (Appendix 6.15). This study shows that SNF sustains plant growth better than N fertilization of Jemalong A17 and R108 plant grown under water limiting conditions.

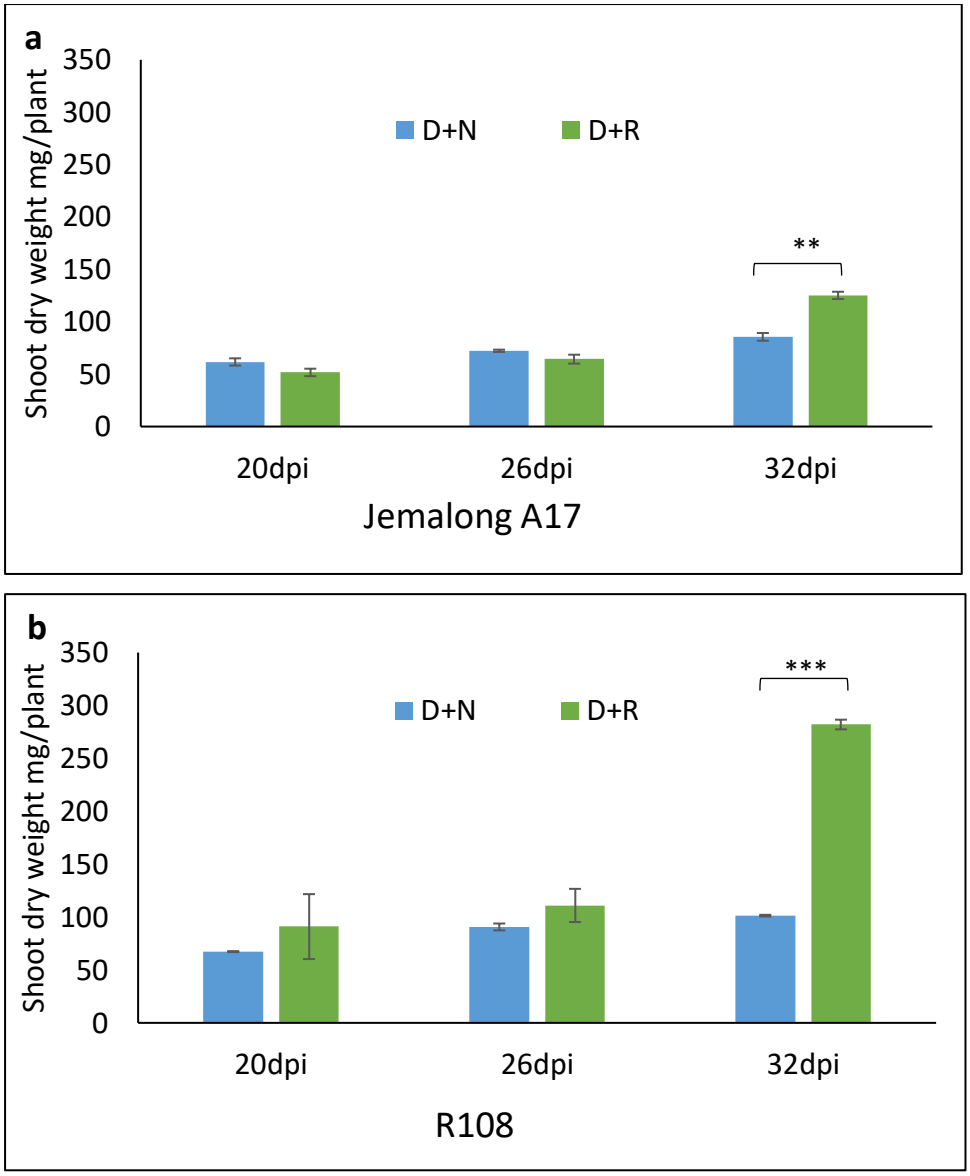

Fig. 10. Effect of *E. meliloti* inoculation and N fertilization on plant growth under drought stress. Shoot dry weight of *E. meliloti* inoculated (+R) and N fertilizer treated (+N) Jemalong A17 (a) and R108 (b) wild type plants grown under drought stress. Plant were well-watered until 20dpi and water was with-holded (D) until 32dpi. Values are the mean of three biological replicates. Error bars represent the standard errors of mean and asterisks indicate the significant differences between two treatments at $p<0.01$ (**) and $p<0.001$ (***), according to student's *t*-test.

4.2.12 *E. meliloti*-inoculated plants induce expression of abscisic acid-related genes and reduce expression of stress-associated genes in *M. truncatula* leaves

As shown above, SNF contributed more to total N assimilation in *E. meliloti*-inoculated and drought-treated R108 than in Jemalong A17 plants. Therefore, the R108 plant was chosen to further investigate drought-induced transcriptional changes of stress-associated genes. As seen above, *E. meliloti* inoculation resulted in plant growth maintenance when grown under water limiting conditions. I therefore speculate that *E. meliloti* inoculation may affect the expression of stress-related genes in *M. truncatula* R108 plants in response to drought stress. Plants were grown for 20 days after inoculation with *E. meliloti* or were not inoculated but treated with N fertilizer. Water was subsequently withheld at 20 dpi for 12 days to impose drought stress as mentioned in Chapter 2. To determine drought-induced changes in gene expression of stress-related genes in *E. meliloti*-inoculated and fertilizer-treated plants, gene expression analysis was performed from leaf tissue using qRT-PCR. For this study, I measured the transcriptional abundance changes of gene(s) involved in ethylene biosynthesis (*MtAcs* and *MtAco*), Reactive Oxygen Species (ROS) levels (*MtCat* and *MtRboh*), ABA biosynthesis (*MtZep and MtNced*), ABA signalling (*MtZip*), salicylic acid-biosynthesis (*MtPal* and *MtIcs*) and proline biosynthesis (*MtP5cs3*). From the results of this study I found that genes *MtAcs* and *MtAco*, which can provide a measure for biosynthesis of the stress hormone ethylene (Zhao *et al.,* 2014), showed significantly less expression (8-10 fold) in *E. meliloti* inoculated plants than in uninoculated plants (Fig. 11c,d) at 32 dpi. *MtCat* and *MtRboh* genes encode proteins involved in regulating levels of ROS and are used as a measure for cellular redox status as a stress indicator in *A. thaliana* (Jimenez-Quesada *et al.,* 2016; Barry *et al.,* 2000). Expression of these genes was significantly less (2-2.5 fold) in *E. meliloti*-inoculated plants as compared to uninoculated plants at 32 dpi (Fig. 11a,b). Then, I found At 32 dpi, that SNF plants showed 2-2.5 fold higher *MtZep* and *MtNced* expression (genes involved in ABA biosynthesis; Luchi *et al*., 2001; Shi-Shuai Luo *et al*., 2016) as compared to uninoculated N fertilizer-treated plants (Fig. 12a,b). The ABA signalling gene *MtZip,* which was shown to be a transcription factor for ABA responsive genes (Belamkar *et al*., 2014), showed a 7-fold increase in expression in *E. meliloti* inoculated plants as compared to in uninoculated N fertilizer-treated plants at 26 and 32 dpi (Fig. 12c). In contrast, there was no significant difference in the expression of genes encoding enzymes involved in the biosynthesis of salicylic acid (*MtPal* and *MtIcs*) between *E. meliloti*-inoculated and N fertilizer treated plants (Appendix 6.16a,b). In addition, expression of a gene encoding pyrroline-5-carboxylate synthetase (*MtP5cs3*), involved in proline biosynthesis, increased over time, but expression did not differ significantly between *E. meliloti*-inoculated and N fertilizer-treated plants at 32 dpi (Appendix 6.16c). This study specifies that upon growth under water-limiting conditions, *E. meliloti* inoculation

increased the expression of ABA-related genes and reduced the expression of ethylene and ROS related genes.

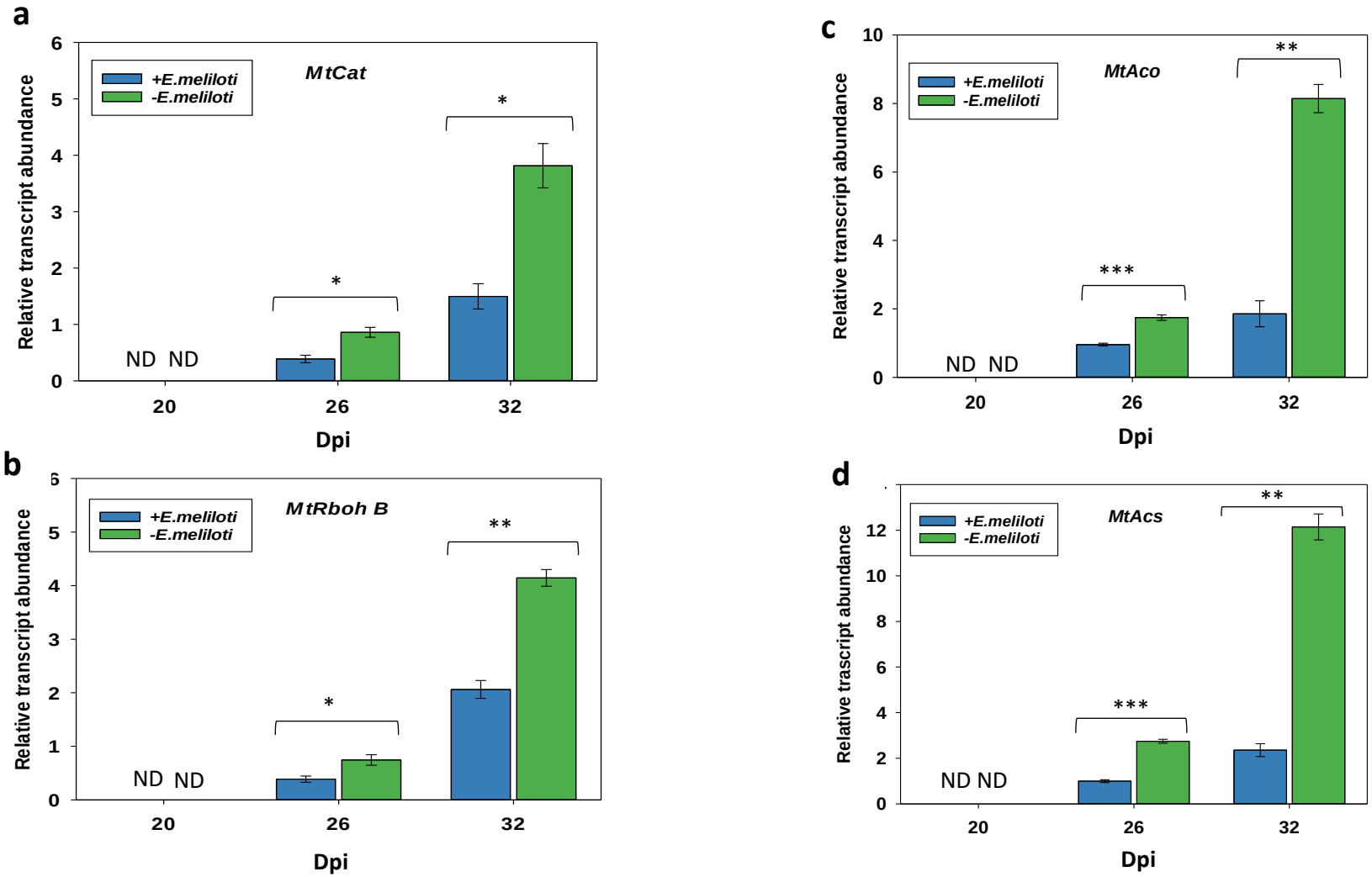

Fig. 11. Transcriptional changes of genes involved in ROS and ethylene synthesis under drought stress. Plants were inoculated with *E. meliloti* (+*E. meliloti*) or were not inoculated (-*E. meliloti*). After 20 days (20 dpi), water was withheld and gene expression of the indicated genes was measured at the indicated days-post-inoculation (dpi). The transcript level for each gene is shown relative to housekeeping genes, *MtElf2* and *MtTub2*, and normalized to the 20dpi time-point as described in chapter 2. Values are the mean of three biological replicates. Error bars represent the standard errors of mean and asterisks indicate a significant difference between *E. meliloti* inoculated and uninoculated plants at $p<0.05$ (*), $p<0.01$ (**) and $p<0.001$ (***) according to student's *t*-test.

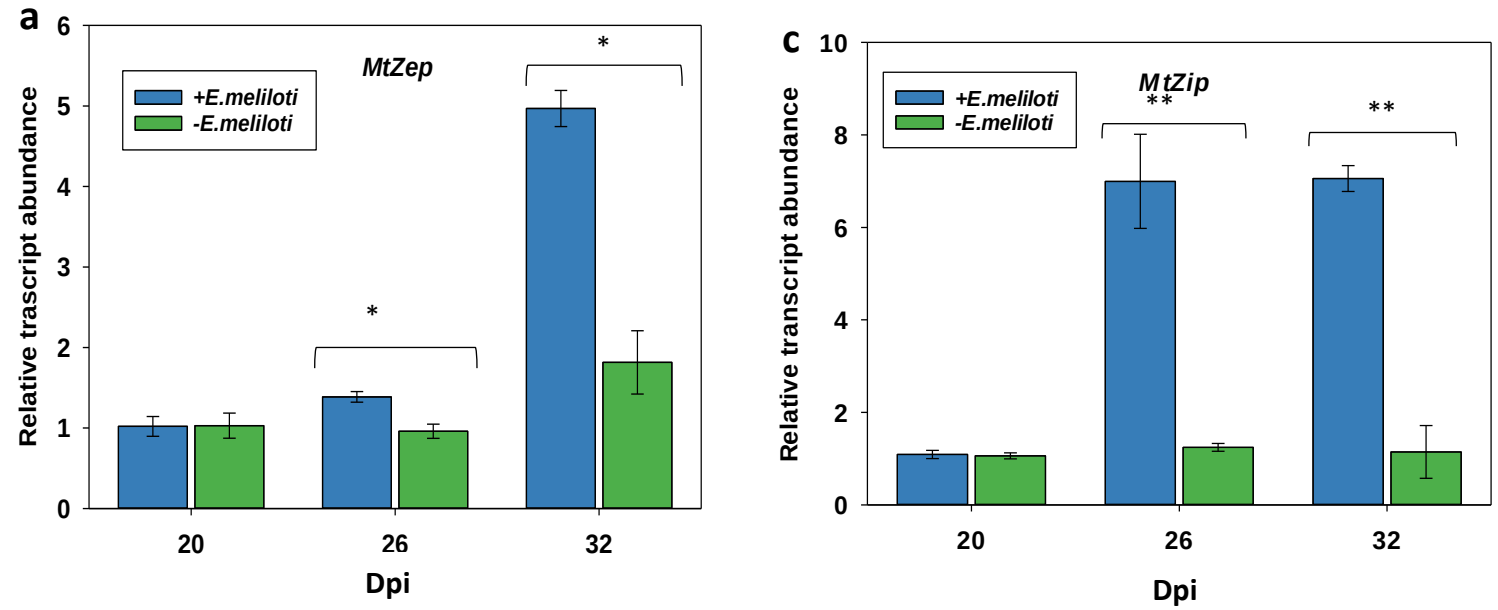

Fig. 12. Transcriptional changes of genes involved in ABA biosynthesis and the post-ABA regulating pathway under drought stress. Plants were inoculated with *E. meliloti* (+*E. meliloti*) or were not inoculated (-*E. meliloti*). After 20 days (20 dpi), water was withheld and gene expression of the indicated genes was measured at the indicated days-post-inoculation (dpi). The transcript level for each gene is shown relative to housekeeping genes, *MtElf2* and *MtTub2*, and normalized to the 20dpi time-point as described in chapter 2. Values are the mean of three biological replicates. Error bars represent the standard errors of mean and asterisks indicate a significant difference between *E. meliloti* inoculated and uninoculated plants at $p<0.05$ (*) and $p<0.01$ (**) according to student's *t*-test.

4.3 Discussion

Jemalong A17 and R108 balance the internal N level by differentially controlling N uptake from two N sources

N is a constituent of proteins, nucleic acids and other indispensable organic compounds that are required for photosynthetic activity, increasing seed quality and enhancing crop yield under optimal and suboptimal conditions (Nobuyasu *et al*., 2003; Roekel & Purcell, 2014; Evans & Terashima, 1987; Poorter & Evans 1998; Makino *et al*, 1997). SNF in legume and non-legume plants offer important benefits for use in sustainable agricultural production and reducing the reliance on N-fertilizers. The detection of the limiting factors that could be managed or modified to increase the symbiotic benefits in grain and forage legumes is a major research goal. The work presented here studies how different *M. truncatula* genotypes performs their symbiosis with *E. meliloti* under external N fertilizer treatment and drought stress.

In the beginning of this study, I found that only WT plants in association with *E. meliloti* exhibited sufficient plant growth while uninoculated and non-N_2 fixing plants resulted in severe plant growth reduction (Fig.2a,b). Moreover, it has been found that phenotypes of symbiosis such as nitrogenase activity, nodule size and nodule biomass varied in WT Jemalong A17 and R108 plants. R108 produced a relatively higher nodule biomass and nodule nitrogenase activity than Jemalong A17 and mutants. This furthermore coincided with more plant growth in R108 plants (Fig. 1a,c, 2a,b).

In addition to symbiotic N_2 fixation, legumes also access other forms of inorganic nitrogen from soil when available, such as nitrate and ammonium. I therefore next investigated the relative contribution of SNF in *M. truncatula*, under conditions where another available source of N, KNO_3, was available. The results of this study emphasize that despite of N fertilization in addition to *E. meliloti* inoculation, both Jemalong A17 and R108 maintain the N level equally as that of plants grown under either *E. meliloti* inoculation or N fertilization. In Jemalong A17, total N level in shoot was balanced by the plant through uptaking N only from fertilizer and inhibiting the N uptake from the N_2 fixation process completely (Fig. 3a, 4a, 5a). A study by Goh *et al*. (2016) supports N uptake level in Jemalong A17 seen in this study that under a low N fertilizer treatment (0.1mM), SNF contributed >70% for shoot N levels, but this decreased drastically up to 0% under a high N fertilizer (10mM) supply. The suppression of N uptake from N_2 fixation process under N fertilizer treatment could possibly be due to the reduction of nodule activity (Table 1a,b, Appendix 6.4). It has been well demonstrated that SNF can be suppressed if N fertilizer is externally added or available in the soil (Gentili *et al*., 2006; Herrmann *et al*., 2014). External N fertilizer treatment reduces nodule activity and as such limits the high-energy cost required for N fixation. External N fertilizer may also lead to an impaired balance of C and N metabolism and

phloem-mediated amino acid loading in nodules, which results in reduced nodulation and nitrogenase activity (Dixon & Kahn, 2004; Liu *et al*., 2005; Streeter, 1988). Liese *et al*. (2017) also described that an external N supply alters the nodule transcriptome and reduces nitrogenase activity simultaneously. Furthermore, treating legumes with nitrate increases oxygen diffusion resistance in their nodules, which consequently results in reduced nitrogenase activity (Denison & Harter, 1995). These previous studies correlate with the data from this study and suggest that the reduction of nitrogenase activity in Jemalong A17 caused by external N fertilizer treatment (Table 1a) could possibly be due to amino acid feedback regulation, changes in nodule oxygen diffusion or alterations to the regulators required for N_2 fixation (Rosov *et al*., 2001; Neo & Layzell, 1997; Bacanambo & Harper, 1997). In contrast to Jemalong A17, R108 plant suppressed the N uptake from N fertilizer, while N uptake from the N_2 fixation process did occur. Nevertheless, in both Jemalong A17 and R108, total N uptake from both N sources was balanced to maintain a similar total N level (Fig. 3b, 4b, 5b).

When the host senses a sufficient amount of N internally due to access to inorganic N present in the soil, it undergoes a process called Autoregulation Of Nodulation (AON) to avoid excess carbon energy consumption by the symbiosis (Okamoto et al., 2009). AON limits nodule formation and disruption of this process may lead to excess nodule formation (Saha & Dasgupta, 2015). The present study showed that R108 nodules cluster in response to N fertilization without reducing its numbers. From the results of this study I postulate that in response to N fertilizer treatment, R108 plant may have disrupted the AON and consequently developed the nodules as a cluster and close to root collar. As a result, R108 plant may have reduced the SNF suppression and continued uptaking N from the N_2 fixation process (Fig. 6a,b, Table 1a,b, Appendix 6.4). In principle, uptake of N will be converted to amino acids, loaded into the xylem and exported to shoots. After a certain level of N export to shoots, plants sense the internal N level and control the nitrate uptake from soil and/or nitrogenase activity through phloem-loaded amino acids to balance the internal N level. Therefore, N uptake in roots depends on N levels in shoots as described by Crawford & Glass (1998). Here I speculate that in the case of R108 plants, the phloem-loaded amino acids from the shoot might not have accumulated in or around the nodule, resulting in uninterrupted nitrogenase activity. It has been reported in soybean that amino acids from the phloem sap downregulate nitrate uptake after a plant senses a high internal N status (Muller & Touraine, 1992). These reports and the result of reduced N uptake from fertilizer seen in nitrogen fixing R108 plants together suggest that R108 plant does not inhibit the SNF (by an unknown mechanism) but limits the N uptake from N fertilizer to control the internal N level (Fig. 4b, 5b). However, further study is required to decipher and determine the regulatory mechanism involved in controlling the AON and N fixation under N treatment. Taken together, the results of SNF contribution

in Jemalong A17 and R108, specifies that SNF contributes substantially to total N supply as detected in R108, despite of availability of another form of fixed Nitrogen.

***M. truncatula* symbiosis with *E. meliloti* increased the drought resistance of the host**

In addition to externally available N in soil, symbiosis also confronts major environmental stresses such as drought. This study was then focused to determine which source of N (SNF, through *E. meliloti* association or N fertilizer) benefits the plant when grown under drought stress. The total N level in drought-stressed Jemalong 17 and R108 treated with *E. meliloti* and N fertilizer, was found similar as that of plants treated with N fertilizer alone (Fig. 7a,b, 8a,b). Under drought stress Jemalong A17 and R018 plant increased the N uptake to 39% and 48% respectively from N_2 fixation process (Ndfix) (Fig. 5a,b). The increase in Ndfix, coincided with a reduced N uptake from N fertilizer. The increase of N uptake from N_2 fixation process in both genotypes could be due to reduced inhibition of nodule activity under drought stress (Table. 2). This reduced inhibition of nodule activity was further found coincided with controlled nodule senescence in N_2 fixing Jemalong A17 and R108 genotypes. Almost 70-75% of nodule tissues hosted differentiated and matured bacteroids in both wild type genotypes (Fig. 9). A reduction of nitrate uptake from N fertilizer in drought-stressed host plants is in general agreement with previous studies suggesting that drought affects the mobility of nitrates to roots. The reduced mobility of nitrates to roots then inhibits N uptake from the soil (Buljovcic & Engels., 2001; Tobar *et al*., 1994; He & Dijkstra., 2014). Therefore, the above findings indicate that reduced suppression of SNF in Jemalong A17 and R108 under N availability and drought stress could be due to reduced soil moisture content, which resulted in reduction of N uptake from N fertilizer. Furthermore, this suggests that under drought stress, SNF becomes a competent N producer in both Jemalong A17 and R108 in comparison with N fertilizer.

It was found that both Jemalong A17 and R108 grown under drought stress, showed drought resistance when inoculated with *E. meliloti*, as compared to uninoculated plants (Fig. 6a,b). The gene expression analysis of this study proved that in response to the drought treatment, inoculated plants modulated the expression of stress-associated genes. Nitrogen fixing plants incited the Zeathanxin epoxidase (*MtZep*) and 9- cis-epoxycarotenoid dioxygenase gene *(MtNced)* genes involves in ABA biosynthesis in leaves (Fig. 12a,b). Previous reports suggested that the loss of function of *MtZep* in mutant plants causes a strong reduction in the levels of the hormone ABA (Xiong & Zhu, 2003). Moreover, overexpression of the orthologous *Zep* genes in *A. thaliana* and *Nicotiana tabacum* enhanced the ABA production and consequently increased drought and salt tolerance (Nambara & Marion-Poll, 2005; Yue *et al*., 2011). Similarly, Zhang *et al*. (2014) illustrated that during mild and severe drought stress, *M. truncatula* expresses another ABA biosynthesis gene, *Nced,* which coincides

with increased endogenous ABA levels (Yue *et al*., 2011). Interestingly, an ABA-signalling gene *Zip*, which acts as a transcription factor for inducing abscisic acid-regulated genes (Kang *et al*., 2002; Yoshida *et al*., 2015; Belamkar *et al*., 2014) and was shown involved in stress tolerance, was also found to be expressed significantly higher in symbiotic N_2 fixing plants (Fig. 12c). This indicates that SNF incites a higher level of expression of ABA biosynthesis and signalling genes upon drought stress. Most interestingly, SNF plants downregulated the expression of ROS and ethylene stress-related genes, as compared to N fertilizer-treated plants under drought conditions (Fig. 11a,b,c,d). This downregulation could be due to an increased positive regulation of ABA-related genes, which are known to mitigate drought stress (Yue *et al*., 2011; Belamkar *et al*., 2014). This suggest that SNF better prepares the host plant to drought stress, such that it can respond faster or more strongly to the imposed drought stress. Such preparation is reminiscent to 'priming' which is a faster and stronger induction of basal mechanism that the plant incites to survive and increase the tolerance under stress condition (Jakab *et al.,* 2005; Conrath *et al*., 2006; Borges *et al*., 2014). The priming-like effect thus may have enabled the host plant to strongly induce ABA regulatory genes, resulting in drought tolerance and reduced stress-induced damage. However, further extensive study is required to understand the SNF-induced molecular changes in response to drought stress. Luo *et al*., (2016) described that Jemalong A17 is more tolerant to drought stress than R108 under uninoculated, but N fertilized, conditions. This study brings an important finding that the maximized benefit of SNF and induction of ABA responsive genes by *E. meliloti* inoculation seen in R108 results in increased plant growth and drought resistance as compared to Jemalong A17 (Fig. 7a,b, 9b, Table 2, Fig. 10a, Appendix 6.12, 6.13, 6.14). The plant growth promoting rhizobacteria reported in many crops were found to be involved in plant growth promotion and confer stress tolerance to plants (Chen *et al*., 2013; Vurukonda *et al*., 2016; Lodeiro *et al*., 1999). This study therefore emphasizes that SNF, in addition to being important for fixing atmospheric nitrogen, also appears to function as a plant growth supporter in *M. truncatula* under drought stress.

4.4 Conclusion

In legumes, improving SNF would be an ideal strategy for sustainable crop production. Determining the contribution and benefit of SNF in the host under N available conditions and drought stress brings an important tool to identify top-performing legume- symbiotic partners and to develop legume crops with increased yield and a reduced N fertilizer dependency. Our study determined that under well-watered conditions, N fertilized R108 plants used SNF for N uptake, when inoculated with *E. meliloti*, and reduced N fertilizer uptake to balance total N uptake. Under drought stress, both Jemalong A17 and R108 plants derived assimilated N from SNF while they significantly reduced the N uptake from N fertilizer. SNF in association with *E. meliloti* not only benefitted the host by increasing the N supply but also primed the host plant to better tolerate drought stress by controlling the expression of drought-associated genes. However, it remains to be shown precisely how the metabolic and transcriptional changes are regulated in a potent N_2 fixing plant under different levels of N availability and drought stress. Given that many studies show a need to focus on increasing N use efficiency in plants to eliminate synthetic fertilizer use and improve crop productivity (Zhang *et al.*, 2015: Galloway *et al*., 2003; Steffen *et al*., 2015), the observed increase of N uptake from SNF and the observed growth adaptation to drought in N-fixing plants in this study is of important agronomic significance for sustainable legume production. This study, therefore, may help with the selection and development of host-legume genetic background traits which reduce SNF suppression and N fertilizer use through breeding strategies.

Chapter 5

Drought-induced senescence of *Medicago truncatula* nodules involves serpin and ferritin to control proteolytic activity and iron levels

5.1 Introduction

Legumes include staple and forage crops and fix atmospheric N_2 through symbiotic association with rhizobia. The association can fix ~100-300kg/ha of N in one crop season and enriches the soil with substantial N for the benefit to non-legumes, reducing the need of N fertilizer (Smil, 1999; Fox *et al*., 2007; Miransari *et al.*, 2013). The actual N_2 fixation amount depends on the efficiency of infection, symbiotic partners and nodule growth and development (Sulieman & Tran, 2014; Mus *et al*., 2016). The model legume *Medicago truncatula* develops indeterminant nodules which possess a permanent nodule meristem and elongate to become cylindrically shaped (Franssen *et al*., 2015). These nodules comprise four different zones: (I) the meristematic zone which ensures the indeterminate growth of the nodule, (II) the infection zone where the *M. truncatula*-specific symbiotic rhizobacterium *Ensifer meliloti* infects the host cell, (III) the fixation zone where bacteroid differentiation and active N fixation takes place and (IV) the senescence zone where the bacteroids degrade as a result of aging or environmental stress (Matamoros *et al*., 1999; Dupont *et al*., 2012).

The process of nodule senescence involves the elevation of proteolytic activity which can function in removal of misfolded or modified proteins and remobilizing nutrients (Pladys & Vance, 1993). However, if the activity is unlimited or uncontrolled, it may affect the symbiosome membrane proteins and key regulators which are involved in N_2 fixation (Vierstra, 1996; Salvesen *et al*., 2015). In soybean and *M. truncatula* nodules, expression of cysteine protease genes was induced during different developmental stages. Particularly, legumain (vacuolar processing) and papain proteases (*MtCP6*) were identified in *M. truncatula* and found to be involved in degrading bacteroids in the senescence zone (Pierre *et al*., 2014). Under drought stress, protease activity may further increase as a result of H_2O_2 production and vacuolar protein accumulation (Kinoshita *et al*., 1999; Solomon *et al*., 1999; Vandenabeele *et al*., 2003). However, plants may regulate the release of protease inhibitors (PI's) to control the activity of proteases to balance proteolysis-dependent cellular damage (Hartl *et al*., 2011; Mosolov & Valueva, 2005). Serine protease inhibitors (serpins) are ubiquitous in plants and have a rigid bait loop that can form covalent, irreversible complexes with endoproteases, such as cysteine and serine proteases through the mechanism of Acyl enzyme intermediates formation (Huntington *et*

al., 2000; Fluhr *et al*., 2011). Serpins play roles in stress responses and Srinivasan *et al*. (2009) found serpins that inhibit stress-induced proteolysis of tobacco leaves. In *Arabidopsis thaliana*, *Atserpin1* was found to interact and inactivate the papain-like protease 'Responsive to Dessication' (*RD1*) and Atmetacaspases (*AtMC9*) that caused programmed cell death (PCD) and tissue decay (Vercammen *et al*, 2006; Lampl *et al*., 2013).

The plant responds to drought stress with a rapid closure of stomata to avoid further loss of water through transpiration (Cornic, 1994; Lawlor, 1995). As a consequence, the diffusion of CO_2 into the leaf will be restricted. The decrease in net photosynthetic rate under drought stress is explained by a lowered internal CO_2 concentration that results in a limitation of photosynthesis at the acceptor site of ribulose-1,5-bisphospate carboxylase/oxygenase (Rubisco) (Cornic et al., 1992) and by the direct inhibition of Rubisco (Haupt-Herting and Fock, 2000). During drought-induced nodule senescence, legheamoglobins (lb) degrade resulting in the release of free iron. Excess iron can react with H_2O_2 to produce more deleterious ROS through the Fenton reaction (Puppo *et al*., 2005; Becana *et al*., 1998; Delaat *et al*., 2014). Plants therefore express the iron scavenger ferritin when high iron availability (Briat *et al*., 2010). Ferritin multimere complexes can accommodate several thousands of free iron atoms in its central cavity and as such control ROS-induced damage (Harrison & Arosio, 1996; Theil *et al*., 2006). Ferritins are also proposed to regulate iron homeostasis to control oxidative damage and to aid in the synthesis of iron-containing proteins during various developmental programmes (Lobreaux & Briat, 1991; Theil *et al.,* 1993; Briat & Lobreaux, 1997; Ravet *et al.*, 2009). Thus, ferritins not only function as iron scavengers, but also provide an iron reservoir for various cellular activities.

This study hypothesizes that nodule senescence is tightly regulated in order to limit detrimental effects of this process to plant survival. We show that drought-induced nodule senescence occurs prior to plant growth limitation and this involves the elevation of proteolytic activity and free iron levels. Nodule senescence is limited by means of *serpin* and *ferritins* expression to control excess proteolytic activity and iron levels.

5.2 Results

5.2.1 Prolonged drought stress affects the growth of *M. truncatula*

Water limitation induces various responses to plants and we first measured physiological and growth responses of *M. truncatula* Jemalong A17 to drought stress in 72 days experiment (Experiment 6, Chapter 2). *M. truncatula* was grown on a vermiculite: perlite: sand mix and inoculated with *E. meliloti* 2 days after sowing. Then, at 30 dpi, water was withheld to keep the soil moisture content to 70% field capacity (FC) for drought treated plants (Day 0 of the drought treatment), while control plants were kept at soil moisture content of 95% FC. Drought-induced physiological changes and growth were subsequently measured for 42 days. To investigate the effect of the drought treatment on leaf water status, RWC and LWP were measured in leaves of control and drought stressed plants. As compared to control plant leaves, a significant difference in RWC and LWP of leaves from drought stressed plants was first observed at 7 DAD and showed lower than those of well-watered control leaves (Fig. 1a,b). We also observed that transpiration rate of drought stressed plants was significantly reduced as compared to control plants at 7 DAD but reduction of stomatal conductance was seen only at 25 DAD (Fig. 2a,b). Similarly, chlorophyll content and photosynthetic rate of drought-stressed plants was significantly reduced at 25 DAD as compared to control plants (Fig. 2c, 3a). Nevertheless, shoot biomass of drought-stressed plants was reduced significantly only at 37 DAD as compared to control plant (Fig. 3b). Thus, drought treatment affected leaf water status within 7 DAD but the effect on plant growth was seen only at 25 DAD.

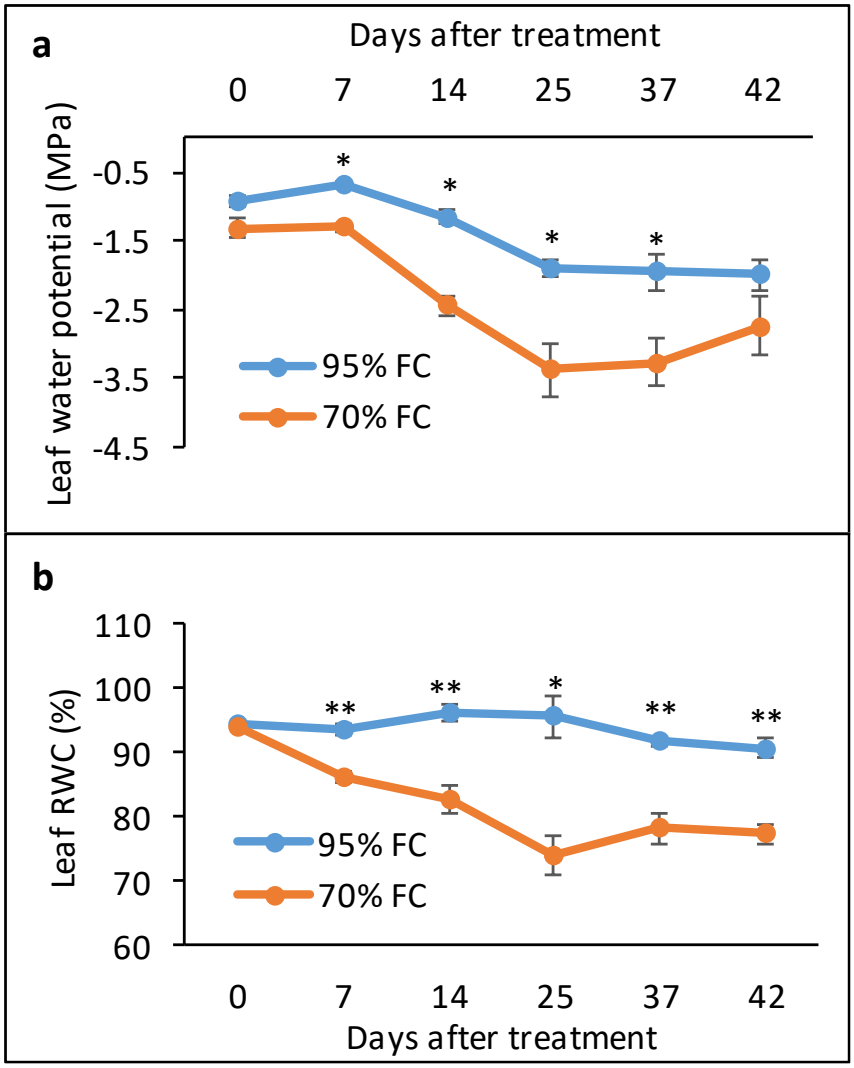

Fig. 1. Drought-induced changes of leaf-water content in *M. truncatula.* (a) Leaf-water potential and (b) leaf relative leaf-water content (RWC) were measured at each time point and at two different soil moisture contents as indicated. Values are the mean of 3 biological replicates. Error bars represent the standard errors of mean and asterisks indicate a significant difference between 95% FC and 70% FC (field capacity) treatment at $p<0.05$ (*) and $p<0.01$ (**), according to student's *t*-test.

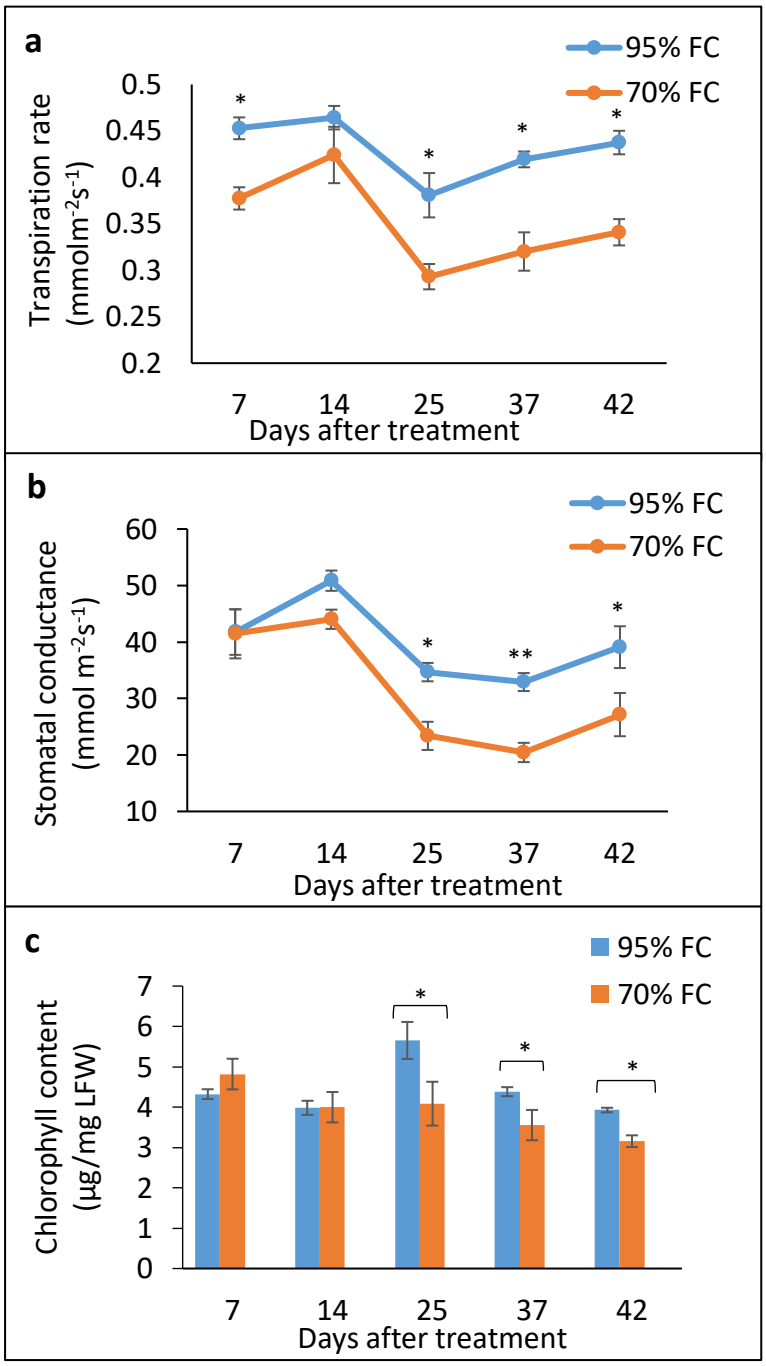

Fig. 2. Effect of drought on *M. truncatula* leaves. (a) Transpiration rate, (b) stomatal conductance and (c) chlorophyll content were measured from the plants at two different soil moisture contents as indicated and at each time point of harvesting. LFW denotes leaf fresh weight. Values are the mean of 3 biological replicates. Error bars represent the standard errors of mean and asterisks indicate a significant difference between 95% FC and 70% FC (field capacity) treatment at $p<0.05$ (*) and $p<0.01$ (**), according to student's *t*-test.

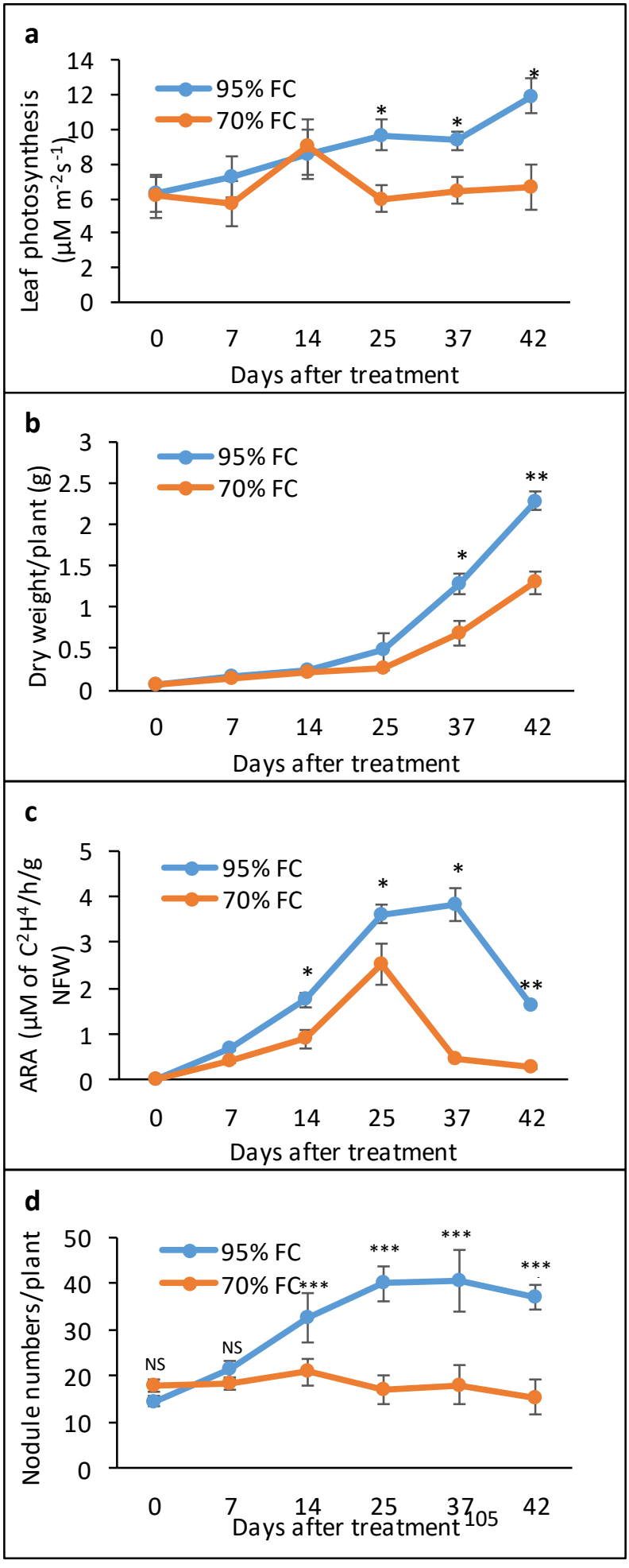
a
Leaf photosynthesis (µM m-2s-1)
95% FC
70% FC
Days after treatment
b
Dry weight/plant (g)
95% FC
70% FC
Days after treatment
c
ARA (µM of C2H4/h/g NFW)
95% FC
70% FC
Days after treatment
d
Nodule numbers/plant
95% FC
70% FC
NS
Days after treatment

Fig. 3. Effect of drought stress on *M. truncatula* growth and nodule nitrogenase activity. (a) Leaf photosynthetic rate (b) shoot dry weight, (c)nodule nitrogenase activity by acetylene reductase assay (ARA) and (d) nodule numbers. Parameters were measured at each time point of harvesting and at two different soil moisture contents as indicated. NFW denotes nodule fresh weight. Values are the mean of 3 biological replicates. Error bars represent the standard errors of mean and asterisks indicate a significant difference between 95% FC and 70% FC (field capacity) treatments at p<0.05 (*) and p<0.01 (**), according to student's *t*-test (a-c) or chi square test (d): *, *P*< 0.05; ** *P*< 0.01; ***, *P*< 0.001; ns, not significant.

5.2.2 Prolonged drought stress disrupts the nodule activity of *M. truncatula*

As the drought stress had a negative effect on plant growth only at 25 days, we hypothesized that it would also take that amount of time to affect the nodule activity and nodulation. We first observed the discoloration of nodules at the senescence zone and found that drought stressed nodules started to loose pink colour at 14 DAD as compared to no change in colour of control nodules. This was further manifested as an increased senescence zone as the drought period extended. At the end of 42 DAD, the whole nodule tissue appeared discoloured as compared to control nodules (Fig. 4). To study the effect of drought on N_2 fixation rate, nitrogenase enzyme activity was measured based on its acetylene reduction capacity from the nodules of plants grown under 95% (control) and 70% FC as mentioned in Chapter 2. The loss of pink colour at 14 DAD in nodules of plants grown at 70% FC coincided with lower nodule nitrogenase activity as compared to control nodules. Nevertheless, activity steadily increased until 25 DAD and dropped subsequently (Fig. 3c). Concurrently, a significant effect of drought stress on nodulation was seen only at 25 DAD. The number of nodules on drought stressed plants was ~15–20 per plant throughout the experiment while control plants showed 37 nodules per plant at 42 days (Fig. 3d). This study showed that drought stress affected the senescence and the nitrogenase activity at 14 DAD.

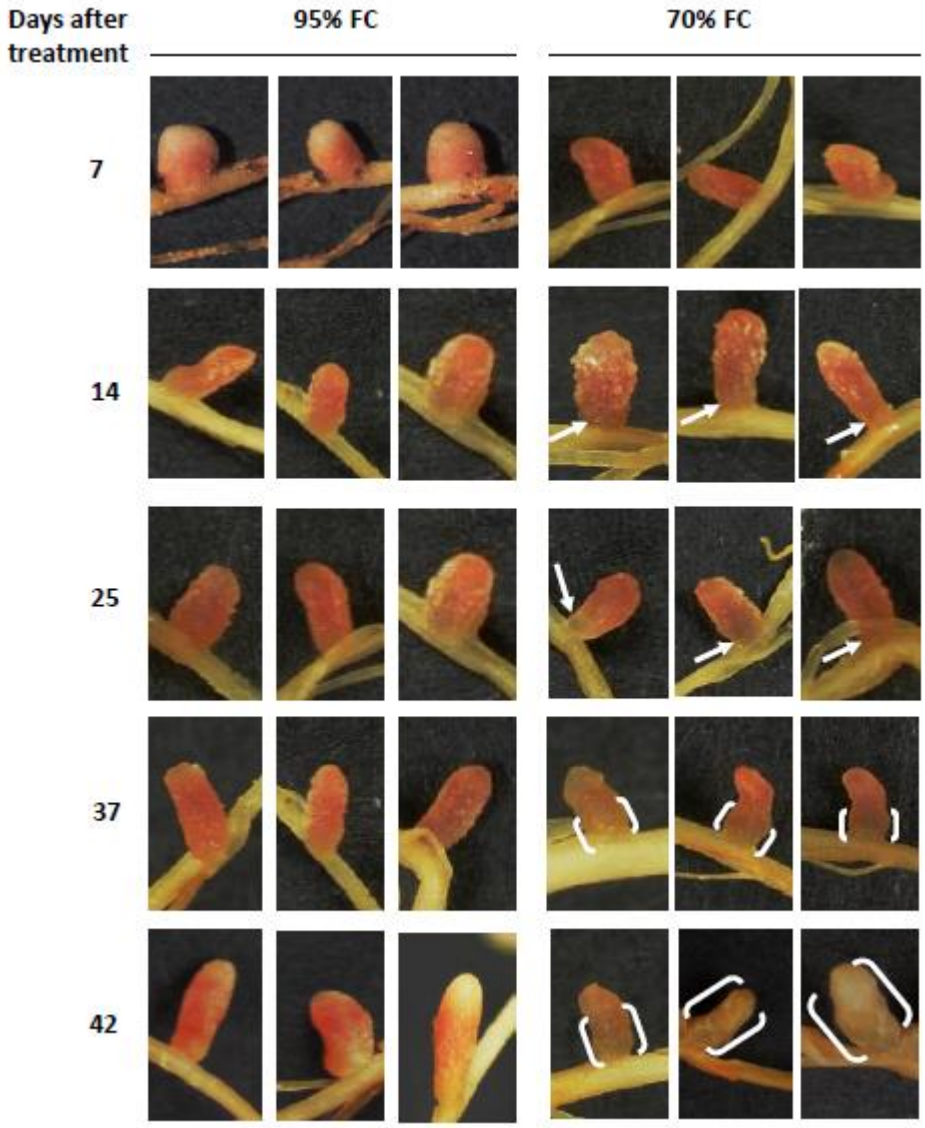

Fig. 4. Change of *M. truncatula* nodule colour under drought stress. Nodule images of *M. truncatula* grown under at two different soil moisture contents as indicated were captured at each time point of harvesting. Time points are at days after treatment. Arrow (white) indicates the sign of initiation of senescence and circle indicates the extend of the loss of pink colour.

5.2.3 Drought induced nodule senescence involves the elevation of proteolytic activity and iron content

We observed that changes of nitrogenase activity correlated with drought-induced nodule senescence. As a key feature of nodule senescence involves the elevation of proteolytic activity and

excess iron increase (Pladys & Vance, 1993; Pierre *et al*., 2014), we hypothesized that drought induced nodule senescence exhibits increased proteolytic activity and excess iron at 14 DAD. We measured the protease activity in the nodule and found that drought stressed plant nodules showed a significant increase at 25 days as compared to well-watered control plant nodules (Fig. 5a). Moreover, this was found to correlate with nodule protein content. At 37 and 42 DAD, protein content of drought-stressed plant nodules reduced by 37% and 55% respectively as compared to nodules of well-watered plants (Fig. 5b). As increased proteolytic activity may cause lb degradation, lb and iron content were also measured in the nodules of all plants and the observed proteolytic activity changes were found to coincide with lb degradation. At 25 DAD, lb content was significantly reduced in the drought stressed plant nodules as compared to nodules of control plants (Fig. 5c). A significant difference in iron content, however, was only observed at 42 DAD (Fig. 5d). Thus, drought stress promoted the proteolytic activity at 25 DAD and this coincided with reduced protein and lb content. However, excess iron increase was observed only at 42 DAD.

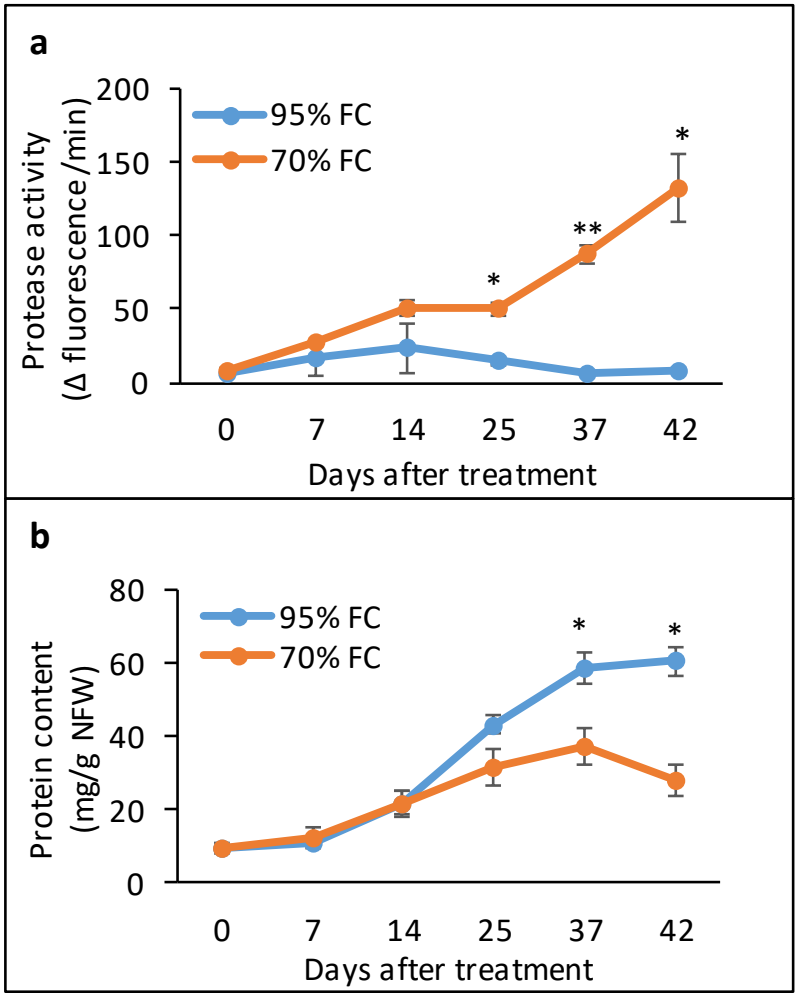

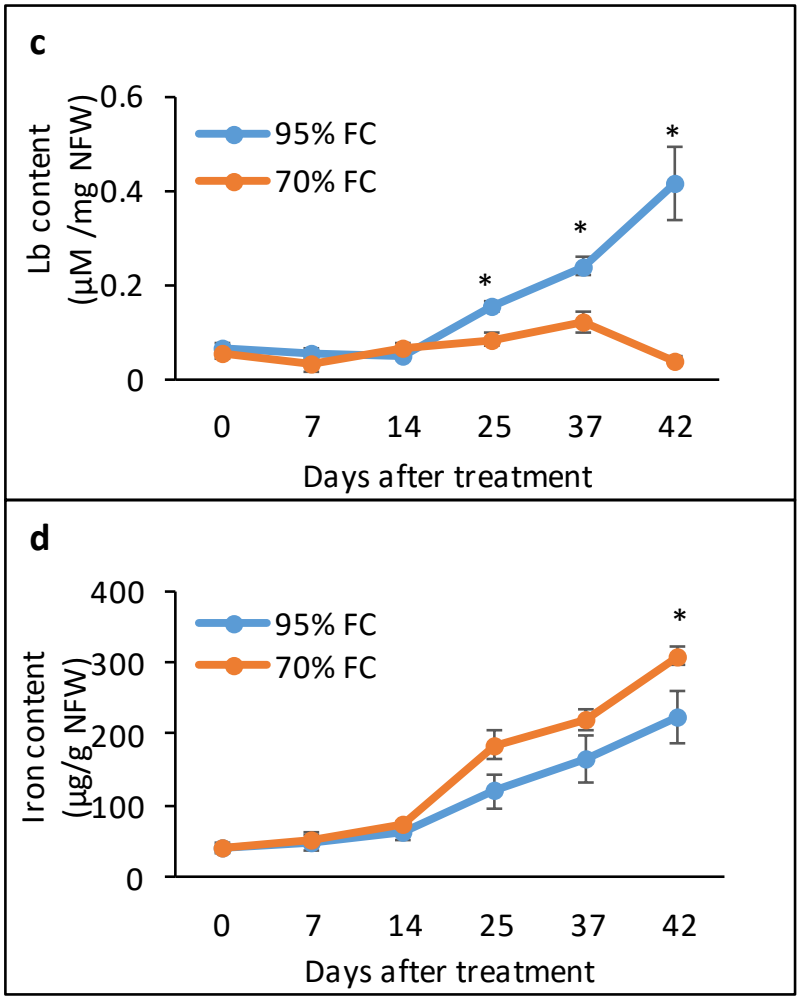

Fig. 5. Drought-induced changes in *M. truncatula* nodules. (a) total protease activity, (b) protein content, (c) leghaemoglobin content and (d) iron content. Assays were performed at each time point of harvesting and at two different soil moisture contents as indicated. NFW denotes nodule fresh weight. Values are the mean of 3 biological replicates. Error bars represent the standard errors of mean and asterisks indicate a significant difference between 95% FC and 70% FC (field capacity) treatment at $p<0.05$ (*) and $p<0.01$ (**), according to student's *t*-test.

5.2.4 Nodule expresses *MtSer6, MtFer2* and *MtFer3* genes during early drought stress

We observed that drought-induced senescence and a decrease in SNF occurred at 14 DAD, but elevation in proteolytic activity and increase in iron occurred at 25 and 42 DAD respectively. Therefore, we speculate that nodule senescence may involve a mechanism to fine-tune the proteolytic activity and limit excess iron levels. It has been reported that serpin can covalently bind and inhibit the activity of highly abundant proteases that causes nodule senescence and that ferritins can act as iron scavengers during early drought stress (Lampl *et al*., 2013; Vorster *et al*., 2013; Pierre *et al*., 2014; Wyk *et al*., 2014). We envisaged that nodules might express *serpin* and *ferritin* genes under drought stress. Hence, we aimed to identify *serpin* and *ferritin* genes in *M. truncatula* and detect their expression in the nodule under drought stress. In total, 28 *serpin* and 4 *ferritin* genes were identified from the *M. truncatula* genome database and their complete coding sequence was retrieved to design primers (Table 1). Using reverse transcriptase PCR and primers (Appendix 2), we measured the expression of these genes in the nodules of well-watered plants at 14 and 25 days. Out of 28 *serpin* genes, *MtSer5, MtSer6, MtSer8*, *MtSer9* and *MtSer10* were found to be expressed at 14 days and only *MtSer6* was found to be expressed at 25 days (Fig. 6). Similarly, when we tested *ferritin* genes, *MtFer2* and *MtFer3* were found to be expressed at 14 and 25 days while *MtFer1* was expressed only at 14 days. The expression of the nodule-expressed genes was subsequently measured in nodules of drought-treated plants and only expression of those genes which were expressed in 25 days well-watered control nodules (*MtSer6*, *MtFer2* and *MtFer3*) were found to be induced by drought stress at 14 DAD (Fig. 7).

	Gene ID	Locus tag	Accession number	Organism
Serpin family	*MtSer1*	MTR_3g018740	XM_003598595	*M.truncatula*
	MtSer2	MTR_2g045980*	XM_003598595	*M.truncatula*
	MtSer3	MTR_8g027420*	XM_003598595	*M.truncatula*
	MtSer4	MTR_2g046030*	XM_003598595	*M.truncatula*
	MtSer5	MTR_3g101030	XM_003602927	*M.truncatula*
	MtSer6	MTR_3g101010	XM_003602925	*M.truncatula*
	MtSer7	MTR_4g045707*	XM_003602925	*M.truncatula*
	MtSer8	MTR_7g050810	XM_003622635	*M.truncatula*
	MtSer9	MTR_3g10120	XM_003602943	*M.truncatula*
	MtSer10	MTR_3g101180	XM_003602941	*M.truncatula*
	MtSer11	MTR_3g015760	XM_003598529	*M.truncatula*
	MtSer12	MTR_3g101190	XM_003602942	*M.truncatula*
	MtSer13	MTR_7g050830	XM_003622637	*M.truncatula*
	MtSer14	MTR_3g099970	XM_003602833	*M.truncatula*
	MtSer15	MTR_3g100990	XM_003602923	*M.truncatula*
	MtSer16	MTR_3g101110	XM_003602934	*M.truncatula*
	MtSer17	MTR_3g101050	XM_003602929	*M.truncatula*
	MtSer18	MTR_3g111160	XM_003603640	*M.truncatula*
	MtSer19	MTR_3g100520	XM_003602885	*M.truncatula*
	MtSer20	MTR_3g101130	XM_003602936	*M.truncatula*
	MtSer21	MTR_7g050750	XM_003622631	*M.truncatula*
	MtSer22	MTR_3g111150	XM_003603639	*M.truncatula*
	MtSer23	MTR_3g048000	XM_003599803	*M.truncatula*
	MtSer24	MTR_3g015620	XM_003598519	*M.truncatula*
	MtSer25	MTR_3g101020	XM_003602926	*M.truncatula*
	MtSer26	MTR_4g093550	XM_003608337	*M.truncatula*
	MtSer27	MTR_3g101120	XM_003602935	*M.truncatula*
	MtSer28	MTR_6g046890	XM_003619290	*M.truncatula*
Ferritin family	*MtFer1*	MTR_7g069980	XM_003623311	*M.truncatula*
	MtFer2	MTR_5g083170	XM_003616637	*M.truncatula*
	MtFer3	MTR_4g014540	XM_003604515	*M.truncatula*

Table 1. Chromosome locus tag and accession number of 28 *serpin* and 3 *ferritin* genes retrieved from *Medicago* genome database (MGDB). Using the locus tag given for individual gene in MGDB, complete coding sequences were retrieved from NCBI BLAST tool. Locus tags with asterisk indicate the genes which didn't show 100% similarity but partially matches with the genes of given accession number. This table is reproduced from Table 1 and 2 of Chapter 3.

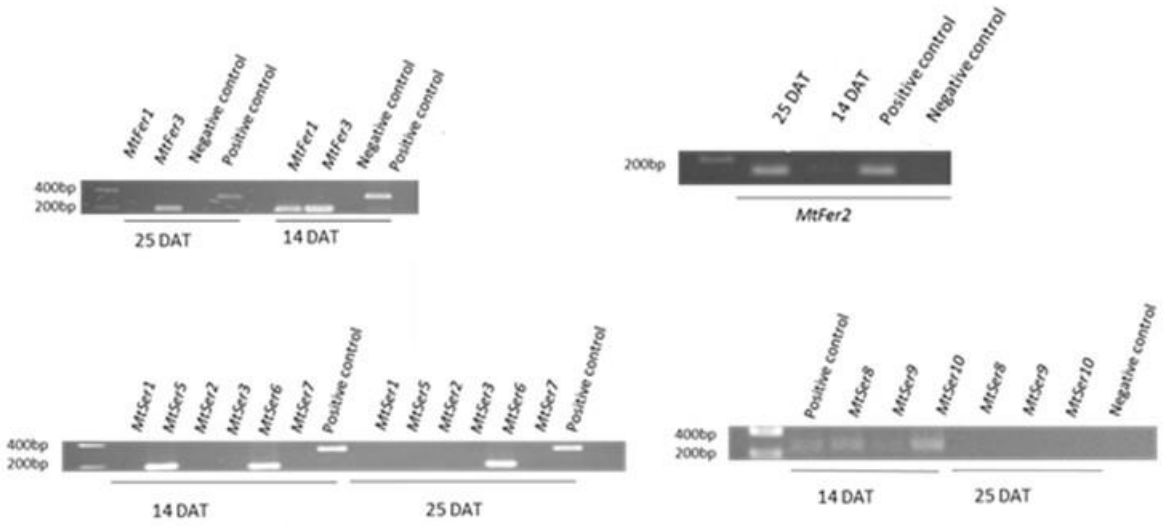

Fig. 6. Expression of 9 *serpin* and 3 *ferritin* genes in *M. truncatula* nodules. Nodules were harvested from 14 and 25 DAT plants grown at 95%FC and expression of genes was determined using reverse transcriptase PCR. *MtELF1* was used for a positive control and no template cDNA was used for negative control. This figure is reproduced from Fig. 6 of Chapter 3.

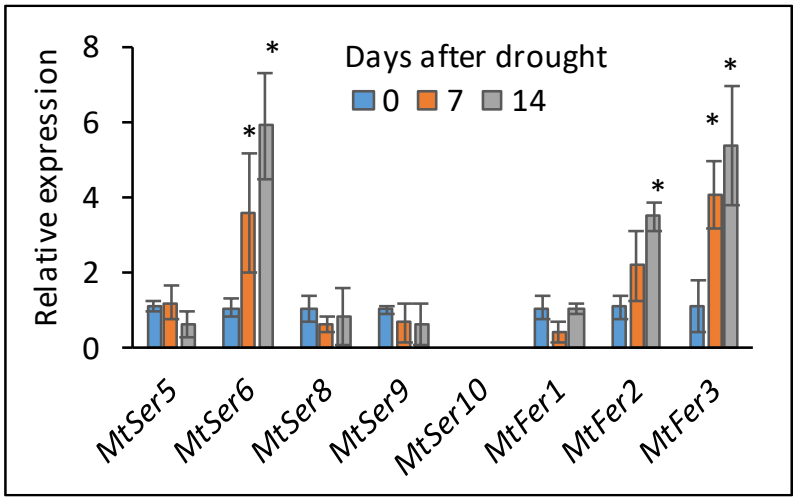

Fig. 7. Response of to drought stress of *serpin* and *ferritin* genes in the nodule of *M. truncatula*. Nodules were harvested from plants grown at 70% FC for 0, 7 and 14 days. The relative transcript abundance (fold change) was determined by qRT-PCR. Data were normalized to control treatment using two internal reference control genes (*βTubulin* and *MtPDF2*). Values are the mean of 3 biological replicates. Error bars represent the standard errors of mean and asterisks indicate a significant difference from day 0 at $p<0.05$ (*), according to student's *t*-test.

5.2.5 Down-regulated expression of *MtSer6, MtFer2* and *MtFer3* in RNAi knockdown lines

As shown above, protease activity was increased only at 25 DAD and free iron increased only at 42 DAD. Therefore, we postulated that *MtSer6* is expressed to limit proteolytic activity and *MtFer2* and *MtFer3* to limit free iron levels. To test this, we used a reverse genetic approach and developed single (*RNAiMtSer6, RNAiMtFer2* and *RNAiMtFer3*), double (*RNAiMtFer2Fer3*) and triple (*RNAiMtSer6Fer2Fer3*) knockdown (KD) constructs to analyse the function of these genes during drought stress. All the constructs were transformed into the *M. truncatula* R108 genotype through *A. rhizogenes* mediated root transformation as this host has been widely used for its fast *in vitro* regeneration capacity (Hoffmann *et al*., 1997; Wang *et al*., 2014). As a control, an empty vector construct was transformed as mentioned in Chapter 2. After transformation, seedlings were transferred and grown with *E. meliloti* in N-free medium for 20 days and then water was withheld completely for another 12 days to impose drought stress (Experiment 7, Chapter 2). After withholding water for 12 days, the FC of the medium was reduced to 51% (Fig. 8a). At this time point (12 DAD), 5 plants were chosen from each RNAi line (single, double, triple and control) and a reverse transcriptase PCR was conducted to check the expression level of the respective target genes. The RNAi transgenic lines where expression of targeted genes were not detected in the nodules (Fig. 8b), were chosen further to confirm the level of expression using quantitative real-time PCR. For each line, at least 3 independent lines were selected along with control lines (Fig. 8b). Quantitative RT-PCR data showed that nodules transformed with the control RNAi construct showed 6 to 10-fold higher expression of the tested genes at 12 days of drought as compared to day 0. In contrast, in single, double and triple RNAi KD nodules, no drought-induced increase of expression of the targeted genes was found (Fig. 9). Thus the RNAi KD effectively suppressed the drought-induced increase of expression of targeted genes.

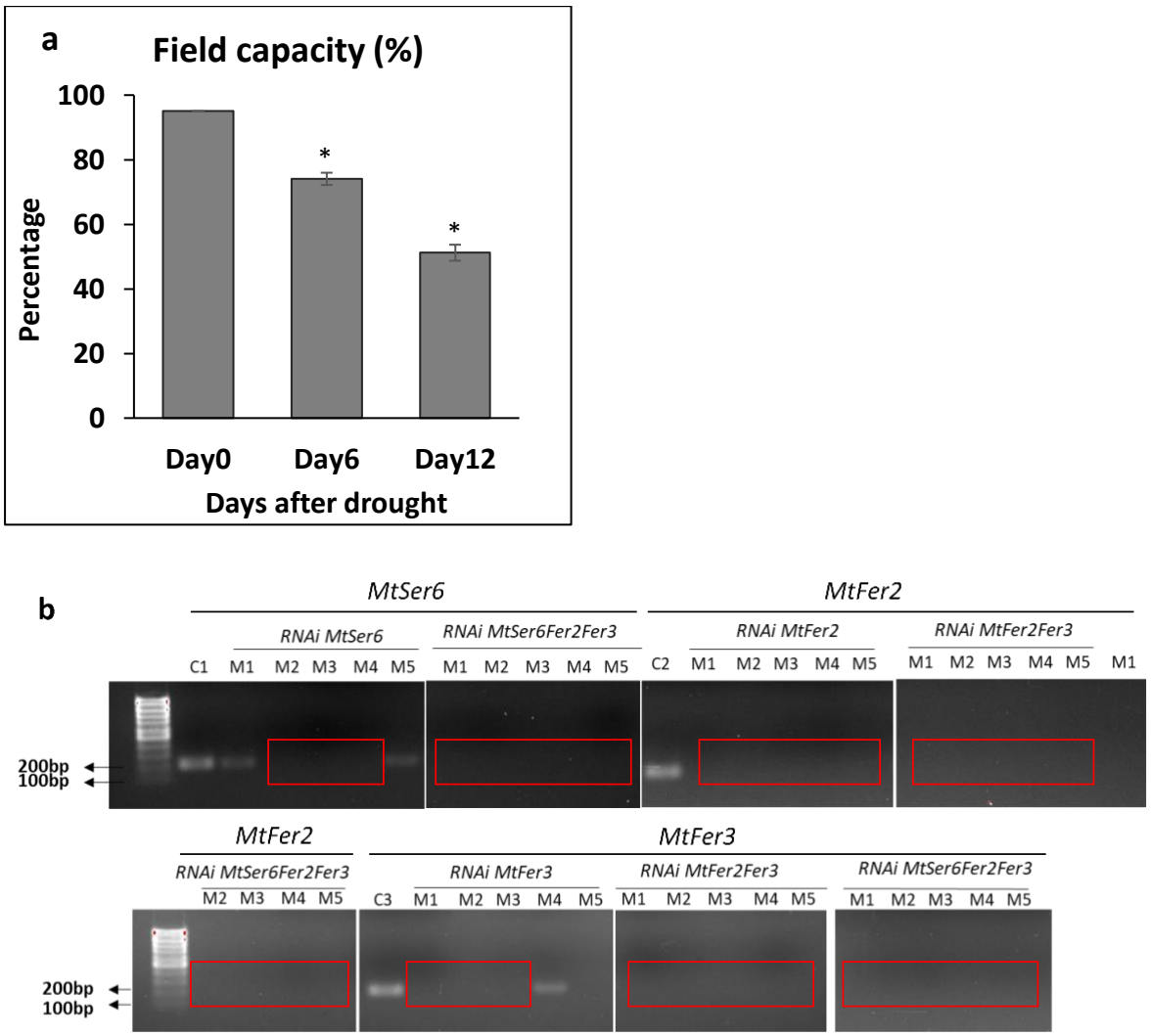

Fig. 8. Effect of RNAi KD on expression of targeted genes in *M. truncatula* nodules grown under drought stress. (a) Field capacity of vermiculite: perlite: sand mix medium used for growing RNAi transgenic plants and (b) reverse transcriptase PCR of *MtSer6, MtFer2* and *MtFer3* genes in RNAi transgenic and control nodules harvested at 12 DAD. M1-M5 indicate independent transgenic plants transformed with the indicated RNAi construct. C1, C2 and C3 indicate independent transgenic plants transformed with an empty vector construct. Red rectangles indicate the RNAi plant lines in which expression of the targeted genes was not detected and those lines were used for further experiments. Error bars represent the standard errors of mean and asterisks indicate a significant difference from day 0 at $p<0.05$ (*), according to student's *t*-test.

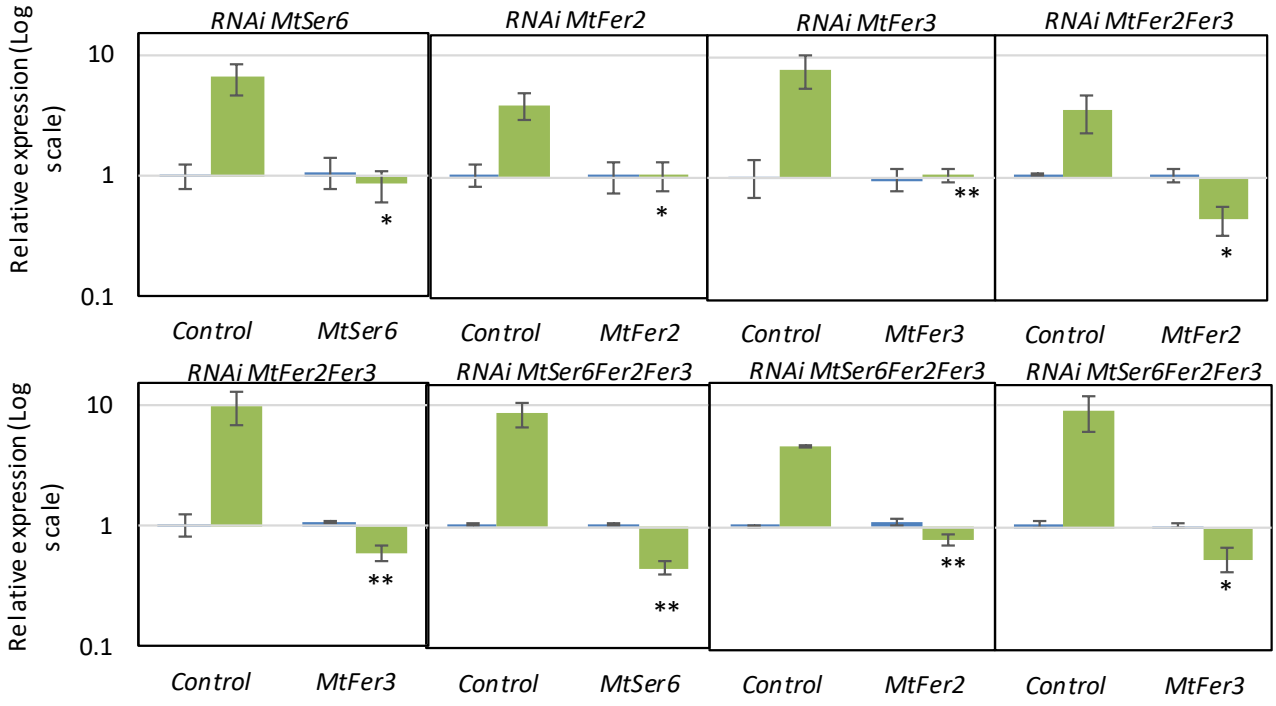

Fig. 9. Effect of RNAi knockdown of *MtSer6, MtFer2* and *MtFer3* expression in *M. truncatula* nodules under drought. Relative transcript abundance changes of the indicated genes in single, double and triple RNAi transgenic nodules of the plants were determined using qRT-PCR. Data were normalized to the control treatment using two internal reference control genes (*βTubulin* and *MtPDF2*). The relative transcript level of each gene was determined from RNAi and control nodules at day 0 (blue bar) and day 12 (green bar) of the drought treatment. Values are the mean of 3 biological replicates. Error bars represent the standard errors of mean and asterisks indicate a significant difference between 12 days old RNAi and control plant nodules carrying an empty vector at $p<0.05$ (*) and $p<0.01$ (**), according to student's *t*-test.

5.2.6 Knockdown of *MtSer6* in *RNAiMtSer6* nodules results in increased papain-like cysteine protease activity, iron levels and *MtFer3* expression

As reported previously, serpin might be involved in controlling cysteine proteolytic activity (RD1) (Vercammen *et al*., 2006; Srinivasan *et al*., 2009). Therefore, we hypothesized that loss of expression of *MtSer6* in drought stressed RNAi transgenic nodules, would result in increased proteolytic activity and concomitant total protein and lb degradation. Therefore, papain like cysteine and legumain like caspase-1- protease activities were measured in 12 days-old drought stressed *RNAiMtSer6* nodules. KD of *MtSer6* in *RNAiMtSer6* nodules provoked papain like cysteine protease activity significantly as compared to control nodules. However, no significant changes of legumain like caspase-1- protease activity was found (Fig. 10a). Moreover, increased papain like cysteine protease activity correlated with nodule protein and lb degradation at 12 DAD (Fig. 10b,c). In addition, we speculated that degradation of lb may liberate iron and increase the excess iron level as described by Puppo *et al*. (2005) and we measured the iron content of 12 days old drought stressed *RNAiMtSer6* nodules. Figure 10(d) shows that degradation of lb coincided with a significant increase of nodule iron content. Furthermore, as increase of iron content might regulate the expression of *ferritins* in plants as reported by Briat *et al*. (2010), we measured the transcript abundance of *MtFer2* and *MtFer3* genes using qRT-PCR. The results showed that *RNAiMtSer6* nodules had a two-fold increase in *MtFer3* expression, while *MtFer2* expression was not affected (Fig. 11). Thus, loss of *MtSer6* expression increases papain like cysteine protease activity and concomitant nodule protein and lb degradation.

5.2.7 Knockdown of *ferritins* result in excess iron increase and nodule protein and lb degradation

Ferritins function in free iron scavenging and we next hypothesised that KD of *MtFer2* and *MtFer3* expression would result in excess iron increase and that consequent increase in oxidative stress will induce protein and lb degradation. We measured the iron content in *RNAiFer2* and *RNAiFer3* single KD nodules at 12 DAD and found that reduced expression of either *ferritin* resulted in significant iron level increases (Fig. 10d). Furthermore, this coincided with increased nodule protein and lb degradation (Fig. 10b,c). In particular, *RNAiFer3* nodules showed significantly higher excess iron and lb degradation as compared to *RNAiFer2* nodules. However, loss of expression of both *ferritin* genes in double *RNAiMtFer2Fer3* KD nodules did not further increase iron levels and lb degradation as compared to single *RNAiMtFer3* nodules (Fig. 10c,d). To investigate whether KD of *MtFer2* or *MtFer3* genes resulted in expression changes of the other *ferritin* or *MtSer6*, we performed qRT-PCR to measure the relative transcript abundance changes. Interestingly, we observed higher *MtFer3*

expression in single *RNAiMtFer2* KD nodules. Furthermore, neither *MtFer2* nor *MtFer3* KD affected expression of *MtSer6* (Fig. 11). Similarly, we didn't observe significant changes of papain like cysteine protease and legumain like caspase-1- protease activities in *ferritin* KD nodules (Fig. 10a). This study shows that loss of *ferritin* expression resulted in excess iron increase and nodule protein and lb degradation. In particular, loss of *MtFer3* in RNAi nodule was seen to have a greater effect on iron increase and lb degradation than *MtFer2*.

5.2.8 Reduced expression of *MtSer6, MtFer2* and *MtFer3* in triple RNAi nodules exhibits further nodule protein and lb degradation

The KD expression of both *serpin MtSer6* and *ferritins MtFer2* and *MtFer3* resulted in increased protein degradation and iron increase. We hypothesized that *serpin* and *ferritins* affect protein degradation in independent ways and therefore that loss of all three genes in triple *RNAiMtSer6Fer2Fer3* KD nodules would further increase degradation of nodule proteins and iron levels under drought stress. Thus, we measured the protein content, lb level, proteolytic activity and iron content in nodules of triple KD lines *RNAiMtSer6Fer2Fer3*. We observed that KD of *MtFer2* and *MtFer3* in addition to *MtSer6* did not further increase the proteolytic activity as compared to KD of *MtSer6* alone, but it did result in significantly less nodule protein content (Fig. 10a,b). Triple KD nodules furthermore showed significantly less lb content than only *RNAiMtSer6* nodules but not as compared to *RNAiFer2Fer3* nodules (Fig. 10c). However, the iron level in triple KD nodules was not significantly different from *MtSer6* and *ferritin KD* nodules (Fig. 10d). This study showed that triple KD of *MtSer6, MtFer2* and *MtFer3* in nodule resulted in increase of degradation of nodule protein and lb further without further increasing proteolytic activity and iron levels.

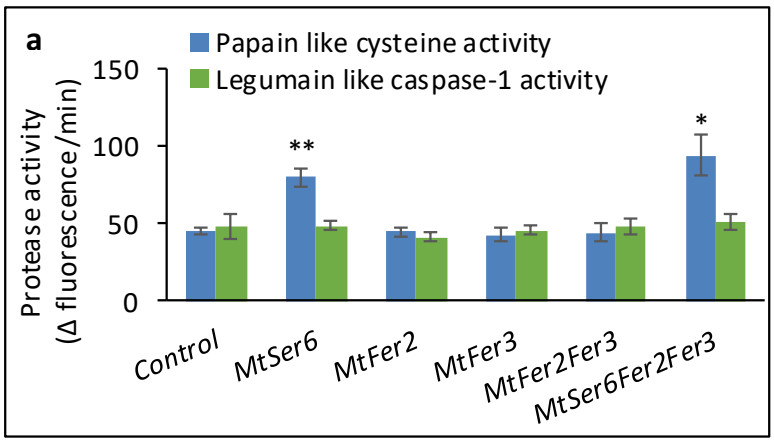

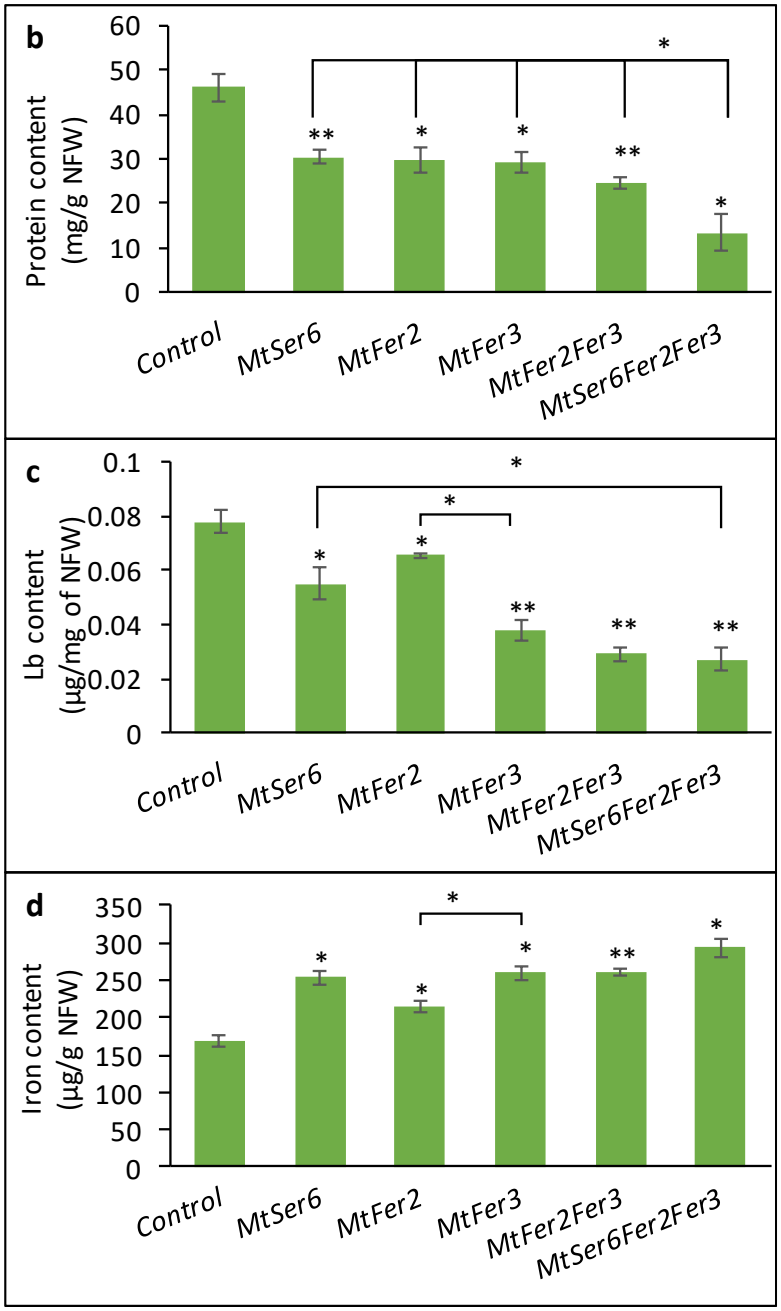

Fig. 10. Effect of reduced *MtSer6, MtFer2* and *MtFer3* expression on nodules. (a) Cysteine like papain and caspase-1 like legumain activity, (b) nodule protein content (c) lb content, and (d) iron content in nodules of drought-stressed RNAi KD plants. Assays were performed from nodules of control and RNAi plants harvested after 12 days of drought treatment. NFW denotes nodule fresh weight. Values are the mean of 3 biological replicates and error bars represent the standard errors of mean. Asterisks indicate a significant difference between control (empty vector) and RNAi KD lines and between two *RNAi* plants (as indicted by line) at $p<0.05$ (*) and $p<0.01$ (**), according to student's *t*-test.

5.2.9 Knockdown of *Mtser6* and *ferritins* causes early nodule senescence and reduced plant growth

The KD of *MtSer3, MtFer2* and *MtFer3* expression resulted in increased nodule protein and lb degradation. Therefore, we expected that drought-stressed RNAi transgenic nodules would show precocious senescence, and reduced nitrogenase activity and that this would negatively affect plant growth. To examine senescence, we sectioned the nodules and observed the bacteroids in RNAi lines harvested at 12 DAD (Fig. 12). Indeed, KD of *MtSer6* in RNAi transgenic nodules resulted in a larger senescent zone, in which symbiosome membrane degradation was visible. Similarly, KD of both *ferritins* in single or double KD RNAi nodules showed larger senescent zones. Surprisingly, KD of all three genes in triple RNAi nodules exhibited complete degradation of bacteroids and a senescent zone that almost completely encompassed the nodule. In contrast, WT plant nodules and control nodules carrying an empty RNAi vector showed no signs of bacteroid degradation or a senescent zone (Fig. 12, 13). Determination of nitrogenase activity of all RNAi nodules furthermore showed that nodule senescence coincided with 30-95% reduced nitrogenase activity (Fig. 14a). Next, the effect of the KD's on plant growth was determined and significantly less photosynthetic rate and shoot biomass (~40-50%) was found in all RNAi KD plants as compared to empty vector control plants (Fig. 14b,c). In particular, triple KD plants had the largest senescent zone, and the lowest nitrogenase activity and this coincided with an 80% reduction in photosynthetic rate as compared to control plants (Fig. 14b). Thus, KD of *MtSer6, MtFer2* and *MtFer3* resulted in early nodule senescence and reduced plant growth.

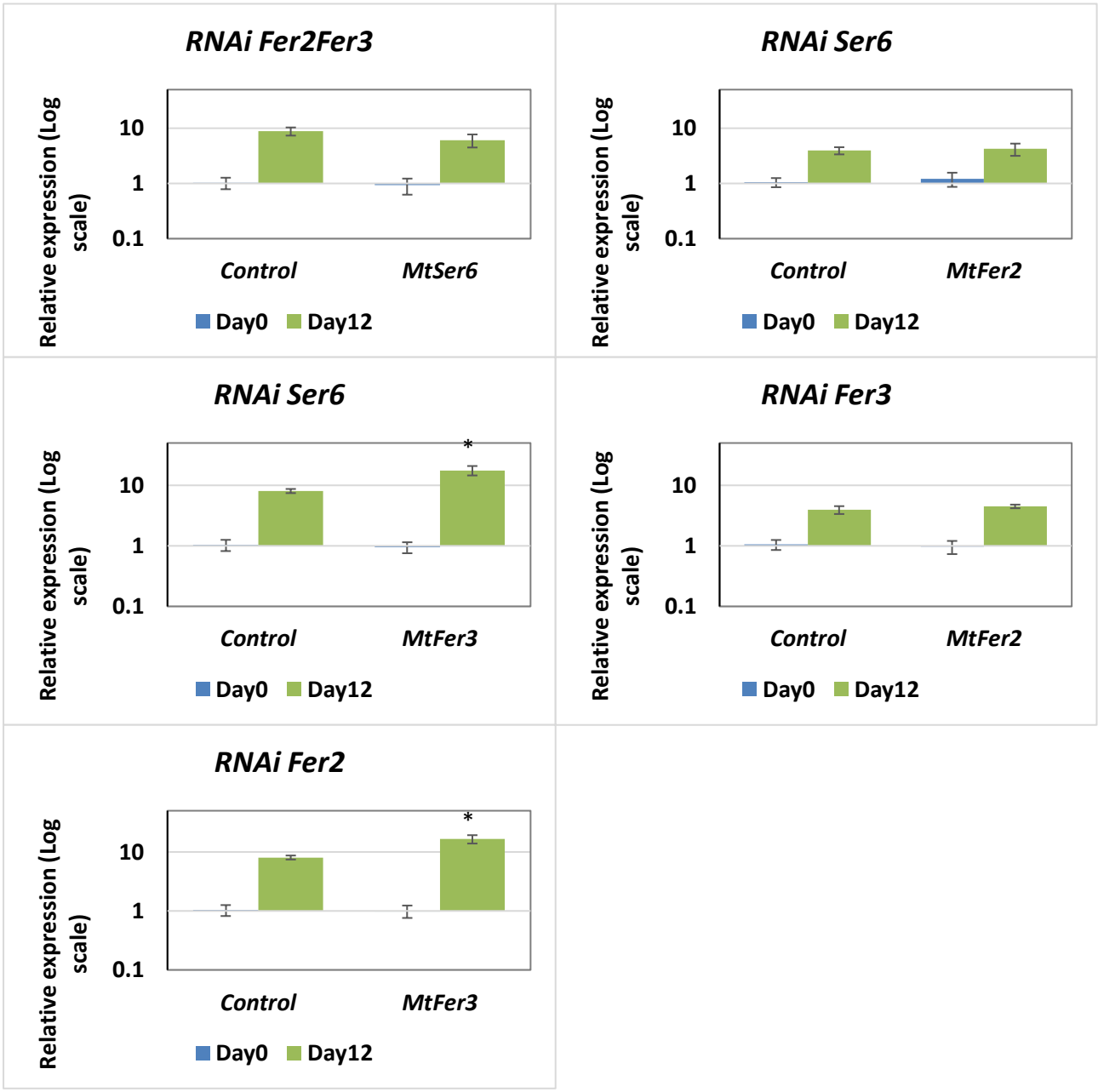

Fig. 11. Ectopic effects of RNAi KD on *Mtser6*, *MtFer2* and *MtFer3* expression. Relative transcript abundance of *MtSer6, MtFer2* and *MtFer3* genes in different RNAi transgenic nodules of the plants at 12 DAD was determined by qRT-PCR. Data were normalized to control treatment using two internal reference control genes (*βTubulin* and *MtPDF2*). The transcript level of each gene was determined from RNAi and control nodules at 0 DAD (blue bar) and 12 DAD (green bar). Values are the mean of 3 biological replicates. Error bars represent the standard errors of mean and asterisks indicate a significant difference between 12 days old RNAi and control plant nodules carrying an empty vector at $p<0.05$ (*), according to student's *t*-test.

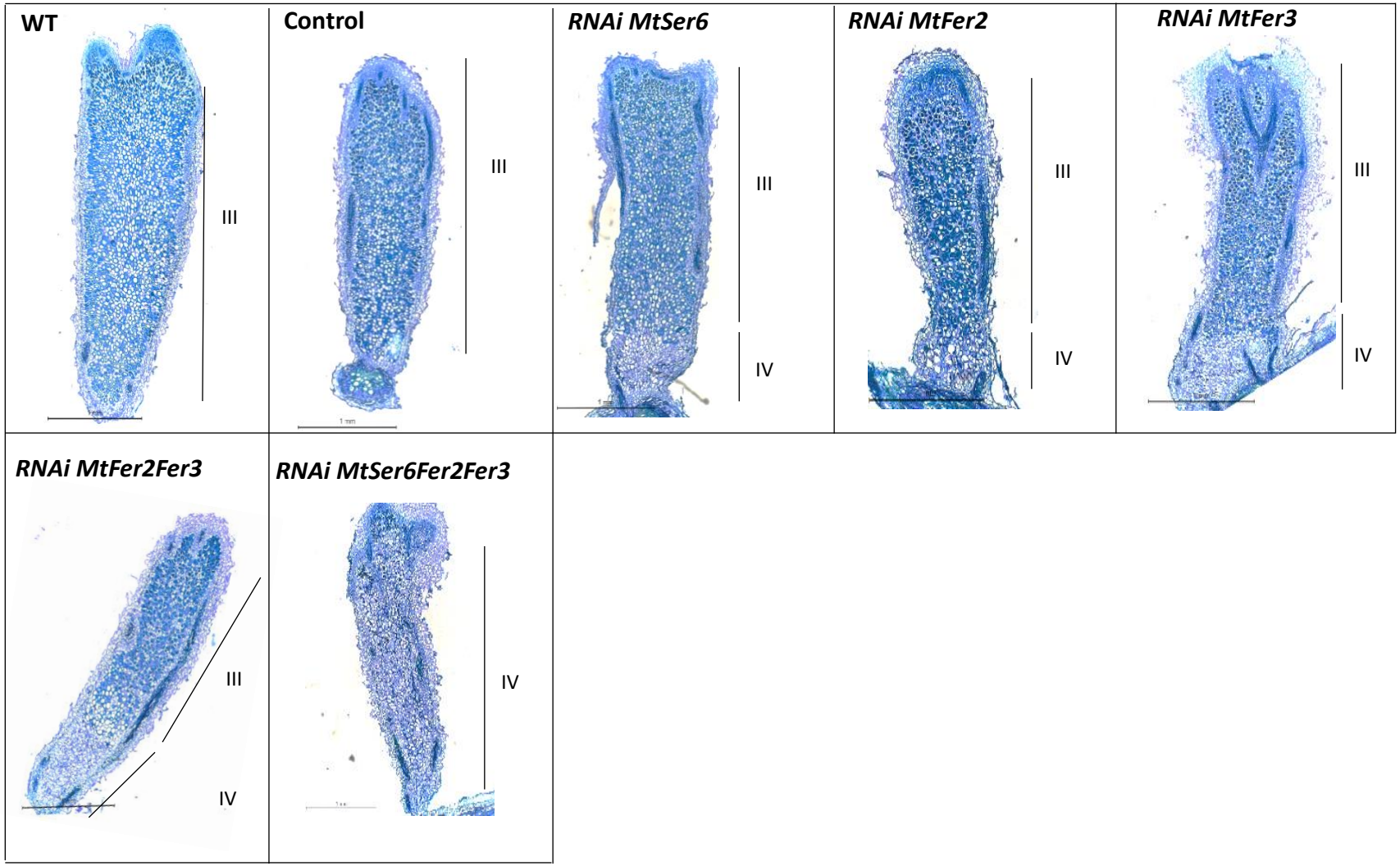

Fig. 12. Impact of reduced *MtSer6, MtFer2* and *MtFer3* expression on nodule senescence of drought-stressed *M. truncatula*. The RNAi, control (empty vector) and WT nodules were harvested from plants at 12 days of drought treatment. Nodules were sectioned as describe in Chapter 2 and light microscopic images taken after toluidine blue staining. Images are representative of 3 biological replicates and 3 independent nodules from each replicate. N_2 fixation (III) and senescence zones (IV) are indicated. Length of the scale bar is 1mm.

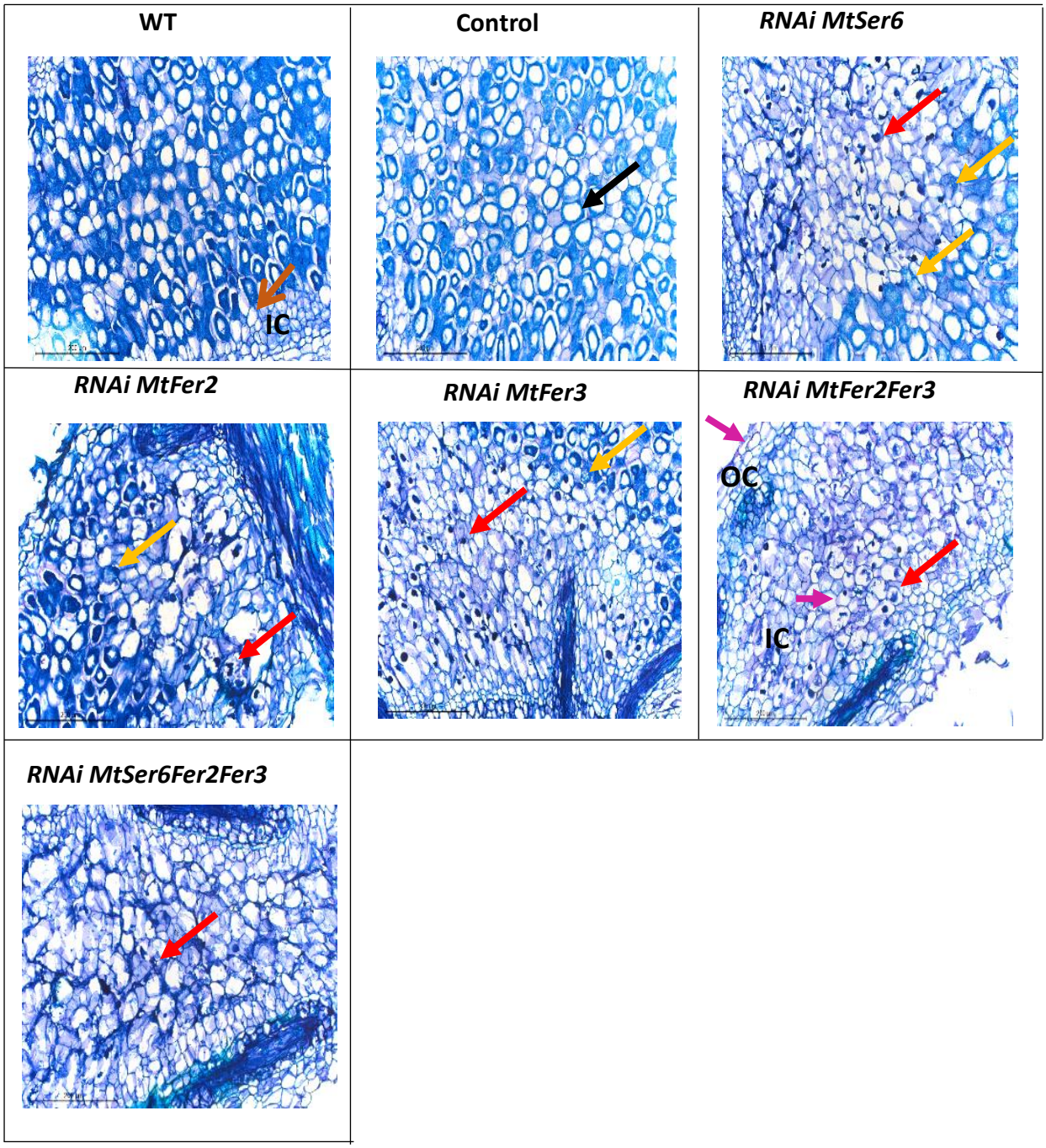

Fig. 13. Effect of reduced *MtSer6, MtFer2* and *MtFer3* expression on *M. truncatula* nodule bacteroids at the senescence zone. Nodules of WT, empty vector control and RNAi KD plants at 12 DAD were prepared as described in Chapter 2. Images were taken (20X) from the senescence Zone IV. Arrows indicate active (black), degrading (yellow) and completely senescent (red) bacteroids. IC; inner cortex, OC; outer cortex (Guerra *et al*., 2010; Brear *et al*., 2013). Length of the scale bar is 200µm.

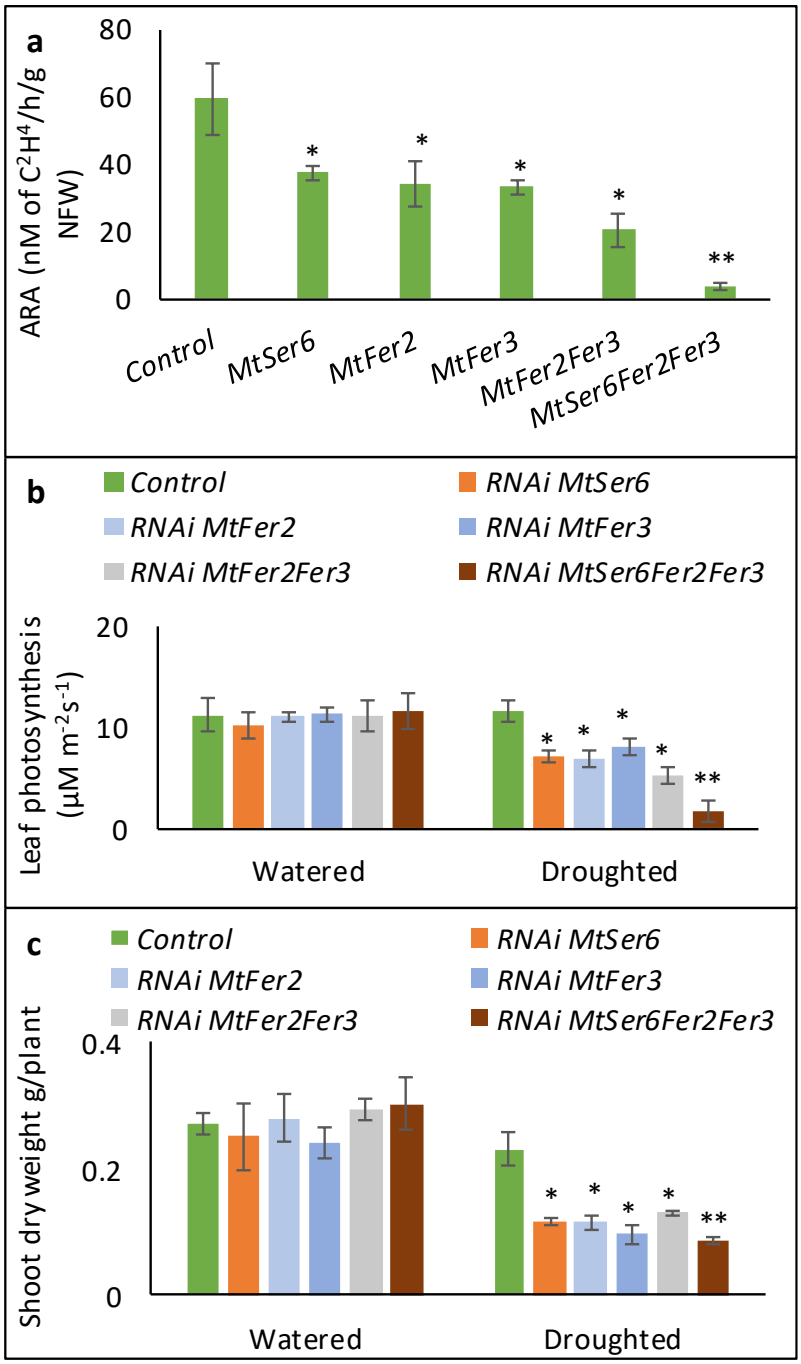

Fig. 14. Effect of reduced *MtSer6*, *MtFer2* and *MtFer3* expression on *M. truncatula* nodule nitrogenase activity and plant growth. (a) Acetylene reductase assay (ARA), (b) Leaf photosynthetic rate and (c) shoot biomass were measured from the control (empty vector) and RNAi plants at 12 days of drought treatment. NFW denotes nodule fresh weight. Values are the mean of least 3 biological replicates. Values are the mean of 3 to 5 biological replicates and error bars represent the standard errors of the mean. Asterisks indicate a significant difference between control and RNAi lines at $p<0.05$ (*) and $p<0.01$ (**), according to student's *t*-test.

5.3 Discussion

Plants respond to drought stress to reduce the risk of drought-induced damage. Reduction of leaf water loss involves primary responses such as adjustment of LWP, stomatal conductance and transpiration rate (Baena-Gonzalez *et al*., 2007; Grzesiak *et al*., 2006; Stanton & Mickelbart, 2014). Our results for drought-treated *M. truncatula* plants were in general agreement with those authors, and early responses comprised more negative LWP and reduced RWC, while stomatal conductance and transpiration rate was reduced at a later stage (Fig. 1a,b, 2a,b). Several reports in different legume species show that drought stress affects the symbiotic process through inhibiting rhizobial infection, nodule development and nitrogenase activity, due to lack of water transport from rhizosphere (Ramos *et al*., 2003; Marino *et al*., 2007; Esfahani *et al*., 2014; Kunert *et al*., 2016). However, the response of the SNF-dependent plants and their associative symbiotic relationship to drought stress is poorly understood. This study is aimed at specifying the response of N-fixing *M. truncatula* to drought stress and deciphering the roles of *serpins* and *ferritins* therein.

Following imposition of a 42-day drought-stress treatment, we observed that nitrogenase activity was affected within 14 DAD and this coincided with the initiation of nodule senescence. However, negative effects of drought stress on plant shoot biomass was seen only at 37 DAD (Fig. 3b,d, 4). This shows that drought-stressed *M. truncatula* limits nodule function prior to plant growth. These results are consistent with previous studies in legumes suggesting that nodules are the first organs being affected by drought stress (Purcell *et al*., 2000; Streeter, 2003; Ladrera *et al*., 2007). Drought stress affects the process of N_2 fixation by various factors such as limiting the carbon supply through suppressing CO_2 fixation, increasing the ureids accumulation in the nodule and transporting aminoacids (majorly glutamate and aspartate) from leaves to nodules (King & Purcell, 2005; Ladrera *et al*., 2007; Marquez-Garcia *et al*., 2015). Since N_2 fixation is crucial for accomplishing the N demand set by SNF-dependent plants (Vitousek *et al*., 2013), drought stressed legumes may experience severe N-deficiency in addition to the water stress. Indeed, we found that reduced nodule function coincided with symptoms of N deficiency such as decreased photosynthesis and chlorophyll levels after 25 DAD, before an effect on plant biomass was seen (Fig. 2c, 3a). Furthermore, RNAi lines, in which drought-induced nodule function was further reduced because of knocked down *serpin* or *ferritin* expression, exhibited even lower photosynthetic rate and shoot biomass, likely due to the limited N supply (Fig. 14a,b,c). These results suggest that nodule senescence during drought stress is likely an effective survival strategy while nodule senescence *per se* is detrimental to plant survival. Although senescence is programmed for nutrient remobilization (Schiltz *et al*. 2004; Distelfeld *et al*., 2014), the question then remains why nodule senescence is induced first and at such an early stage of drought stress.

To begin answering this question, we first investigated mechanisms of nodule senescence. Pierre *et al*. (2014) found that an increase in proteolytic activity is a key feature of nodule senescence and we showed that proteolytic activity of *M. truncatula* nodules increased from 25 DAD. In addition, total nodule protein content and lb content in particular decreased (Fig. 5a,b,c,d). These results are in agreement with previous reports suggesting that elevation of proteolytic activity during nodule senescence results in nodule protein and lb degradation (Pladys & Vance, 1993; Chungopast *et al*., 2014). It seems logical to propose that the nutrients obtained from the protein degradation are recycled and used as a N source to sustain plant growth. Indeed, several reports hypothesized that nutrient remobilization during environmental stress by early induction of senescence in older tissues may help to sustain plant growth (Fischer, 2007; Distelfeld *et al*., 2014; Chen *et al*., 2015; Maillard *et al*., 2015; Diaz-Mendoza *et al*., 2016). It was also reported in *M. truncatula* and *Glycine max* that nodules affected by drought stress succumb to early senescence and as such influence nutrient remobilization (Van de Velde *et al*., 2006; Ladrera *et al*., 2007). Thus, senescence of protein-rich nodules may extend the useful lifespan of nodules in times where reduced water and carbon supply (Atkins *et al*., 1984; Marquez-Garcia *et al*., 2015; Yuan *et al*., 2017), limit the nodules' ability to fix gaseous N.

However, in order for senescence to benefit plant growth it needs to be controlled as enhanced drought stress-induced senescence in the RNAi KD plants coincided with lower plant biomass. Since increased senescence also coincided with lower nitrogenase activity and lb contents, functional SNF was likely affected as well. It has been shown previously also that increase of nodule senescence decreases the N fixation and plant growth (Evans *et al*., 1999; Ramos *et al*., 1999; Voisin *et al*., 2003; Marino *et al*., 2007; Li *et al*., 2008). Thus a controlled progression of nodule senescence may allow the plant to maximise the positive effects of both nutrient recovery by senescence and remaining nutrient biosynthesis by SNF that is still sustainable, given the water and carbon availability. Here, we demonstrate the presence of two mechanisms that help assure a controlled senescence. First of all, expression of *M. truncatula MtSer6* (*serpin6*) seems to control or fine-tune nodule protease activity during drought-stress: Expression of this gene is induced in nodules of drought-stressed plants and KD of this induction causes higher papain like cysteine protease activity, lower protein levels, increased nodule senescence and reduced plant growth (Fig. 10a,b, 7, 8c). This is consistent with previous studies in Arabidopsis leaves showing that a *serpin* controlled the activity of papain-like cysteine protease that caused ROS damage and PCD (Vercammen *et al*. 2006; Lampl *et al*., 2013) and another in *M. truncatula* that elevation of papain-like cysteine protease activity causes degradation of bacteroids and induction of nodule senescence (Pierre *et al*., 2014). The increased papain-like cysteine protease activity coincided with lower lb levels and increased iron levels, suggesting that this activity

is directly involved in lb degradation (Fig. 10a,c,d). While lb are an N-rich nutrient source, they also harbour iron, which at elevated concentrations can induce ROS damage (Ravet *et al*., 2009). Therefore, we proposed that iron levels also needed to be controlled and here we show that expression of the ferritin encoding genes, *MtFer2* and more importantly *MtFer3*, is a second mechanism to assure controlled drought-induced nodule senescence. Expression of these genes is upregulated in response to drought stress while their RNAi KD resulted in increased iron and decreased nodule protein and lb levels (Fig. 10b,c,d). The effect of *ferritins* KD on protein levels is likely a result of iron-induced toxicity and ROS damage to bacteroids (Fig. 12, 13; Ravet *et al*., 2009; DeLaat *et al*., 2014).

The two mechanisms are likely to function largely independently of each other. Although, KD of *MtSer6* had a positive feedback regulation on *MtFer3* expression, it also resulted in excess iron increase (Fig. 10c, 11). Because *MtFer3* expression in the nodule is induced by high iron content (Briat *et al*., 2010), the feedback regulation is likely a secondary result of the increased iron levels, rather than a direct result of the increased papain-like cysteine protease levels. Conversely way around, KD of *ferritins* did not affect *MtSer6* expression or protease activities, but it did result in lower nodule protein levels (Fig. 10a,b 11), indicating that this was a result of oxidative damage to nodule proteins. Furthermore, KD of both *Serpin6* and the two *ferritins* resulted in much lower nitrogenase activity and more senescence than when knocked down separately, suggesting they have an additive effect on nodule function. Thus the combined data suggests that under drought stress, *M. truncatula* responds with the early senescence of nodules that is tightly controlled by the expression of *MtSer6* to regulate papain-like cysteine protease activity and *ferritins* to limit excess iron levels.

5.4 Conclusion

We showed that *M. truncatula* initiates nodule senescence as one of the early responses to drought stress and well before plant growth is affected. However, the senescence needs to be tightly regulated and increased senescence is detrimental to plant growth. The nodule achieves this in part by controlling the expression of protease inhibitor *serpin6* and *ferritins Fer2* and *Fer3*. We propose that this strategy allows the plant to maximise survival by continuing to benefit from remaining symbiotic N_2 fixation in a water-limiting environment for as long as possible and in the meantime also benefit from nutrients recovered during nodule senescence.

Chapter 6

Summary and conclusion

The symbiotic relationship in legumes is an important biological process that feeds the plant with N through the process called symbiotic nitrogen fixation (SNF). In sustainable agriculture system, this SNF has an important agronomical significance and can reduce the need of synthetic N fertilizer use. A large body of research has deciphered the crucial role of SNF in legumes and several researchers suggested that enhancing the SNF process through developing a suitable host-rhizobial partner would be an ideal strategy to reach sustainable legume production (Jensen & Hauggaard-Nielsen, 2003; Kneip *et al*., 2007; Mus *et al*., 2016). Legume plants may respond internally to changes in N availability in the rhizosphere as well as periods of drought stress. Elucidating the SNF process in response to N availability and nodule senescence regulation under drought conditions is essential to predict efficient symbiotic partners for use in sustainable agricultural systems. The theme of this thesis is centred on the *M. truncatula* SNF process under two different environmental conditions, N availability and drought stress, and the mechanisms involved in the drought-induced nodule senescence process.

In chapter 3, I assessed the symbiotic characteristics of *M. truncatula* Jemalong A17, a WT genetic background, in association with *E. meliloti* and identified the key serpin and ferritin genes expressed in nodule which are speculated to be involved in the drought-induced nodule senescence process. In chapter 4 I showed variation in the symbiotic efficiency of Jemalong A17 and another WT genetic background, R108, and in particular, R108 exhibited higher nitrogenase activity, bacteroid numbers and plant growth than Jemalong A17. To explain the variations I found, I began by determining the SNF process in both the genotypes in response to external N treatment. In contrast to the reports which elucidated that external N suppresses nodulation and N fixation (Saito *et al*., 2014; Ohyama *et al*., 2008; Reed *et al*., 2011; Walch-Liu *et al*., 2005), I found that R108 plants show only limited SNF suppression in response to external N treatment. Moreover, I show that R108 plants alter the nodules' location to cluster close the root collar in response to external N treatment. It was shown in *M. truncatula*, *M. sativa* and *T. subterraneum* by Goh *et al*. (2016) that internal N availability alters the root and nodule lengths and mass ratio depending upon the ability to fix N. This report is in favour of our argument and suggests that N treatment in the N-fixing R108 plant can change the nodule plasticity to increase or maintain the N input from the N fixation process. Interestingly, under drought stress both the Jemalong A17 and the R108 plants showed no SNF suppression and an increased N derivation from the fixation process to 38.99% and 48.35% respectively. Conversely, these plants have limited the N uptake from fertilizer under drought stress (Fig. I). As the Jemalong A17 and R108 plants prefer to uptake N from nodules rather than N fertilizer under drought stress, I focused on defining

the importance of SNF and N fertilization on plant growth maintenance under drought. This result highlighted that the benefit of SNF on plant growth recovery was well pronounced in both Jemalong A17 and R108 as compared to plants fertilized with N fertilizer alone. Luo *et al*. (2016) described that as compared to Jemalong A17, the R108 plant showed more drought tolerance under N-fertilized conditions. In contrast, this study shows that R108 plants exhibited significantly higher nodule and plant growth than Jemalong A17 under drought stress. It could be argued that *E. meliloti* inoculation and efficient SNF has an impact on plant growth maintenance under drought. I therefore chose R108 for further study to analyse the transcriptional changes of genes involved in stress and drought tolerance. Results showed that the N-fixing R108 plant expressed significantly higher transcripts of abscisic acid-related genes, such as *MtNced, MtZep* and *MtZip*, than the N-fertilized plant. Conversely, R108 plants exhibited significantly less expression of ethylene-responsive genes, *MtAcs* and *MtAco,* and ROS-responsive genes, *MtCat* and *MtRbohB.* This indicated that *E. meliloti* inoculation primed the host to cope with drought stress by inducing ABA-related gene expression and continued uptake of N from symbiosis.

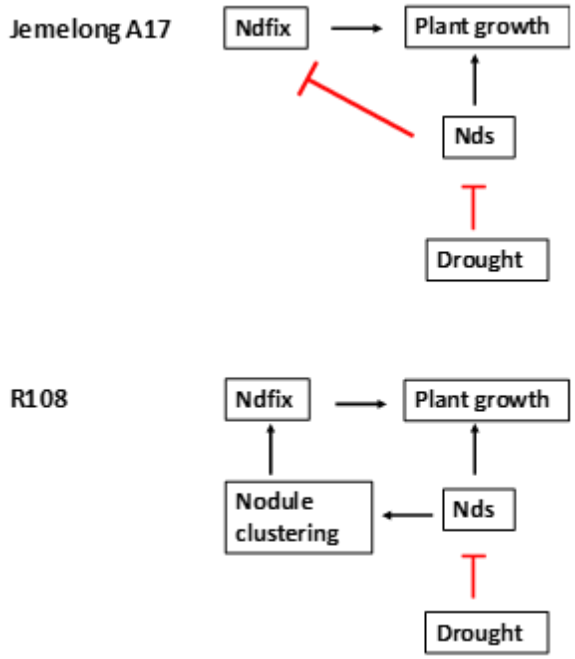

Fig. I. Proposed model of the response of two *M. truncatula* genotypes to external N fertilizer treatment and drought. During well-watered growth conditions, plant growth is supported by N uptake from N fertilizer present in the soil (Nds) in both Jemalong A17 and R108 genotypes. However, Nds suppresses N uptake from SNF (Ndfix) in Jemalong A17, but not in R108. In R108, Nds stimulates nodule clustering around the root collar, which is suggested to stimulate Ndfix and therefore also plant growth. In response to drought, Nds is suppressed in both genotypes, resulting in increased Ndfix in Jemalong A17 and R108 genotypes.

Drought stress is a major threat for both legume growth and SNF as limited moisture in the rhizosphere may limit the rhizobial infection, nodule development and plant growth. To cope with or adapt to drought stress, plants may induce early senescence in old tissues to remobilize the nutrients for growth recovery (Gregersen, 2011; Thomas, 2013; Maillard *et al*., 2015). Two reasons for early induction of nodule senescence in legumes could be; i) In order to reduce the investment of more carbon cost for bacteroid respiration and N_2 fixation under stress condition and ii) nodules have rich protein sources (Perlick *et al*., 1997; Kevei *et al*., 2002) such as, leghaemoglobins; amino acid rich proteins; and nodulins and enzymes for N, carbon and sulfur metabolisms which can be remobilized by a plant in order to recover the plant growth (Witty &Minchin, 2005). However, a legume plant may experience severe N deficiency and stress if drought-induced nodule senescence continues without controlled regulation. As SNF was sustained and nodules did not senesce during 12 days of drought (Chapter 4), I hypothesized in chapter 5 that drought-induced nodule senescence in *M. truncatula* is tightly regulated to maximize the benefit of nutrient recovery from the degrading nodules. The initial study in this chapter was performed to confirm the effect of drought stress on plant growth and N_2 fixation. Results showed that nodule senescence was induced prior to plant growth reduction in *M. truncatula.* Nodule senescence furthermore coincided with the elevation of proteolytic activity, degradation of nodule proteins including Lb and reduction in nitrogenase activity. This result was consistent with the previous study which suggested that the elevation of proteolytic activity causes bacteroid damage and nodule senescence in *Glycine max* and *M. truncatula* (Vorster *et al*., 2013; Wyk *et al*., 2014; Quain *et al*., 2015; Pierre *et al*., 2014). As a result of nodule protein and Lb degradation, *M. truncatula* nodules accumulate free iron ions, which are known to cause H_2O_2-mediated oxidative damage in cell organelles (Delaat *et al*., 2014; Ravet *et al*., 2009). For the purposes of identifying the mechanisms that ensure the controlled nodule senescence to minimize the SNF and plant growth reduction in drought-stressed *M. truncatula* nodules, I investigated the function of genes encoding an identified serpin (*Mtser6*) and two ferritins (*MtFer2,* and MtFer3; Chapter 3). Serpins interact and inhibit cysteine and papain proteases (Roberts *et al*., 2003; Lampl *et al*., 2013) and ferritins (Chapter 3) are known as iron scavengers (Delaat *et al*., 2014). Results show that these genes regulate *M. truncatula* nodule senescence under drought stress (Fig. II). A reverse genetic study revealed that *MtSer6* controls the elevation of papain-like cysteine protease activity which causes nodule protein and Lb degradation. The study also showed that ferritins can reduce the excess iron levels in nodules which cause iron toxicity. Knock-down of *Serpin6* and *ferritins* in *M. truncatula* showed bacteroid degradation and early nodule senescence at 12 days of drought. A qRT-PCR test to investigate the feedback regulation of these genes by knock-down effect suggests that these two mechanisms function independently under drought stress. As a consequence of these two independent

mechanisms, loss of gene expression in nodules in which both *ser6* and *ferritins* are knocked down, nodules exhibited further nodule protein degradation and severe senescence.

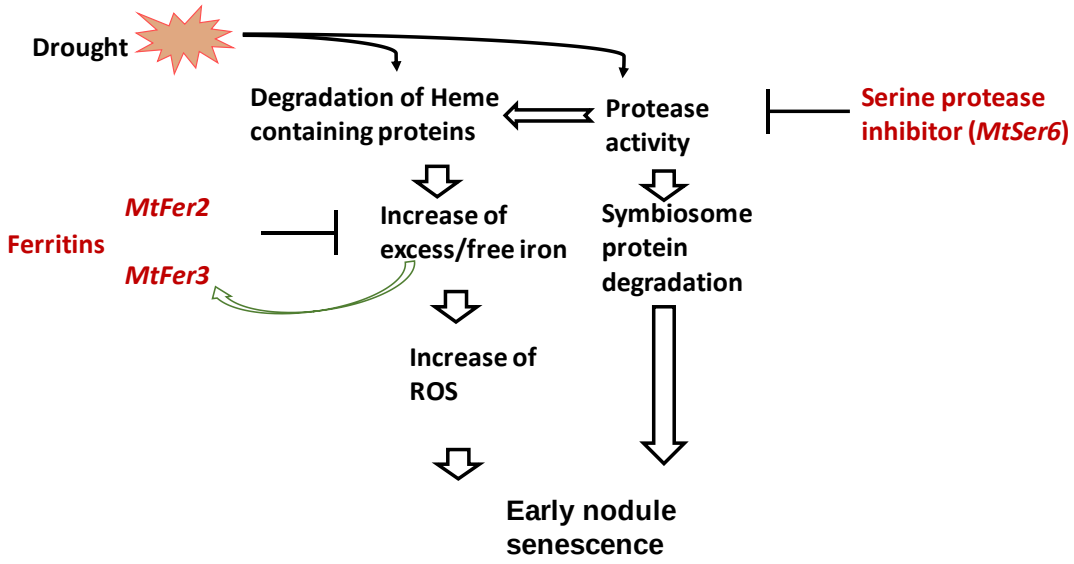

Fig. II. Proposed model for the regulation of drought-induced nodule senescence in *M. truncatula.* This process involves *Serpin MtSer6* to control the increase of proteolytic activity which could potentially degrade Lb and cause early nodule senescence. Similarly, under drought stress *M. truncatula* provokes *ferritins MtFer2* and *MtFer3* to scavenge excess free iron ions (released from Lb degradation) that causes H_2O_2-mediated ROS damage to bacteroids in nodules. These two mechanisms are functionally independent in controlling nodule senescence.

Taken together, the results of this study show that the varying responses of *M. truncatula-E. meliloti* symbiosis to external N and drought stress in different host genotypes can result in variable SNF suppression. Moreover, under drought stress *M. truncatula* may regulate the controlled nodule senescence process by involving serpin and ferritin to retain residual SNF and to maximize plant survival. As compared to drought-treated, N-fertilized plants, which have limited capacity to uptake N from soil, SNF plants sustained better plant growth as a result of controlled nodule senescence and abscisic acid-related gene induction. The results of this study are of important agronomical significance as the establishment of efficient symbiosis and controlled regulation of the nodule senescence mechanisms can reduce the reliance on N fertilizer and help to sustain sufficient levels of plant growth under changing climatic conditions.

Bibliography

Abolhasani M, Lakzian A, Tajabadipour A, Haghnia G. 2010. The study salt and drought tolerance of Sinorhizobium bacteria to the adaptation to alkaline condition. *Australian Journal of Basic and Applied Sciences* 4: 882–886.

Alami-Milani M, Amini R, Mohammedinasab AD, Shafaghkalvanegh J, Asgharzade A, Emaratpardaz J. 2013. Yield and yield components of lentil (*Lens culinaris* Medick.) affected by drought stress and mulch. *International Journal of Agriculture and Crop Sciences* 5: 1228–1231.

Alvarez-Alfageme F, Maharramov J, Carrillo L, Vandenabeele S, Vercammen D, van Breusegem F, Smagghe G. 2011. Potential use of a serpin from arabidopsis for pest control. *PLoS One* 6: e20278.

Annals of Botany 89: 907–916.

Annapurna K, Ramadoss D, Bose P, Vithal Kumar L. 2013. In situ localization of *Paenibacillus polymyxa* HKA-15 in roots and root nodules of soybean (*Glycine max* L.). *Plant Soil* 373: 641–648.

Appleby CA. 1984. Legbemoglobin and Rhizobium respiration. *Annual Review of Plant Physiology* 35: 443–178.

Arrese-Igor C, Gonzalez EM, Gordon AJ, Minchin FR, Galvez L, Royuela M, Cabrerizo PM, Aparicio-Tejo PM. 1999. Sucrose synthase and nodule nitrogen fixation under drought and other environmental stresses. *Symbiosis* 27: 189–212.

Aslam SN, Newman MA, Erbs G, Morrisey KL, Chinchilla D, Boller T, Jensen TT, De Castro C, Ierano T, Molinaro A. 2008. Bacterial polysaccharides suppress induced innate immunity by calcium chelation. *Current Biology* 18: 1078–1083.

Atkins CA, Shelp BJ, Kuo J, Peoples MB, Pate JS. 1984. Nitrogen nutrition and the development and senescence of nodules on cowpea seedlings. *Planta* 162: 316–326.

Bacanamwo M, Harper JE. 1997. The feedback mechanism of nitrate inhibition of nitrogenase activity in soybean may involve asparagine and/or products of its metabolism. *Physiologia Plantarum* 100: 371–377.

Baena-Gonzalez E, Rolland F, Thevelein JM, Sheen J. 2007. A central integrator of transcription networks in plant stress and energy signalling. *Nature* 448: 938–942.

Barrios AN, Hoogenboom G, Nesmith DS. 2005. Drought stress and the distribution of vegetative and reproductive traits of a bean cultivar. *Scientia Agricola* 62: 18–22.

Barry CS, Llop-Tous MI, Grierson D. 2000. The regulation of 1-aminocyclopropane-1-carboxylic acid synthase gene expression during the transition from system-1 to system-2 ethylene synthesis in tomato. *Plant Physiology* 123:979–986.

Barthelemy-Delaux C, Marburger D, Delaux PM, Conley S, Ané JM. 2014. Effect of drought on Bradyrhizobium japonicum populations in Midwest soils. *Plant Soil* 382: 165–173.

Becana M, Klucas RV. 1992. Oxidation and reduction of leghemoglobin in root nodules of leguminous plants. *Plant Physiology* 98: 1217–1221.

Becana M, Moran JF, Iturbe-Ormaetxe I. 1998. Iron-dependent oxygen free radical generation in plants subjected to environmental stress: toxicity and antioxidant protection. *Plant Soil* 201: 137– 147.

Belamkar V, Weeks NT, Bharti AK, Farmer AD, Graham MA, Cannon SB. 2014. Comprehensive characterization and RNA-Seq profiling of the HD-Zip transcription factor family in soybean (*Glycine max*) during dehydration and salt stress. *BMC Genomics* 15: 950.

Benedito VA, Torres-Jerez I, Murray JD, Andriankaja A, Allen S, Kakar K, Wandrey M, Verdier J, Zuber H, Ott T *et al*. 2008. A gene expression atlas of the model legume *Medicago truncatula. The Plant Journal* 55: 504–513.

Benjamin JG, Nielsen DC. 2006. Water deficit effects on root distribution of soybean, field pea and chickpea. *Field Crops Research* 97: 248–253.

Berrabah F, Bourcy M, Eschstruth A, Cayrel A, Guefrachi I, Mergaert P, Wen J, Jean V, Mysore KS, Gourion B, Ratet P. 2014. A nonRD receptor-like kinase prevents nodule early senescence and defense-like reactions during symbiosis. *New Phytologist* 203:1305–1314.

Bethlenfalvay GJ, Phillips DA. 1977. Ontogenetic interactions between photosynthesis and symbiotic nitrogen fixation in legumes. *Plant Physiology* 60: 419–421.

Bethlenfalvay GJ, Phillips DA. 1977. Ontogenetic interactions between photosynthesis and symbiotic nitrogen fixation in legumes. *Plant Physiology* 60: 419–421.

Bhalerao R, Keskitalo J, Sterky F, Erlandsson R, Bjorkbacka H, Birve SJ, Karlsson J, Gardestrom P, Gustafsson P, Lundeberg J, Jansson S. 2003. Gene expression in autumn leaves. *Plant Physiology* 131: 430–42.

Blaha D, Prigent-Combaret C, Mirza MS, Moenne-Loccoz Y. 2006. Phylogeny of the 1aminocyclopropane-1-carboxylic acid deaminase-encoding gene *acdS* in phytobeneficial and

pathogenic *Proteobacteria* and relation with strain biogeography. *FEMS Microbiology Ecology* 56: 455–470.

Blilou I, Ocampo JA, García-Garrido JM. 1999. Resistance of pea roots to endomycorrhizal fungus or Rhizobium correlates with enhanced levels of endogenous salicylic acid. *Journal of Experimental Botany* 50: 1663–1668.

Boddey RM, Victoria RL. 1986. Estimation of biological nitrogen fixation associated with Brachiaria and paspalum grasses using ^{15}N labelled organic matter and fertilizer. *Plant and Soil* 90: 265–292.

Bollman MI, Vessey, JK. 2006. Differential effects of nitrate and ammonium supply on nodule initiation, development, and distribution on roots of pea (*Pisum sativum*). *Canadian Journal of Botany* 84: 893–903.

Bournier M, Tissot N, Mari S, Boucherez J, Lacombe E, Briat JF, Gaymard F. 2013. *Arabidopsis* ferritin 1 (*AtFer1*) gene regulation by the phosphate starvation response 1 (*AtPHR1*) transcription factor reveals a direct molecular link between iron and phosphate homeostasis. *Journal of Biological Chemistry* 288: 22670–22680.

Branca G, McCarthy N, Lipper L, Jolejole MC. 2011. Climate-Smart Agriculture: A Synthesis of Empirical Evidence of Food Security and Mitigation Benefits from Improved Cropland Management. Mitigation of Climate Change in Agriculture Series no. 3. *Food and Agriculture Organization of the United Nations (FAO)*, Rome, Italy.

Brear EM, Day DA, Collina-Smith PM. 2013. Iron: an essential micronutrient for the legumerhizobium symbiosis. *Frontiers in Plant Science* 4: 359.

Briat JF, Lobreaux S. 1997. Iron transport and storage in plants. *Trends in plant science* 2: 187– 193.

Briat JF, Ravet K, Arnaud N, Duc C, Boucherez J, Touraine B, Cellier F, Gaymard F. 2010. New insights into ferritin synthesis and function highlight a link between iron homeostasis and oxidative stress in plants. *Annals of Botany* 105: 811–822.

Brodribb TJ, Holbrook NM. 2003. Stomatal closure during leaf dehydration, correlation with other leaf physiological traits. *Plant Physiology* 132: 2166–2173.

Buljovcic Z, Engels C. 2001. Nitrate uptake ability by maize roots during and after drought stress. *Plant Soil* 229: 125–135.

Cam Y, Pierre O, Boncompagni E, Herouart D, Meilhoc E, Bruand C. 2012. Nitric oxide (NO): a key player in the senescence of *Medicago truncatula* root nodules. *New Phytologist* 196: 548–560.

Cercos M, Gomez-Cadenas A, Ho THD. 1999. Hormonal regulation of a cysteine proteinase gene, *EBP1*, in barley aleurone layers: *Cis*- and *trans*-acting elements involved in the co-ordinated gene expression regulated by gibberellins and abscisic acid. *The Plant Journal*. 19**:** 107–118.

Chabaud M, Boisson-Dernier A, Zhang J, Taylor CG, Yu O, Barker DG. 2006. *Agrobacterium rhizogenes*-mediated root transformation. *The Medicago truncatula Handbook, The Samuel Roberts Noble Foundation.* 1-8.

Chaves MM, Pereira JS, Maroco J, Rodrigues ML, Ricardo CPP, Osorio ML, Carvalho I, Faria T, Pinheiro C. 2002. How plants cope with water stress in the field: photosynthesis and growth.

Chen Y, Xiao C, Wu D, Xia T, Chen Q, Chen F, Yuan L, Mi G. 2015. Effects of nitrogen application rate on grain yield and grain nitrogen concentration in two maize hybrids with contrasting nitrogen remobilization efficiency. *European Journal of Agronomy* 62: 79–89.

Chungopast S, Hirakawa H, Sato S, Handa Y, Saito K, Kawaguchi M, Tajima S, Nomura M. 2014. Transcriptomic profiles of nodule senescence in *Lotus japonicus* and *Mesorhizobium loti* symbiosis. *Plant Biotechnology* 31: 345–U115.

Clement M, Lambert A, Heroulart D, Boncompagni E. 2008. Identification of new up-regulated genes under drought stress in soybean nodules. *Gene* 426:15–22.

Cornic G, Ghashghaie J, Genty B, Briantais JM. 1992. Leaf photosynthesis is resistant to a mild drought stress. *Photosynthetica* 27: 295-309.

Cornic G. 1994. Drought stress and high light effects on leaf photosynthesis. *In:* Photoinhibition of photosynthesis: from molecular mechanisms to the field. Baker N.R., Boyer J.R. (eds.). *Bios Scientific Publishers, Oxford*. 297-313.

Crawford NM, Glass ADM. 1998. Molecular and physiological aspects of nitrate uptake in plants *Trends in Plant Science* 3: 389–395.

Crews TE, Peoples MB. 2004 Legume versus fertilizer sources of nitrogen: ecological trade-offs and human needs. *Agriculture, Ecosystems & Environment* 102: 279–297.

Crop Science 24: 297–303.

Dai A. 2013. Increasing drought under global warming in observations and models. *Nature Climate Change* 3: 52–58.

D'Apuzzo E, Valkov TV, Parlati A, Omrane S, Barbulova A, Sainz MM, Lentini M, Esposito S, Rogato A, Chiurazzi M. 2015. PII overexpression in *Lotus japonicus* affects nodule activity in permissive low

nitrogen conditions and increases nodule numbers in high nitrogen treated plants. *Molecular Plant Microbe Interaction* 28: 432–442.

Daryanto S, Wang L, Jacinthe PA. 2015. Global synthesis of drought effects on food legume production. *PLoS ONE* 10: e0127401.

David KAV, Apte SK, Banerji A, Thomas J. 1980. Acetylene reduction assay for nitrogenase activity: gas chromatographic determination of ethylene per sample in less than one minute. *Applied and Environmental Microbiology* 39: 1078–1080.

Davies KM, Deroles SC, Boase MR, Hunter DA, Schwinn KE. 2012. "Biolistics-based gene silencing in plants,". In: Sudowe S, Reske-Kunz A. eds. *Methods in Molecular Biology*. Heidelberg: SpringerVerlag. 63–74.

Deakin WJ, Broughton WJ. 2009. Symbiotic use of pathogenic strategies: rhizobial protein secretion systems. *Nature Reviews Microbiology* 7: 312–20.

DeLaat DM, Colombo CA, Chiorato AF, Carbonell SAM. 2014. Induction of ferritin synthesis by water deficit and iron excess in common bean (*Phaseolus vulgaris* L.). *Molecular Biology Reports* 41: 1427–1435.

Denison RF, Harter BL. 1995. Nitrate effects on nodule oxygen permeability and leghemoglobin. Nodule oximetry and computer modeling. *Plant Physiology* 107: 1355–1364.

Diaz-Mendoza M, Velasco-Arroyo B, Santamaria ME, Gonzalez-Melendi P, Martinez M, Diaz I. 2016. Plant senescence and proteolysis: two processes with one destiny. *Genetics and Molecular Biology* 39: 329–338.

Distelfeld A, Avni R, Fischer AM. 2014. Senescence, nutrient remobilization, and yield in wheat and barley. *Journal of Experimental Botany* 65: 3783–3798.

Dixon R, Kahn D. 2004. Genetic regulation of biological nitrogen fixation. *Nature Reviews Microbiology* 2: 621–631.

Djordjevic MA, Oakes M, Wong CE, Singh M, Bhalla P, Kusumawati L, Imin N. 2011. Border sequences of Medicago truncatula CLE36 are specifically cleaved by endoproteases common to the extracellular fluids of Medicago and soybean. *Journal of Experimental Botany* 62: 4649–4659.

Drake R, John I, Farrell A, Cooper W, Schuch W, Grierson D. 1996. Isolation and analysis of cDNAs encoding tomato cysteine proteases expressed during leaf senescence. *Plant Molecular Biology* 30: 755–767.

Dupont L, Alloing G, Pierre O, El Msehli S, Hopkins J, Herouart D, Frendo P. 2012. The legume root nodule: from symbiotic nitrogen fixation to senescence. *In Senescence,* Ed. Tetsuji Nagata, Intech Publisher. 137–157.

Durgo H, Klement E, Hunyadi-Gulyas E, Szucs A, Kereszt A, Medzihradszky KF, Kondorosi E. 2015. Identification of nodule-specific cysteine-rich plant peptides in endosymbiotic bacteria. *Proteomics* 15: 2291–2295.

Elboutahiri N, Thami-Alami I, Udupa SM. 2010. Phenotypic and genetic diversity in*Sinorhizobium meliloti* and *S. medicae* from drought and salt affected regions of Morocco. *BMC Microbiology* 10: 15.

Ellwood SR, D'Souza NK, Kamphuis LG, Burgess TI, Nair RM, Oliver RP. 2006. SSR analysis of the Medicago truncatula SARDI core collection reveals substantial diversity and unusual genotype dispersal throughout the Mediterranean basin. *Theoretical and Applied Genetics* 112: 977–983.

El-Yahyaoui F, Küster H, Amor BB, Hohnjec N, Pühler A, Becker A, Gouzy J, Vernié T, Gough C, Niebel A *et al*. 2004. Expression profiling in *Medicago truncatula* identifies more than 750 genes differentially expressed during nodulation, including many potential regulators of the symbiotic program. *Plant Physiology.* **136**, 3159–3176.

Esfahani MN, Sulieman S, Schulze J, Yamaguchi-Shinozaki K, Shinozaki K, Tran LS. 2014. Mechanisms of physiological adjustment of N2 fixation in *Cicer arietinum* L. (chickpea) during early stages of water deficit: single or multi-factor controls. *The Plant Journal* 79: 964–980.

Evans JR, Terashima I. 1987. Effects of Nitrogen Nutrition on Electron Transport Components and Photosynthesis in Spinach. *Functional Plant Biology* **14**: 59–68.

Evans PJ, Gallesi D, Mathieu C, Jesus Hernandez M, de Felipe M, Halliwell B, Puppo, A. 1999. Oxidative stress occurs during soybean nodule senescence. *Planta* 208: 73–79.

Farkas A, Maroti G, Durgo, H., Györgypál, Z., Lima RM, Medzihradszky KF, Kereszt A, Mergaert P, Kondorosi E. 2014. Medicago truncatula symbiotic peptide NCR247 contributes to bacteroid differentiation through multiple mechanisms. *Proceedings of the National Academy of Sciences,* USA 111: 5183–5188.

Feng HM, Yan M, Fan XR, Li BZ, Shen QR, Miller AJ, Xu GH. 2011. Spatial expression and regulation of rice high-affinity nitrate transporters by nitrogen and carbon status. *Journal of Experimental Botany* 62: 2319–2332.

Fenta BA, Beebe SE, Kunert KJ, Burridge JD, Barlow KM, Lynch PJ, Foyer CH. 2014. Field phenotyping of soybean roots for drought stress tolerance. *Agronomy* 4: 418–435.

Fischer A. 2007. Nutrient remobilization during leaf senescence. *In SGan, ed, Annual Plant Reviews, Vol 26.* Blackwell Publishing, Oxford*:* 87–107.

Fischer G, Winiwarter W, Ermolieva T, Cao GY, Qui H, Klimont Z, Wiberga D, Wagner F. 2010. Integrated modeling framework for assessment and mitigation of nitrogen pollution from agriculture: concept and case study for China. *Agriculture Ecosystem & Environment* 136: 116– 124.

Fluhr R, Lampl N, Roberts TH. 2012. Serpin protease inhibitors in plant biology. *Physiologia Plantarum* 145: 95–102.

Follett, RF. 2001. Nitrogen Transformation and Transport Processes. pp. 17-44, In R.F. Follett and J. Hatfield. (eds.). 2001. Nitrogen in the Environment; Sources, Problems, and Solutions. Elsevier Science Publishers. The Netherlands. 520 pp.

Foreman J, Demidchik V, Bothwell JH, Mylona P, Miedema H, Torres MA, Linstead P, Costa S, Brownlee C, Jones JD, Davies JM, Dolan L. 2003. Reactive oxygen species produced by NADPH oxidase regulate plant cell growth. *Nature* 422: 442–446.

Fox JE, Gulledge J, Engelhaupt E, Burow ME, McLachlan, JA. 2007. Pesticides reduce symbiotic efficiency of nitrogen-fixing rhizobia and host plants. *Proceedings of the National Academy of Sciences, USA* 104: 10282–10287.

Foyer CH, Rasool B, Davey JW, Hancock RD. 2016. Cross-tolerance to biotic and abiotic stresses in plants: a focus on resistance to aphid infestation. *Journal of Experimental Botany* 67: 2025– 2037.

Franssen HJ, Xiao TT, Kulikova O, Wan X, Bisseling T, Scheres B, Heidstra R. 2015. Root developmental programs shape the *Medicago truncatula* nodule meristem. *Development* 142: 2941–50.

Fricker MD, Meyer AJ. 2001. Confocal imaging of metabolism in vivo: pitfalls and possibilities. *Journal of Experimental Botany* 52: 631–640.

Galloway JN, Aber JD, Erisman JW, Seitzinger SP, Howarth RH, Cowling EB, Cosby BJ. 2003. The nitrogen cascade. *BioScience* 53: 341–356.

Galvez L, Gonzalez EM, Arrese-Igor C. 2005. Evidence for carbon flux shortage and strong carbon/nitrogen interactions in pea nodules at early stages of water stress. *Journal of Experimental Botany* 56: 2551–2561.

Gaymard F, Boucherez J, Briat JF. 1996. Characterization of a ferritin mRNA from Arabidopsis thaliana accumulated in response to iron through an oxidative pathway independent of abscisic acid. *Biochemical Journal* 318: 67–73.

Gentili F, Wall LG, Huss-Danell K. 2006. Effects of phosphorus and nitrogen on nodulation are seen already at the stage of early cortical cell divisions in *Alnus incana*. *Annals of Botany* 98: 309–315.

Goh CH, Nicotra AB, Mathesius U. 2016. The presence of nodules on legume root systems can alter phenotypic plasticity in response to internal nitrogen independent of nitrogen fixation. *Plant Cell & Environment* 39: 883–896.

González EM, Gordon AJ, James CL, Arrese-Igor C. 1995. The role of sucrose synthase in the response of soybean nodules to drought. *Journal of Experimental Botany* 46: 1515–1523.

Gordon AJ, Minchin FR, Skot L, James CL. 1997. Stress-induced declines in soybean N2 fixation are related to nodule sucrose synthase activity. *Plant Physiology* 114: 937–946.

Gosti F, Bertauche N, Vartanian N, Giraudat J. 1995. Abscisic acid-dependent and -independent regulation of gene expression by progressive drought in Arabidopsis thaliana. *Molecular Genetics and Genomics* 246: 10–18.

Gourion B, Berrabah F, Ratet P, Stacey G. 2015. Rhizobium–legume symbioses: the crucial role of plant immunity. *Trends Plant Sci* 20: 186–194.

Graham PH, Vance CP. 2003. Legumes: importance and constraints to greater use. *Plant Physiology* 131: 872–877.

Gregersen PL. 2011. Senescence and nutrient remobilization in crop plants. In: Hawkesford MJ, Barraclough P, eds. Oxford, UK: Wiley-Blackwell *The molecular and physiological basis of nutrient use efficiency in crops*. 83–102.

Groten K, Dutilleul C, van Heerden PDR, Vanacker H, Bernard S, Finkemeier I, Dietz KJ, Foyer CH. 2006. Redox regulation of peroxiredoxin and proteinases by ascorbate and thiols during pea root nodule senescence. *FEBS Letter* 580: 1269–1276.

Grzesiak MT, Grzesiak S, Skoczowski A. 2006. Changes of leaf water potential and gas exchange during and after drought in triticale and maize genotypes differing in drought tolerance. *Photosynthetica* 44: 561–568.

Grzesiak S, Iijima M, Kono Y, Yamauchi A. 1997. Differences in drought tolerance between cultivars of field bean and field pea. A comparison of drought-resistant and drought-sensitive cultivars. *Acta Physiologiae Plantarum* 19: 349–357.

Gubry-Rangin C, Bena G, Cleyet-Merel JC, Brunel B. 2013. Definition and evolution of a new symbiovar, sv. *rigiduloides*, among *Ensifer meliloti* efficiently nodulating Medicago species. *Systematic and Applied Microbiology* 36: 490–496.

Guerra JC, Coussens G, De Keyser A, De Rycke R, De Bodt S, Van De Velde W, Goormachtig S, Holsters M. 2010. Comparison of developmental and stress-induced nodule senescence in *Medicago truncatula*. *Plant Physiology* 152: 1574–1584.

Ha CV, Leyva-Gonzalez MA, Osakabe Y, Tran UT, Nishiyama R, Watanabe Y, Tanaka M, Seki M, Yamaguchi S, Dong NV *et al*. 2014. Positive regulatory role of strigolactone in plant responses to drought and salt stress. *Proceedings of the National Academy of Sciences, USA. 111: 851–6.*

Harper JE, Gibson AH. 1984. Differential nodulation tolerance to nitrate among legume species.

Harrison PM, Arosio P. 1996. Molecular properties, iron storage function and cellular regulation. *Biochimica et Biophysica Acta* 1275: 161–203.

Hartl FU, Bracher A, Hayer-Hartl M. 2011. Molecular chaperones in protein folding and proteostasis. *Nature* 475: 324–332.

Haupt-Herting S, Fock HP. 2000. Exchange of oxygen and its role in energy dissipation during drought stress in tomato plants. Physiologia Plantarium. 110: 489-495.

Haynes JG, Czymmek KJ, Carlson, CA, Veereshlingam H, Dickstein, Sherrier DJ. 2004. Rapid analysis of legume root nodule development using confocal microscopy. *New Phytologist* 163: 661–668.

He M, Dijkstra FA. 2014. *Drought effect on plant nitrogen and phosphorus: A metaanalysis*. *New Phytologist* 204: 924–931.

Hellens RP, Edwards EA, Leyland NR, Bean S, Mullineaux, PM. 2000. pGreen: a versatile and flexible binary Ti vector for Agrobacterium-mediated plant transformation. *Plant Molecular Biology* 42: 819–832.

Hellmann C, Grosse-Stoltenberg A, Laustro V, Oldeland J, Werner C. 2015. Retrieving nitrogen isotopic signatures from fresh leaf reflectance spectra: Disentangling delta δ15N from biochemical and structural leaf properties. Frontiers in Plant Science 6: 307.

Herridge DF, Peoples MB, Boddey RM. 2008. Global inputs of biological nitrogen fixation in agricultural systems. Plant Soil 311: 1–18.

Herrmann L, Chotte JL, Thuita M, Lesueur D. 2014. Effects of cropping systems, maize residues application and N fertilization on promiscuous soybean yields and diversity of native rhizobia in Central Kenya. *Pedobiologia* 57: 75–85.

Hoffmann B, Trinh TH, Leung J, Kondorosi A, Kondorosi E. 1997. A new *Medicago truncatula* line with superior in vitro regeneration, transformation, and symbiotic properties isolated through cell culture selection. *Molecular Plant Microbe Interactions* 10: 307–315.

Huang S, Cerny RE, Bhat DS, Brown SM. 2001. Cloning of an Arabidopsis patatin-like gene, STURDY, by activation T-DNA tagging. *Plant Physiology* 125: 573–584.

Huntington JA, Read RJ, Carrell RW. 2000. Structure of a serpin-protease complex shows inhibition by deformation. *Nature* 407: 923–926.

Iuchi S, Kobayashi M, Taji T, Naramoto M, Seki M, Kato T, Tabata S, Kakubari Y, Yamaguchi-

Jamet A, Mandon K, Puppo A, Herouart D. 2007. H_2O_2 is required for optimal establishment of the *Medicago sativa/Sinorhizobium meliloti* symbiosis. *Journal of Bacteriology* 189: 8741–8745.

Jensen ES, Hauggaard-Nielsen H. 2003. How can increased use of biological N2 fixation in agriculture benefit the environment. *Plant Soil* 252: 177–186.

Jiang S S, Liang X N, Li X, Wang S, Lv D, Max C Y, Li X H, Ma W, Yan Y. 2012. Wheat DroughtResponsive Grain Proteome Analysis by Linear and Nonlinear 2-DE and MALDI-TOF Mass Spectrometry. *International Journal of Molecular Sciences* 13:16065–16083.

Jiménez-Quesada MJ, Traverso JÁ, Alché Jde D. 2016. NADPH oxidase-dependent superoxide production in plant reproductive tissues. *Front Plant Science* 7: 359.

Jones KM, Sharopova N, Lohar DP, Zhang JQ, VandenBosch KA, Walker GC. 2008. Differential response of the plant *Medicago truncatula* to its symbiont *Sinorhizobium meliloti* or an exopolysaccharide-deficient mutant. *Proceedings of the National Academy of Sciences, USA* 108: 704–709.

Joo JH, Bae YS, Lee JS. 2001. Role of auxin-induced reactive oxygen species in root gravitropism. *Plant Physiology* 126: 1055–1060.

Kakar K, Wandrey M, Czechowski T, Gaertner T, Scheible WR, Stitt M, Torres-Jerez I, Xiao Y, Redman JC, Wu HC *et al.* 2008. A community resource for high-throughput quantitative RT-PCR analysis of transcription factor gene expression in *Medicago truncatula. Plant Methods* 4: 18–30.

Kang SG, Choi JH, Suh SG. 2002. A leaf-specific 27 kDa protein of potato Kunitz-type protease inhibitor is induced in response to abscisic acid, ethylene, methyl jasmonate, and water deficit. *Molecules and Cells* 13: 144–147.

Kang Y, Udvardi M. 2012. Global regulation of reactive oxygen species scavenging genes in alfalfa root and shoot under gradual drought stress and recovery. *Plant Signalling & Behaviour* 7: 539– 543.

Karim S, Liu X, Lu Z, Yuan Z, Zhu Y and Cao W. 2016. In-season estimation of rice grain yield using critical nitrogen dilution curve. *Field Crops Research* 195: 1–8.

Kevei Z, Vinardell J M, Kiss G B, Kondorosi A, Kondorosi E. 2002. Glycine-rich proteins encoded by a nodule-specific gene family are implicated in different stages of symbiotic nodule development in *Medicago* spp. *Molecular Plant Microbe Interaction* 15: 922–931.

Kidric M, Kos J, Sabotic J. 2014. Protease and their endogenous inhibitors in the plant response to abiotic stress. *Botanica Serbica* 38: 139–158.

King CA, Purcell LC. 2005. Inhibition of nitrogen fixation in soybean is associated with elevated ureides and amino acids. *Plant Physiology* 137: 1389–1396.

Kinoshita T, Yamada K, Hiraiwa N, Kondo M, Nishimura M, Hara-Nishimura I. 1999. Vacuolar processing enzyme is up-regulated in the lytic vacuoles of vegetative tissues during senescence and under various stress conditions. *The Plant Journal* 19: 43–53.

Kinoshita T. 1999. Vacuolar processing enzyme is up-regulated in the lytic vacuoles of vegetative tissues during senescence and under various stressed conditions. *The Plant Journal* 19: 43–53.

Kirizii DA, Vorobei NA, Kots SY. 2007. Relationships between nitrogen fixation and photosynthesis as the main components of the productivity in alfalfa. *Russian Journal of Plant Physiology* 54: 589– 594.

Kizilkaya R. 2009. Nitrogen fixation capacity of *Azotobacter spp*. Strains isolated from soils in different ecosystems and relationship between them and the microbiological properties of soils. *Journal of Environmental Biology* 30: 73-82.

Kneip C, Lockhart P, Voss C, Maier UG. 2007. Nitrogen fixation in eukaryotes—new models for symbiosis*. BMC Evolutionary Biology* 7: 55.

Kondorosi E, Mergaert P, Kereszt A. 2013. A paradigm for endosymbiotic life: cell differentiation of *Rhizobium* bacteria provoked by host plant factors. *Annual Review of Microbiology* 67: 611– 628.

Krouk G, Tillard P, Gojon A. 2006. Regulation of the high-affinity NO3- uptake system by NRT1.1mediated NO3- demand signaling in Arabidopsis. *Plant Physiology* 142: 1075–1086.

Ku YS, Au-Yeung WK, Yung YL, Li MW, Wen CQ, Liu X, Lam HM. 2013. Drought Stress and Tolerance in Soybean. In A Comprehensive Survey of Internaitonal Soybean Research—Genetics. Board, J.E., Ed.; InTech: New York, NY, USA. *Physiology, Agronomy and Nitrogen Relationships* 209–237.

Kunert KJ, Vorster BJ, Fenta BA, Kibido T, Dionisio G, Foyer CH. 2016. Drought stress responses in soybean roots and nodules. *Frontiers in Plant Science* 7: 1015–1021.

Kusumawati L, Imin N, Djordjevic MA. 2008. Characterization of the secretome of suspension cultures of Medicago species reveals proteins important for defense and development. *Journal of Proteome Research* 7: 4508–4520.

Ladrera R, Marino D, Larrainzar E, Gonzalez EM, Arrese-Igor C. 2007. Reduced carbon availability to bacteroids and elevated ureides in nodules, but not in shoots, are involved in the nitrogen fixation response to early drought in soybean. *Plant Physiology* 145: 539–546.

Lampl N, Alkan N, Davydov O, Fluhr R. 2013. Set-point control of RD21 protease activity by *AtSerpin1* controls cell death in Arabidopsis. *The Plant Journal* 74: 498–510.

Lampl N, Budai-Hadrian O, Davydov O, Joss TV, Harrop SJ, Curmi PMG, Roberts TH, Fluhr R. 2010. Arabidopsis *AtSerpin1*, crystal structure and in vivo interaction with its target protease RESPONSIVE TO DESICCATION-21 (RD21). *Journal of Biological Chemistry* 285: 13550–13560.

Larrainzar E, Wienkoop S, Scherling C, Kempa S, Ladrera R, Arrese-Igor C, Weckwerth W, Gonzalez EM. 2009. Carbon metabolism and bacteroid functioning are involved in the regulation of nitrogen fixation in *Medicago truncatula* under drought and recovery. *Molecular Plant–Microbe Interactions* 22: 1565–1576.

Larrainzar E, Wienkoop S, Weckwerth W, Ladrera R, Arrese-Igor C, Gonzalez EM. 2007. *Medicago truncatula* root nodule proteome analysis reveals differential plant and bacteroid responses to drought stress. *Plant Physiology* 144: 1495–1507.

LaRue TA, Child JJ. 1979. Sensitive fluorometric assay for leghemoglobin. *Analytical Biochemistry* 92: 11–15.

Latif AA, Osman G. 2017. Comparison of three genomic DNA extraction methods to obtain high DNA quality from maize. *Plant Methods* 13:1-9.

Lawlor DW, Cornic G. 2002. Photosynthetic carbon assimilation and associated metabolism in relation to water deficits in higher plants. *Plant, Cell & Environment* 25: 275–294.

Lawlor DW, Tezara W. 2009. Causes of decreased photosynthetic rate and metabolic capacity in water-deficient leaf cells: a critical evaluation of mechanisms and integration of processes. *Annals of Botany* 103: 561–579.

Lawlor DW. 1995. Effects of water deficit on photosynthesis. *In:* Environment and plant metabolism. Smirnoff N. (ed.). *Bios Scientific Publishers Ltd., Oxford*. 129-160.

Lawn RJ, Brun WA. 1974. Symbiotic nitrogen fixation in soybeans. I. Effects of photosynthetic source-sink manipulations. *Crop Science* 14: 11-16.

Li Y, Zhou L, Li Y, Chen D, Tan X, Lei L, Zhou J. 2008. A nodule-specific plant cysteine proteinase, *AsNODF32*, is involved in nodule senescence and nitrogen fixation activity of the green manure legume *Astragalus sinicus*. *New Phytologist* 180: 185–192.

Liang Y, Cao Y, Tanaka K, Thibivilliers S, Wan J, Choi J, Kang C, Qiu J, Stacey G. 2013. Nonlegumes respond to rhizobial Nod factors by suppressing the innate immune response. *Science* 341: 1384–1387.

Libault M, Farmer A, Brechenmacher L, Drnevich J, Langley RJ, Bilgin DD, Radwan O, Neece DJ, Clough SJ, May GD *et al.* 2010. Complete transcriptome of soybean root hair cell, a single cell model, and its alteration in response to *Bradyrhizobium japonicum* infection. *Plant Physiology* 152: 541–552.

Liese R, Schulze J, Cabeza RA. 2017. Nitrate application or P deficiency induce a decline in *Medicago truncatula*N_2-fixation by similar changes in the nodule transcriptome. *Scientific Reports* 7: 462–64.

Lobreaux S, Briat JF. 1991. Ferritin accumulation and degradation in different organs of pea (*Pisum sativum*) during development. *The Biochemical Journal* 274: 601–606.

Lodeiro AR, Gonzalez P, Hernandez A, Balague LJ, Favelukes G. 2000. Comparison of drought tolerance in nitrogen-fixing and inorganic nitrogen-grown common beans. *Plant Science* 154: 31–41.

Lodwig EM, Hosie AHF, Bordes A, Findlay K, Allaway D, Karunakaran R, Downie JA, Poole PS. 2003. Amino-acid cycling drives nitrogen fixation in the legume–Rhizobium symbiosis. *Nature* 422: 722–726.

Lohar DP, Sharopova N, Endre G, Penuela S, Samac D, Town C, Silverstein KA, VandenBosch K A. 2006. Transcript analysis of early nodulation events in *Medicago truncatula*. *Plant Physiology* 140: 221–234.

López-Gómez M, Hidalgo-Castellanos J, Iribarne C, Lluch C. 2014. Proline accumulation has prevalence over polyamines in nodules of *Medicago sativa* in symbiosis with *Sinorhizobium meliloti* during the initial response to salinity. *Plant Soil* 374: 149–159.

Lucas MM, Van de Sype G, Herouart D, Hernfindez MJ, Puppo A, De Felipe MR. 1993. Immunolocalization of ferritin in determinate and indeterminate legume root nodules. *Protoplasma* 204: 61–70.

Luo N, Yu X, Nie G, Liu J, Jiang Y. 2016. Specific peroxidases differentiate *Brachypodium distachyon* accessions and are associated with drought tolerance traits. *Annals of Botany* 118: 259–270.

Luscher A, Muller-Harvey I, Soussana JF, Rees RM, Peyraud JL. 2014. Potential of legume-based grassland-livestock systems in Europe: A review. *Grass and Forage Science* 69: 206–228.

Ma W, Guinel FC, Glick BR. 2003. *Rhizobium leguminosarum* biovar viciae 1-aminocyclopropane-1-carboxylate deaminase promotes nodulation of pea plants. *Applied and Environmental Microbiology* 69: 4396–4402.

Maillard A, Diquelou S, Billard V, Laine P, Garnica M, Prudent M, Garcia-Mina JM, Yvin JC, Ourry A. 2015. Leaf mineral nutrient remobilization during leaf senescence and modulation by nutrient deficiency. *Frontiers in Plant Science* 6: 317.

Makino A, Shimada T, Takumi S, Kaneko K, Matsuoka M, Shimamoto K, Nakano H, MiyaoTokutomi M, Mae T, Yamamoto N. 1997. Does decrease in ribulose-1,5-bisphosphate carboxylase by antisense rbcS lead to a higher N-use efficiency of photosynthesis under saturating CO2 and light in rice plants? *Plant Physiology* 114: 483–491.

Malik NSA, Pfeiffer NE, Williams DR, Wagner FW. 1981. Peptidohydrolases of soybean root nodules. Identification, separation and partial characterization of enzymes from bacteroid-free extracts. *Plant Physiology* 68: 386–392.

Mansfield TA. Davies WJ. 1981. Stomata and stomatal mechanisms. In: Aspinall D, editor; Page JR, Aspinall D, editors. Sydney, Australia: Academic Press. *The Physiology and Biochemistry of Drought Resistance in Plants* 315–346.

Mao G, Turner M, Yu O, Subramanian S. 2013. miR393 and miR164 influence indeterminate but not determinate nodule development. *Plant Signaling & Behavior* 8: e26753.

Marino D, Frendo P, Ladrera R, Zabalza A, Puppo A, ArreseIgor C, Gonzalez EM. 2007. Nitrogen fixation control under drought stress. Localized or systemic? *Plant Physiology* 143: 1968–1974.

Marquez-Garcia B, Shaw D, Cooper J, Karpinska B, Quain MD, Makgopa EM, Kunert K, Foyer CH. 2015. Redox markers for drought induced nodule senescence, a process occurring after droughtinduced senescence of the lowest leaves in soybean (*Glycine max*). *Annals of Botany* 116: 497–510.

Martínez-Abarca F, Herrera-Cervera JA, Bueno P, Sanjuan J, Bisseling T, Olivares J. 1998. Involvement of salicylic acid in the establishment of the *Rhizobium meliloti*-alfalfa symbiosis. *Molecular Plant Microbe Interaction* 11: 153–155.

Matamoros MA, Moran JF, Iturbe-Ormaetxe I, Rubio MC, Becana M. 1999. Glutathione and homoglutathione synthesis in legume root nodules. *Plant Physiol*ogy 121: 879–888.

Maunoury N, Redondo-Nieto M, Bourcy M, Bourcy M, Van de Velde W, Alunni B, Laporte P, Durand P, Agier N, Marisa L *et al*. 2010. Differentiation of symbiotic cells and endosymbionts in *Medicago truncatula* nodulation are coupled to two transcriptome-switches. *PLoS ONE* 5: e9519.

Merbach W, Schilling G. 1980. Effectiveness of symbiotic N2-fixation in leguminous plants, as affected by inoculation with rhizobia, by substrate, N-fertilizing, and 14C-sucrose application. *Zentralblatt Fur Bakteriologie* 135: 99–118.

Mergaert P, Nikovics K, Kelemen Z, Maunoury N, Vaubert D, Kondorosi A, Kondorosi E. 2003. A novel family in *Medicago truncatula* consisting of more than 300 nodule-specific genes coding for small, secreted polypeptides with conserved cysteine motifs. Plant Physiology 132**:** 161-173.

Mergaert P, Uchiumi T, Alunni B, Evanno G, Cheron A, Catrice O, Mausset AE, Barloy-Hubler F, Galibert F, Kondorosi A. 2006. Eukaryotic control on bacterial cell cycle and differentiation in the *Rhizobium*-legume symbiosis. *Proceedings of the National Academy of Sciences, USA.* 103: 5230–5235.

Mhadhbi H, Fotopoulos V, Mylona PV, Jebara M, Elarbi Aouani M, Polidoros AN. 2011. Antioxidant gene-enzyme responses in Medicago truncatula genotypes with different degree of sensitivity to salinity. *Physiologia Plantarium* 141: 201–14.

Miransari M, Riahi H, Eftekhar F, Minaie A, Smith DL. 2013. Improving soybean (*Glycine max* L.) N2 fixation under stress. *Journal of Plant Growth Regulation* 32: 909–921.

Moeder W, Barry CS, Tauriainen AA, Betz C, Tuomainen J, Utriainen M, Grierson D, Sandermann H, Langebartels C, Kangasjarvi J. 2002. Ethylene synthesis regulated by biphasic induction of 1aminocyclopropane-1-carboxylic acid synthase and 1-aminocyclopropane-1-carboxylic acid oxidase genes is required for hydrogen peroxide accumulation and cell death in ozone-exposed tomato. *Plant Physiology* 130**:** 1918–1926.

Moghaddam A, Raza A, Vollmann J, Ardakani MR, Wanek W, Gollner G, Friedel JK. 2015. Biological nitrogen fixation and biomass production stability in alfalfa (*Medicago sativa* L.) genotypes under organic management conditions. *Biological Agriculture & Horticulture* 31: 177– 192.

Mohammad RM, Akhavan-Kharazian M, Campbell WF, Rumbaugh MD. 1991. Identification of salt- and drought-tolerant *Rhizobium meliloti* L. strains. *Plant and Soil* 134: 271-276.

Morais RF, Quesada DM, Reis VM, Urquiaga S, Alves BJ, Boddey RM (2012). Contribution of biological nitrogen fixation to Elephant grass (*Pennisetum purpureum* Schum.). *Plant Soil* 356: 23–34.

Moreau D, Voisin AS, Salon C, Munier-Jolain N. 2008. The model symbiotic association between *Medicago truncatula* cv. Jemalong and *Rhizobium meliloti* strain 2011 leads to Nstressed plants when symbiotic N2 fixation is the main N source for plant growth. *Journal of Experimental Botany* 59: 3509–3522.

Mortier V, De Wever E, Vuylsteke M, Holsters M, Goormachtig S. 2012. Nodule numbers are governed by interaction between CLE peptides and cytokinin signaling. *The Plant Journal* 70: 367– 376.

Mosolov VV, Valueva TA. 2005. Proteinase inhibitors and their function in plants: A review. *Applied Biochemistry and Microbiology* 41: 227–246.

Muller B, Touraine B. 1992 Inhibition of NO3- uptake by various phloem-translocated amino acids in soybean seedlings. *Journal of Experimental Botany* 43: 617–623.

Muller J, Boller T, Wiemken A. 2001. Trehalose becomes the most abundant non-structural carbohydrate during senescence of soybean nodules. *Journal of Experimental Botany*. 52: 943– 947.

Munos S, Cazettes C, Fizames C, Gaymard F, Tillard P, Lepetit M, Lejay L, Gojon A. 2004. Transcript profiling in the chl1-5 mutant of *Arabidopsis* reveals a role of the nitrate transporter NRT1.1 in the regulation of another nitrate transporter, NRT2.1. *The Plant Cell* 16: 2433–2447.

Mus F, Crook MB, Garcia K, Garcia Costas A, Geddes BA, Kouri ED, Paramasivan P, Ryu MH, Oldroyd GE, Poole PS *et al*. 2016. Symbiotic Nitrogen Fixation and the Challenges to Its Extension to Nonlegumes. *Applied and Environmental Microbiology* 82: 3698–710.

Nambara E, Marion-Poll M. 2005. Abscisic acid biosynthesis and catabolism. *Annual Review of Plant Biology* 56: 165–185.

Nascimento F, Brígido C, Alho L, Glick BR, Oliveira S. 2012. Enhanced chickpea growth promotion ability of a mesorhizobia expressing an exogenous ACC deaminase gene. *Plant Soil* 353: 221–230.

Naveed M, Hussain MB, Mehboob I, Zahir ZA. 2017. Rhizobial Amelioration of Drought Stress in Legumes. In: Zaidi A., Khan M., Musarrat J. (eds) Microbes for Legume Improvement. *Springer*, Cham.

Nelson MS, Sadowsky MJ. 2015. Secretion systems and signal exchange between nitrogen-fixing rhizobia and legumes. *Frontiers in Plant Science* 6: 491.

Neo HH, Layzell DB. 1997. Phloem glutamine and the regulation of O2 diffusion in legume nodules. Plant Physiology 113: 259–267.

Nobuyasu H, Liu S, Adu-Gyamfi JJ, Mohapatra PK, Fujita K. 2003. Variation in the export of 13C and 15N from soybean leaf: the effects of nitrogen application and sink removal. *Plant Soil* 253: 331–339.

Noctor G, Veljovic-Jovanovic S, Driscoll S, Novitskaya L, Foyer C H. 2002. Drought and oxidative load in the leaves of C_3 plants: a predominant role for photorespiration? *Annals of Botany* 89: 841– 850.

Ohyama T, Ohtake T, Sueyoshi K, Tewari K, Takahashi Y, Ito S, Nishiwaki T, Nagumo Y, Ishii S, Sato T. 2008. Nitrogen fixation and metabolism in soybean plants. In Nitrogen Fixation Research Progress, Ed. Couto GN, *Nova Science Publishers Inc, New York* 15–109.

Okamoto S, Ohnishi E, Sato S, Takahashi H, Nakazono M, Tabata S, Kawaguchi M. 2009. Nod factor/nitrate-inducible CLE genes that drive systemic regulation of nodulation. *Plant Cell Physiology* 50: 67–77.

Oono Y, Ooura C, Rahman A, Aspuria ET, Hayashi K, Tanaka A, Uchimiya H. 2003. *p*Chlorophenoxyisobutyric acid impairs auxin response in Arabidopsis root. *Plant Physiology* 133: 1135–1147.

Ott T, Van Dongen JT, Gunther C, Krusell L, Desbrosses G, Vigeolas H, Bock V, Czechowski T, Geigenberger P, Udvardi MK. 2005. Symbiotic leghemoglobins are crucial for nitrogen fixation in legume root nodules but not for general plant growth and development. Current Biology 15**:** 531–535.

Ozturk ZN, Talame V, Deyholos M, Michalowski CB, Galbraith DW, Gozukirmizi N, Tuberosa R, Bohnert HJ. 2002. Monitoring large-scale changes in transcript abundance in drought- and saltstressed barley. *Plant Molecular Biology* 48: 551–573.

Pankievicz VCS, Do Amaral FP, Santos KFDN, Agtuca B, Xu Y, Schueller MJ, Arisi ACM, Steffens MBR, de Souza EM, Pedrosa FO *et al*. 2015. Robust biological nitrogen fixation in a model grassbacterial association. *The Plant Journal* 81: 907–919.

Pascual M, De Lorenzo CA, De Felipe MR, Rajalakshmi S, Gordon AJ, Thomas BJ, Minchin FR. 1996. Possible reasons for relative salt stress tolerance in nodules of white lupin cv. Multolupa. *Journal of Experimental Botany* 47: 1709–1716.

Pei ZM, Murata Y, Benning G, Thomine S, Klüsener B, Allen GJ, Grill E, Schroeder JI. 2000. Calcium channels activated by hydrogen peroxide mediate abscisic acid signalling in guard cells. *Nature* 406**:** 731–734.

Pereira NA, Song Z. 2008. Some commonly used caspase substrates and inhibitors lack the specificity required to monitor individual caspase activity. *Biochemical and Biophysical Research Communications* 377: 873–877.

Perlick AM, Kuster H, Puhler A. 1997. Analysis of genes expressed in root nodules of broad bean (V. faba L.). A. Legocki, H. Bothe, and A. Puhler, eds. Springer-Verlag, Berlin. *Biological Fixation of Nitrogen for Ecology and Sustainable Agriculture.* 91–94.

Petit JM, Briat JF, Lobreaux S. 2001. Structure and differential expression of the four members of the *Arabidopsis thaliana* ferritin gene family. *Biochemical Journal* 359: 575–582.

Pfaffl MW.2004. Quantification strategies in real-time PCR. Bustin SA Ed. *A-Z of quantitative PCR*. *Chapter 3. International University Line La Jolla, CA, USA*. 87–112.

Pfeiffer NE, Torres CM, Wagner FW. 1983. Proteolytic Activity in soybean root nodules: activity in host cell cytosol and bacteroids throughout physiological development and senescence. *Plant Physiology* 71: 797–802.

Pierre O, Hopkins J, CoJmbier M, Baldacci F, Engler G, Brouquisse R, Herouart D, Boncompagn E. 2014. Involvement of papain and legumain proteinase in the senescence process of *Medicago truncatula* nodules. *New Phytologist* 202: 849–863.

Pislariu CI, Murray JD, Wen J, Cosson V, Muni RR, Wang M, Benedito VA, Andriankaja A, Cheng X, Jerez IT *et al*. 2012. A *Medicago truncatula* tobacco retrotransposon insertion mutant collection with defects in nodule development and symbiotic nitrogen fixation. *Plant Physiology* 159: 1686– 1699.

Pladys D, Vance CP. 1993. Proteolysis during Development and Senescence of Effective and Plant Gene-Controlled Ineffective Alfalfa Nodules. *Plant physiology* 103: 379–384.

Poorter H, Evans JR. 1998. *Photosynthetic nitrogen-use efficiency of species that differ inherently in specific leaf area*. *Oecologia* 116: 26–37.

Prousek. 2007. Fenton chemistry in biology and medicine. *Pure and Applied Chemistry* 79: 2325– 2338.

Puppo A, Groten K, Bastian F, Carzaniga R, Soussi M, Lucas MM, de Felipe MR, Harrison J, Vanacker H, Foyer CH. 2005. Legume nodule senescence: roles for redox and hormone signalling in the orchestration of the natural aging process. *New Phytologist* 165: 683–701.

Purcell LC, King CA, Ball RA. 2000. Soybean cultivar differences in ureides and the relationship to drought tolerant nitrogen fixation and manganese nutrition. *Crop Science* 40: 1062–1070.

Quain MD, Makgopa ME, Cooper J, Kunert KJ, Foyer CH. 2015. Ectopic phytocystatin expression alters nodule numbers and influences the responses of soybean (*Glycine max)* to nitrogen deficiency. *Phytochemistry* 112: 179–187.

Quintana E, Larrainzar E, Seminario A, Diaz-Leal JL, Alamillo JM, Pineda M, Arrese-Igor C, Wienkoop S, Gonzalez EM. 2013. Local inhibition of nitrogen fixation and nodule metabolism in drought-stressed soybean. *Journal of Experimental Botany* 64: 2171–2182.

Ramos MLG, Gordon AJ, Minchin FR, Sprent JI, Parsons R. 1999. Effect of water stress on nodule physiology and biochemistry of a drought tolerant cultivar of common bean (*Phaseolus vulgaris* L.). *Annals of Botany* 83: 57–63.

Ramos MLG, Parsons R, Spront JI, James EK. 2003. Effect of water stress on nitrogen fixation and nodule structure of common bean *Pesquisa Agropecuaria Brasileira* 38: 339–347.

Ranawake AL, Dahanayaka N, Amarasingha UGS, Rodrigo WDRJ, Rodrigo UTD. 2011. Effect of water stress on growth and yield of mung bean (*Vigna radiata* L). *TARE* 14: 98–102.

Ravet K, Touraine B, Boucherez J, Briat, JF, Gaymard F, Cellier F. 2009. Ferritins control interaction between iron homeostasis and oxidative stress in Arabidopsis. *The Plant Journal* 57: 400–412.

Reed SC, Cleveland CC, Townsend AR. 2011. Functional ecology of free-living nitrogen fixation: A contemporary perspective*. Annual Review of Ecology, Evolution, and Systematics* 42: 489– 512.

Rehman A, Nautiyal CS. 2002. Effect of drought on the growth and survival of the stress-tolerant bacterium *Rhizobium sp*. NBRI2505 sesbania and its drought-sensitive transposon n5 mutant. Current Microbiology 45: 368–377.

Reid D, Li D, Ferguson BJ, Gresshoff PM. 2013. Structure-function analysis of the GmRIC1 signal peptide and CLE domain required for nodulation control in soybean. *Journal of Experimental Botany* 64: 1575–1585.

Remans R, Ramaekers L, Schelkens S, Hernandez G, García A, Luis Reyes J, Mendez N, Toscano V, Mulling M, Galvez L, Vanderleyden J. 2008. Effect of *Rhizobium-Azospirillum* coinoculation on nitrogen fixation and yield of two contrasting *Phaseolus vulgaris* genotypes cultivated across different environments in Cuba. *Plant Soil* 312: 25–37.

Ritchie RJ. 2006. Consistent sets of spectrophotometric chlorophyll equations for acetone, methanol and ethanol solvents. *Photosynthesis Research* 89: 27-41.

Roberts TH, Marttila S, Rasmussen SK, Hejgaard J. 2003. Differential gene expression for suicidesubstrate serine proteinase inhibitors (serpins) in vegetative and grain tissues of barley. *Journal of Experimental Botany* 54: 2251–2263.

Rodríguez-Celma J, Lin WD, Fu GM, Abadia J, Lopez-Millan AF, Schmidt W. 2013. Mutually exclusive alterations in secondary metabolism are critical for the uptake of insoluble iron compounds by Arabidopsis and *Medicago truncatula*. *Plant Physiology* 162: 1473–1485.

Rodriguez-Haas B, Finney LA, Vogt S, Gonzalez-Melendi P, Imperial J, Gonzalez-Guerrero M. 2013. Iron distribution through the developmental stages of *Medicago truncatula* nodules. *Metallomics* 5: 1247–125310.

Roekel R, Purcell LC. 2014. Soybean biomass and nitrogen accumulation rates and radiation use efficiency in a maximum yield environment. *Agronomy Journal* 54: 1189–1196.

Roponen I. 1970. The effect of darkness on the leghaemoglobin content and amino acid levels in the root nodules of pea plants. *Physiologia Plantarium* 23: 452–460.

Rosov FN, Shleev SV, Petrova NE, Tsyganov VE, Borisov AY, Topunov AF, Tikhonovich IA. 2001. The Sym31Gene Responsible for Bacteroid Differentiation Is Involved in Nitrate-Dependent Nodule Formation in Pea Plants. *Russian Journal of Plant Physiology* 48: 459–463.

Roux B, Rodde N, Jardinaud MF, Timmers T, Sauviac L, Cottret L, Carrere S, Sallet E, Courcelle E, Moreau S *et al*. 2014. An integrated analysis of plant and bacterial gene expression in symbiotic root nodules using laser-capture microdissection coupled to RNA sequencing. *The Plant Journal* 77: 817–37.

Ruijter JM, Ramakers C, Hoogaars WMH, Karlen Y, Bakker O, van den Hoff MJB, Moorman AFM. 2009. Amplification efficiency: Linking baseline and bias in the analysis of quantitative PCR data. Nucleic Acids Research: 3712.

Rustgi S, Boex-Fontvieille E, Reinbothe C, von Wettstein D, Reinbothe S. 2017. Serpin1 and WSCP differentially regulate the activity of the cysteine protease RD21 during plant development in Arabidopsis thaliana. *Proceedings of the National Academy of Sciences, USA* 114: 2212–2217.

Saha S, DasGupta M. 2015. Does SUNN-SYMRK Crosstalk occur in Medicago truncatula for regulating nodule organogenesis?. *Plant Signal and Behaviour*. 10: e1028703.

Saito A, Tanabata S, Tanabata T, Tajima S, Ueno M, Ishikawa S, Ohtake N, Sueyoshi K, Takuji Ohyama. 2014. Effect of Nitrate on Nodule and Root Growth of Soybean (*Glycine max* (L.) Merr.). *International Journal of Molecular Sciences* 15: 4464-4480.

Saito A, Tanabata S, Tanabata T, Tajima S, Ueno M, Ishikawa S, Ohtake N, Sueyoshi K, Ohyama T. 2014. Effect of nitrate on nodule and root growth of soybean (*Glycine max* (L.) Merr.). *International Journal of Molecular Sciences* 15: 4464–4480.

Salvagiotti F, Cassman KG, Specht JE, Walters DT, Weiss A, Dobermann A. 2008. Nitrogen uptake, fixation and response to fertilizer N in soybeans. *Field Crops Research* 108: 1–13.

Salvesen GS, Hempel A, Coll NS. 2015. Protease signalling in animal and plant-regulated cell death. *The FEBS Journal* 283: 2577–2598.

Samarah NH. 2005. Effects of drought stress on growth and yield of barley. *Agronomy for Sustainable Development* 25: 145–149.

Sambrook, Joseph. (2001). Molecular cloning: a laboratory manual. Cold Spring Harbor, N.Y. :Cold Spring Harbor Laboratory Press.

Sarker AM, Rahman MS, Paul NK. 1999. Effect of soil moisture on relative leaf water content, chlorophyll, proline and sugar accumulation in wheat. *Journal of Agronomy and Crop Science* 183: 225–229.

Schiltz S, Gallardo K, Huart M, Negroni L, Sommerer N, Burstin J. 2004. Proteome reference maps of vegetative tissues in pea. An investigation of nitrogen mobilization from leaves during seed filling. *Plant Physiology* 135: 2241–2260.

Serraj R, Vadez V, Denison RF, Sinclair TR. 1999. Involvement of ureides in nitrogen fixation inhibition in soybean. Plant Physiology 119: 289–296.

Serraj R. 2003. Effects of drought stress on legume symbiotic nitrogen fixation: physiological mechanisms. *Indian Journal of Experimental Biology* 41: 1136-1141.

Sharma R, Rawat V, Suresh CG. 2015. Genome-Wide Identification and Tissue-Specific Expression Analysis of UDP-Glycosyltransferases Genes Confirm Their Abundance in *Cicer arietinum* (Chickpea) Genome. *PLoS One* 9: e109715.

Shinozaki K, Shinozaki K. 2001. Regulation of drought tolerance by gene manipulation of 9-cisepoxycarotenoid dioxygenase, a key enzyme in abscisic acid biosynthesis in Arabidopsis. *The Plant Journal* 27: 325–333.

Sieuwerts S, De Bok FA, Mols E, De Vos WM, Van Hylckama Vlieg JE. 2008. A simple and fast method for determining colony forming units. Letters in Applied Microbiology 47: 275–278.

Simova-Stoilova L, Vassileva V, Petrova T, Tsenov N, Demirevska K, Feller U. 2006. Proteolytic activity in wheat leaves after drought stress and recovery. *General and Applied Plant Physiology* 9: 1–100.

Simsek S, Ojanen-Reuhs T, Stephens S B, and Reuhs B L. 2007. Strain-ecotype specificity in *Sinorhizobium meliloti-Medicago truncatula* symbiosis is correlated to succinoglycan oligosaccharide structure. *Journal of Bacteriology* 189: 7733–7740.

Smil V. 1999. Nitrogen in crop production: An account of global flows. *Global Biogeochemical Cycles* 13: 647–662.

Solomon M, Belenghi B, Delledonne M, Menachem E, Levine A. 1999. The involvement of cysteine proteases and protease inhibitor genes in the regulation of programmed cell death in plants. *The Plant Cell* 11: 431–443.

Soper FM, Boutton TW, Sparks JP. 2014. Investigating patterns of symbiotic nitrogen fixation during vegetation change from grassland to woodland using fine scale δ15N measurements. *Plant, Cell & Environment* 38: 89–100.

Souza RD, Ambrosini A, Passaglia LMP. 2015. Plant growth-promoting bacteria as inoculants in agricultural soils. *Genetics and Molecular Biology* 38: 401–419.

Srinivasan T, Kumar KR, Kirti PB. 2009. Constitutive expression of a trypsin protease inhibitor confers multiple stress tolerance in transgenic tobacco. *Plant Cell Physiology* 50: 541–553.

Stacey G, Libault M, Brechenmacher L, Wan J, May GD. 2006. Genetics and functional genomics of legume nodulation. *Current Opinion in Plant Biology* 9: 110–121.

Stanton KM, Mickelbart, MV. 2014. Maintenance of water uptake and reduced water loss contribute to water stress tolerance of *Spiraea alba* Du Roi and *Spiraea tomentosa* L. *Horticulture Research* 1: 14033–14039.

Steenhoudt O, Vanderleyden J. 2000. Azospirillum a free-living nitrogen-fixing bacterium closely associated with grasses: genetic, biochemical and ecological aspects. *FEMS Microbiology Review* 24: 487 – 506.

Steuer B, Stuhlfauth T, Fock HP. 1988. The efficiency of water use in water stressed plants is increased due to ABA induced stomatal closure. *Photosynthesis Research* 8: 327–336.

Straub D, Ludewig U, Neuhauser B. 2014. A nitrogen dependent switch in the high affinity ammonium transport in *Medicago truncatula*. *Plant Molecular Biology* 86: 485–494.

Streeter J. 1988. Inhibition of legume nodule formation and N_2 fixation by nitrate. *Critical Reviews in Plant Science* 7: 1–23.

Streeter JG. 1985. Nitrate inhibition of legume nodule growth and activity: 1. Long-term studies with a continuous supply of nitrate. *Plant Physiology* 77: 321–324.

Streeter JG. 2003. Effect of trehalose on survival of *Bradyrhizobium japonicum* during desiccation. *Journal of Applied Microbiology* 95: 484–491.

Sugawara M, Sadowsky MJ. 2014. Enhanced nodulation and nodule development by *nolR* mutants of *Sinorhizobium medicae* on specific *Medicago* host genotypes. *Molecular Plant Microbe Interaction* 27: 328–335.

Sulieman S, Tran LP. 2014. Symbiotic Nitrogen Fixation in Legume Nodules: Metabolism and Regulatory Mechanisms. *International Journal of Molecular Sciences* 15: 19389–19393.

Sulieman S, Van Ha C, Esfahani NM, Watanabe Y, Nishiyama R, Pham CT, Nguyen VD, Tran LS. 2015. DT2008: a promising new genetic resource for improved drought tolerance in soybean when solely dependent on symbiotic N2 fixation. *BioMed Research International* 2015: 7-10.

Suzaki T, Yoro E, Kawaguchi M. 2015. Leguminous plants: inventors of root Nodules to accommodate symbiotic bacteria. *International Review of Cell and Molecular Biology* 316: 111– 158.

Tahir J, Watanabe M, Jing HC, Hunter DA, Tohge T, Nunes-Nesi A, Brotman Y, Fernie AR, Rainer H, Dijkwel PP. 2012. Activation of R-mediated innate immunity and disease susceptibility is affected by mutations in a cytosolic O-acetylserine (thiol) lyase in Arabidopsis. *The Plant Journal* 73: 118–130.

Takeda N, Maekawa T, Hayashi M. 2012. Nuclear-localized and deregulated calcium- and calmodulin-dependent protein kinase activates rhizobial and mycorrhizal responses in *Lotus japonicus*. *The Plant Cell* 24: 810–822.

Talbi C, Sanchez C, Hidalgo-Garcia A, Gonz Alez EM, Arrese-Igor C, Girard L, Bedmar EJ, Delgado MJ. 2012. Enhanced expression of *Rhizobium etli* cbb3 oxidase improves drought tolerance of common bean symbiotic nitrogen fixation. *Journal of Experimental Botany* 63: 5035–5043.

Talebi R, Ensafi MH, Baghebani N, Karami E, Mohammadi K. 2013. Physiological responses of chickpea (*Cicer arietinum*) genotypes to drought stress. *Environmental and Experimental Botany* 11: 15.

Tang Q, Puri A, Padda KP, Chanway CP. 2017. Biological nitrogen fixation and plant growth promotion of lodgepole pine by an endophytic diazotroph *Paenibacillus polymyxa* and its GFPtagged derivative. *Botany* 95: 611–619.

Terpolilli JJ, O'Hara GW, Tiwari RP, Dilworth MJ, Howieson JG. 2008. The model legume *Medicago truncatula* A17 is poorly matched for N_2 fixation with the sequenced microsymbiont *Sinorhizobium meliloti* 1021. *New Phytologist* 179: 62–66.

Theil EC, Hase T, Barton LL, Hemings B. 1993. Plant and microbial ferritins, Iron chelation in plants and soil microorganisms. *New York, NY Academic Press*: 133–156.

Theil EC, Matzapetakis M, Liu X. 2006. Ferritins: iron/oxygen biominerals in protein nanocages. *Journal of Biological Inorganic Chemistry* 11: 803–810.

Thoiron S, Pascal N, Briat JF. 1997. Impact of iron deficiency and iron re-supply during the early stages of vegetative development in maize (*Zea mays* L.). *Plant Cell & Environment* 20: 1051–1060.

Thomas H. 2013. Senescence, ageing and death of the whole plant. *New Phytologist* 197: 696– 711.

Tilak KVB, Ranganayaki RN, Pal KK, Desaxena R, Shekhar-Nautiyal AK, Shilpi Mittal C, Tripathi AK, Johri BN. 2005. Diversity of plant growth and soil health supporting bacteria. *Current Science* 89: 136–150.

Timmers ACJ, Soupene E, Auriac M-C, de Billy F, Vasse J, Boistard P, Truchet G. 2000. Saprophytic intracellular rhizobia in alfalfa nodules. *Molecular Plant Microbe Interaction* 13**:** 1204–1213.

Tobar R, Azcon R, Barea JM. 1994. Improved nitrogen uptake and transport from ^{15}N-labelled nitrate by external hyphae of arbuscular mycorrhiza under water-stressed conditions. *New Phytologist* 126: 119–122.

Toker C, Canci H, Ceylan FO. 2006. Estimation of outcrossing rate in chickpea (*Cicer arietinum* L.) sown in autumn. *Euphytica* 151: 201–205.

Udvardi M, Brodie EL, Riley W, Kaeppler SS, Lynch J. 2015. Impacts of agricultural nitrogen on the environment and strategies to reduce these impacts. *Procedia Environmental Sciences* 29: 303.

Van de Velde W, Zehirov G, Szatmari A, Debreczeny M, Ishihara H, Kevei Z, Farkas A, Mikulass K, Nagy A, Tiricz H. *et al*. 2010. Plant peptides govern terminal differentiation of bacteria in symbiosis. *Science* 327: 1122-1126.

Van de Velde W, Guerra JC, De Keyser A, De Rycke R, Rombauts S, Maunoury N, Mergaert P, Kondorosi E, Holsters M, Goormachtig S. 2006. Aging in legume symbiosis. A molecular view on nodule senescence in *Medicago truncatula*. *Plant Physiology* 141: 711–720.

Vandenabeele S, Van Der Kelen K, Dat J, Gadjev I, Boonefaes T, Morsa S, Rottiers P, Slooten L, Montagu MV, Zabeau M *et al*. 2003. A comprehensive analysis of hydrogen peroxide-induced gene expression in tobacco. *Proceedings of the National Academy of Sciences, USA* 100: 16113– 16118.

Vargas LK, Volpiano CG, Lisboa BB, Giongo A, Beneduzi A, Passaglia LMP. 2017. Potential of rhizobia as plant growth–promoting rhizobacteria. In: Khan MS, Zaide A, Musarrat J (eds) Microbes for legume improvement. *Springer*, Berlin: 153–174.

Vaseva I, Zehirov G, Stoychev V, Kirova E, Simova-Stoilova L, Sabotic J, Sustar-Vozlic J, Meglic V, Kidric M. 2014. Semi-quantitative RT-PCR analysis of selected protease inhibitors in droughtstressed *Triticum aestivum. Genetics and Plant Physiology* 4: 57–67.

Vensel WH, Tanaka CK, Cai N, Wong JH, Buchanan BB, Hurkman WJ. 2005. Developmental changes in the metabolic protein profiles of wheat endosperm. Proteomics 5: 1594–1611.

Vercammen D, Belenghi B, van de Cotte B, Beunens T, Gavigan JA, De Rycke R, Brackenier A, Inze D, Harris JL, Van Breusegem F. 2006. Serpin1 of *Arabidopsis thaliana* is a suicide inhibitor for *metacaspase 9. Journal of Molecular Biology* 364: 625–636.

Verma DPS, Hu CA, Zhang M. 1992. Root nodule development: origin, function and regulation of nodulin genes. *Physiologia Plantarium* 85: 253–265.

Vierstra RD. 1996. Proteolysis in plants: mechanisms and functions. *Plant Molecular Biology* 32: 275–302.

Vitousek PM, Menge DNL, Reed SC, Cleveland CC. 2013. Biological nitrogen fixation: rates, patterns, and ecological controls in terrestrial ecosystems. *Philosophical Transactions of the Royal Society* 368: 1–9.

Voisin AS, Salon C, Jeudy C, Warembourg FR. 2003. Seasonal patterns of 13C partitioning between shoot and nodulated roots in *Pisum sativum* L. under different air CO2 concentrations. *Annals of Botany* 91: 539–546.

Vorster BJ, Schluter U, Du Plessis M, van Wyk S, Makgopa ME, Ncube I, Quain MD, Kunert K, Foyer CH. 2013. The cysteine protease–cysteine protease inhibitor system explored in soybean nodule development. *Agronomy* 3: 550–570.

Vurukonda SSKP, Vardharajula S, Shrivastava M, SkZ A. 2016. Enhancement of drought stress tolerance in crops by plant growth promoting rhizobacteria. *Microbiology Research* 184: 13–24.

Walch-Liu P, Ivanov II, Filleur S, Gan Y, Remans T, Forde BG. 2006. Nitrogen regulation of root branching. *Annals of Botany* 97: 875–881.

Wang TZ, Tian QY, Wang BL, Zhao MG, Zhang WH. 2014. Genome variations account for different response to three mineral elements between *Medicago truncatula* ecotypes *Jemalong A17* and *R108*. *BMC Plant Biology* 14: 22.

Waterer JG, Vessey JK. 1993. Effect of low static nitrate concentrations on mineral nitrogen uptake, nodulation, and nitrogen fixation in field pea. *Journal of Plant Nutrition* 16: 1775–1789.

Westhoek A, Field E, Rehling F, Mulley G, Webb I, Poole PS, Turnbull LA. 2017. Policing the legume-Rhizobium symbiosis: a critical test of partner choice. Scientific Reports 7: 1419.

Witty JF, Minchin FR. 1997. Dynamic control of oxygen diffusion resistance in nodules. In: Legocki A, Bothe H, Puhler A, eds. NATO ASI Series G39. Berlin, Heidelberg: Springer-Verlag. *Biological fixation of nitrogen for ecology and sustainable agriculture* 241–4.

Wollaston VB, Earl S, Harrison E, Mathas E, Navabpour S, Page T, Pink D. 2003. The molecular analysis of leaf senescence-a genomics approach. *Plant Biotechnology Journal* 1: 3–22.

Wyk SG, Du Plessis M, Cullis CA, Kunert KJ, Vorster BJ. 2014. Cysteine protease and cystatin expression and activity during soybean nodule development and senescence. *BMC Plant Biology* 14: 294.

Xia X, Ma C, Dong S, Xu Y, Gong Z. 2017. Effects of nitrogen concentrations on nodulation and nitrogenase activity in dual root systems of soybean plants. *Soil Science and Plant Nutrition* 63: 470–482.

Xuan Z, Manning L, Nelson J, Richmond JE, Colon-Ramos DA, Shen K, Kurshan PT. 2017. Clarinet (CLA-1), a novel active zone protein required for synaptic vesicle clustering and release. *eLife* 6: e29276.

Yadav SS, Kumar J, Yadav SK, Singh S, Yadav VS, Turner NC, Redden R. 2006. Evaluation of *Helicoverpa* and drought resistance in desi and kabuli chickpea. *Plant Genetic Resources: Characterisation and Utilisation* 4: 198–203.

Yamaguchi M, Valliyodan B, Zhang J, Lenoble ME, Yu O, Rogers EE, Nguyen HT, Sharp RE. 2010. Regulation of growth response to water stress in the soybean primary root. I. Proteomic analysis reveals region−specific regulation of phenylpropanoid metabolism and control of free iron in the elongation zone. *Plant Cell & Environment* 33: 223–243.

Yanni Y, Zidan M, Dazzo F, Rizk R, Mehesen A, Abdelfattah F, Elsadany A. 2016. Enhanced symbiotic performance and productivity of drought stressed common bean after inoculation with tolerant native rhizobia in extensive fields. *Agriculture, Ecosystems & Environment* 232: 119–128.

Yoshida T, Fujita Y, Maruyama K, Mogami J, Todaka D, Shinozaki K, Yamaguchi-Shinozaki K. 2015. Four *Arabidopsis* AREB/ABF transcription factors function predominantly in gene expression downstream of SnRK2 kinases in abscisic acid signalling in response to osmotic stress. *Plant Cell & Environment* 38: 35–49.

Yousfi N, Sihem N, Ramzi A, Abdelly C. 2016. Growth, photosynthesis and water relations as affected by different drought regimes and subsequent recovery in *Medicago laciniata* (L.) populations. *Journal of Plant Biology* 59: 33–43.

Yuan SL, Li R, Chen HF, Zhang CJ, Chen LM, Hao QN, Chen SL, Shan ZH, Yang ZL, Zhang XJ *et al*. 2017. RNA-Seq analysis of nodule development at five different developmental stages of soybean (*Glycine max*) inoculated with *Bradyrhizobium japonicum* strain 113-2. *Scientific Reports* 7: 42248.

Yue YS, Zhang MC, Zhang JC, Duan LS, Li ZH. 2011. *Arabidopsis LOS5/ABA3* overexpression in transgenic tobacco (*Nicotiana tabacum* cv. *Xanthinc*) results in enhanced drought tolerance. *Plant Science* 181: 405–411.

Zahran HH. 1999. Rhizobium-legume symbiosis and nitrogen fixation under severe conditions and in an arid climate. *Microbiology and Molecular Biology Reviews* 63: 968–989.

Zegada-Lizarazu W, Monti A. 2013. Photosynthetic response of sweet sorghum to drought and re-watering at different growth stages. *Physiologia Plantarium* 149: 56–66.

Zhang JY, Cruz DE, Carvalho MH, Torres-Jerez I, Kang Y, Allen SN, Huhman DV, Tang Y, Murray J, Sumner LW *et al*. 2014. Global reprogramming of transcription and metabolism in *Medicago truncatula* during progressive drought and after re-watering. *Plant Cell & Environment* 37: 2553–2576.

Zhao, Liu M, Xia W, Wang X, Zhang T, Wen-Hao. 2014. Cold acclimation-induced freezing tolerance of *Medicago truncatula* seedlings is negatively regulated by ethylene. *Physiologia plantarum*. 152: pp12161.

Zhu JK. 2002. Salt and drought signal transduction in plants. *Annual Review of Plant Biology* 53: 247–73.

Zimmermann IM, Heim MA, Weisshaar B, Uhrig JF. 2004. Comprehensive identification of *Arabidopsis thaliana* MYB transcription factors interacting with R/ B-like BHLH proteins. *The Plant Journal* 40: 22–34.

Appendices

Appendix 1. Growth media and nutrients used in this study

TAE buffer (50X)

Components	**g or ml/L**
Tris free base	242
Disodium EDTA	18.61
Glacial Acetic Acid	57.1ml
Deionized water	1L

TBE buffer (10X)

Components	**g or ml/L**
Tris free base	108
Na2EDTA	9.3
Boric acid	55
Deionized water	1L

Yeast Extract Mannitol medium (YEM broth)

Components	**g/L**
Yeast extract	1.0
Mannitol	10.0
Sodium chloride	1.0
Di-potassium hydrogen phosphate	0.5
Magnesium sulfate	0.2
Calcium chloride	1.0
Agar (for solid media)	18

Jenson's seedling medium

Components	**g/L**
Calcium phosphate	1.0
Di-potassium hydrogen phosphate	0.2
Magnesium sulfate	0.2
Sodium chloride	0.2
Ferric chloride	0.1
Potassium nitrate (If N source needed)	0.2

TY/calcium medium

Components	**amount/L**
Bactro tryptone	5g
Yeast extract	3g
CaCl2	6mM
Agar (for soild media	18

Modified Fahraeus medium

Stock solutions	**Stock concentration**	**Volume (ml) (for 1 liter of 1x medium)**	**Final Concentration**
Macro nutrients			
$MgSO_4$, 7 H_2O	0.5M	1.0	0.5mM
KH_2PO_4	0.7M	1.0	0.7mM
Na_2HPO_4, $2H_2O$	0.4M	2.0	0.8mM
Fe-EDTA	20mM	2.5	50µM
Micronutreints			

$MnSO_4$, $CuSO_4$, $ZnSO_4$ H_3BO_3, Na_2MoO_4	1mg/ml each	0.1 each	0.1 µg / l each

LB broth

Components	**g or ml/L**
Peptone	10
Yeast extract	5
Sodium chloride	5
Deionized water	1L

Appendix 2. Primers used in this study

Primers used for amplifying 7 serpin and 1 ferritin groups

Primers	Forward	Reverse
S1	CCCTTTCTCTTCAAMCTT C	CACCATYTTWGTMARACCT
S2	CTTCCYGAYGMAAAAGATGGG	AGGGTGGTCAGCTACAAAGTC
S3	TGGGCTGAAAARRAGACAAA	Anchored oligo dT primer(Roche)
S4	GAAGTAGGTGAYTTYAGRATTCCA	Anchored oligo dT primer(Roche)
S5	GGAGGTTTKACAAAAATKGYGGA	Anchored oligo dT primer(Roche)
S6	TATGGCYTRAAAARAGACAAATGG	Anchored oligo dT primer(Roche)
S7	ATGACTTYCATCYGYGAATCAA	Anchored oligo dT primer(Roche)
F1	TTTCTTTGGCTCGTCAGAATT T	ACACCRTGACCCTTTCCA

Primers used in this study for amplifying 9 serpin and 3 ferritin genes

Group	Gene	Forward	Reverse
S1	*MtSer1*	TTGTTGGACAAGTCGATGAAG	GAGTGCATTAGCAAAGATGAGTC
	MtSer3	CCTTTTATGAGCAGCAACCTT	GCTCTAGGAACTCAAATTCAGA
	MtSer2	CCAATCATCTTAACTCCTTCACC	GGCGTTGCTTTGTAATTATCA
	MtSer5	CTCGTTTCCGTCATTCTCAAA	TGTAGTGAAAAGAGAGCAGATAT
	MtSer6	TCTTGGGTCGGTCAACAATG	AAACTGCTTCTTCTTGCTGGT
	MtSer7	CAAGTTGGCTTCCGTTGATT	TGTTGACCGACCCTGGTT
S2	*MtSer8*	ACATCAGAGCAGAATCTCATCG	GGCAGTGATCATAATGAGTACG
	MtSer9	GTTGCCTTCTCAAGAGCGATT	CGTAGTTTGGAGTGACAAGG
	MtSer10	CTTTGTCACTCCACGTTGTG	GGCAAGCAAGTAAGAAACG
F1	*MtFer1*	TGAGTGTTGGTAAGAAATGGGG	GATCACAGATTCACATTCATCAGC
	MtFer2	TCAACGACCCTTTTCGTTATTC	TCACCATCCATAGGAAGATTCA
	MtFer3	TGCACCCTATTGTGAGTCCT	GCTCTACCAAAAACTCGCTC
Reference genes	*MtELF1*	CCACCAACCTTGACTGGTAC	CCACGCTTGAGATCCTTCAC
	MtPDF2	GTGTTTTGCTTCCGCCGTT	CCAAATCTTGCTCCCTCATCTG
	β Tubulin	TTTGCTCCTCTTACATCCCGTG	GCAGCACACATCATGTTTTTGG
Primers used for RNAi construction	*Ser6*	**Xba I** GCCTCTAGAAAGAACTTCTTCCTCTTGG	**BamHI** CGCGGATCCAATTGACGCTTATCTT
	Fer3	**Xba I** GCCTCTAGAGGCTGATCGTAACAA	**BamHI** CGCGGATCCACACAGCTTCTACTT

	Fer2	**Xba I** GCC TCT AGA TGC CTC AAA GAC TGG	**BamHI** CGCGGATCCCTATATGAACAGAGA
	35S	**35S** CCACTGACGTAAGGGATGA	……
	NAN F	ATCTGCATGCAAGCTACTTAGA	……
	NOS R	…….	TGTTTGAACGATCGGGGAAATTCG

Primers used for qRT-PCR

No	Gene	Forward	Reverse
1	*MtZEP*	GAGGAAAGGGTTTGAGGTAGTG	GCTTCCAAAGCAGCCAAAG
2	*MtNCED*	ACCGTTTGGCCCAAGAAA	CAGAGGCTACGAGCATAGTAAAG
3	*MtPAL*	TAGTGACTGGGTGATGGATAGT	AGGCACCACCTTGTTTAGTT
4	*MtICS*	GCACCAGCATTTAGTGGAAAC	TTCAGACTGGTAAGCAGGTAAAG
5	*MtZIP*	GTCACAAACAAGCTACCAAAGG	TCTTCATCTCTCTCCCTCTTCA
6	*MtP5CS3*	GAGTAGTCTCATGGCTCTGTATG	CGAGGTAATTGTGTCGGATAGT
7	*MtRbohB*	AGAAGCAGGCAGAGGAATATG	CTCCTCGTGTAGAATGAGTTGG
8	*MtCAT*	GCGCACCTGTTTGGAATAAC	TGGGATCCGTTCCCTATCA
9	*MtACO*	AGTTCAAGTGGCAGAGACATT	GCCCATAGCTGGTCCATTATTA
10	*MtACS*	GTGAGAGGTGGTAGGGTAAGA	ATCACCAGGATCAGCCAAAC

Appendix 3. Nucleotide sequence of the genes used for qRT-PCR

MtZep

>XM_003611692.2:257-1780 Medicago truncatula zeaxanthin epoxidase mRNA
ATGGTTTCTACTTTGTCTCACAAATGTCTCAGTCCCTCAATGACAACTTTCTCAAGAACCCACTTCTCAA
ATCCTTTTGTGAGCTATGGAAACAGAACAACCAAGCAGAGGAGAAAACTGATGCAAGTAAAAGCAACAGT
AATGCATGAAGCACCTTTTTCTGTCTCAAAGTCAACGCATAGTGTAGCTGAGATTGACATGGATCAAACT
CCTCAGAAGAAGCAGCTTAAGGTACTTGTGGCTGGTGGAGGGATTGGTGGGTTGGTTTTTGCTTTGGCTG
CTAAGAGGAAAGGGTTTGAGGTAGTGGTTTTTGAGAAGGATTTGAGTGCTATAAGAGGGGAGGGACAGTA
TAGAGGTCCAATTCAGATACAAAGCAATGCTTTGGCTGCTTTGGAAGCAATAGATATGAATGTTGCTGAT
GAAGTTATGAGAGTTGGTTGCATCACAGGTGATAGAATCAATGGGCTTGTGGATGGAGTTTCTGGGTCTT
GGTACATTAAGTTTGATACATTCACTCCTGCAGCAGAACGAGGGCTTCCAGTTACTAGAGTTATTAGCCG
AATGGCTTTGCAAGAGATTCTTGCACGTGCAGTCGGGGATGATGTCATTATGAATGGTAGTAATGTTGTC
GATTTCATTGATCATGAAACTAAGGTAACAGTGGTGTTGGATAATGGTCAGAAGTATGATGGAGATCTCT
TGGTTGGAGCAGATGGGATTTGGTCCAAGGTGCGGACAAAGTTATTTGGGTCAACAGAAGCTACATACTC
GGGCTATACTTGTTATACTGGTATAGCAGACTTTGTGCCACCTGACATTGAATCGGTTGGGTACCGGGTA
TTCTTAGGACACAAACAATACTTTGTATCTTCAGACGTCGGTGCTGGAAAGATGCAATGGTATGCATTTC
ACCAAGAACCTGCAGGAGGTGTTGATACCCCCAATGGGAAAAAGGAAAGGTTACTGAAGATATTTGAGGG
GTGGTGTGATAATGCAATAGATTTGATAGTTGCCACTGAAGAAGAGGCAATTCTGCGACGAGATATATAT
GATCGGACGCCAACACTAACATGGGGAAAAGGACGTGTGACCTTACTTGGTGATTCTGTTCATGCCATGC
AGCCAAATATGGGCCAAGGAGGATGCATGGCTATTGAGGATGGATATCAACTTGCATTTGAGTTGGATAA
TGCATGGCAGCAAAGTGCAAAATCAGGCTCTACAATTGACATTGCTTCTTCCCTTAAGAGCTACGAGAGG
GAGCGAAGATTACGAGTTACTTTTGTTCATGGAATGGCTAGAATGGCAGCTTTGATGGCTTCCACCTACA
AGGCATATCTAGGTGTTGGTCTTGGACCCTTTGAGTTTTTAACCAAGTTTAGAATACCACATCCGGGAAG
AGTTGGAGGAAGGTTTTTTATTCAAAAGTCGATGCCTTTGATGTTGAATTGGGTGTTAGGTGGCAATAGC
TCCAAACTTGAAGGCAGACCACTATGTTGCAGGCTCTCAGACAAAGTATGTTAG

MtNced

>XM_013608915.1:166-1998 Medicago truncatula 9-cis-epoxycarotenoid
dioxygenase mRNA
ATGGCAACATCAACGGCTTCATCAAACACATGGATTAACACCAAACTTGGTTCATCATCTTCATACTCTT
CTCCTTTCAAAGATTCAAGATCAAATTCAATCACTTTAAAGAAGAAAAGATCTATCTCCCAAAACAACAA
AATCTCATGCTCACTTCAAACAACACTACCTTTTCCTAAACAATACCAACCTAGTAAACCAAAAACGGTA
ATTCCCACAAAAGAACCAAAACCAAACCAACCCATAACAAAAACATTACCAAAACAACAACAAGAACAAA
AACAACACAAATGGAACCTTCTACAAAAAGCCGCCGCCACCGCCCTCGACTTCGTCGAAACAACCTTAAT
CAAACAAGAACAAAAACACCCACTACCCAAAACCTCCGACCCACGTGTTCAAATTGCCGGTAACTTCGCC
CCAGTACCGGAACACCCGGTAACCCAATCTCTTCCAATTACCGGCAAAATCCCAACCAACATTGACGGTG
TTTACCTCCGTAACGGCGCCAATCCACTTTACGAGCCAGTAGCCGGTCACCACTTCTTCGACGGAGACGG
TATGGTCCACGCCGTTAAATTCACAAACGGCTCCGTAAGTTACTCTTGCCGCTTCACCGAAACCCACCGT
TTGGCCCAAGAAAAAGCCCTGGGCCGGCCCGTTTTTCCAAAAGCCATAGGTGAACTTCATGGTCATTCAG
GCATAGCACGTTTAGCACTTTACTATGCTCGTAGCCTCTGTGGGCTTGTTGATGGGACCCACGGAATGGG
TGTTGCTAACGCTGGTTTGGTTTATTTCAATAACCGTTTGTTAGCTATGTCTGAAGATGATATTCCTTAT
CATATTCGTGTCACACCTAACGGTGATTTAACCACCGTTTGCCGTTATGATTTCGATAATCAACTCAAAT
CTACAATGATAGCTCATCCCAAGGTTGATCCAGTTGATAAGAATATGTATGCTTTGAGCTATGACGTAGT
TCAAAAGCCTTATTTGAAATACTTTCGTTTTGATGCGTCCGGAGTTAAGTCTCCGGACGTTGAGATTCCG
TTGGAGCAGCCTACTATGATGCATGACTTCGCGATCACTGAGAATTTCGTTGTTGTGCCTGATCAACAAG
TTGTGTTTAAATTGGGTGAAATGATCCGTGGTGGGTCGCCTGTTGTTTACGATAAGGAGAAAGTCTCGAG
GTTCGGGGTTTTATCCAAGAATGCTGAAGATTCTTCTGAGATGATTTGGATTGATGCACCAGAGTGTTTC
TGTTTTCATCTGTGGAATGCGTGGGAAGAGCCTGAAAATGATGAAGTTGTGGTGATTGGATCATGTATGA
CACCGGCTGATTCGATATTCAATGAATGTGAAGAGAATTTGGAGAGTGTTTTGTCTGAAATTCGGTTGAA
TTTGAAGACAGGGAAATCAACTAGAAGACCTATAATCAAAGAATCTGAACAAGTGAATTTGGAAGCTGGA
ATGGTGAACAAGAACAAATTGGGAAGAAAGACACAATTTGCTTATCTTGCTCTTGCTGAACCATGGCCTA
AAGTTTCCGGGTTCGCGAAAGTTGATCTTTTCAGCGGCGAAGTTAAGAAATATATTTACGGTGAAAACAG
ATTTGGCGGGGAGCCTCTGTTTTTACCAAATTCCGATTCTGAGAACGAAGATGATGGTTATATTTTGACA
TTTGTTCATGATGAGAAAGAATGGAAATCAGAATTGCAGATTGTGAATGCTGCTACTTTGAAGCTTGAAG
CTTCTATTCAGCTTCCTTCTCGTGTTCCTTATGGATTTCATGGAACTTTCATTAATTCAAATGATTTGAA
GAAACAAGAATGA

MtPal

>XM_003590423.2:257-2395 Medicago truncatula phenylalanine ammonia-lyase-like protein mRNA
ATGGAGGGAATTACCAATGGCCATGTTGAAGCAACCTTTTGTTTGAGCAAAAATGGTGGTGATCCACTCA
ACTGGGGCGCGGCGGCGGAGTCATTGACAGGGAGTCATTTGGATGAGGTGAAGCGTATGGTGGAGGAGTA
TCGTAACCCGTTGGTTAAAATCGGCGGTGAGACACTTACCATTGCTCAGGTGGCTGGAATTGCTTCCCAT
GATAGTGGTGTTAGGGTGGAGCTTTCGGAGTCGGCAAGGGCCGGTGTTAAGGCAAGTAGTGACTGGGTGA
TGGATAGTATGAATAAAGGTACGGACAGTTATGGTGTTACCACCGGTTTTGGTGCTACTTCTCACCGGAG
AACTAAACAAGGTGGTGCCTTGCAGAAGGAGCTAATTAGGTTTTTGAATGCCGGAATATTTGGCAATGGT
ACAGAATCAAATTGTACACTACCACATACAGCAACAAGAGCTGCAATGCTTGTGAGGATCAACACTCTTC
TTCAAGGGTATTCTGGTATTAGATTTGAAATCTTGGAAGCTATCACAAAGCTCTTGAACAACAATATTAC
CCCATGTTTACCACTTCGCGGTACAATCACAGCTTCCGGTGATCTTGTTCCACTCTCTTACATTGCCGGT
TTATTAACGGGCAGACCCAACTCTAAAGCCGTTGGACCGTCTGGAGAAATTCTCAATGCCAAGGAAGCTT
TTCAACTTGCTGGCATTGGTTCTGATTTCTTTGAATTGCAACCTAAGGAAGGTCTTGCTCTTGTTAATGG
AACTGCTGTTGGTTCTGGTTTAGCTTCTATTGTTCTGTTCGAAGCAAATGTACTAGCGGTTTTGTCTGAA
GTTATGTCGGCAATTTTCGCTGAAGTTATGCAAGGGAAACCTGAATTTACTGATCATTTGACTCATAAGT
TGAAGCATCACCCTGGTCAAATTGAAGCTGCTGCTATTATGGAGCATATTTTGGATGGAAGCGCTTATGT
TAAAGCCGCTAAGAAGTTACACGAGACTGATCCTTTGCAAAAGCCTAAACAAGATCGTTATGCACTTAGA
ACTTCACCTCAATGGCTTGGTCCTTTGATTGAAGTGATAAGATTTTCGACCAAGTCTATTGAAAGAGAGA
TTAACTCGGTCAACGACAACCCTTTGATCGATGTTTCAAGGAACAAGGCCATACATGGTGGTAACTTTCA
AGGAACACCTATCGGAGTTTCAATGGACAACACTCGTTTAGCTCTTGCTTCGATCGGTAAACTCATGTTT
GCTCAATTCTCTGAGCTTGTTAATGATTTTTACAACAATGGTTTGCCTTCGAATCTTACTGCAAGTAGAA
ACCCAAGTTTGGATTATGGTTTCAAGGGATCTGAAATTGCTATGGCTTCTTATTGCTCCGAGTTACAATA
TCTTGCTAACCCTGTCACCACCCATGTGCAAAGTGCTGAGCAACACAACCAAGACGTTAACTCTTTGGGT
TTGATTTCTTCTAGAAAAACAAACGAGGCTATTGAGATCTTAAAGCTCATGTCTTCCACTTTCTTGATCG
CGCTTTGCCAAGCAATTGACTTGAGGCATTTGGAAGAGAATTTGAGGAACACTGTCAAGAACACTGTAAG
CCAAGTTGCTAAGAGAACACTCACAACCGGTGTCAATGGAGAACTTCATCCTTCAAGATTTTGCGAGAAA
GATTTGCTCAAAGTTGTCGACAGGGAGTATGTGTTTGCCTATGCTGATGATCCTTGCCTAGCTACATACC
CTTTGATGCAAAAGTTGAGACAAGTGCTTGTGGATCATGCATTAGTGAATACCGAAGGAGAGAAGAATTC
GAACACATCAATCTTCCAAAAGATTGCAACATTTGAGGATGAATTGAAGGCTATCTTGCCAAAGGAAGTT
GAAAGTGCAAGGACAGCATATGAAAATGGACAAAGTGGAATTTCAAACAAGATTAAGGAATGTAGGTCTT
ATCCATTGTACAAGTTTGTTAGAGAGGAGTTGGGAACAGCGTTGCTAACCGGTGAAAAAGTGATATCGCC
AGGAGAAGAGTGCGACAAATTGTTCACAGCTATGTGCCAAGGTAAAATTGTTGATCCTCTTATGGAATGT
CTCGGAGAGTGGAACGGCGCTCCTCTTCCAATTTGTTAA

MtIcs

>XM_003621235.2 Medicago truncatula isochorismate synthase partial mRNA
ATGTTTCAATTAGGGTTACAAAGAATCATCTCAGACCAAACCTCTAATGGATTTAATGTCATCAAAGGTG
ACAATGCTTACCAGTATTTCCTTCAGCCGCCTAATGCACCAGCATTTAGTGGAAACACACCAGAGCAACT
ATTTCACAGAAAAGGCCTACATATCACTAGTGATGCTTTGGCCGCAACCCGTGCTAGAGGAGTGTCACTA
GAACTAGACCATCAAATTGAACTTTACCTGCTTACCAGTCTGAAGGACGACATCGAGTTTACTATAGTAA
GAGAGACCATAAGAAGAAAATTAGAGGCAATCTGTGAAAAAGTTACAATCGATTCAACGAAAATGGTCAG
AAAACTACTGAGGATCCAACATTTATTTGCTCAACTAACTGGCAGGTTAAGAAGTGAAGAGGATGAGTTT
GAAATTTTGTCATCACTTCACCCAAGTCCCGCAGTTTGTGGATTTCCAACAGAAGAGGCACAACTTTTAA
TTGCAGAAACAGAAGTGTTTGATCGAGGAATGTATGCTGGACCTGTTGGTTGGTTTGGAGGAGGAGAGAG
TGACTTTGCCGTTGGCATCAGATCAGCATTGGTGGAACAGGAACTAGGTGCTTTGATATATGCAGGGACA
GGAATAGATGAAGGAAGCAATCCATACTTGGAGTGGGATGAGCTAGAACTCAAGACATCTAAGGAGTGTT
TGTCTGTCAATGCATACATTCACCGCAAACGATTGCTAGCAAGTTTGTTATTCTACTTTATTTCCGACAG
TGTTGCCAAATAG

MtZip

>XM_003611476.2:245-1057 Medicago truncatula homeobox associated leucine zipper protein mRNA
ATGGGTCTTAATGATCAAGATTCTCTTCACCTTGTTCTAGGTTTATCTTTGAATACTTCTACTACTCCAA
AGGAAATAACTACCACCACCCCCATGAATCCCTATTCCACCTCCAACGAGCCATCCTTAACGTTAGGACT
CTCTGGTGAGAGTTATAACCTTATAAGTCACAAACAAGCTACCAAAGGTTATGGTGAGGAACTTTGTAGA
CAAACTTCATCACCTCATAGTGTTGTTAATTCATCTTTCTCAAGTGGGAGAGTACTGCAAGTGAAGAGGG
AGAGAGATGAAGAAGAAGAAGAAGTAGAAGAAGAGAGGGTTTCTTCAAGAGTTAGTGATGAAGATGAAGA
TGCTACAAATGCTAGAAAGAAATTGAGGCTTACCAAAGAACAATCACTATTGCTTGAAGAAAGCTTCAAA
CTACACAGCACTCTCAATCCTAAACAAAAACAAGCTTTAGCGAGACAGTTGAATCTAAGGCCACGACAAG
TTGAAGTATGGTTCCAGAATCGGAGAGCCAGAACAAAGCTGAAACAAACAGAGGTGGATTGCGAGTTCTT
GAAAAAATGTTGTGAAACATTAACAGACGAAAACAGGAGGCTCAAAAAGGAGTTACAAGAGCTGAAGTCA

TTGAAAGTAGCACAACCTTTGTACATGCCTATGCCTGCAGCCACCCTCTCCATCTGCCCGTCTTGCGAAA
GACTCGGCCGCGTCGCCGACGGTGGTGGTGGTTCCAATAAGATCACTGCCTTCACTATGGCTCCAAATAC
TCATTTCTACAATCCTTTCAACAATCCTTCTGCAGCATGTTAA

MtP5cs3

Medicago truncatula clone BAC mtb1-34m03 delta-1-pyrroline-5-carboxylate synthetase (P5CS3) gene, complete cds

ATGGATCCAACTCGAGCTTTCGTCACTTCTGTTAATCGTGTTATCGTCAAGGTTGGAACAGCTGTGGTTA
CTAGAAGTGATGGAAGATTAGCATTGGGAAGACTTGGAGCTCTATGTGAGCAGCTTAAAGATCTAAACCT
TCAAGGCTATGAAGTTATATTGGTGACTTCGGGTGCTGTTGGTCTTGGCAGACAAAGACTTAGATATAGG
AAATTGGCTAATAGCAGCTTTTCTGATCTTCAAAAGCCACAAGGTGACCTTGATGGAAAAGCATGTGCGG
CTGTTGGGCAGAGTAGTCTCATGGCTCTGTATGATACTATGTTTAGCCAGCTAGATGTGACTTCCTCCCA
ACTACTAGTGAATGATGGGTTTTTTAGGGATTCAGGTTTCAGAAAACAACTATCCGACACAATTACCTCG
TTATTAGAATCGAAGGTCATCCCCATTTTCAATGAAAATGATGCTGTTAGTACTAGGAAGGCGCCATATG
AGGATTCTTCTGGTATTTTTTGGGACAATGACAGTTTGGCTGGTCTATTAGCCCTTGAACTTAAAGCTGA
CCTTTTAGTTTTATTAAGTGATGTTGAGGGCCTTTATAGTGGTCCTCCAAGTGACCCAAACTCAAAATTA
ATTCATACATATATAAAAGAGAAACATCAAAGAGAAGTTACTTTTGGAGACAAATCAAGATTGGGCAGAG
GGGGTATGACTGCTAAAGTCAATGCTGCTGTTTGTGCTGCTCATGCTGGCATCCCTGTTATTATAACTAG
TGGCTATGCCACAGACAACATTATACGAGTGCTTCAAGGGGAGAAAATAGGCACTGTCTTTCATAGAGAT
GCACATCTGTGGAAAAACATAAAGGAAGAGAGCGCGCATGAAATGGCCGTCGCAGCACGTAACAGTTCTA
GAAGACTTCAGGCCCTAAAATCTGAAGAAAGGAGGAAAATATTGCTGGCAGTGGCTGATGCATTGGAGAA
AAACCAAAATATGATTATGCTTGAAAATCAGGCTGATGTTGCTGTTGCTGTGGCAGCTGGATATGACAAG
TCTCTGATATCACGTTTAACCCTGAAGCCTGAGAAGATCTCTAGTCTTGCAAAGTCTGTGCGCGTGCTGG
CAGATATGGAAGAACCAATTGGTCAAATTTTGAAGAGAACTGAGCTAGCTGATGAACTCGTTCTGGAGAA
AATATCATGTCCTCTGGGTGTCCTCCTGATTATATTTGAGTCTCGACCTGATGCTCTTGTTCAGATAGCA
GCATTGGCAATTCGAAGTGGGAATGGCTTATTACTTAAAGGAGGAAAGGAAGCCCGAAGATCAAATGCGG
TCTTACACAAGGTCATAACTTCAGCAATACCGGATACAGTCAGTGGCAAACTTATTGGGCTTGTGACTTC
AAGAGATGAAATTCCAGATCTACTCAAGCTTGATGATGTGATAGATCTTGTGGTCCCTAGAGGCAGTAAT
AAGCTTGTTTCTCAAATCAAGGAGTCAACAAGAATCCCTGTTCTTGGACATGCTGATGGAATTTGTCATG
TATATGTCGACAAGTCTGCTAATATTGAGATGGCAAAGCAGATAGTTAGGGATGCAAAGACTGATTATCC
TGCAGCCTGCAATGCAATGGAGACTCTTCTTGTACACAAGGATCTATGTAATGGTGGACTTAACGAGCTT
ATCCTTGAACTCCAACGTGAAGGTGTTCAAATATATGGTGGACCAAAAGCTAGTGCTGTGCTAAATATTT
CTGAAGCGAGTTCTTTGCATCATGAGTACAGCTCACTTGCTTGCACAATTGAAATTGTAGAGGACGTCTT
TGTTGCCATTGACCACATAAATAAACATGGAAGTGCGCATACTGAGTGCATTGTCACAGAAGACTCTGAA
GTGGCTGAGACATTCTTATCTCAAGTTGACAGTGCTGCTGTATTCCACAATGCAAGTACACGGTTTTGTG
ATGGAGCACGCTTTGGACTAGGGGCAGAGGTTGGAATAAGTACAAGTCGGATTCATGCTCGAGGTCCTGT
AGGAGTCGAGGGATTGTTGACAAAAAAATGGATATTGAGGGGGAATGGACAGGTAGTCGATGGTGATCGA
GGAGTCTCTTATACTTACAAAGAGCAGCTAATAGAAGCATAA

MtRbohB

>XM_003602678.2:81-2852 Medicago truncatula respiratory burst oxidase-like protein mRNA

ATGGGAACTGACGAAGTTGAAGGAGAAATCCACAATCATCGTGACTCTGATACAGAACTCATTGCTCTTC
ACAATGGTTCCTTCAGTGGACCTTTGAACAAAAGGGTAGGAAGAAGAAGTGCAAAGTTAAACGTTTCAAA
TTCAACTTCTGCCATAGATCTTAACCATCAAGAACAAGATGAAGAAAAAGCAGAGCAAGATTACGTTGAA
GTTACTATGGATATTCAAGGTGACTCTGTTGCTTTACACAGTGTTAAAACTGTTCCTGGAAACAATGGTG
AAGATGAGAAACTTGTTTTGCTTGGTAAAGGAATGGAGAAGAAAAGATCTTTTGGTGCTTCTTTTGTTAG
AACTGCTTCGATTCGTATGAAACATGTTTCTCAGGAGTTGAAGAAATTAACTTCTTTTTCGAAACAAGTT
GGACCTCAGAAAGTTTATGATAGGACTAAGTCTGCAGCTTCTCATGCTCTTAGAGGACTCAAGTTTATCA
ATAATAAGACTGATGTTGGATGGTTTGAGGTTGAAAAGCAGTTTGATATTCTTTCAACTCATGATGCTTT
TCTTCATCGCTCTCTCTTTGCCAAATGCATAGGGATGAACAAGGAGTCTGAGGCATTTGCAGGTGAGCTA
TTTGATGCTATGTCTAGGAGGAGGAATATTCATGGAGATTCAATTAATAAGCCACAATTGAAGGATTTCT
GGGACCAGATATCTGACAATAGTTTTGATTCTAGGCTCAGAACATTCTTTGACATGGTTGATAAAGATGC
GGATGGCAGAATCACCGAGGATGAAATTAAAGAGATTATTTGCCTTAGTGCCACTACAAACAAACTCTCA
AACATACAGAAGCAGGCAGAGGAATATGCTGCTTTGATCATGGAAGAACTAGACCCTGATGATACTGGAT
TTATCATGGTAAATGACCTAGAGATACTCTTGTTGCATGGACCAACTCATTCTACACGAGGAGATAGTAA
GTACCTGAGCCAAATGCTAAGCATAAAGCTTAAGGGTACATATGAATACAATCCTGTTCGGAAGAGGTAT
AGAGATGCCATTTACTTTCTGCAGGACAATTGGCAAAGAACTTGGATATTGGTACTATGGATTGGTGTTA
TGTGTGGTCTATTTGCCTACAAATTCATGCAGTACAGAAGAAAAGATGCTTATGAAGTAATGGGTCATTG
TGTGTGCATGGCTAAAGGTGCAGCTGAGACACTCAAATTGAACATGGCTATTATCTTGTTACCTGTTTGT
CGAAACACCATCACATGGCTTAGGAACAAGACCAAACTAGGCATTGCTGTTCCTTTTGATGATAACCTCA
ACTTCCACAAGGTGATTGCTGTGGCAGTAGCAACTGGAGTTGGTATACATGCTATTTATCATCTTACTTG

CGACTTTCCTCGCCTTCTTCATGCAAATAGTGAAAAGTACAAGCTCATGGAACCATTTTTTGGAAAGCAA
CCAACAAGTTATTGGCATTTTGTGAAATCATGGGAAGGAGTAACGGGGATTGTAATGGTTGTTTTAATGA
CAATAGCCTTCACACTGGCTAGTCCTTGGTTCAGGAAAGGAAGGGTTAAGCTACCTAAACCCCTCAATAG
TCTAACTGGTTTCAATGCCTTTTGGTACTCTCATCATCTCTTTGTATTTGTCTATGCCCTTTTGGTTGTG
CATGGAATCAAACTTTACTTGACTCGGGAATGGCACAAAAAAACGACTTGGATGTATTTGGTTATTCCCA
TCATCATTTATGCATTGGAACGACTGACTAGAGCACTCAGATCAAGCATCAAGCCTGTAAGAATATTAAA
GGTGGCTGTTTATCCTGGAAATGTGTTGGCTCTTCATATGTCAAAGCCTCAGGGGTTTAGATACAAGAGT
GGACAATACATGTTTGTAAATTGTGCTGCTGTCTCTCCATTTGAATGGCATCCGTTTTCCATAACCTCTT
CCCCAGGAGATGACTACCTTAGTGTTCACATCAGAACATTAGGTGACTGGACCAGAAGTCTCAGAGTCAA
ATTCTCAGAGAGTTGCCTTCCACCGACCCATGGGAAGAGTGGACTTCTAAGAGCTGAATGCATGCAAGGG
GATAGCAGCCCAAGTACTCTCCCTAAAGTTTTGATCGATGGTCCTTATGGAGCGCCTGCACAAGACTACA
AGCAATATGATGTAGTTTTACTTGTAGGCCTAGGAATTGGGGCTACCCCAATGATAAGTATACTAAAGGA
CATTGTGAATAATTTCAAGGCTATGGAAGAAGATGAAGGGACCACTATAGAGGAGGGAACAAGTAGTAAA
TCACCGAGACCATCACAACACAAGAGAACCGGTTTGAATAGCTTTAAAACTAAGAGGGCTTATTTTTACT
GGGTTACTAGAGAACAGGGTTCATTTGATTGGTTTAAAGGAGTAATGAATGAGGTGGCTGAAGATGATCA
TAGGGGAGTAATTGAGCTACACAATTATTGTACTAGTGTTTATGAAGAGGGTGATGCTCGCTCTGCTCTT
ATTGCTATGCTCCAATCACTTAATCATGCTAAAAATGGTGTGGATATCGTCTCTGGAACACGCGTCAAGT
CTCACTTTGCTAAACCTAATTGGCGTAGTGTCTACAAGCGCATTGCACTTAATCATCCACAAACACGCGT
TGGGGTGTTTTACTGTGGGCCACCTGCACTTACTAAAGAGCTTCGTCAATTAGGTTCGGACTTTTCTCAC
AACACAACCACCAAATATGATTTCCACAAGGAGAATTTCTAG

MtCat

>XM_013606823.1:175-1653 Medicago truncatula catalase heme-binding enzyme mRNA
ATGGATCCATACAAGCACCGTCCGTCCAGCGCTTACAATTCTCCTTTCTGGACTACAAATTCTGGCGCAC
CTGTTTGGAATAACAACTCATCCCTAACCGTTGGATCCAGAGGTCCAATTCTCTTGGAAGATTATCATCT
TGTGGAAAAGCTTGCCCAATTTGATAGGGAACGGATCCCAGAACGTGTTGTCCATGCCAGGGGAGCAAGT
GCAAAGGGTTTCTTTGAAGTCACACATGATATTTCGCACCTGACTTGTGCAGATTTCCTACGAGCTCCTG
GAGTTCAGACACCCGTCATTGTGCGTTTCTCCACTGTCATTCATGAACGTGGTAGCCCTGAAACCTTGAG
AGACCCTCGAGGTTTTGCTGTGAAATTTTACACCAGAGAGGGTAACTTTGACCTTGTTGGAAACAACTTT
CCTGTCTTCTTCGTTCACGACGGGATGAATTTTCCAGATATGGTCCATGCTCTTAAACCCAACCCCAAGT
CCCACATTCAGGAGAATTGGAGAATCCTTGACTTCTTTTCTCACTTTCCAGAAAGCCTTCACATGTTCTC
CTTCCTATTTGATGATGTGGGTGTCCCACAAGATTATAGGCACATGGATGGTTTTGGAGTTAACACATAT
TCCCTGATCAACAAGGCTGGGAAAGCAGTGTACGTGAAATTTCACTGGAAGCCCACATGTGGTGTGAAGT
GTCTGTTGGAGGAAGAGGCCATTAAGGTGGGAGGAGCCAACCACAGCCATGCTACTCAAGACCTGTATGA
TTCAATTGCTGCTGGTAACTATCCTGAGTGGAAACTGTTTGTTCAAACAATAGATCCTGCTCACGAAGAC
AAATTTGATTTTGACCCACTTGATGTAACTAAGACTTGGCCTGAGGACATTATACCCCTTCAGCCCGTAG
GTCGCCTGGTCTTGAACAAGAACATAGACAATTTCTTTGCTGAGAATGAACAACTTGCATTTTGTCCTGC
CATTATTGTGCCTGGTGTATATTACTCGGATGATAAGATGCTTCAAACCAGGATTTTCTCTTATGCTGAT
TCACAGAGGCACAGGCTTGGGCCAAACTATCTGCAACTTCCTGCTAATGCTCCCAAGTGTGCTCACCACA
ACAATCACCATGAGGGTTTCATGAATTTCATTCACAGGGATGAAGAGGTCAATTACTTCCCTTCAAGGCA
TGATCCTGTTCGTCATGCAGAAAAGGTTCCCATTCCTACTGCTAATTTCTCTGCATGCCGTGAAAAGTGC
AATATTCCAAAGCAGAACAACTTCAAGCAGCCTGGAGAGCGATACCGATCTTGGGCACCCGACAGGCAAG
ATAGATTTCTCCGCAGATGGGTGGATGCTTTATCCGATCCACGCGTCACCCATGAAATCCGCAGCATCTG
GATCTCATACTGGTCTCAGGCTGATCGTTCTCTTGGACAAAAGATTGCATCTCATCTGAACATGAGGCCT
AGCATTTAA

MtAcs

>XM_003624037.2:717-1856 Medicago truncatula 1-aminocyclopropane-1-carboxylate synthase mRNA
ATGTCAAAAGTGAGAGGTGGTAGGGTAAGATTTGATCCTGACCGTATATTGATGAGTGGTGGAGCAACAG
GAGCAAATGAGTTAATCATGTTTTGTTTGGCTGATCCTGGTGATGCTTTTTTGGTTCCTAGCCCTTATTA
TCCAGCATTTGTCCGTGACTTATGTTGGAGAACCGGTGTGCAACTAATTCCTGTCCAATGTCATAGCTCA
AACAATTTCAAGATAACAAGAGAAGCACTTGAAGAAGCTCATAAAAAAGCACAAGAAGAAAACATCAATG
TAAAAGGGTTAATCATAACAAATCCATCAAATCCTTTAGGAACAACATTAGAAAAAGATACACTAAAGAG
CATAGTGAGTTTCATCAATGAAAACAACATCCATTTGGTATGTGATGAAATTTATTCGGGGACCGTTTTC
AACACACCAACGTACGTAAGTGTCGCGGAAGTTATCCAAGAAATGGAAGAATGCAAGAAAGATCTCATTC
ACATTATCTATAGTTTATCAAAAGACATGGGTCTTCCGGGTTTTAGAGTTGGTTTGGTTTATTCGTACAA
CGATGAAGTTGTGAACTGCGGTAGAAAAATGTCGAGCTTTGGATTAGTCTCATCGCAGACACAACATTTT

CTAGCCGCAATGCTTTCGGATGACATATTTGTGGATAAATTTTTGGAAGAGAGTTCAAGAAGATTACGAG
AGCGACGTGAATTTTTTACAAAGGGACTTGAGAAAGTCAACATTACTTGCTTACCAAGTAATGCAGGACT
ATTCTTTTGGATGAATTTGAGGGGTTTGTTGAAAGAGAAAACATTTGAAGGTGAAATGAAACTTTGGCGT
TTGATTATCAATGAAGTAAAGCTTAATGTTTCGCCGGGTTCGGCTTTTAATTGCTCTGAGCCTGGTTGGT
ATAGAGTTTGTTTTGCTAACATGGATCATGAAACAGTTGAGATTGCATTGAGGAGAATTAGAGCATTTGT
TAATGGAAGAGAAAAAGGGAAAACAGTTGAAATCAAACGTTGGAAGAGTAATCTTAGACTTAGCTTTTCT
TCAAGAAGGTTTGATGAGAATGTTATGTCTCCTCACATGATGTCTCCTCATTCACCAATGCCTCATTCAC
CACTTGTTCGAGCTACTTAA

MtAco

>XM_003620886.2:38-949 Medicago truncatula 1-aminocyclopropane-1-carboxylate oxidase mRNA
ATGGCAATTCCTGTGATAGATTTTAGCACTCTCAATGGTGACAAAAGAGGTGAAACTATGGCTCTTTTGC
ATGAAGCTTGTCAAAAATGGGGTTGCTTTCTGATTGAGAACCATGATATTGAGGGGAAGTTGATGGAGAA
GGTGAAGAAGGTAATTAATAGTTACTATGAAGAAAATTTGAAGGAAAGTTTTTACCAATCTGAGATAGCA
AAGAGGTTGGAGAAAAAGGAGAACACCTGTGATGTTGACTGGGAAAGTTCATTCTTCATTTGGCATCGTC
CGACGTCTAACATTAGGAAAATTCCAAACCTCTCTGAGGATCTTTGTCAAACAATGGATGAGTACATTGA
CAAACTAGTTCAAGTGGCAGAGACATTATCTCAGATGATGAGTGAAAATCTTGGTTTGGAGAAAGATTAC
ATAAAGAAAGCATTTTCAGGAAATAATAATAATGGACCAGCTATGGGCACAAAAGTGGCAAAGTACCCTG
AATGTCCATATCCAGAATTGGTAAGAGGTTTAAGAGAGCATACAGATGCTGGTGGAATCATCCTATTGCT
TCAAGATGACAAAGTACCTGGTCTTGAATTCTTCAAAGATGGAAAATGGATTGAGATACCACCTTCAAAA
AACAATGCTATCTTTGTCAACACAGGTGACCAAATTGAAGTGTTGAGCAATGGTTTATACAAAAGTGTTG
TGCATAGGGTGATGCCTGACAAGAATGGAAGTAGACTATCTATTGCAAGTTTCTATAATCCAGTTGGTGA
AGCTATTATTTCTCCAGCTCCTAAACTCTTGTATCCAAGTAATTACTGCTATGGTGACTATTTGGAGCTT
TATGGAAAAACTAAGTTTGGTGATAAGGGTCCTAGATTTGAATCCATCAAGAATAAGGCCAATGGGAACT
AG

Appendix 4. *RNAi* sense strand with introduced restriction sites for generating *MtSer6, MtFer2* and *MtFer3* RNAi lines

Appendix 5. Multiple alignment of members of serpin and ferritin family

S1 group

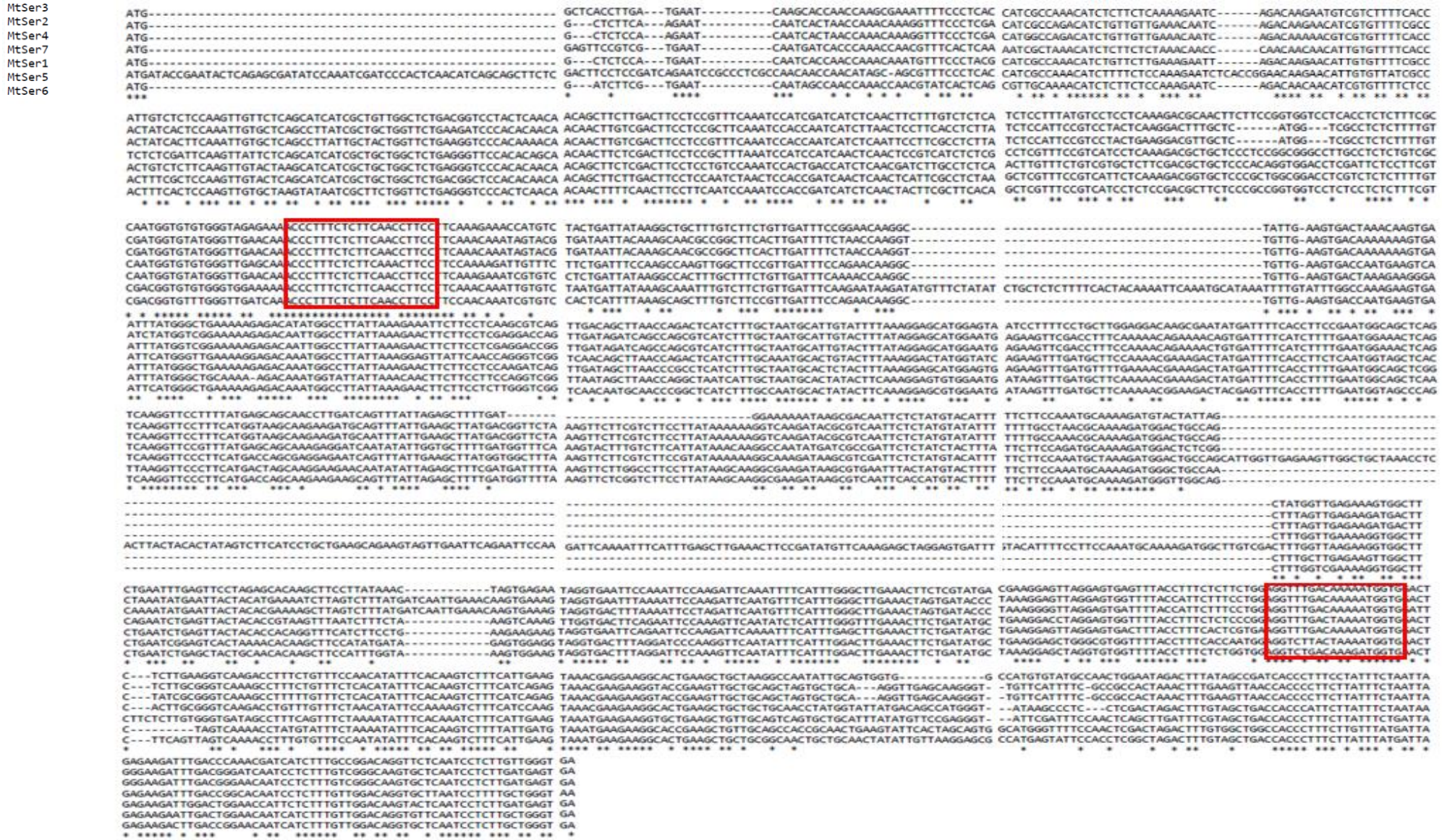

Fig. a.

S2 group

Fig. b.

S3 group

Fig. c.

S4 group

Fig. d.

S5 group

Fig. e.

S6 group

Fig. f.

S7 group

Fig. g.

F1 group

Fig. h.

Fig. Multiple sequence alignment of complete serpin and ferritin coding sequences (MUSCLE output). Serpins were grouped into S1 (Fig. a), S2 (Fig. b), S3 (Fig. c), S4 (Fig. d), S5 (Fig. e), S6 (Fig. f) and S7 (Fig. g) and ferritins were grouped into F1 (Fig. h). The conserved regions of each group are marked with red rectangles and are used to design the primers.

Appendix 6. Supplementary figures for chapter4

6.1. Length of the WT and mutant nodules. Length of the nodules measured under microscope from the plants grown under N limited condition at 32 dpi. Values are the mean of three biological replicates. Error bars represent the standard errors of mean and asterisks indicate a significant difference between Jemalong A17 and R108 plants at $p<0.05$ (*) according to student's *t*-test.

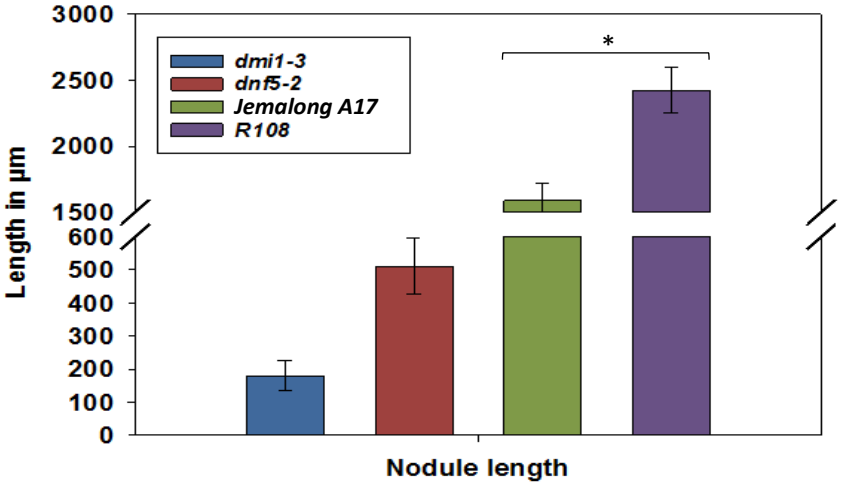

6.2 Effect of SNF on leaf chlorophyll content and photosynthesis. Chlorophyll content (a) and the photosynthesis rate (b) of two WT genotypes, Jemalong A17 and R108, and non-N fixing mutants, *dnf5-2* and *dmi1-3*, were measured at each time point of harvesting. Values are the mean of three biological replicates. Error bars represent the standard errors of mean and asterisks indicate a significant difference between uninoculated and *E. meliloti* inoculated plants at $p<0.05$ (*) according to student's *t*-test.

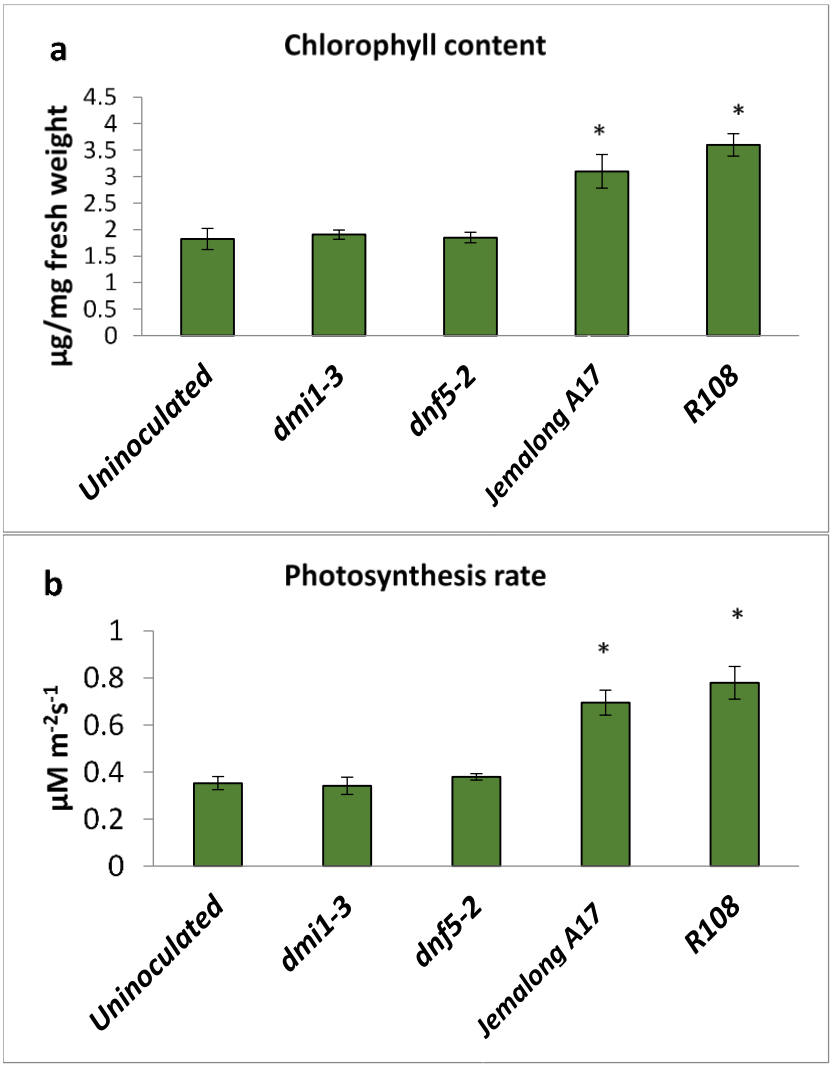

6.3. Effect of drought treatment on N derivation from SNF. Percentage of Ndfix in shoots of Jemalong A17 (a) and R108 plants (b). Plant were well-watered until 20 dpi and were subsequently watered normally (W) or water was with-holded (D). R denotes +/- *E. meliloti* inoculated. Values are the mean of three biological replicates. Error bars represent the standard errors of mean.

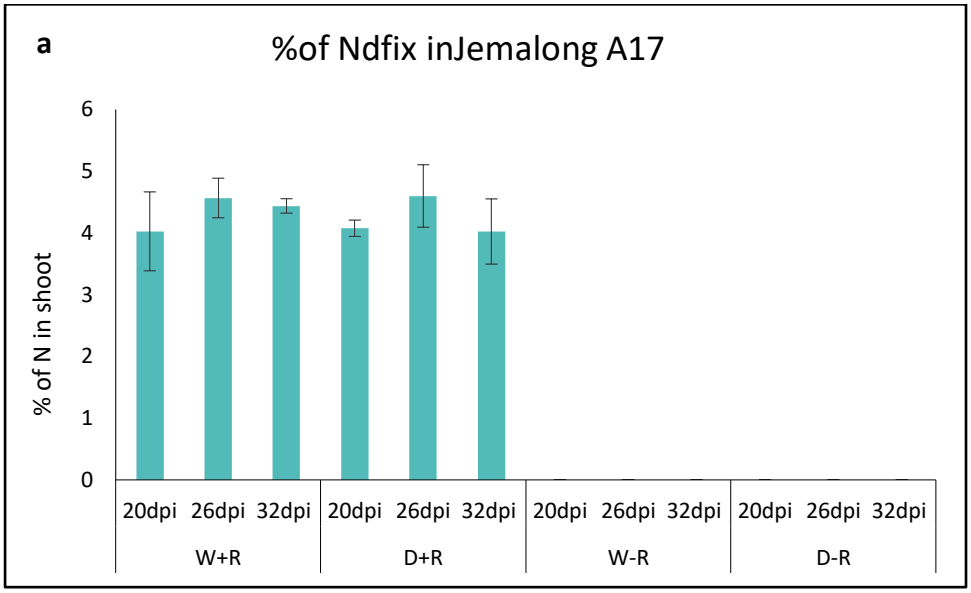

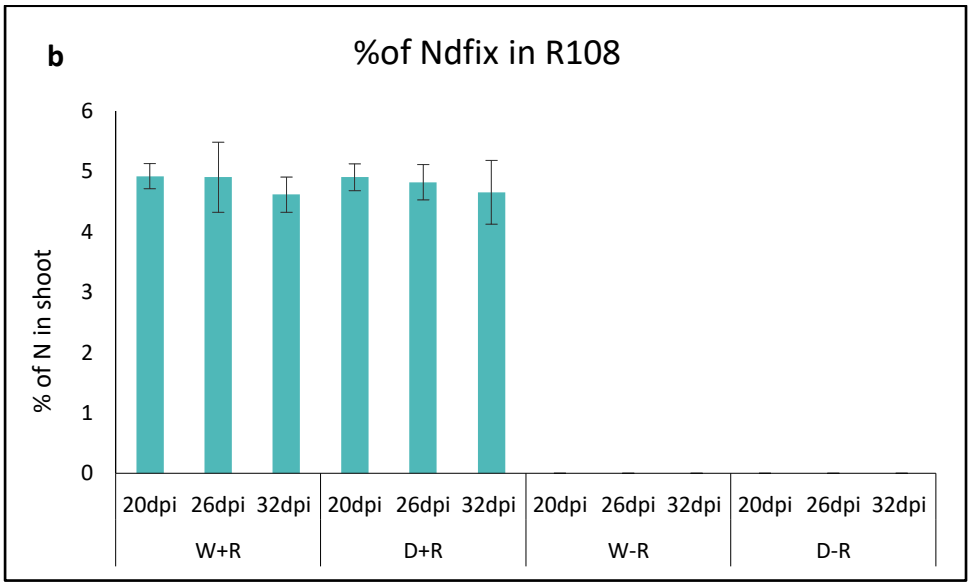

6.4. Effect of external N fertilizer treatment on bacteroid numbers in *M. truncatula.* Bacteroid numbers were counted at 20, 26 and 32 dpi in Jemalong A17 and R108 plants grown under external N fertilizer treatment (+/- N) and well-watered conditions. Values are the mean of three biological replicates. Error bars represent the standard errors of mean and different letters on each bar represents the significant differences at $p<0.05$ according to ANOVA-Post Hoc Tukey's test.

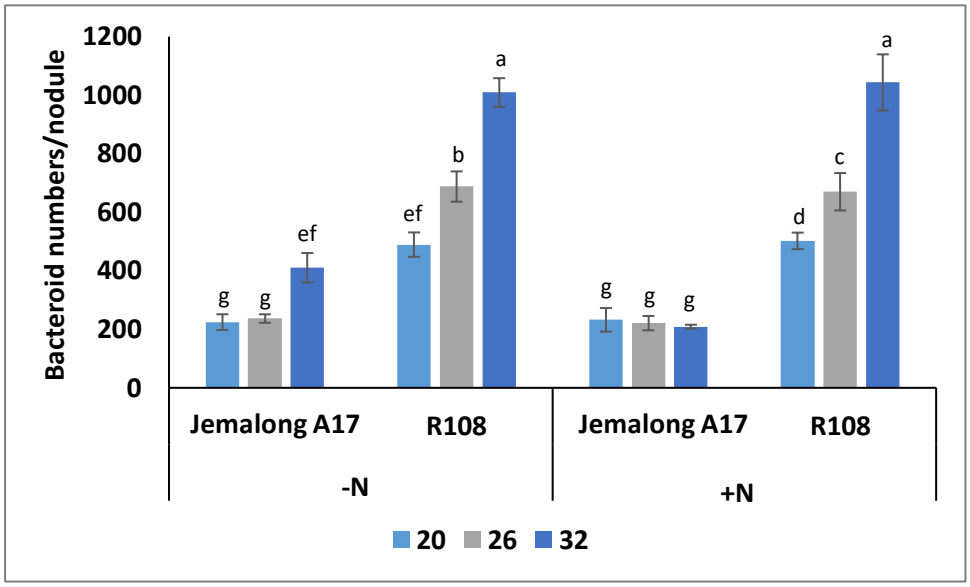

6.5. Effect of external N fertilizer treatment on nodule localization in roots of *M. truncatula* Jemalong A17. Root image containing nodules (a) and the distance of nodules from root collar (b) at 32 dpi. 20 nodules from three plants were measured. Treatments are watered (+/- W) and N fertilizer treated (+/-N).

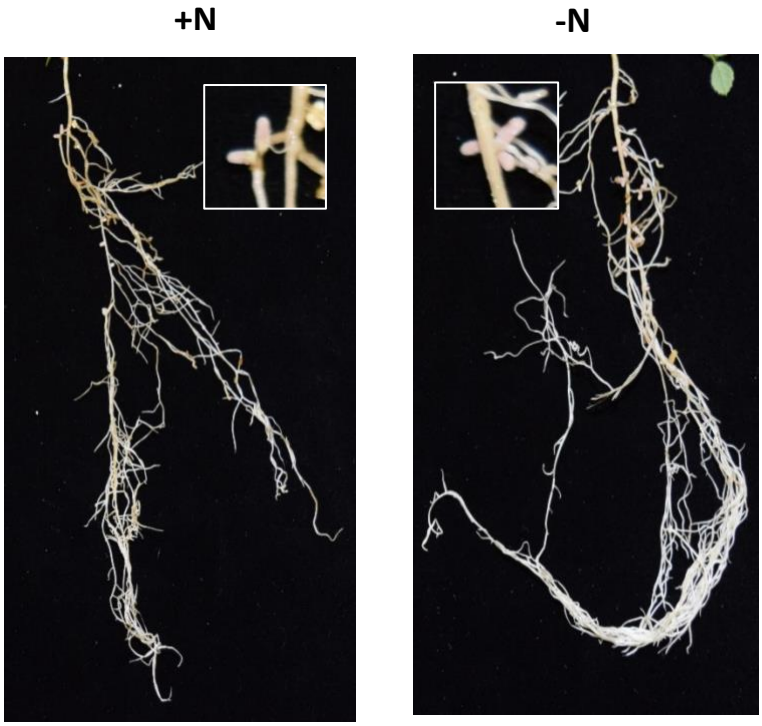

6.6. Effect of drought stress and N fertilization on nodulation. After water was withheld at 20 dpi, nodule numbers were counted in the N fertilizer treated Jemalong A17 and R108 plants at 20, 26 and 32 dpi. Values are the mean of three biological replicates. Error bars represent the standard errors of mean different letters on each bar represents the significant differences at $p<0.05$ according to ANOVA-Post Hoc Tukey's test.

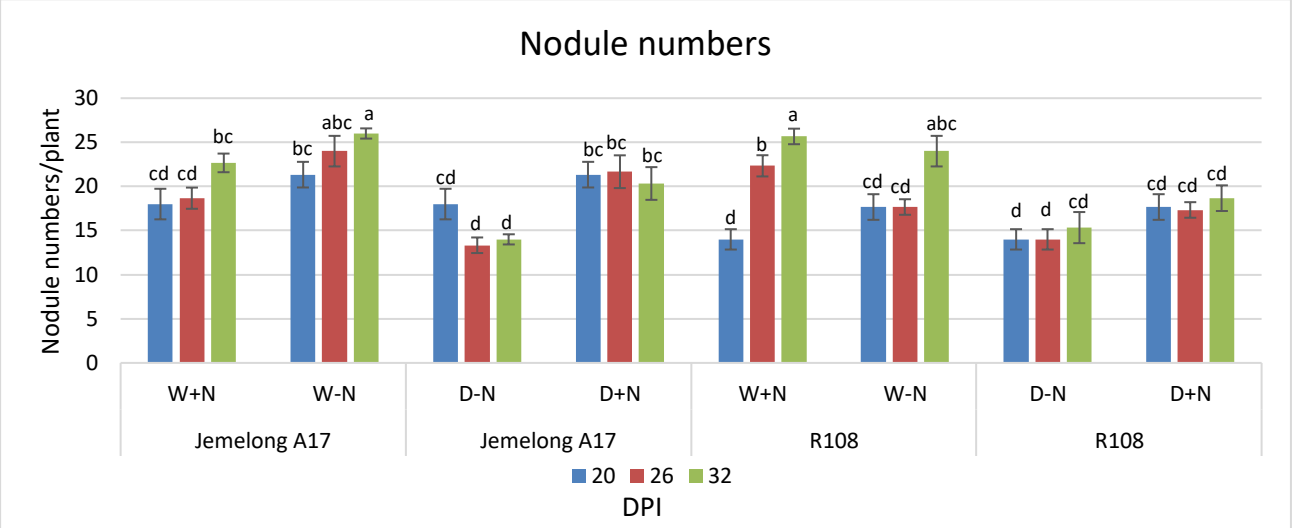

6.7. Effect of drought stress and N fertilization on bacteroid numbers. After water was withheld at 20 dpi active bacteroid numbers were counted in the N fertilizer treated Jemalong A17 and R108 plants at 20, 26 and 32dpi. Treatments are well watered (+W) or drought stressed (-W). Values are the mean of three biological replicates. Error bars represent the standard errors of mean and different letters on each bar represents the significant differences at $p<0.05$ according to ANOVA-Post Hoc Tukey's test.

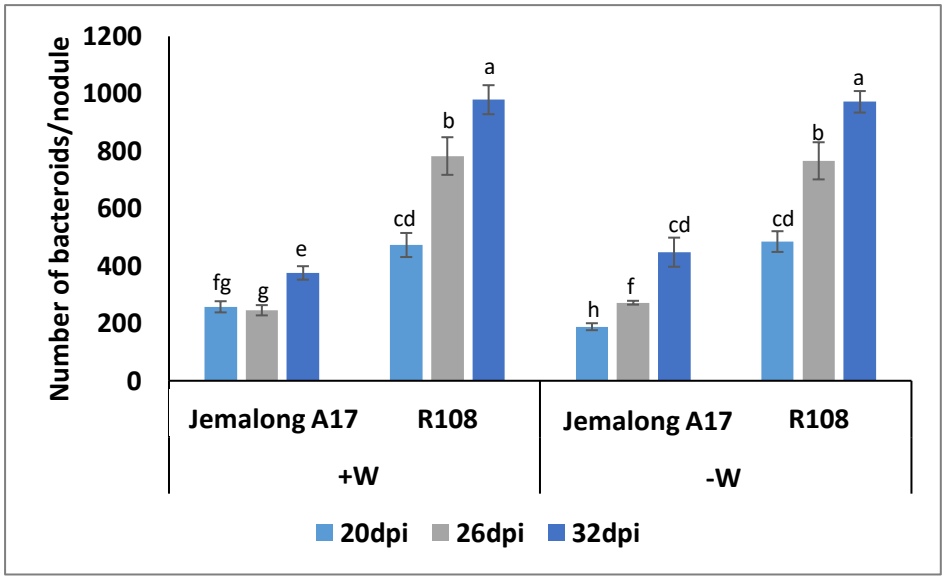

6.8. Percentage field capacity of vermiculite: perlite: sand mix in a 12-day water holding period. Potting mix was completely saturated with water overnight and a maximum water holding capacity was calculated as described in Chapter 2. Values are the mean of three biological replicates. Error bars represent the standard errors of mean asterisks indicate the significant difference from 20dpi time point at p<0.001(***) according to student's *t*-test.

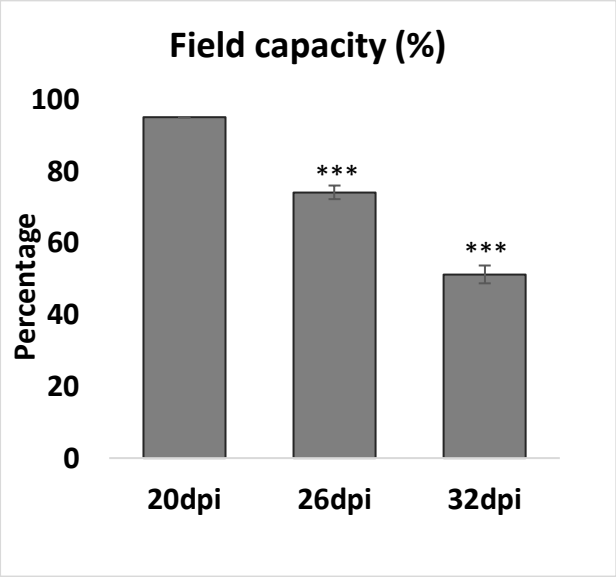

6.9. Effect of drought stress on transpiration rates. Transpiration rate of *E. meliloti*-inoculated Jemalong A17 and R108 plants grown under well-watered (+W) and drought stress (-W) conditions. Values are the mean of three biological replicates. Error bars represent the standard errors of mean and different letters on each bar represents the significant differences at $p<0.05$ according to ANOVA-Post Hoc Tukey's test.

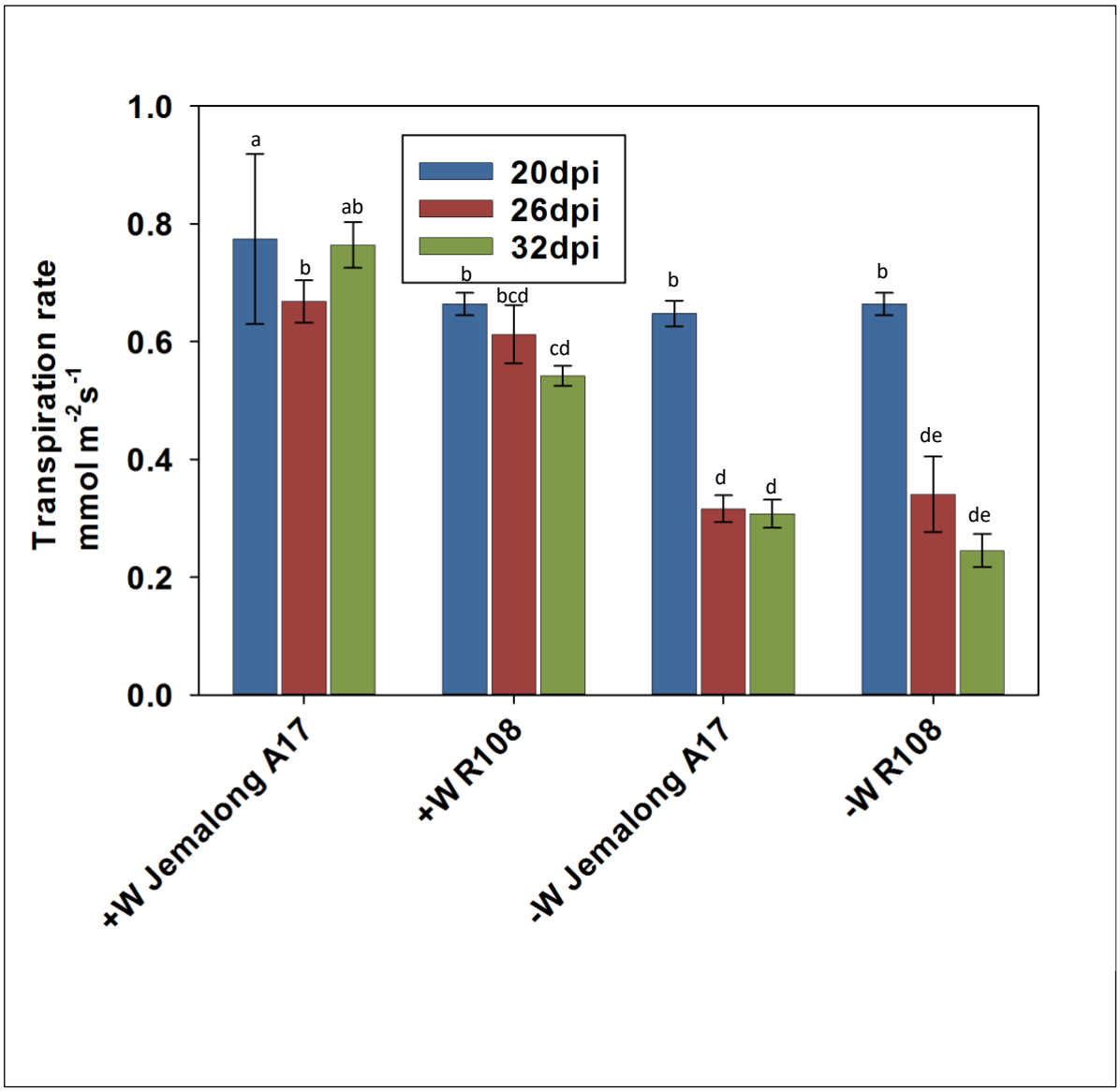

6.10. Effect of drought stress on stomatal conductance. Stomatal conductance of *E. meliloti*-inoculated Jemalong A17 and R108 plants grown under well-watered (+W) and drought stress (-W) conditions. Values are the mean of three biological replicates. Error bars represent the standard errors of mean and different letters on each bar represents the significant differences at $p<0.05$ according to ANOVA-Post Hoc Tukey's test.

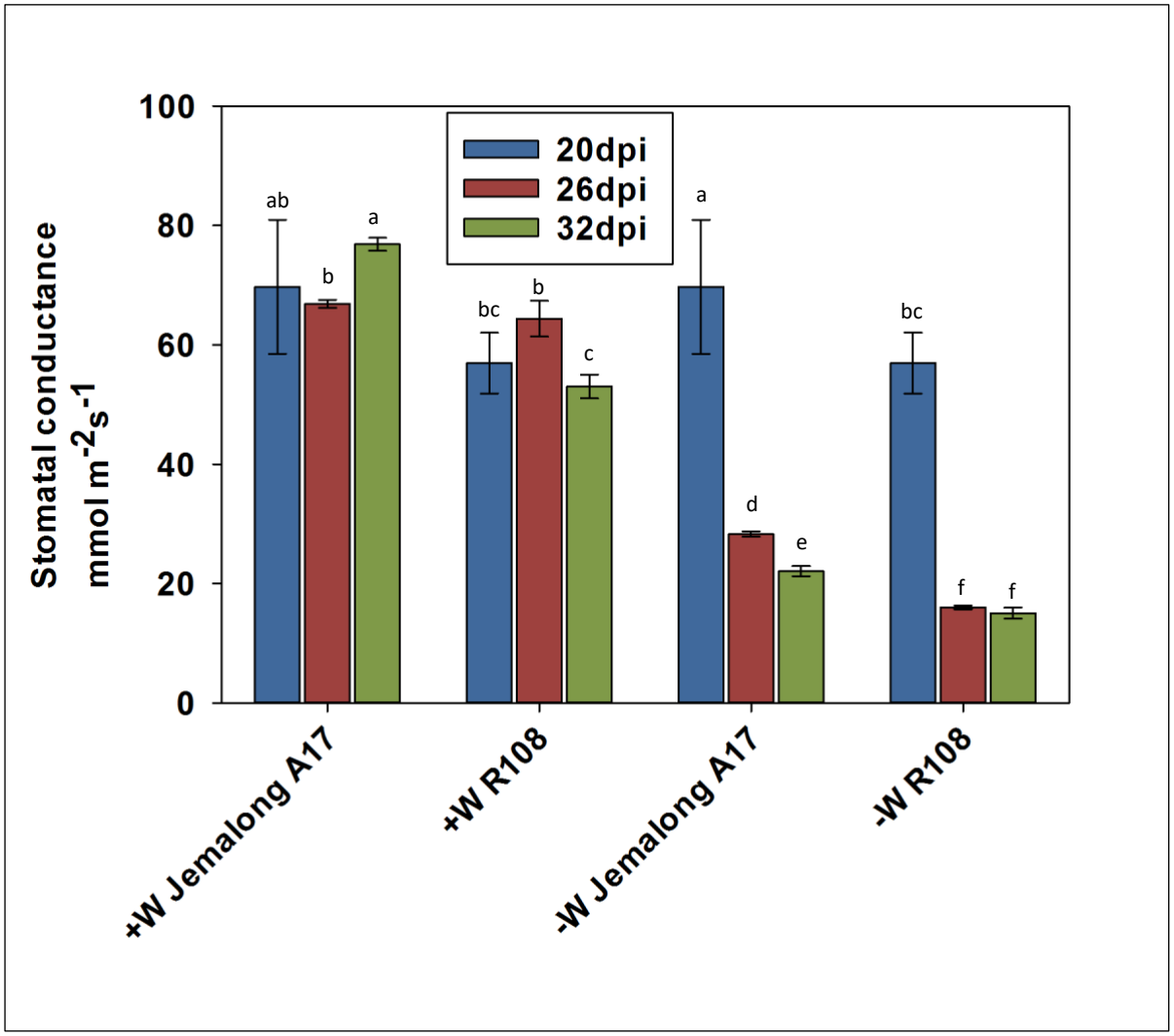

6.11. Effect of *E. meliloti* inoculation and N fertilization on photosynthesis under drought stress. Photosynthetic rates of *E. meliloti*-inoculated mutants and WT genotypes grown under either *E. meliloti* (+R) inoculation or N fertilization (+N). Values are the mean of three biological replicates. Error bars represent the standard errors of mean and different letters on each bar represents the significant differences at $p<0.05$ according to ANOVA-Post Hoc Tukey's test.

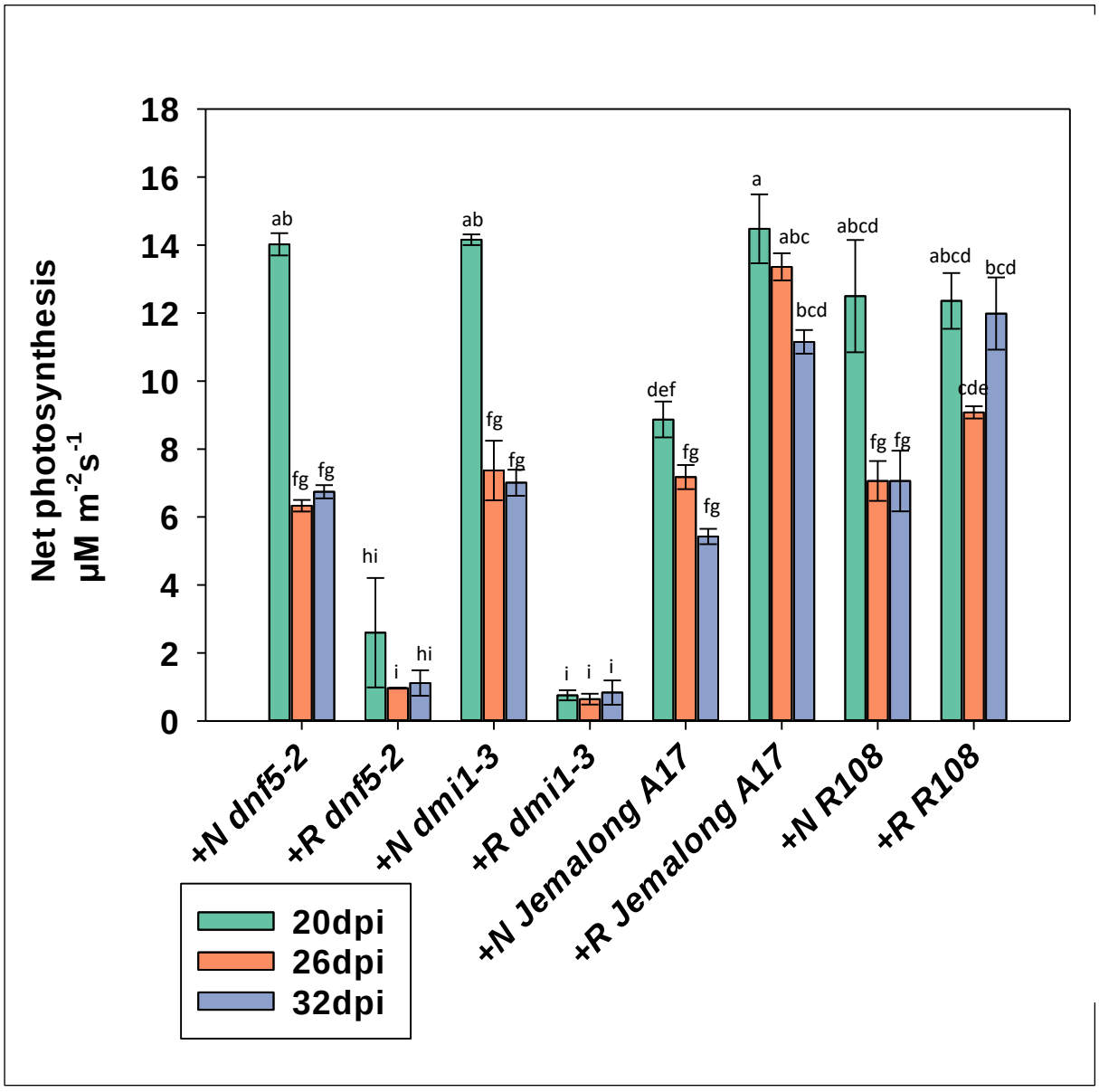

6.12. Growth of *M. truncatula* under different conditions at 20dpi. Plants are mutants, *dmi1-3 and dnf5-2* and WT genotypes, Jemalong A17 and R108. Treatments are *E. meliloti*-inoculated (+R/-R), N fertilizer treated (+N/-N) and well-watered or drought stressed (+W/-W).

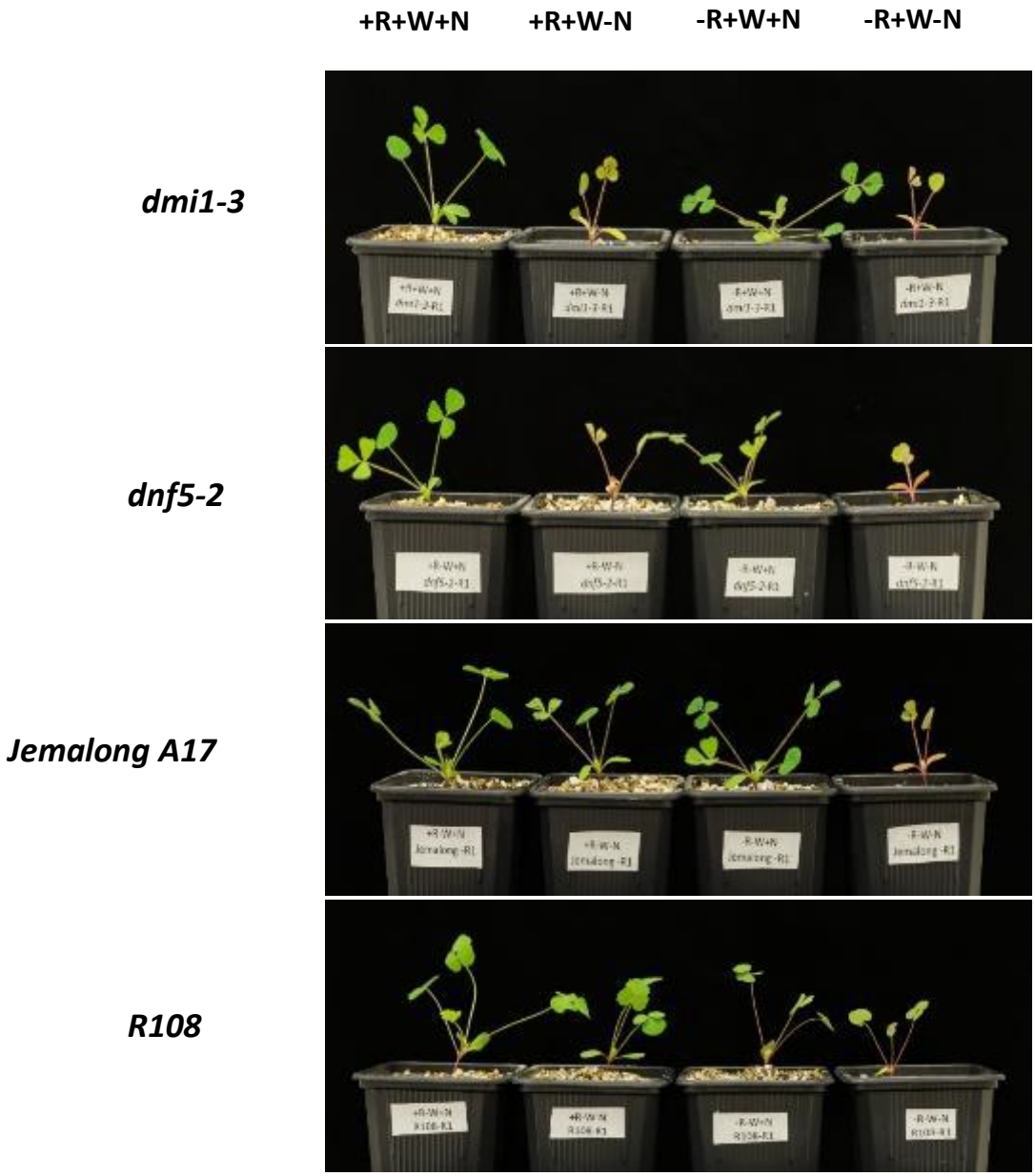

6.13. Growth of *M. truncatula* under different conditions at 26dpi. Plants are mutants, *dmi1-3 and dnf5-2* and WT genotypes, Jemalong A17 and R108. Treatments are *E. meliloti*-inoculated (+R/-R), N fertilizer treated (+N/-N) and well-watered or drought stressed (+W/-W).

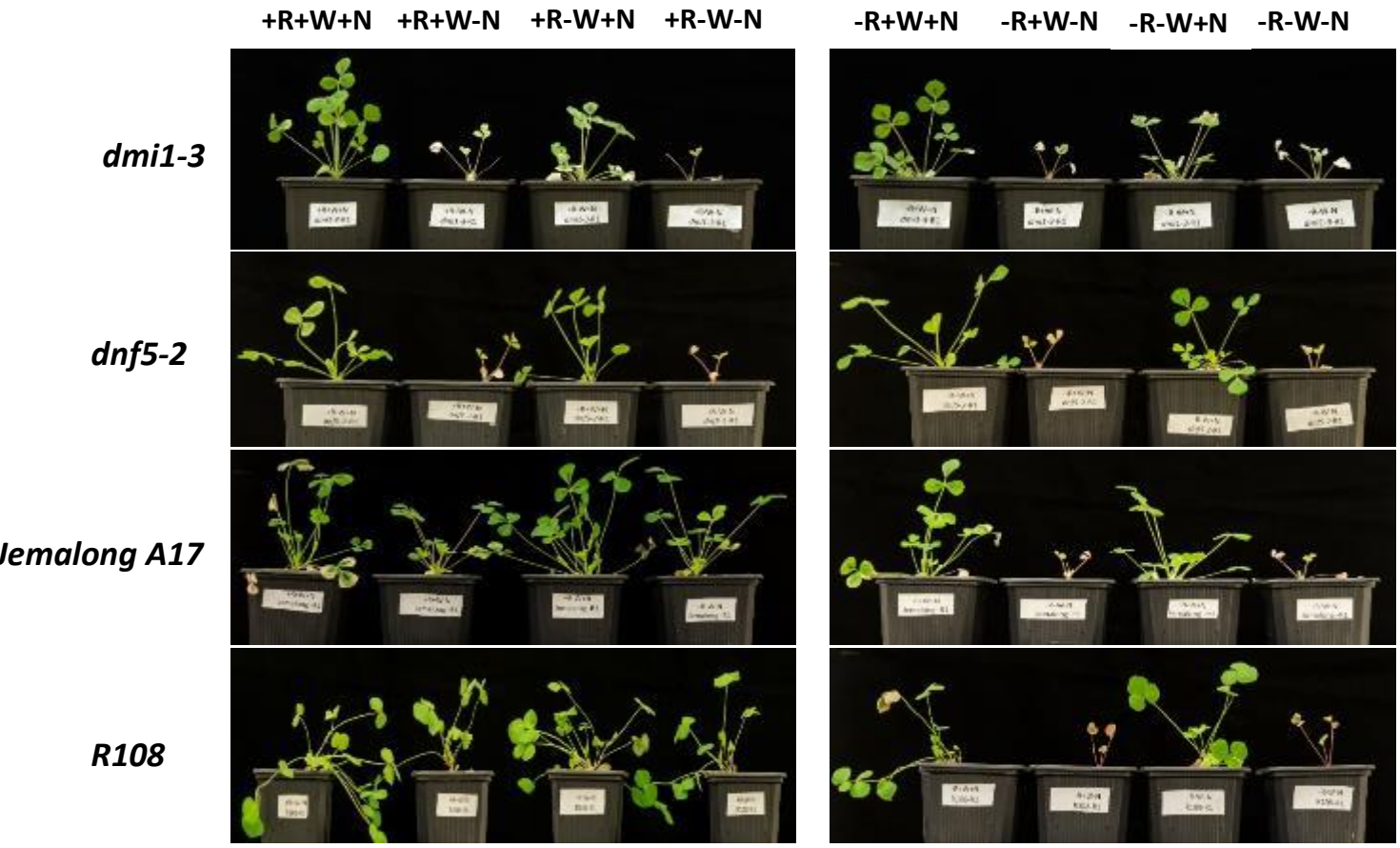

6.14. Growth of *M. truncatula* under different conditions at 32dpi. Plants are mutants, *dmi1-3 and dnf5-2* and WT genotypes, Jemalong A17 and R108. Treatments are *E. meliloti*-inoculated (+R/-R), N fertilizer treated (+N/-N) and well-watered or drought stressed (+W/-W).

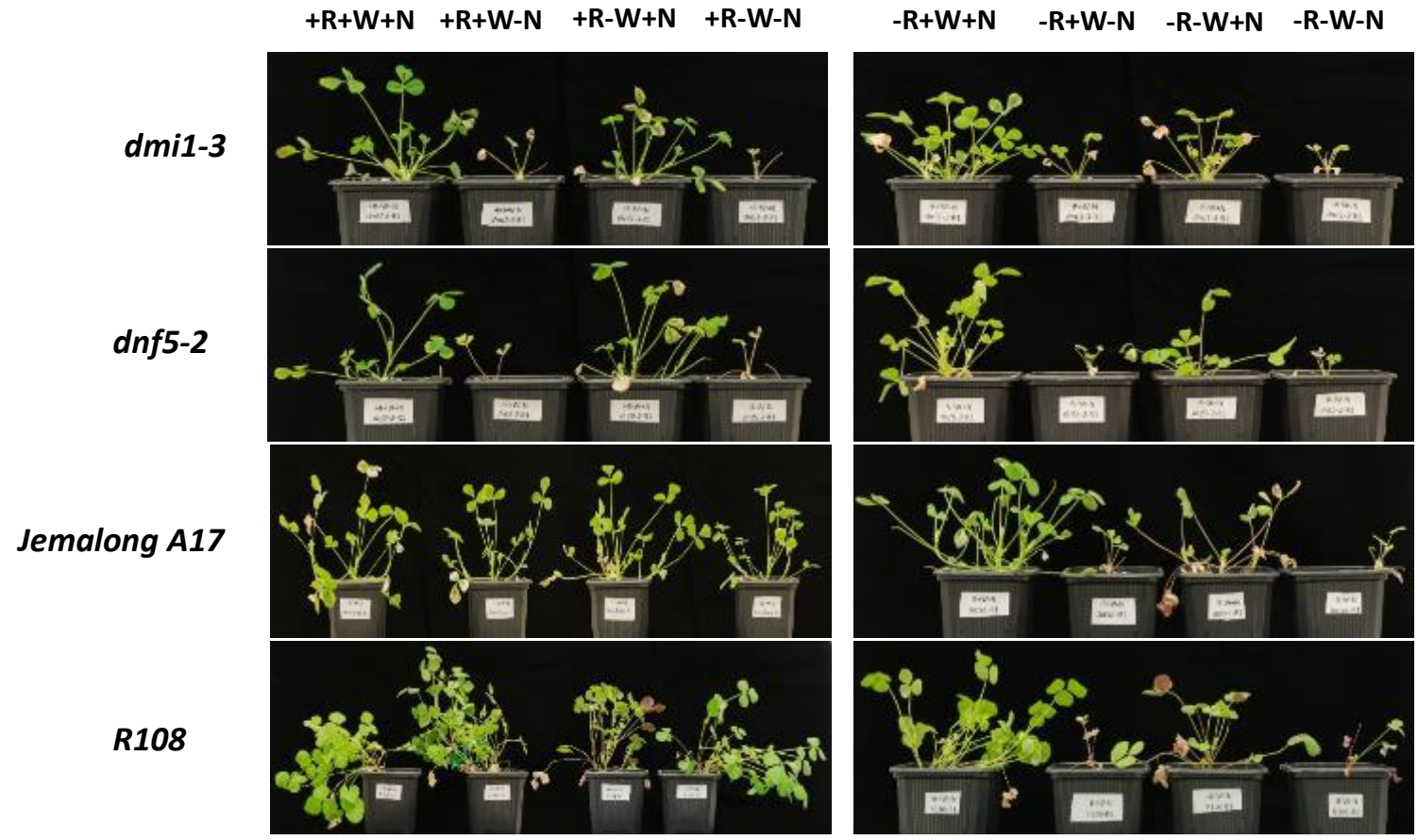

6.15. Relative comparison of nodule dry weight and shoot growth in Jemalong A17 and R108 plants under drought stress. Plants were grown under drought stress for 12 days after water was withheld at 20 dpi. Values are the mean of three biological replicates. Error bars represent the standard errors of mean and different letters on each bar represents the significant differences at $p<0.05$ according to ANOVA-Post Hoc Tukey's test.

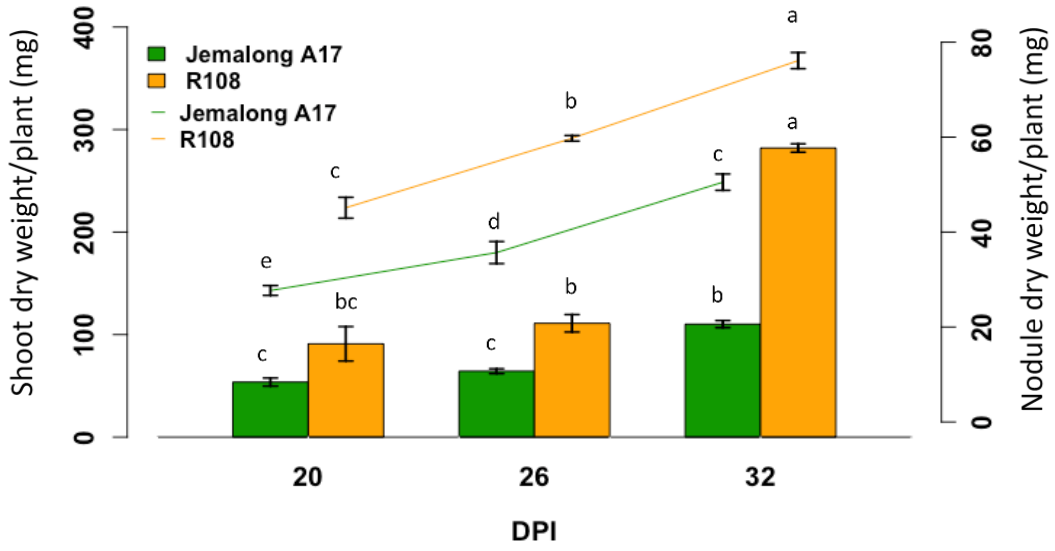

6.16. Transcriptional changes of genes involved in salicylic acid and proline biosynthesis under drought stress. Salicylic acid (a,b) and proline biosynthesis (c) genes in *E. meliloti*-inoculated and N fertilizer treated plants at 32 dpi (after water was withheld at 20 dpi). The transcript level for each gene relative to housekeeping genes, *MtElf2* and *MtTub2*, was determined by qRT-PCR. Values are the mean of three biological replicates. Error bars represent the standard errors of mean and asterisks indicate a significant difference between well-watered and droughted plants at $p<0.05$ (*) according to student's *t*-test.

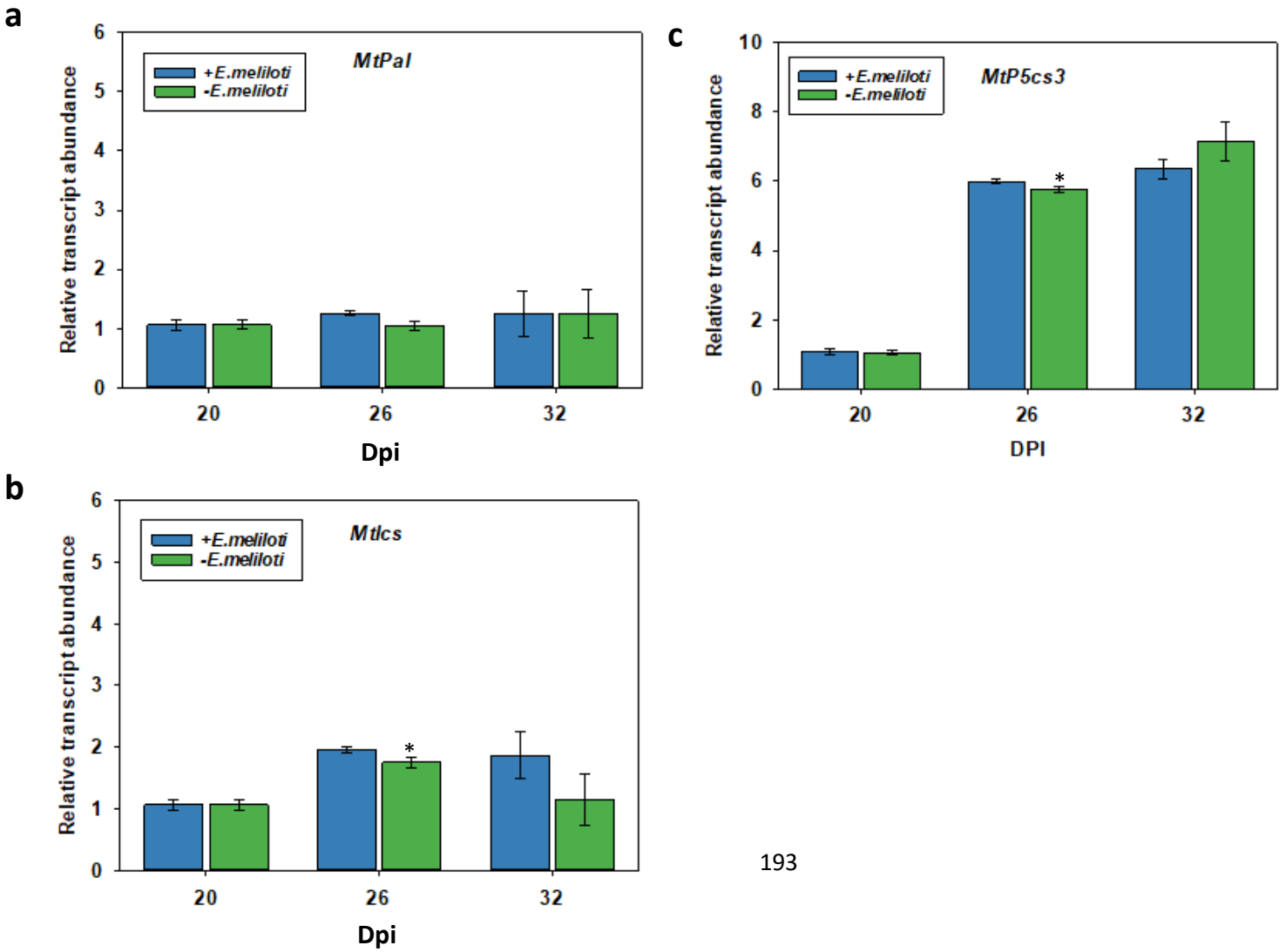

Appendix 7

DRC 16

MASSEY UNIVERSITY
GRADUATE RESEARCH SCHOOL

STATEMENT OF CONTRIBUTION TO DOCTORAL THESIS CONTAINING PUBLICATIONS

(To appear at the end of each thesis chapter/section/appendix submitted as an article/paper or collected as an appendix at the end of the thesis)

We, the candidate and the candidate's Principal Supervisor, certify that all co-authors have consented to their work being included in the thesis and they have accepted the candidate's contribution as indicated below in the *Statement of Originality*.

Name of Candidate: Ramadoss Dhanushkodi

Name/Title of Principal Supervisor: Dr Paul Dijkwel

Name of Published Research Output and full reference:

Drought-induced senescence of Medicago truncatula nodules involves serpin and ferritin to control proteolytic activity and excess iron levels- New Phytologist (submitted)

In which Chapter is the Published Work: Chapter 5

Please indicate either:

- The percentage of the Published Work that was contributed by the candidate 80%

  and / or

- Describe the contribution that the candidate has made to the Published Work:

  Ideas were discussed, concept was designed, research was conducted and manuscript was written

Ramadoss Dhanushkodi — Digitally signed by Ramadoss Dhanushkodi Date: 2018.03.28 02:29:14 +13'00'

Candidate's Signature — 28/03/2018 Date

Paul Dijkwel — Digitally signed by Paul Dijkwel Date: 2018.03.29 16:33:44 +13'00'

Principal Supervisor's signature — 28/3/18 Date

The research presented in Chapter 5 was published in the Journal *New Phytologist*. A copy of the title page is shown here.

Research

New Phytologist

Drought-induced senescence of *Medicago truncatula* nodules involves serpin and ferritin to control proteolytic activity and iron levels

Ramadoss Dhanushkodi[1], Cory Matthew[2], Michael T. McManus[1†] and Paul P. Dijkwel[1]

[1]Institute of Fundamental Sciences, Massey University, Private Bag 11-222, Palmerston North, New Zealand; [2]Institute of Agriculture and Environment, Massey University, Private Bag 11-222, Palmerston North, New Zealand

Author for correspondence:
Paul P. Dijkwel
Tel: +64 6 951 7731
Email: P.Dijkwel@massey.ac.nz

Received: *19 February 2018*
Accepted: *20 May 2018*

New Phytologist (2018) **220**: 196–208
doi: 10.1111/nph.15298

Key words: drought stress, ferritin, *Medicago truncatula*, nodule senescence, serpin, symbiotic nitrogen fixation.

Summary

• Drought is a major constraint for legume growth and yield. Senescence of nitrogen-fixing nodules is one of the early drought responses and may cause nutrient stress in addition to water stress in legumes. For nodule senescence to function as part of a drought-survival strategy, we propose that the intrinsically destructive senescence process must be tightly regulated.

• *Medicago truncatula* protease inhibitor and iron scavenger-encoding genes, possibly involved in controlling nodule senescence, were identified. RNA interference (RNAi) lines were constructed in which expression of a *serpin* or *ferritins* was knocked down. Both wild-type and RNAi lines were subjected to drought stress and nodule activity and plant physiological responses were measured.

• Drought caused *M. truncatula* to initiate nodule senescence before plant growth was affected and before an increase in papain-like proteolytic activity and free iron levels was apparent. Knock-down expression of *serpin6* and *ferritins* caused increased protease activity, free iron levels, early nodule senescence and reduced plant growth.

• The results suggest that *M. truncatula* nodule-expressed *serpin6* and *ferritins* mediate ordered drought-induced senescence by regulating papain-like cysteine protease activity and free iron levels. This strategy may allow the drought-stressed plants to benefit maximally from residual nitrogen fixation and nutrient recovery resulting from break down of macromolecules.

Introduction

Legumes include staple and forage crops and fix atmospheric N_2 through symbiotic association with rhizobia. The association can fix *c.* 100–300 kg ha^{-1} of N in one crop season and enriches the soil with substantial N for the benefit to non-legumes, reducing the need for nitrogen fertilizer (Smil, 1999; Fox *et al.*, 2007; Miransari *et al.*, 2013). The actual amount of nitrogen fixation depends on the efficiency of infection, symbiotic partners and nodule growth development (Sulieman & Tran, 2014; Mus *et al.*, 2016). The model legume *Medicago truncatula* develops indeterminate nodules, which possess a permanent nodule meristem and elongate to become cylindrically shaped (Franssen *et al.*, 2015). These nodules comprise four different zones: (1) the meristematic zone which ensures indeterminate growth of the nodule, (2) the infection zone where the *M. truncatula*-specific symbiotic rhizobacterium *Ensifer meliloti* infects the host cell, (3) the fixation zone where bacteroid differentiation and active N fixation takes place and (4) the senescence zone where the bacteroids degrade as a result of aging or environmental stress (Matamoros *et al.*, 1999; Dupont *et al.*, 2012).

The process of nodule senescence involves the elevation of proteolytic activity, which can function in removal of misfolded or modified proteins and remobilizing nutrients (Pladys & Vance, 1993). However, if the activity is unlimited or uncontrolled, it may affect the symbiosome membrane proteins and key regulators which are involved in nitrogen fixation (Vierstra, 1996; Salvesen *et al.*, 2015). In soybean and *M. truncatula* nodules, expression of cysteine protease genes was induced during different developmental stages. In particular, legumain (also known as vacuolar processing enzyme) and papain proteases (*MtCP6*) were identified in *M. truncatula* and found to be involved in degrading bacteroids in the senescence zone (Pierre *et al.*, 2014). Under drought stress, protease activity may further increase as a result of H_2O_2 production and vacuolar protein accumulation (Kinoshita *et al.*, 1999; Solomon *et al.*, 1999; Vandenabeele *et al.*, 2003). However, plants may regulate the release of protease inhibitors (PIs) to control the activity of

†Dedicated to the memory of Michael T. McManus (1957–2015).

The full paper can be accessed via https://nph.onlinelibrary.wiley.com/doi/abs/10.1111/nph.15298